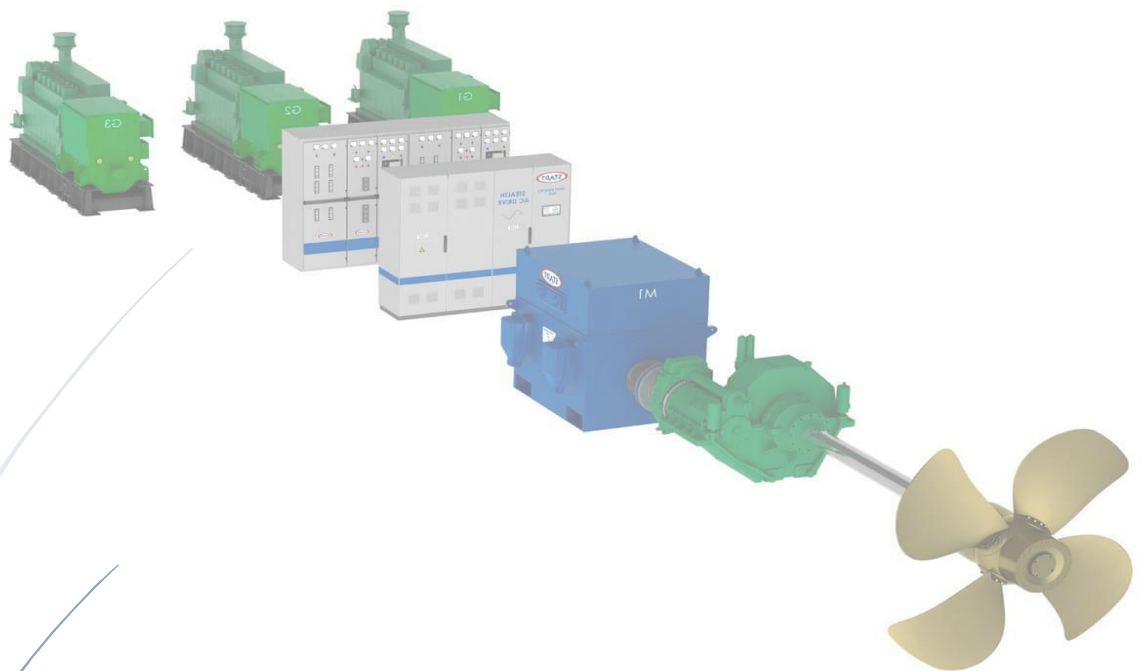


Version: Final
15-6-2018

Automatic Selection of an Optimal Power Plant Configuration

Using Client Preferences and time based Operational Profiles



J.S. van Dijk
4162056

[This page has intentionally been left blank]

The picture used on the cover:

Diesel-Electric Propulsion System, Inc. a reduction gearbox

Obtained from :

<http://www.nauticexpo.com/prod/stadt/product-32120-200622.html>

Thesis for the degree of MSc in Marine Technology in the specialization of
Marine Engineering

Automatic Selection of an Optimal Power Plant Configuration

By

J.S. van Dijk

Performed at

Nevesbu

This thesis SDPO.18.017.m is classified as confidential in accordance with the general conditions for projects performed by the TUDelft.

To be defended in public on

26-06-2018

Thesis exam committee

Chair/Responsible Professor	:	Rear-Admiral (ret.) Ir. K. Visser	TU Delft, Faculty 3mE - Department of DPO
Staff Member	:	Ir. P. de Vos	TU Delft, Faculty 3mE - Department of DPO
Staff Member	:	Dr. B.K. Atasoy	TU Delft, Faculty 3mE - Department of TEL
Company Member	:	Ir. R.M. Boogaart	Nevesbu

Company supervisor

Responsible Supervisor : Ir. R.M. Boogaart

E-mail : Not included for privacy purposes

Author Details

Author contact e-mail : Not included for privacy purposes

Student number : 4162056

[This page has intentionally been left blank]

Abstract

An increase in environmental awareness and regulations and a desire to maximize profits, pressure ship owners to optimize their ships, and more specifically the power plant of those ships. During the design and optimization of these power plants a large number of different systems is considered. Most of these considerations are found in an early design stage where data is limited and the impact of the choices made is major. These choices are mainly influenced by the mission of the ship and the wishes (or preferences) of the owner of said ship.

To investigate the influence of these choices, this research aims to enable design space exploration while taking those wishes into account. To do so the preferences of a ship owner are translated into a multi criteria weight factors for different design objectives (or characteristics). This research considers four different characteristics; fuel consumption, emissions, system mass and system volume.

The preferences and the (time based) operational profile of the ship are then used to populate a design space with every possible power plant configuration.

To be able to populate the design space, the most important design choices (related to the design of a ship borne power plant) are identified and implemented into objective functions. These functions decrease the number of design solutions that have to be considered during the selection of the optimal power plant configuration. The developed objective functions present results which are also seen in practice and these are therefore considered to be verified on an individual basis.

Following the application of the objective functions, the performance of every system is simulated over the entire operational profile.

The results of this simulation are then, together with the results of the objective functions, used in a multi criteria analysis which selects the power plant configuration which according to the client's preferences is the optimal.

The entire power plant selection process is executed for three different (generalized) cases; a (Handymax size) general cargo vessel, a harbor tugboat and a trailing hopper suction dredger. For each of the three cases an optimal power plant configuration is found and the selection of these configurations can be explained. Additionally, the selected power plant configurations can (to a certain extent) be found in practice. Both of these reasons give some initial confidence in the working principles of the tool.

Because the client preferences have a subjective nature, a sensitivity analysis is executed. This analysis shows that the majority of the configurations are influenced by the client preference, with maximum deviations around 10 %, although there are some extreme deviations. These extreme deviations are caused by the stacking of design choices and an increase in electrical power demand.

The magnitude of the deviations changes not only under the influence of a changing weight factor, but also when the power demand changes. This indicates the influence of the design choices is not only dependent on the weight factors but also on the operational profile.

The observed sensitivity is mainly present when the numerical results are compared. During the final concept selection the influence is reduced and two different power plant configurations are dominantly selected, for varying preferences.

It is recommended to investigate the influence of the operational profile during this design process as well. Additionally the expansion of the considered systems and the inclusion of more design criteria is advised.

Preface

This thesis is part of the final assessment for the degree of Master of Science in Marine Technology, with a specialization in Marine Engineering, as it is taught at the Delft University of Technology (DUT). The subject is the selection of an optimal power plant configuration for surface ships. The required research has been performed at Nevesbu (Nederlandse Verenigde Scheepsbouw Bureaus) located in Alblasserdam, the Netherlands.

I would like to thank Nevesbu for giving me the opportunity to work on this project, and specifically the employees located at the Alblasserdam offices, for their interest in this project and for the great experience I had while performing this research.

An additional word of gratitude to my supervisor at Nevesbu, Rolf Boogaart, who despite his busy schedule, was available to give advice when needed.

Another word of gratitude to my supervisor at DUT: Peter de Vos, who during my first lecture on the subject of marine engineering, piqued my interest with the statement;

“Marine engineering depends on three things; the operational profile, the operational profile and ... the operational profile.”

Many marine engineers will confirm that this is largely true. However, there are additional factors, one of which is investigated during this research.

All jokes aside; I want to thanks to Peter for the fact that he, while in the final stages of his own PhD research, managed to find time for meaningful discussions on the contents of this thesis when needed. Additionally I would like to thank Iona Georgescu, who is currently working on her PhD at DUT, for sharing her experiences with the creation of large concept libraries and for giving advice on how I might be able to limit the size of those libraries.

I would also like to thank Klaas Visser for being the chairman of my graduation committee and his very interesting lectures on Diesel Engines, which were filled with (diesel engine related) knowledge and his personal experience with these machines.

I would also like to thank Dr. Atasoy for finding the time to be part of my graduation committee.

And last, but certainly not least, I would like to thank my girlfriend, Daisy Heemskerk, for her support during my studies and especially during this project and for her (non-engineering) point of view on some issues I encountered.

Without these people this thesis would not be the document that lies before you.

Jitte van Dijk
Alblasserdam, June 2018

Table of Contents

ABSTRACT	V
PREFACE	VI
LIST OF FIGURES	3
LIST OF TABLES	4
LIST OF ACRONYMS	5
1. INTRODUCTION	7
1.1. BACKGROUND	7
1.2. PROBLEM STATEMENT.....	8
1.3. OBJECTIVE	8
1.4. REPORT STRUCTURE.....	9
2. SCOPE OF THE RESEARCH	11
2.1. CONCEPT GENERATION METHODOLOGY	11
2.2. SYSTEM BOUNDARIES AND COMPONENTS	13
2.3. ENERGY FLOW DIAGRAM	19
3. CREATION OF THE CONCEPT LIBRARY	23
3.1. GENERATION OF ALL CONCEPTS.....	23
3.2. REDUCING THE NUMBER OF CONCEPTS.....	25
4. INPUT FOR THE TOOL	27
4.1. OPERATIONAL PROFILES	27
4.2. PROPULSIVE POWER - RPM RELATIONSHIP	32
4.3. MULTI CRITERIA ANALYSIS WEIGHT FACTORS AND EMISSION CONTROL AREA	33
5. DESIGN ALGORITHMS	35
5.1. SYSTEM DESIGN SELECTION AND OVERALL DESIGN PROCESS	35
5.2. POWER MANAGEMENT STRATEGY.....	36
5.3. SHAFT CONFIGURATION GEARBOX DESIGN.....	41
5.4. PROPULSIVE POWER GENERATION SYSTEM DESIGN.....	41
5.5. ELECTRICAL ENERGY STORAGE AND GENERATION SYSTEMS DESIGN	50
5.6. FUELS: CHEMICAL PROPERTIES AND STORAGE	60
5.7. ENGINE EMISSIONS & EXHAUST GAS TREATMENT SYSTEM DESIGN	62
6. PERFORMANCE MODELS	79
6.1. EXISTING MODELS.....	79
6.2. EXHAUST GAS TREATMENT SYSTEMS.....	81
7. RESULTS	85
7.1. FINAL MULTI CRITERIA ANALYSIS.....	85
7.2. GENERAL CARGO VESSELS.....	86
7.3. HARBOR TUG	89
7.4. TRAILING SUCTION HOPPER DREDGERS	90
7.5. REMARKS.....	93
7.6. SENSITIVITY ANALYSIS	94
8. CONCLUSIONS AND DISCUSSION	103

8.1.	CONCLUSIONS	103
8.2.	DISCUSSION	106
9.	RECOMMENDATIONS	109
9.1.	RECOMMENDATIONS CONCERNING THE CONCEPT DATABASE.....	109
9.2.	RECOMMENDATION CONCERNING THE INPUT.....	110
9.3.	RECOMMENDATIONS BASED ON THE GENERATED RESULTS	111
	BIBLIOGRAPHY	112
	APPENDICES	118

List of Figures

Figure 1: Global Process Flow Diagram of the concept exploration tool.....	8
Figure 2: Concept Generation Principles	11
Figure 3: Different concept definitions given the chosen concept generation principle	13
Figure 4: EFD of a possible Propulsion power Generation System	20
Figure 5: Energy Flow Diagram with all possible connections	22
Figure 6: Defined Nodes and their numbering	23
Figure 7: Operational Profile Cargo Vessel	28
Figure 8: Partial Operational Profile Harbor Tug	29
Figure 9: Complete operational Profile Harbor Tug.....	30
Figure 10: Operational Profile TSH Dredgers.....	31
Figure 11: Propulsive power Generation Management flowchart	37
Figure 12: Engine Management flowchart (example for a PGS containing 3 engines).....	38
Figure 13: PMS of Hybrid Generation Systems	39
Figure 14: Components Propulsive power Generation System	42
Figure 15: Process Flow Diagram Engine Design	43
Figure 16: Total System mass per possible engine design	44
Figure 17: Total System Volume per possible engine design.....	45
Figure 18: Average Fuel Consumption per possible engine design	45
Figure 19: Process Flow Diagram, Propulsive power Generation System Design	46
Figure 20: Engine, Gearbox and Total Mass versus Gearbox Ratio	49
Figure 21: Engine, Gearbox and Total Volume versus Gearbox Ratio	49
Figure 22: Engine and Total efficiency versus Gearbox Ratio	49
Figure 23: Detailed Energy Flow Diagram of the Electrical Grid	50
Figure 24: Grid Voltage, Current and Current Limits as function of the electrical Power	51
Figure 25: Process Flow Diagram, Electrical Grid Design	52
Figure 26: Battery Based EES Lay-Out.....	53
Figure 27: Main dimensions of an inverter as function of power.....	54
Figure 28: Inverter mass as function of inverter power	54
Figure 29: Lead-Acid Batteries, Cell voltage as function of discharge current	55
Figure 30: Li-Ion Batteries, Cell voltage as function of discharge current	55
Figure 31: Process Flow Diagram of the PEMFC design Algorithm	57
Figure 32: Hybrid Generation System Design Flow	59
Figure 33: NOx emissions as function of engine loading for Diesel Engines.....	64
Figure 34: NOx emissions as function of engine loading for Dual fuel Engines	64
Figure 35: NOx emissions as function of engine loading for DF engines supplied with ammonia	65
Figure 36: Scrubber System Components.....	66
Figure 37: Scrubbing Tower floor area and principal dimensions	66
Figure 38: Regression of Spray Tower dimensions [12]	67
Figure 39: Regression of the 'Hydrocyclone' Dataset [12].....	69
Figure 40: Schematic representation of SCR dimensions	71
Figure 41: Reactor Construction (derived from [20] & [42])	74
Figure 42: SCR dimension Prediction results - Main dimensions.....	77
Figure 43: SCR dimension Prediction results - Spatial Requirements.....	78
Figure 44: SCR Efficiency Correction factor as function of Temperature	82
Figure 45: Example of Sensitivity Analysis Results.....	95

List of Tables

Table 1: Summarized comparison of different methods to generate a new concept	12
Table 2: Considered Nodes and their Options	18
Table 3: Summary of every node and the number of options per node.....	24
Table 4: Operational Modes Cargo Vessel	28
Table 5: Operational Modes Harbor Tug.....	29
Table 6: Operational Modes TSH Dredgers	31
Table 7: Propeller law constant 'C ₄ ' for all cases.....	32
Table 8: MCA weight factors for all cases.....	33
Table 9: Design requirements Case study Engine Design.....	43
Table 10: Numerical Results of the MPE design for the example case	44
Table 11: Engine speed Ranges per engine type.....	46
Table 12: Design Requirements Case Study Gearbox Design.....	47
Table 13: Supply Grid Voltage as function of electrical power	51
Table 14: Battery parameters for the considered battery types [3]	56
Table 15: Average Cylinder Data Generator driving Diesel Engines.....	58
Table 16: Fuel Characteristics per fuel	60
Table 17: Dual Fuel blending Ratios for all considered dual fuel types.....	61
Table 18: Sulphur Emission Limits per ECA	63
Table 19: Engine Designations based on engine speed [8]	63
Table 20: IMO NO _x limits per engine designation [11]	65
Table 21: NO _x Limit Reduction factors or for each ECA (valid from 2016 onwards).....	65
Table 22: Availability of performance models for the considered systems.....	79
Table 23: Optimal Concepts, per characteristic, Cargo Vessel.....	86
Table 24: Components, optimal Configuration, Cargo Vessel.....	87
Table 25: Numerical Results Selected Configuration, Cargo Vessel.....	87
Table 26: Optimal Concepts, per characteristic, Harbor Tug	89
Table 27: Components, optimal Configuration, Harbor Tug	90
Table 28: Numerical Results Selected Configuration, Harbor Tug	90
Table 29: Optimal Concepts, per characteristic, TSHD.....	91
Table 30: Components, optimal Configuration, TSHD.....	92
Table 31: Numerical Results Selected Configuration, TSHD.....	92
Table 32: Used Cases for the Sensitivity Analysis.....	94
Table 33: Design Data for a single configuration located at an extreme spikes in fuel consumption	97
Table 34: Selected optimal concepts per sensitivity analysis case.....	99
Table 35: System types present in the most dominantly selected concepts	100

List of Acronyms

(S/N/) ECA	(Sulphur- /Nitrogen) Emission Control Area
(US) EPA	(United States) Environment Protection Agency
AC	Alternating Current
AFR	Air to Fuel Ratio
BMS	Battery Management System
CNG	Compressed Natural Gas
DC	Direct Current
DoH	Degree of Hydrogenization
EFD	Energy Flow Diagram
EGTS	Exhaust Gas Treatment System
EM	Engine Margin
ESS	Electrical power Storage System
FC	Fuel Consumption
HFO	Heavy Fuel Oil
ICE	Internal Combustion Engine
IDeA	Intermediate Design Algorithm
IMO	International Maritime Organisation
ITF	International Transport Forum
LNG	Liquefied Natural Gas
MCA	Multi Criteria Analysis
MDO	Marine Diesel Oil
MPE	Main Propulsive Engine(s)
PEMFC	Proton Exchange Membrane Fuel Cells
PGS	Propulsive power Generation System (MPE and/or PTI)
PMS	Power Management Strategy
PMSM	Permanent Magnet Synchronous Machine
PTI	Power Take In
PTO	Power Take Out
RPM	Rotations Per Minute
SCR	Selective Catalytic Reduction
SoD	State of Discharge
TSH(D)	Trailing Suction Hopper (Dredger)

[This page has intentionally been left blank]

1. Introduction

This chapter serves as an introduction to this research. For a proper introduction the first paragraph presents the background of the problem. The second paragraph then states the problem. The main objective and research questions are then presented in the third paragraph. The final paragraph of this chapter summarizes the global report structure.

1.1. Background

An increase in environmental awareness and regulations (for example the report published by the ITF [1] or the recent IMO agreement on greenhouse gas reduction [2]) and a desire to maximize profits pressure ship owners to optimize their ships. This optimization mainly influences the on board power plant, since this is a large contributor to the operational costs of a ship and the biggest producer of emissions on board.

In the process of designing and optimizing these power plants a lot of possible components are considered, and the number of possibilities is increasing rapidly.

During these considerations design choices are made, so that the power plant configuration does indeed become the optimal one. The majority of these design choices are made in the initial stages of the design of a power plant. At this stage the influence of these choices is often major, while data about their influence is scarce.

For ships which are built in series (bulk cargo carriers for example) this lack of data is often compensated by the fact that similar ships exist, and data from these vessels can be used to obtain insight into the influence of the encountered design choices.

However, for ships which are not built in series, this approach is not applicable (since reference data is not available) and another approach to investigate the influence of the design choices is required.

An example of another approach is the creation of a set of power plant configurations which are pre-selected by an engineer. From this set of designs one is selected which is considered to be optimal, given the wishes of the owner of the vessel.

This approach is very feasible, but requires a longer design phase than the method based on reference vessels. Since a designer has to determine which power plant configurations are interesting and then design those concepts. From which one is then selected (and the remainder discarded).

The wish exists to apply the latter approach to more commonly build vessels, so that their power plant designs becomes less dependent on previously build versions. Which in turn could open the door towards more innovative (and possibly improved) power plant designs for these commonly build vessels.

However, these vessels have a relatively short design phase and an elongation of this phase is not wanted, since this increases the investments required to build a new vessel. To prevent an elongation of the design phase it is important to quickly select the optimal power plant configuration.

1.2. Problem Statement

The main problem that this research aims to solve is the selection of the optimal power plant concept, by taking into account the preferences of a client, without increasing the duration the design phase.

To do so a concept exploration tool, which is able to estimate the performance and dimensions of numerous power plant configurations, has to be developed.

The different power plant configurations are then compared to each other so that the one that is optimal, according to the preferences of the client, can be selected.

There are already tools which can be used to optimize a set of predetermined power plants given the operational profile. For example the tools which are developed at Nevesbu for the design of diesel-electric submarines [3] & [4]. However, the number of concepts that can be compared remains limited.

Research is being done to increase the number of concepts that can be investigated ([5] and [6]). These researches show that the number of considered concepts can rapidly escalate into millions (or more) different concepts. A high number of concepts likely requires more computational time, which is unwanted since swift results are required. Therefore a median between a few and far too many has to be found.

1.3. Objective

The main objective of this research is the selection of the optimal power plant configuration based on the operational profile of a vessel and the preferences of the owner, without extending the design phase.

To achieve the objective a concept exploration tool is developed which is able to ‘design’ numerous power plant configurations, and obtaining data about system mass and volume in the process. The designed configurations are then subjected to a performance simulation in order to obtain estimates of the fuel consumption and emissions of CO₂, NO_x and SO_x. During the course of this research these four parameters (fuel consumption, emissions, mass and volume) are referred to as ‘characteristics’. The preferences of a client are to be expressed as Multi Criteria Analysis (MCA) weight factors for each of these four characteristics.

An overview of envisioned concept exploration tool is presented in Figure 1. In which the input required by the tool, the design and simulation stage and the final multi criteria analysis can be recognized.

This figure also shows the library of feasible concepts. This library defines the different power plant configurations that are to be considered as concepts. The content of this library is not related to any of the user defined input.

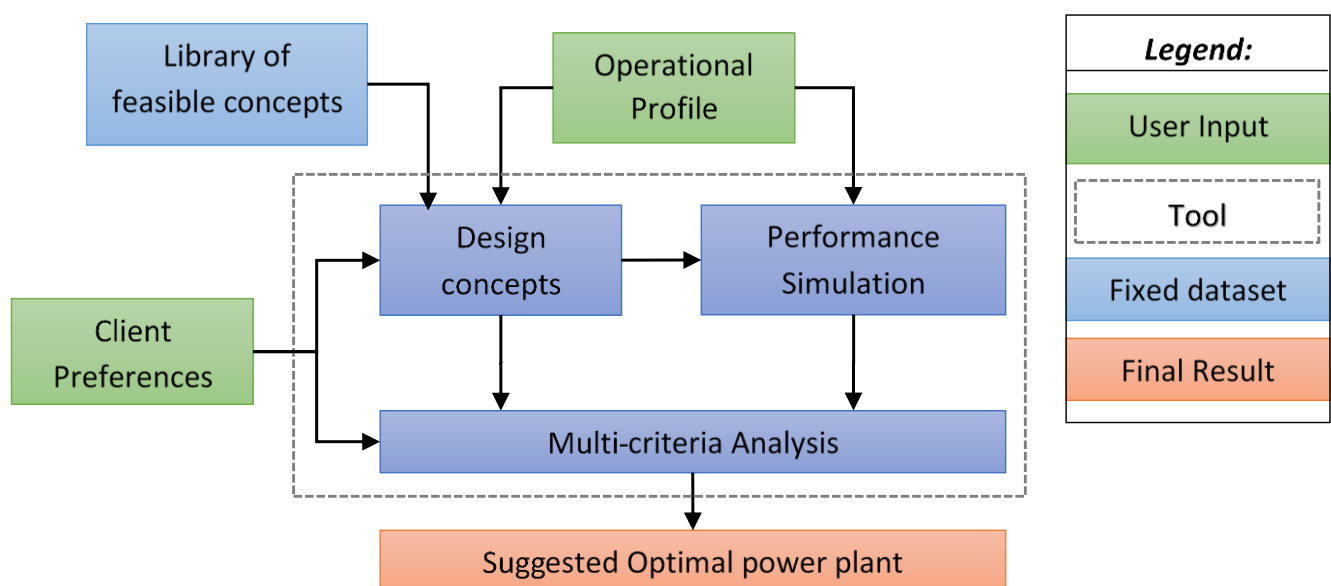


Figure 1: Global Process Flow Diagram of the concept exploration tool

The required input is determined for three different (example) cases, in order for the tool to be developed and tested. During the course of this research these considered cases are defined using a ship type. The three considered cases are; a general cargo carrier, a harbor tug and a trailing hopper suction dredger.

The problem and objective can be translated into the following main question and the sub-research questions that come along with it. The main question of this research is :

“What is the optimal power plant configuration of a surface vessel given its operational profile and the preferences of its owner, when a comparison is made based on the fuel consumption, emissions and spatial requirements?”

Sub questions

What is the most suitable method to create the configuration concept library ?

What is the operational profile and what are possible client preferences ?*

Which design choices are influenced by the preferences of a client ?

For each of the different characteristics considered, which configuration would be the ideal choice ?*

*. For each of the ship types considered

1.4. Report Structure

This report consists of nine chapters and nine appendices. The ninth appendix (which is appendix I) does not contain information that is relevant to this research. Instead it presents a concept paper about this research.

The first chapter presented the introduction to the research. Chapter two discusses the scope of the research, which consist of a list of the considered systems and the method used to develop the library of concepts. The creation of this library is then discussed in chapter three.

Chapter four, then presents the input required for the tool, by defining the required parameters for each of the three case studies.

The different design choices, which are encountered when designing the systems that can be found in a power plant are discussed in chapter five.

Chapter six then discusses the performance models that are used during the simulation of the designed systems.

The results of the concept exploration tool is then presented in chapter seven, for each of the considered cases.

Chapter eight then present the conclusions of this research and reflect on them. The ninth, and final chapter will present the recommendations for future research.

[This page has intentionally been left blank]

2. Scope of the Research

This chapter presents the scope of this research. This is done by first discussing the method used to create the 'library of feasible concepts'. After this method has been determined, the next paragraph will discuss the boundaries of this research. The final paragraph will then combine the presented boundaries into an overall Energy Flow Diagram (EFD).

2.1. Concept Generation Methodology

Before the library of feasible concepts can be created, the method to do so has to be determined. To do so the first step is establishing a definition of a power plant configuration concept. For this research a power plant configuration is considered to be a network of nodes (or systems).

Any network can be defined using a description of the nodes and edges in that network. The description of the edges is referred to as topology.

By defining a power plant configuration as a network, it is possible to define three different methods that can be used to 'create' concept power plant configurations. These methods are defined as follows:

A new concept configuration is created -

1. By varying the topology, while keeping the nodes fixed.
2. By keeping the topology fixed, while changing the nodes.
3. By varying both the topology and the nodes.

These three methods will be discussed separately and following this discussion the method used to create the library of feasible concepts is selected. All of the considered methods are graphically presented in Figure 2, which shows a benchmark concept (concept A) and a new concept (concept B) that would be created using the considered method.

Note that the concepts presented in Figure 2 are purely there to illustrate the working principles of the three concept generation methods, they do not represent actual power plant configurations.

Method	Concept 'A'	Concept 'B'
1.		
2.		
3.		

Figure 2: Concept Generation Principles

The first method allows for the examination of the influence of the topology on the determined characteristics, but is likely to require complex algorithms. These complex algorithms are due to the fact that the nature of the influence that systems have on each other can change. This method allows for the comparison of a huge number of different possible configurations, as shown by 'de Vos' [5] or 'Silvas et al' [7]. Due to the complexity of the algorithms it is difficult, but certainly possible, to develop a performance simulation.

The second method is able to analyze the effect of having different options for each node. While not requiring complicated algorithms to 'design' every possible configuration, since the nature of the effects which components have on each other does not change. Additionally the number of possible configurations remains limited. Both of the aforementioned arguments make this method suitable for a performance simulation.

The third concept creation method is a combination of the aforementioned methods. This method allows for an analysis on both influences and will examine every possible concept that can be dreamt of. However, this comes at the price of incredibly complex algorithms and an (near) infinite number of concepts. These factors make it (almost) impossible, to develop a performance simulation, especially when the wish to obtain quick results is kept in mind.

The presented reasoning, is summarized using keywords/symbols in Table 1.

Table 1: Summarized comparison of different methods to generate a new concept

		Method		
		1	2	3
Criterion	# Concepts (Design space size)	Large	Medium	(Almost) infinite
	Complexity of required algorithms	High	Low	High
	Computational Time Requirement	Medium	Low	High
	Suitability for Performance Simulation	+/-	++	-

The wish to simulate the performance of a power plant configuration over the entire mission of the ship and the fact that quick results are required, force the selection of a method which has a limited design space and does not require complex algorithms. Therefore the second method is selected for this research.

However, even with the selected concept creation method the number of possible power plant configurations can still become quite large when a detailed definition of each system is used, which is necessary for a performance simulation to be possible.

To prevent the number of concepts from escalating to an amount which is infeasible given the wish to quickly obtain results, a power plant configuration will not be defined using a detailed description of the systems. Instead each system is defined using a broad description and dedicated Intermediate Design Algorithm (IDeA) is then used to compare different feasible options, and select the one which, according to the client preferences, is optimal and as such determine the required level of detail.

Both methods are graphically presented in Figure 3, which demonstrates both methods for a fictional node (or system). Method 'A' is the method where each option defines a new power plant concept and method 'B' is the method where an intermediate design choice is made, which is method used during this research.

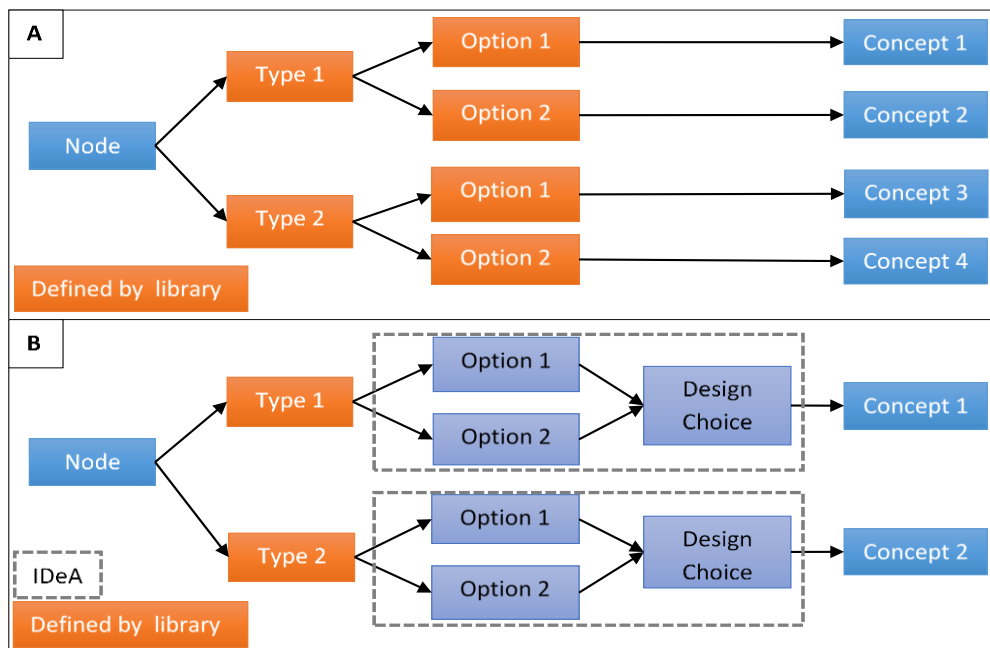


Figure 3: Different concept definitions given the chosen concept generation principle

2.2. System Boundaries and Components

Now that the methodology to create the library of feasible (power plant) concepts has been selected, the boundaries of the research can be determined. The selected methodology requires a fixed topology and the possible values for each of the nodes.

The nodes are considered to be the main machinery inside a power plant and the variable used to define each node is the type of system that is installed.

The topology can only be defined once the possible systems have been determined, since these systems also define the required connections between nodes.

Therefore the boundaries of the power plant are first established, then each of the nodes and the systems that can be present are discussed. The result of this discussion is summarized in Table 2, which is located at the end of this paragraph.

2.2.1. Input and Power plant boundaries

The power plant of a ship has multiple functions, including (but not limited to) providing propulsive power, fuel treatment, generating electrical power and the supply of (heated) water and hydraulic power. For this research the latter functions are considered to be combined into one (electric) auxiliary power demand. The operational systems, such as dredging/ballasting pumps or winches are accounted for as a separate (electrical) power demand. Note that this does assume that pumps (and winches) are always driven by electric motors.

These assumptions allow the functions of a power plant to be simplified to the supply of propulsive- and electrical power. These power demands can be defined as an operational profile, which for this research is defined as a quasi-static time trace of the propulsive, auxiliary and operational power.

For dimensioning purposes, a propeller speed and a voltage of the electrical systems are required. For the determination of the propeller speed a relationship is established based on the propeller law [8, p. 422]. For this relationship a (ship dependent) constant (“ C_4 ” [8, p. 422]) is required, which is added to the input. The electrical grid voltage cannot be related to a ship type in such a way. Instead a dedicated algorithm will be used to determine this during the design of the power plant configuration.

The operational profile does not include any geographical data. However, there are design requirements which depend on the operating area of the vessel. Therefore some sort of geographical data is required. This data is added the input of the tool, in the form of the most stringent Emission Control Area (ECA) in which the vessel has to (be able to) operate. For this research four different emission control areas are defined; a Nitrogen Emission Control Area (NECA), A Sulphur Emission Control Area (SECA), both sulphur and nitrogen Emission Control Area (ECA) or no emission control area. The latter of which means the vessel only has to comply with global IMO limits.

The final components of the input are the multi criteria analysis weight factors. These factors indicate how important a certain characteristic is deemed to be. These weights will have a value between 0 and 10, with a value of 0 indicating that a characteristic is not important at all and a value of 10 implying a value is considered to be very important. It is allowed to assign the same value multiple times, to different weight factors. It is also allowed to use non-integer values. Negative values and values higher than 10 should not be used.

2.2.2. Propeller

A well-known system inside any power plant is the propulsor, of which only one type is considered during this research; the screw type, fixed pitch, propeller. Which is selected because these propulsors are the most conventional type at the time of this research. The type of propeller is not varied during this research so that the initial complexity of the tool remains limited.

The propulsive power will be defined as the delivered power (P_D), which is shown in equation (2.1) [8]. In this equation ‘ k_p ’ represents the number of propellers and P_p the power of each propeller. Using this definition removes the number of propellers as a design choice.

$$P_D = k_p * P_p \quad (2.1)$$

2.2.3. Drive Shaft Configuration

Following the propeller shaft into the ship, the first (considered) node is encountered; the drive-shaft configuration, which divides the propulsive power over propulsive power generation system(s).

Both a single shaft configuration and a power take in (PTI) configuration are considered during this research, since they are both very conventional in practice [8].

For PTI configurations a first design choice is found; the power division ratio (PDR). The PDR is a dimensionless value, which defines the portion of the total power each generation system has to (be able to) deliver. During this research it is defined as shown by equation (1.2). The value for the PDR is variable, but fixed for a specific operational profile.

$$\begin{aligned} P_{MPE} &= P_{\max} * PDR \\ P_{PTI} &= P_{\max} * (1 - PDR) \end{aligned} \quad (1.2)$$

Although Power take off (PTO) systems are conventional systems, they are not included in this research. This is due to the complex power management strategy that would be required, which would cause a complexity that is infeasible given the time constraints posed to this research.

2.2.4. Propulsive Power Generation Systems

Following the driving shaft further into the ship, the next (two) nodes are encountered; the Propulsive power Generation Systems (PGS). There are two separate PGS nodes; the Main Propulsive Engine (MPE) and the Power Take In (PTI) engine. The variables for both these nodes is the engine type and whether a gearbox is present or not.

The values associated with this variable are the most common engines in industry; two and four stroke diesel engine(s), four stroke dual fuel engine(s) and electric motors.

Two - stroke dual fuel engines exist, but these are relatively new, and not as efficient as their 4-stroke counterparts yet [9]. Engines which run on pure gas (i.e. without a pilot fuel) are not included.

The only type of electric motor that considered during this research are Permanent Magnet Synchronous Machines (PMSM). This type is selected because synchronous motors are very well applicable for ship propulsion [10]. Of this type of motors those with permanent magnets are in general; more efficient (especially in part load conditions), have a lower mass, and require less maintenance [4]. All of these advantages together make these machines very viable for ship propulsion.

Gas turbines are not included in this research due to their relatively low efficiency and the fact that maintenance on these machines is somewhat complex and therefore expensive [8, p. 137+138].

Additionally, gas turbines are not really suited for maneuvering, because can only rotate in one direction [8, p. 314]. This in combination with the fact that gas turbines are only practical in applications where very high power densities are necessary (such as frigates), lead to the exclusion of gas turbines.

All the selected engine types are can be used as direct drive or with reduction gearbox. The reduction gearbox is considered to always be a Single Input-Single Output (SiSo) type gearbox, and more complex reduction gearboxes are not included. Instead concepts which require two (or more) input shafts to be reduced to a single output shaft will have a separate gearbox solely for this purpose. This type of gearbox would normally be combined with the reduction gearbox into one (more complex) gearbox. However, separating these different functionalities allows for a less complicated algorithm.

2.2.5. Exhaust Gas Treatment Systems and Emissions

The conversion of chemical energy to either mechanical- or electrical power comes at the price of emissions, some of which are harmful to the environment. These emissions are subjected to international regulations, such as those posed by International Maritime Organization (IMO) [11].

In order for a vessel to meet those regulations exhaust gas treatment systems (EGTS) can be applied, and these systems will also be included in the power plant configuration.

During this research only 'open loop' scrubbing and Selective Catalytic Reduction (SCR) systems are considered. Open loop scrubbers are included because they are in general the smallest and least complex scrubbing systems [12, pp. 11,13,15], while still being very effective at removing SO_x from the exhaust gasses. SCR systems are included because they are the only after treatment method to effectively reduce the amount of NO_x in the exhaust gas [13].

Other methods to reduce the emissions of NO_x exist. However, these all rely on changing the combustion process, which will not be modeled during this research due to time constraints [13].

There are no (economically) feasible methods to remove CO₂ from the exhaust gas, and the only method to reduce CO₂ emissions is the selection of the used fuel and/or improving the overall system efficiency [14, p. 725].

Waste Heat recovery systems are not considered by this research, although they are feasible for maritime applications. This is done because waste heat systems are often used for HVAC purposes or the heating of water, both of these are not included in this research, since these consumers of power are considered to be (part of the) auxiliary power demand.

2.2.6. Electric Power Storage and Generation

Apart from the propulsive power demand, there is also an electrical power demand. This demand can be met using three different supply methods; the storage of (electrical) energy, the generation of electrical energy or a combination of these two.

All of these are applied in industry to some extent and will therefore be included in this research. Which leads to the specification of two additional nodes; the electrical power storage system (ESS) and the electrical power generation system.

Electrical Power Storage

The storage of electricity can be used to reduce fuel consumption and emissions or to smoothen the power demand (which is highly erratic in practice) so that the overall engine loading improves [15].

The latter method is very feasible in practice, but not applicable for this research, due to the quasi-static definition of the operational profile (as discussed in 2.2.1).

Therefore the storage of electrical power is used to reduce the consumption of fuel and to reduce emissions. This application requires large storage capacity at relatively low peak powers. To determine which systems are included, different energy storage methods are compared using a 'Ragone plot' (see also appendix A [16]). If the included fuels and fuel conversion systems seen in this plot are ignored (since they do not store electrical power), batteries, flywheels and supercapacitors remain as storage methods.

From that same Ragone plot it can be seen that both flywheels and supercapacitors are not suitable for applications which require large storage capacities at a lower peak power, leaving only batteries as feasible storage systems. During this research both lead-acid and li-ion batteries are included.

Electrical Power Generation

The most conventional method of generating electrical power at the time of this research are engine driven generators. Both dual fuel and diesel engine driven generators are considered and generators driven by a gas engine are excluded.

Another feasible, less mature, generation system are fuel cell stacks. Which are included because of their efficiency and because they can generate electricity without any harmful emissions. Of the different fuel cell types the 'Proton Exchange Membrane Fuel Cell' (PEMFC) is the most mature technology. It is also considered to be the safer option (in comparison to other fuel cell types), due to the relatively low operating temperature [17].

PEMFC's do however require either a supply of pure hydrogen or a fuel reforming installation. The latter of which is not included, since reformers are only (truly) practical when waste heat can be utilized [18]. Since these were excluded from this research, fuel reformers are also excluded.

There are auto-reforming fuel cell concepts, however these are not a proven technology yet, especially for mobile (maritime) applications [18] and therefore these are not included in this research.

Finally a combination of engine driven and a PEMFC based generation system is also considered. Both dual fuel and diesel engine driven generators are allowed in combination with a fuel cell.

Other electricity generation systems, such as nuclear power or turbines are not included due to their relative inefficiency, size or (general) public opinion. The latter being the most important reason for the exclusion of nuclear power.

2.2.7. Fuel Types

The operation of Internal Combustion Engines (ICE) and fuel cells requires fuel. The type of fuel influences the (fuel tank) dimensions and the performance of the system supplied with that fuel. Therefore different fuel types will also be included in the scope of this research.

The considered fuel options are; Marine Diesel Oil (MDO), Heavy Fuel Oil (HFO), Liquefied Natural Gas (LNG), Compressed Natural Gas (CNG), pressurized Hydrogen (H_2) and Ammonia (NH_3).

The spatial requirements of the systems required for the application of those fuels (fuel treatment systems, supply pumps etc.) are not included. Additionally, the electrical power demand of those systems is assumed to be included in the auxiliary load.

MDO and HFO are selected because they are both very conventional, maritime, fuels and both are quite versatile fuels. Since they can be used as fuel for diesel engines, but also as pilot fuel for dual fuel engines.

Liquefied- and Compressed Natural Gas (LNG and CNG) are included because they are the main fuels on which dual fuel engines operate. Both fuels are also considered a transition fuel towards lower emissions. Due to their lower carbon content, the absence of fuel borne sulphur.

Both compression and liquefaction are considered as storage methods because they are both feasible and mature storage methods. Conventional natural gas (without liquefaction or compression) is not considered due to the immense volume it would take to store a significant amount of gas.

Pressurized Hydrogen is included to allow for the application of a PEM fuel cell. It is possible to use hydrogen as fuel in an ICE, however this application of hydrogen is not considered during this research, because of the low efficiency of an ICE engine running on hydrogen when compared to fuel cell applications [19].

There are other ways of storing the hydrogen than just pressurized, however these often come at the price of high cooling demands or a rather low storage efficiency, as presented by ten Hacken [4]. The storage of hydrogen is done at 700 bar, which is the state of the art [4].

Ammonia is included because it has two, completely different, applications. It can be used in a dual fuel engine (just like LNG and CNG) and it can be used as a reagent in an SCR installation. For this research the SCR installation will always use ammonia.

Other fuel types are not included in this research, due to their limited technological maturity or because they were excluded due to the elimination of the systems that use them as fuel.

All nodes and their possible components have now been determined, and are summarized in Table 2. For the sake of legibility the two Propulsive power Generation Systems (PGS), fuel tanks and exhaust gas treatment systems have each been combined into a single column, while in truth they are divided over multiple, separate, nodes.

Each node will be assigned one value from its specific column, and combinations within that column are not allowed. (E.g. A concept which contains both li-ion batteries and lead-acid batteries does not exist.) The actual separation of the presented options is presented (in a more detailed manner) using an Energy Flow Diagram (EFD), which is discussed in the next paragraph.

Table 2: Considered Nodes and their Options

Shaft Configuration	PGS ^{1,2}	EES	Fuel Types ⁴	EGS	EGTS ⁵
Single Shaft	Diesel engines (DE) 2-stroke	Li-Ion Batteries	MDO	Fuel Cells (PEMFC)	SCR
Power Take In	Diesel engines (4-stroke)	Lead-Acid Batteries	HFO	DE Genset	Open Loop Scrubber
	Dual fuel engines (DF) (4-stroke)	None	LNG	DF Genset	Not Present ⁶
	PMSM		CNG	DE Genset + PEMFC	
	None ³		Ammonia	DF Genset + PEMFC	
			Hydrogen (Pressurized)	None	
			None		

1. This list is applicable to both propulsive power generation systems that can exist.
2. All engines can be present either as geared or as direct drive
3. This option is there since the Power take In system has to be capable of being 'empty' for the cases where a single propulsion generation system is applied.
4. The fuel types are in practice divided over a series of fuel tanks, however for the sake of legibility all fuel types are listed in one column.
5. These systems are also divided over two separate nodes and only listed in one column for the sake of legibility
6. The 'Not Present' option is allowed for both exhaust gas treatment system nodes.

2.3. Energy Flow Diagram

Now that all the considered nodes (or systems) and their options have been determined it is possible to define the invariable topology. An Energy Flow Diagram (EFD) is used to present the topology and is presented by Figure 5 at the end of this paragraph. The definition of the presented EFD required certain choices to be made and these are discussed in the following paragraphs. The EFD shows all possible connections that can occur. However, certain energy flows are not always present, since they are not always required.

2.3.1. Fuel Supply Lines

The first choices that have to be made, concern the fuel supply towards the generation systems. Each combustion engine will have one tank containing the main fuel (or the pilot fuel) and one tank that contains the secondary fuel for dual fuel cases. The fuel cell will have a separate hydrogen storage tank.

This results in a total of seven different fuel tanks. This definition allows for the definition of a relatively simple topology, which in turn is beneficial for both the speed and complexity of the complete tool.

2.3.2. Mechanical Connections

The (significant) mechanical connections are found in the propulsive power generation systems. Which for this research is divided into three nodes; the shaft configuration gearbox and the two propulsive power generation systems.

The installed gearboxes are very often combined into one gearbox, which both reduces the rotational speed and allows for the (dis-) connecting of engines.

This is not done in this research, because keeping these functionalities separate, allows for a simpler algorithms, (possibly) at the cost of a small overestimation of the gearbox losses. However, because the calculations still result in relatively broad estimates and because the results are compared to each other the influence of this error is only minor.

The engines inside one PGS are always identical, both in terms of Maximum Continuous Rating (MCR), rotational speed and in their dimensions (E.g. there can be two 6-cylinder engines, but not one 6- and one 8-cylinder engine).

The combination of different engine types within one propulsive power generation system was already removed from the considered options in the previous paragraph.

Both of these assumptions do discard some possible power plant configurations. However, this is somewhat negated by the fact that it is still possible to have two propulsive power generations systems, which do not necessarily have the same engine type (or engine size) installed.

The overall EFD shows the two mechanical connections which do not dependent on the internal design of the propulsive power generation systems. The first connection is the gearbox encountered when following the propeller shaft inward; the shaft configuration gearbox. This gearbox is only used to (dis-) connect the propulsive power generation systems and it does not alter the rotational speed of the shaft.

The second connection is the reduction gearbox, which is present only when the engine type demands it, this gearbox does alter the rotation speed of the shaft.

As stated earlier in this paragraph it is possible for a PGS to contain more than one engine. In the case that there are more engines, the power provided by each engine is combined into one shaft by a 'combinatory gearbox'. The overall EFD of the power plant does not show such a combinatory gearbox, for the sake of legibility. Instead Figure 4 presents (an example of) the internal configuration of a multi-engine driven PGS.

For electrical engines, only one engine is applied per propulsive power generation system, so that the complexity of the PGS is as low as possible.

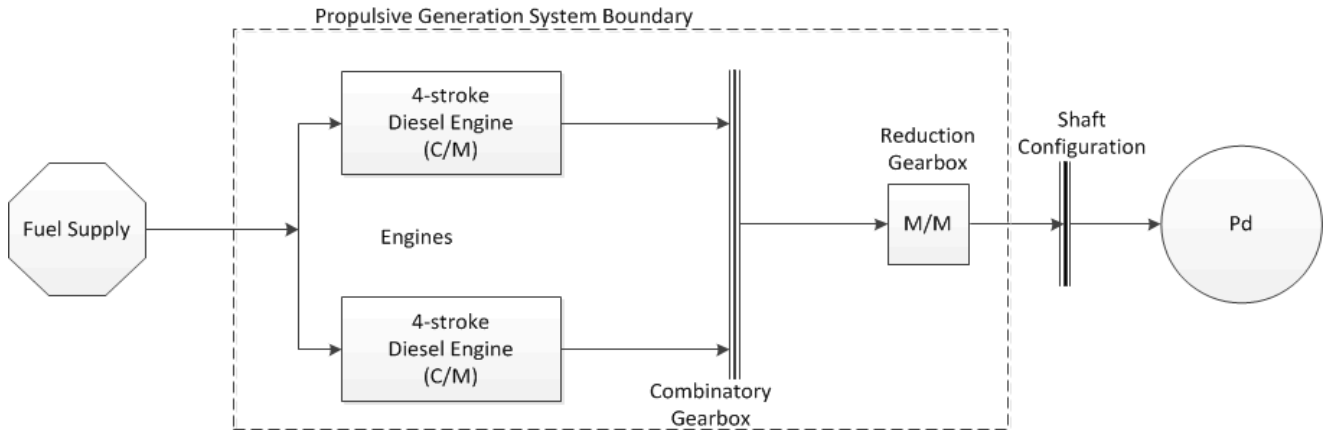


Figure 4: EFD of a possible Propulsion power Generation System

2.3.3. Electrical Grid

The second important set of decisions concern the lay-out of the electrical grid. The grid is assumed to be an Alternating Current (AC) grid at all times, since this is the most conventional type of grid used on board. There are also vessels which use a direct current (DC) grid, however this is mainly done in cases where either a very high or very low voltages are present. These somewhat specialized cases are not implemented during this research.

The choice to use an AC grid limits the amount of DC-AC conversions (which would be required, since most systems operate on AC). Limiting these conversions means that the losses that are associated with them are limited as well.

Inside the electrical grid transformers can be present, so that two electrical grids with different voltages can be connected. The overall EFD shows all transformers that can exist. The actual amount of transformers (and their location) is determined, for each configuration, by the algorithm which determines the electrical grid voltages.

2.3.4. Remark on the predefined topology

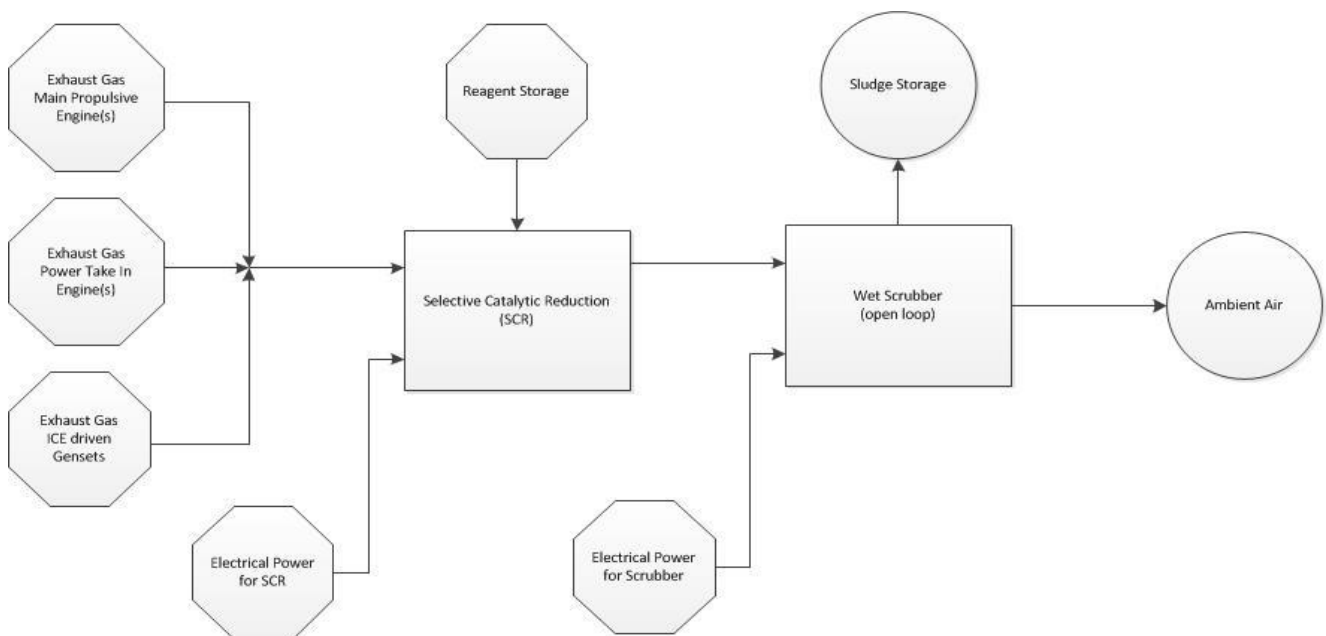
A final remark on the predefined topology concerns the exhaust gas treatment systems. These systems are only present in the EFD as electrical power consumers.

The flow of the exhaust gasses is not shown in the overall EFD, since these gases are not considered to be an energy flow (since waste heat systems are excluded from this research).

However, there is a fixed topology for the exhaust gas treatment systems (as can be seen from a schematics presented by Wärtsilä [12, p. 2]) .

This topology is caused by the fact that SCR system have an operating temperature range of 200 to approximately 430 degree Celsius [20], which is well above the operational temperature of a wet scrubber (since the water used by a scrubbers also lowers the exhaust gas temperature).

Therefore the exhaust gas will, starting at the engine, first encounter the SCR system (when applied) and then the scrubbing system (if this is applied), this topology is shown below. In the figure shown below, the storage of the sludge produced by the scrubber and the reagent storage are seen.



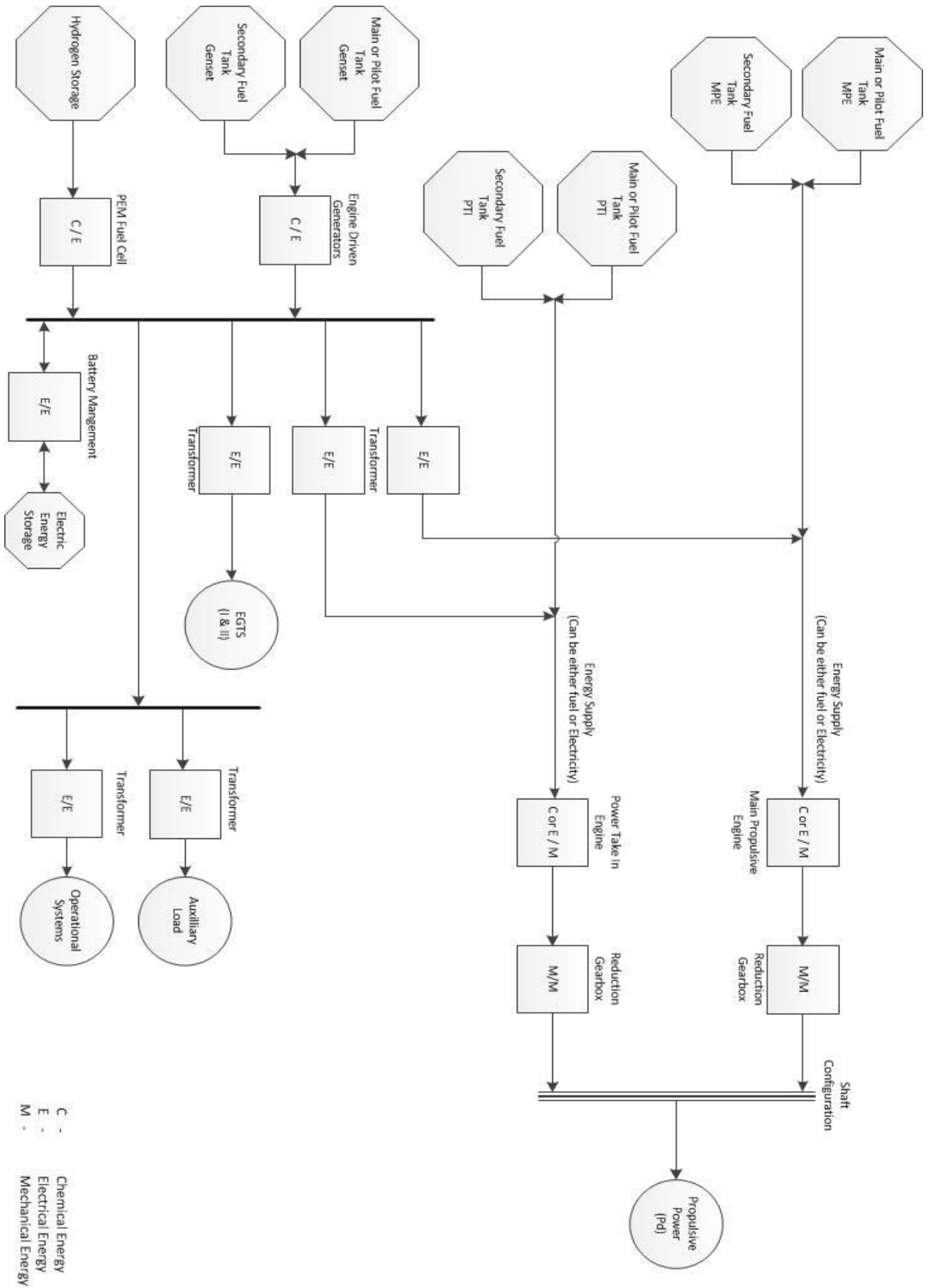


Figure 5: Energy Flow Diagram with all possible connections

3. Creation of the Concept Library

In this chapter the creation of the library of feasible concepts is discussed. The creation of this library is an automated process in order to ensure that every possible concept configuration is considered. The first step is the enumeration of every possible combination of the options discussed in the scope, this process is discussed in paragraph 3.1. Following the complete enumeration a set of constraints is used to reduce the size of the design space and to ensure that only feasible concepts remain. These constraints and their effects are discussed in paragraph 3.2.

3.1. Generation of all Concepts

The first step in the process is the 'creation' of every possible power plant configuration concept. As discussed in chapter 2, such a concept configuration consist of a predetermined topology (which was presented using an EFD) and a set of nodes.

It was also discussed that the systems present in each node are defined using only the type of system present in that node. The detailed information required for a performance simulation is then determined by separate algorithms (see also paragraph 2.1). During the discussion of the scope and the EFD, a total of 14 individual nodes were (implicitly) defined, these nodes are also presented in Figure 6. The numbers in this figure correspond with the first column of Table 3, which also summarized the defined nodes.

The systems summarized in Table 2 (found at the end of paragraph 2.2) can then be combined with the defined topology to determine the number of possible systems per node, which is included in the third column of Table 3.

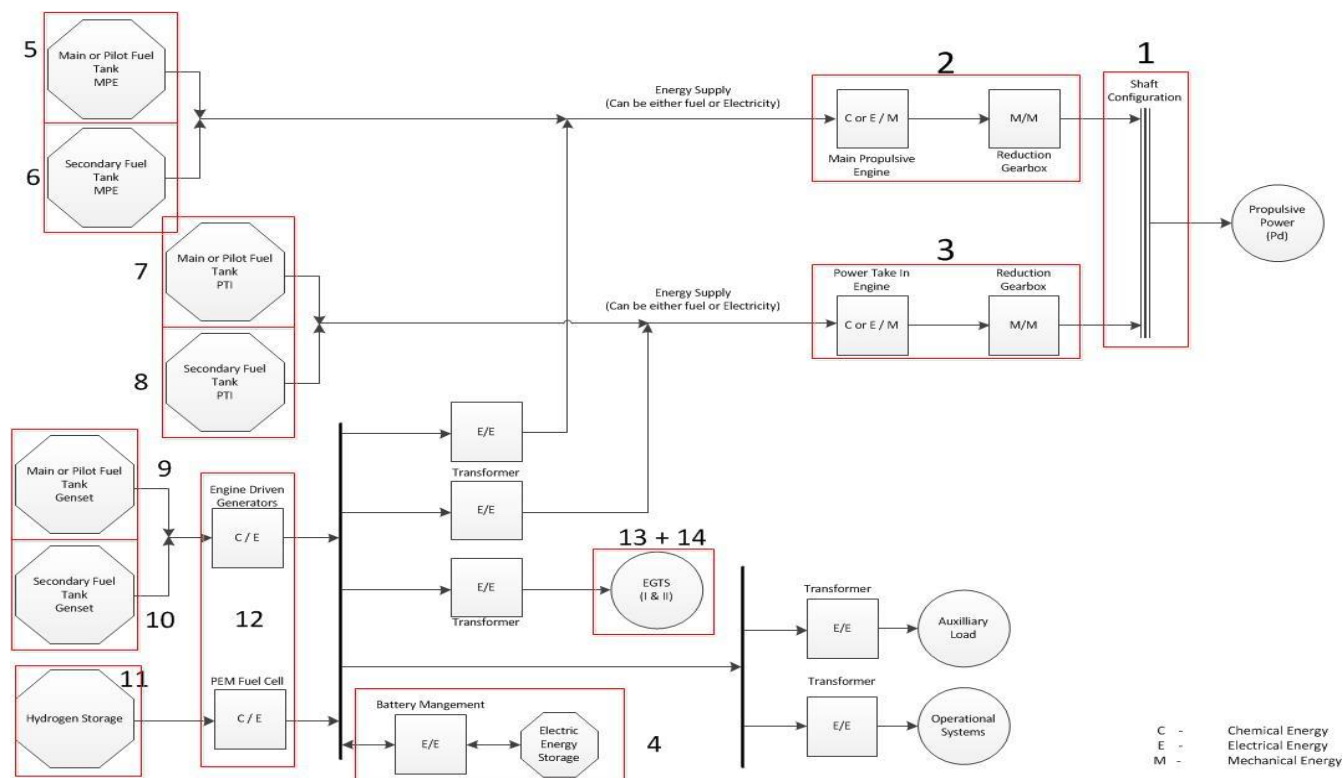


Figure 6: Defined Nodes and their numbering

Table 3: Summary of every node and the number of options per node

Node number	Node Name	Number of Options
1	Shaft Configuration	2
2	Main Propulsive Engine(s) (MPE) (Engine + Reduction Gearbox)	8
3	Power Take in (Engine(s)) (PTI) (Engine + Reduction Gearbox)	9
4	Electrical Energy Storage System	3
5	Main (or Pilot) Fuel Tank - MPE	3
6	Dual Fuel Tank - MPE	4
7	Main (or Pilot) Fuel Tank - PTI	3
8	Dual Fuel Tank - PTI	4
9	Main (or Pilot) Fuel Tank Gensets	3
10	Dual Fuel Tank Gensets	4
11	Hydrogen Storage	2
12	Electricity Generation System	6
13	Exhaust gas Treatment System (SOx)	2
14	Exhaust gas Treatment System (NOx)	2

Because the topology is not varied, a power plant configuration can be completely described by defining the systems inside that configuration. During this research this description (see also equation (3.1) for a generalized example) is from now on referred to as a (concept) ‘blueprint’.

$$\text{Blueprint} = [N_1 \ N_2 \ N_3 \ N_4 \ N_5 \ N_6 \ N_7 \ N_8 \ N_9 \ N_{10} \ N_{11} \ N_{12} \ N_{13} \ N_{14}] \quad (3.1)$$

Given this description of a power plant configuration the maximum number of possible concepts is equal to the maximum amount of combinations that can be made with the considered systems. The maximum number of combination can be determined using equation (3.2).

$$\#_{\text{concepts}} = \prod_{N=1}^{14} \#_{\text{options_node_N}} \approx 35,8 * 10^6 \quad (3.2)$$

With the previously discussed systems a total of 35.831.808 (35,8 mln) possible combinations can be created. Which is significantly less than the number of possibilities that could be created using other methods (as discussed by [5] or [6]), but also significantly larger than the number of considered power plants discussed by [3] or [4]. Therefore the goal of finding a median between a few and far too many (as discussed in paragraph 1.2) seems to have been achieved.

However, the design and simulation of each of these power plant concepts would still require a large amount of time. Spending this large amount of time is not feasible for this research, since quick results are preferred (as discussed in paragraph 1.3). Therefore the total number of power plant concepts has to be reduced.

3.2. Reducing the number of Concepts

This paragraph discusses the required reduction of the number of possible power plant configurations. This reduction is achieved using several constraints. These constraints and their effect are described in this paragraph.

The first constraint that is applied to the library is the fact that the vessel has to (be able to) comply with the emissions regulations that are applicable in the selected emission control area. This constraint causes the application of the exhaust gas treatment systems to become determined by the selected emission control area, instead of being specified by the concept 'blueprint'.

This constraint eliminates power plant configurations which are not able to meet the emission regulation. Additionally configurations which include these treatment systems while they are not required are also removed. The latter of these configurations are feasible, but will never be used in practice due to an unnecessary increase in initial investments (and system dimensions) and therefore their elimination is accepted.

The complete set of power plant configuration also includes configurations which are infeasible and these should also be eliminated prior to the design and simulation stage.

This research considers a configuration to be feasible when it can execute the required mission (generating electrical and propulsive power (see paragraph 2.2.1)), without excess systems.

This definition of feasibility can be translated into several constraints and these are discussed in the remainder of this paragraph.

When starting at the first node, the shaft configuration, the first constraints are also encountered, and are defined as follows:

- A form of propulsive power generation has to be presented in all concepts (although this was already enforced by the fact that 'not present' is not considered as an option for the MPE).
- A single shaft configuration should not have a PTI engine (type).
- A PTI shaft configuration should have both a Main Propulsive Engine type and a PTI engine type.

The next nodes encountered are those which define the engine types inside each of the propulsive power generation systems. These nodes come with a set of constraints, all of which are related to the fuel supply lines. Since for a combustion engine to operate it has to be supplied with the appropriate fuel type. Additionally concepts which have unnecessary fuel tanks should also be discarded. These constraints can be summarized as follows:

- Diesel engines require either HFO or MDO to be present.
- For diesel engines the secondary fuel tanks have to be empty.
- Dual fuel engines require either HFO or MDO as a pilot fuel.
- Dual fuel engines require a main fuel (LNG, CNG or Ammonia).
- Electrical Machines require no fuel, and thus both fuel tanks should be empty.
- For cases where no engine is present, there should also not be any fuel.

The next set of nodes encounters are the systems used to supply electric power to the different users; the electricity generation and storage systems. These systems also come with several constraints, which are summarized below.

- A form of electrical power supply has to be presented in all concepts. This means that there has to be either a generation system or a storage system or a combination of both.
- When a fuel cell is present, there should also be a supply of pure hydrogen
- If a fuel cell is not present, there should also not be any hydrogen storage.
- For the engine driven generation systems the fuel type constraints posed to the diesel and dual fuel engines are applicable as well.

The presented constraints are implemented in the concept generation process and cause 99.93 % of the possible configurations to be eliminated, leaving a total of 26.818 power plant configurations. These are deemed feasible and are therefore included in the library of feasible concepts.

4. Input for the Tool

In this chapter the four parameters of the input are determined. All of these parameters have been discussed (but not determined) in the previous chapters and are summarized below.

- The mission of the vessel
 - The operational profile, defined as a quasi-static time trace of the required power(s).
 - The propeller power/RPM constant ('C₄').

- The preferences of the client
 - The Multi Criteria Analysis weight factors.
 - The Emission Control Area in which the vessel has to operate.

For this research three ship types are selected, for which the input is determined. These three ship types are (ocean going) bulk cargo vessels, harbor tugboats and Trailing Suction Hopper Dredgers (TSHD).

It is however important to be aware of the fact that the input of the tool is not determined when selecting a certain ship type. For this research these ship types are used as a superordinate parameter, to estimate the required input.

Ocean going bulk cargo vessels are selected because both the solution and their operational profile are known with high degree of certainty, and as such this ship type can be used to verify the working principles of the tool. The other two vessel types are included because there is more variation in their power plant designs and because their operational profile and client preferences are quite different from each other.

Paragraph 4.1 presents the operational profile for each ship type. Following this paragraph 4.2 will discuss the determination of the delivered power/RPM constant and present the obtained values for the different ship types. Finally the MCA weight factors and the emission control area are determined in paragraph 4.3.

4.1. Operational Profiles

The operational profile is defined using three, quasi-static, time traces. The first one specifies the required propulsive power. The second trace dictates the auxiliary (electrical) load, which includes, but is not limited to, lighting, control systems and HVAC.

The only systems excluded from this auxiliary power are the mission specific equipment of the vessel, such as (dredging) pumps, winches or cargo handling systems. The third time trace specifies the electrical power required by those systems.

4.1.1. Ocean-going (bulk) Cargo Vessels

Ocean going bulk cargo vessels are built in an extensive range of vessel sizes and a more detailed definition is required to have some accuracy in the determined input. During this research a ship series dubbed 'Handymax' is used. This class of bulk cargo vessels is a fair average between the different sizes and plenty of data is available for these vessels. For these vessels the operational stages presented in Table 4 can be recognized.

The speed profile during departure and while sailing in coastal waters are determined using ‘Marine Traffic’ [21] and “Propulsion Trends in Bulk Carriers” [22]. It is assumed that the duration and vessel speed are identical for arrival and departure and the two coastal water transits.

The duration of the transit phase was determined using the average distance of a trip from Rotterdam to North America, while sailing at the specified transit speed.

The determined ship speeds are then converted to a required propulsive power by establishing a relationship between the propulsive power and the vessel’s speed, using data from “Propulsion Trends in Bulk Carriers” [22].

The loading and discharging together have a duration of 120 hours [23]. This same source indicates that on average unloading takes approximately twice as long as loading does. Which means that both the loading and unloading durations are known.

The auxiliary and operational power are derived from reference material [8, p. 90]. All this data can be combined to form the plot shown by Figure 7.

Table 4: Operational Modes Cargo Vessel

Stage	Speed [kts]	Duration [hours]	$P_{propulsive}$ [kW]	$P_{auxiliary}$ [kW]	$P_{operational}$ [kW]
Loading	0	40	0	100	500
Departure	3	1	85	375	0
Coastal Waters	6	1	680	375	0
Transit	14.5	248	9597	375	0
Coastal Waters	6	1	680	375	0
Arrival	3	1	85	375	0
Unloading	0	80	0	100	500

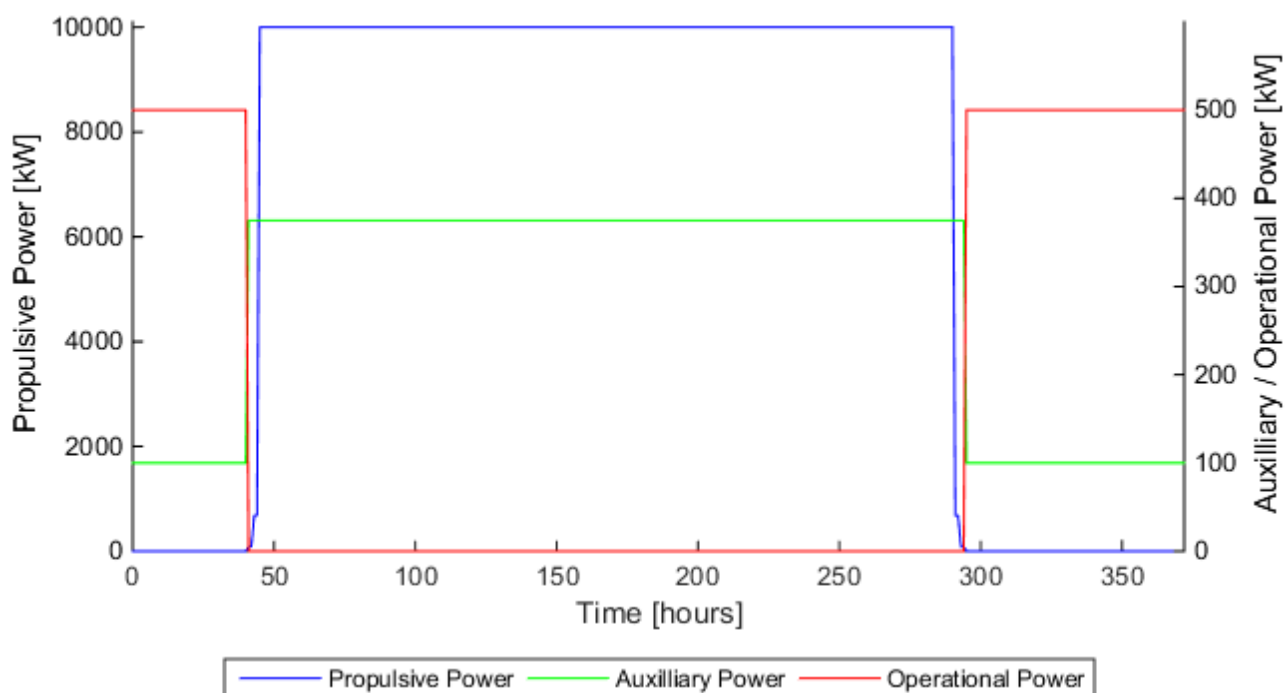


Figure 7: Operational Profile Cargo Vessel

4.1.2. Harbor Tugs

For harbor tugs the operational stages presented by Table 5 are recognized. The vessel speeds found for the different operational stages are commonly seen values [24] & [25]. Because the harbor tug has operating conditions which are very different from each other, the use of a power/ship speed curve would not result in accurate propulsive power estimates. Instead these powers are estimated based on research which focused on the operational profile of a harbor tug [26].

Especially for the ‘loitering’ and ‘hooking on/off’ stages, a power-speed relationship does not suffice, since there is a power requirement, although the ship speed is zero. This power requirement is due to the fact that the captain has to keep the tug in position and maneuver the tug in such a way that the hook on/off procedure can be executed as safe and quickly as possible.

The assumption is made that during hook on/off this power is slightly increased with respect to the loitering, due to the proximity to another ship and the forces caused by the towing lines. The duration of each stage is derived from previous analysis of the operational cycle of a harbor tug [27].

The auxiliary power requirements are based on data obtained from “Offshore Ship Designers” [24]. All the discussed operational stages results in the operational profile shown in Figure 8.

Table 5: Operational Modes Harbor Tug

Stage	Speed [kts]	Duration [minutes]	$P_{\text{propulsive}}$ [kW]	$P_{\text{auxiliary}}$ [kW]	$P_{\text{operational}}$ [kW]
Transit	12	5	1000	50	0
Loitering	0	5	450	50	0
Hook on	0	10	500	50	250
Vessel Assistance	2	15	2000	50	50
Hook Off	0	10	500	50	150
Transit back	12	1	800	50	0
Stand-By	0	20	0	50	0

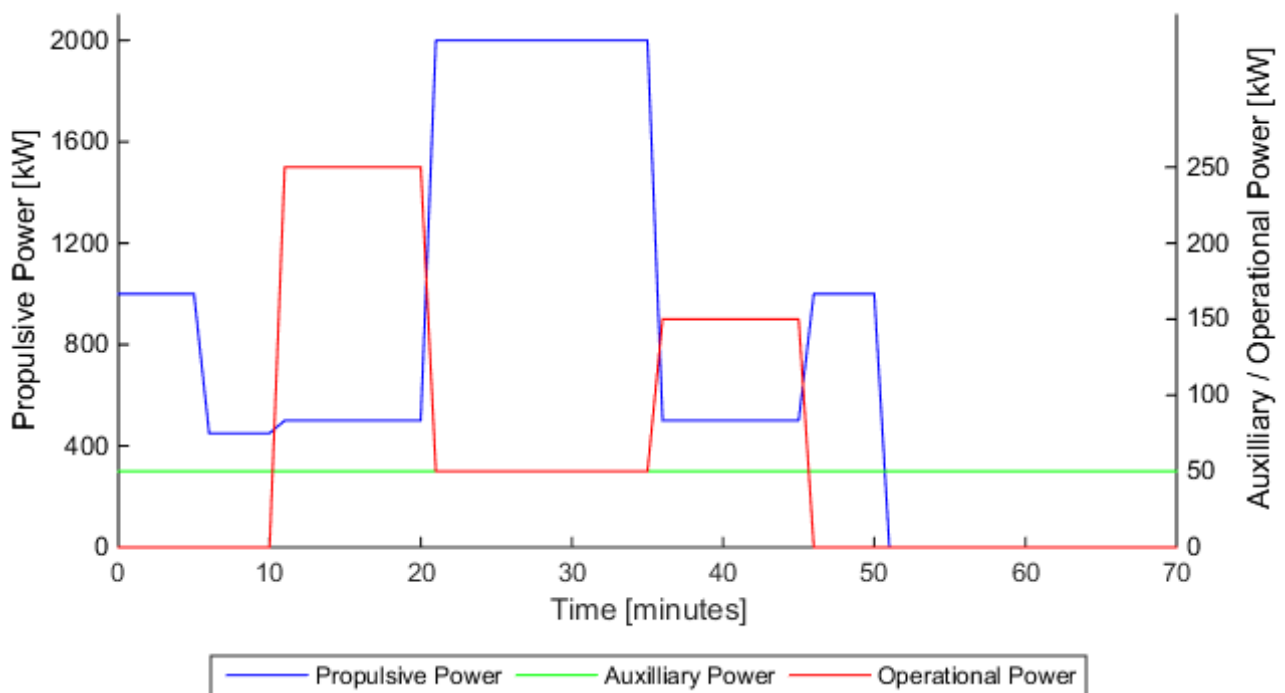


Figure 8: Partial Operational Profile Harbor Tug

The presented operation profile is a typical mission a harbor tug would execute. However, it is not feasible for a harbor tug to refuel/recharge after a single mission. It is assumed that the tug is operational for 8 hours per shift and continuously completing the mission as it is defined previously. As a result a harbor tug would have to be able to execute 7 missions per shift. The assumption is made that there is enough time between shifts to refuel the tug. Therefore the tug has to be able to execute 7 consecutive missions, without interruptions. Which results in the complete operational profile shown by Figure 9.

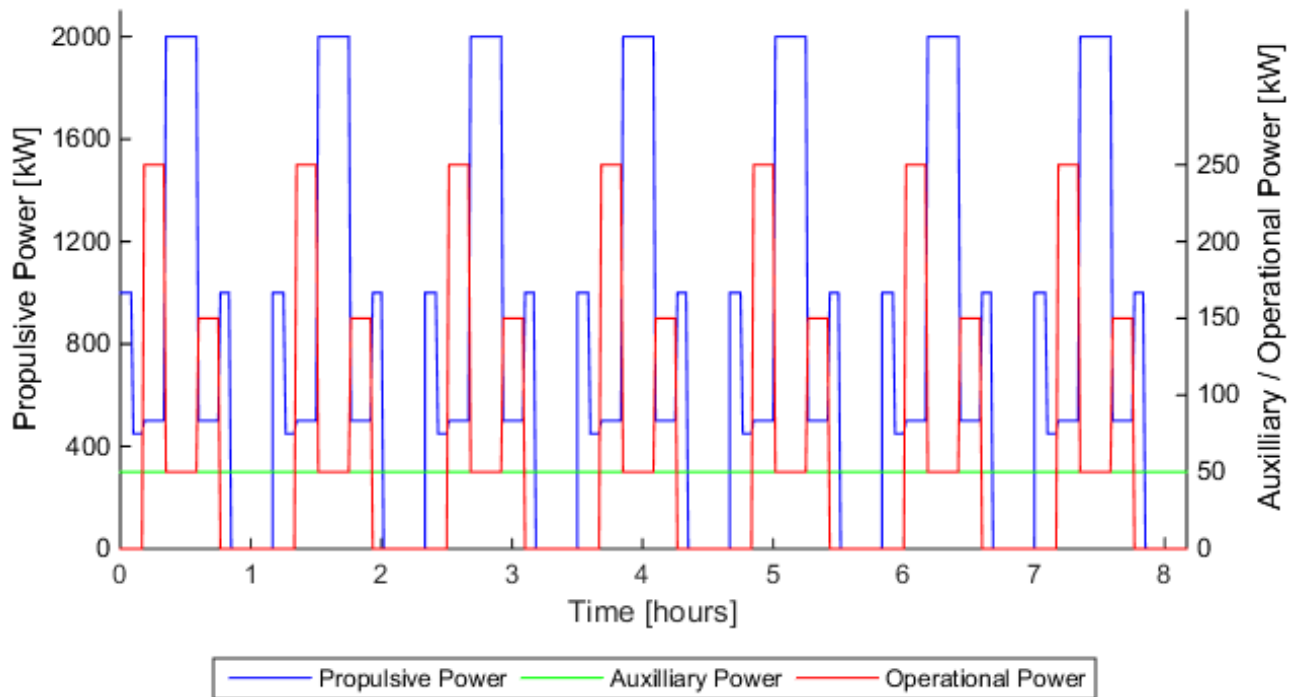


Figure 9: Complete operational Profile Harbor Tug

4.1.3. Trailing Suction Hopper Dredgers

For trailing suction hopper dredgers the stages presented by Table 6 are recognized. The operational modes are derived from a video developed by Boskalis [28] and personal communications with 'Van Oord' [29]. The ship speeds for each of the stages has been estimated using reference vessels, such as the "Gateway" [30].

The speed during transit is assumed to be slightly lower because the vessel is fully loaded. The duration of the loading has been estimated based on an analysis of the dredging cycle [31].

The transit durations are somewhat arbitrary, since they are dependent on the initial location of the vessel and its destination. It is assumed there will always be a suitable port within 24 hours, since these vessels mainly operate in coastal waters. The propulsive power at each stage is determined based on reference vessels and the personal communication with an engineer of 'van Oord Marine Contractors' [29].

During the discharging stage the vessel is kept stationary using its Dynamic Positioning (DP) system. The DP system is considered to be consisting of two components, the trust generators (propellers and a bow thruster) and the DP control system.

The trust generators are all assumed to be powered by the main engines. This does imply that the bow thruster is powered by the same engine as the main propellers. In reality this is not the case, since bow thrusters normally have their own engines. This is however not included as option and neglecting the power of a bow thruster would be more significant error than altering the source of that required power.

The power demand from a DP system is highly variable [32]. Due to the quasi-static nature used to describe the operational profile, this cannot be accounted for and instead an average (constant) value is assumed. The DP control system is assumed to be part of the auxiliary load and therefore the auxiliary load is increased slightly during DP mode.

The other auxiliary loads are again based on reference ships [8, p. 90]. For this research it is assumed that the dredging pumps are electrically driven, which is sometimes done, although pumps driven by the main engines (PTO driven pumps) or by separate diesel engines are also encountered in practice [29]. The latter concepts are however not included in this research. All these considerations combined result in the operational profile shown by Figure 10.

Table 6: Operational Modes TSH Dredgers

Stage	Speed [kts]	Duration [hours]	$P_{\text{propulsive}}$ [kW]	$P_{\text{auxiliary}}$ [kW]	$P_{\text{operational}}$ [kW]
Transit	14	24	9000	1000	0
Dredging	2	3	6000	1500	10000
Loaded Transit	12	3	7200	1000	0
Discharging (Rainbow)	0	5	900	1650	9000
Transit back	14	25	9000	1000	0

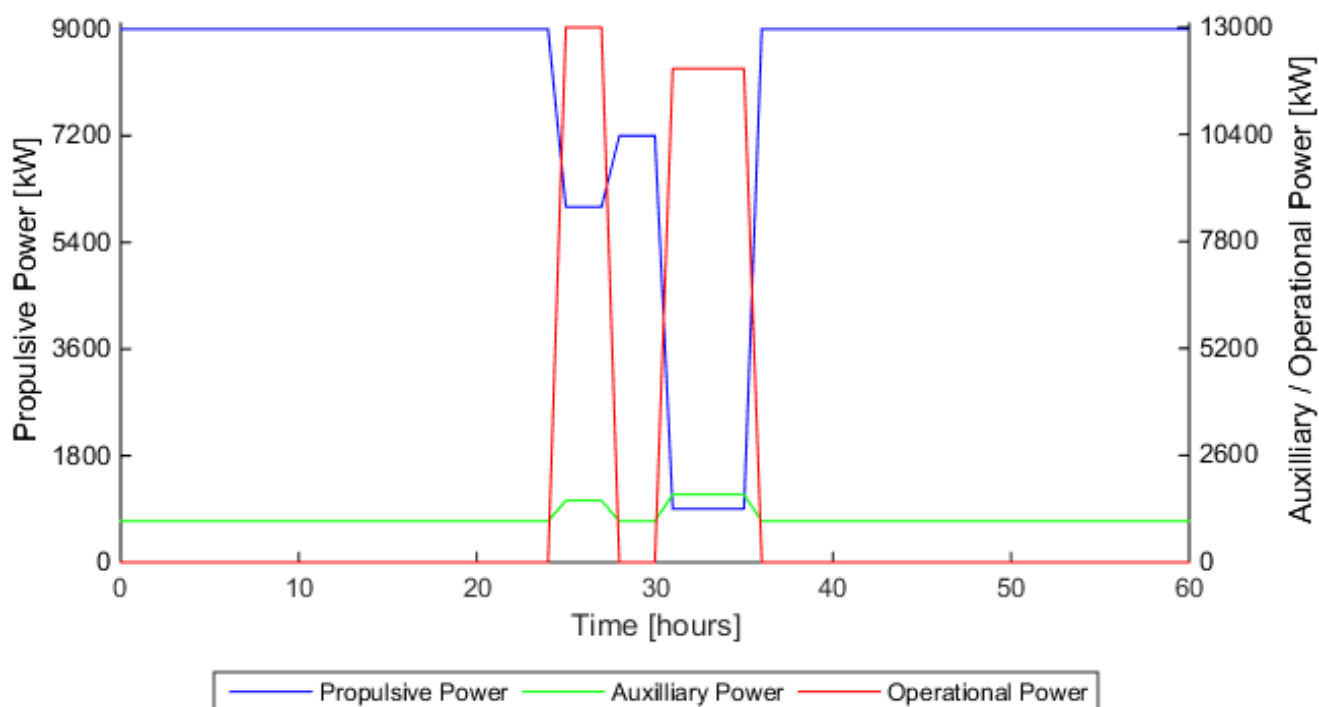


Figure 10: Operational Profile TSH Dredgers

4.2. Propulsive power - RPM Relationship

Another component of the input is the relationship between the delivered propulsive power (P_D) and the propeller RPM. This relationship is presented by equation (4.1). This equation shows a third power relationship between the delivered power and the rotational speed of the propeller, which is scaled using the factor 'C₄'.

$$P_{prop} = C_4 * N_p^3 \quad (4.1)$$

This relationship is valid at all times, because the value of 'C₄' is a function of ship speed and the design of both the propeller and the ship itself. However, this function is quite complex, and more difficult, if not impossible, to accurately determine in an early design stage.

However, if the propeller law is assumed, then 'C₄' becomes a constant value, which only depends on the ship and propeller design [8, pp. 422-423]. This makes it possible to use reference vessels to estimate a value for 'C₄'. When this approach is used, it is paramount that the vessels used to determine the value of C₄ are similar in their main dimensions and propeller design as the vessel for which the power plant is being designed.

This approach is used, and the constant 'C₄' is determined by finding the value for which the power/RPM relationship (shown by equation (4.1)) best matches the data obtained from the reference vessels. The values found using this approach are presented in Table 7. The data obtained from the reference vessels and the resulting power to RPM relationships are included in Appendix B.

Table 7: Propeller law constant 'C₄' for all cases

Ship Type	Value of C ₄
	[kW/RPM ³]
Cargo Vessels	0,0041
Harbor Tugs	2.81 * 10 ⁻⁴
TSH Dredgers	0,0006

Once again it has to be stressed that this approach is only feasible when similar reference ships are used. This can be observed by examining the used reference data. For the bulk cargo vessels, which are all 'Handymax' Cargo Vessels, a good fit could be found. The same holds for the harbor tugs, although there is some deviation present. Which is most likely due to the fact that there is some variation in the power plant configurations and propeller designs.

However, for trailing suction hopper dredgers the used approach is definitely lacking. This can be deduced from the large spread in the obtained data, and the fact the plotted curve has a relatively large error with the provided data points (see Appendix B).

This spread is likely caused by the fact that obtaining accurate data for these vessels has proven to be a challenge, and the data which was available shows a larger spread in vessel sizes than is preferred.

Additionally there are several different power plant configurations currently applied in vessels, and often these configurations contain a Controllable Pitch Propeller (CPP) [29], which renders the propeller law inapplicable.

Because CPP's were excluded from this research (see also chapter 2) and because some sort of power/RPM relationship is needed nonetheless, the found value for 'C₄' is used. This does however cause uncertainty during the design process and the final results. Given the observable deviations from the third power curve, it is however recommended to add CPP's to the considered systems during future research.

4.3. Multi Criteria Analysis Weight factors and Emission Control Area

In this paragraph the multi criteria analysis weights and the emission control area are specified for each of the three considered ship types. The values for each of the client preferences are determined by examining possible priorities that the owner of a ship type could have. It has to be said that these MCA weight factors are very subjective and will therefore be subjected to a sensitivity analysis.

The emission control area is also considered to be a client preference and is therefore also determined in this paragraph, based on indications given by DNV-GL [33].

4.3.1. Ocean-going (bulk) Cargo Vessels

The owner of a bulk cargo vessel will have a preference for a low system volume and a low fuel consumption. Since these two greatly influence the profitability of a vessel. Weight is of a slightly lower importance, though still not entirely unimportant. Emissions are, as long as regulations are met, not important at all.

These vessels travel between ports, some of which some are total emission control areas, and as such an ocean going cargo vessel will have to comply with those emission regulations. The estimated weights and area indication are summarized in Table 8.

4.3.2. Harbor Tugs

The operator of a harbor tug (often this is a port authority) will consider emissions to be of great importance due to the city surrounding the port. Additionally they will not want to operate their tugs at too high costs, since this would decrease the competitiveness and profitability of the port. This is why fuel consumption is also deemed to be important. Weight is not a high priority although not neglectable. Volume is more important since large tugs will have issues with maneuverability.

For this research the harbor tug is assumed to operate in the port of Rotterdam, which currently is a SECA, but will become a total emission control area after 2021 [34], the latter condition is used. The estimated weights and area indication are summarized in Table 8.

4.3.3. Trailing Suction Hopper Dredgers

These vessels are commercially operated and therefore fuel consumption is deemed to be of high importance. However, since these vessels often load/unload close to shore both their emissions will still be somewhat important, since it might increase the chance of the owner being granted a job, if he can execute it using a cleaner ship than his competitors.

The weight and volume of the power plant are of a lower importance since maneuverability or size is not really limited. However, it does influence the cargo capacity of the dredger, and therefore is not completely negligible.

These dredgers operate all around the world, and a lot of areas are not yet subjected to emission control. Therefore these ships are assumed to be subjected to the global limits. The estimated weights and area indication are summarized in Table 8.

Table 8: MCA weight factors for all cases

Characteristic:	Cargo Vessels	Harbor Tugs	TSH Dredgers
Fuel Consumption	10	6	8
Emissions	0	8	6
Weight	5	3	5
Volume	7	5	5
Operating in:	ECA	ECA	Not in any kind of ECA

[This page has intentionally been left blank]

5. Design Algorithms

This chapter will discuss the most important design choices made during the design of a power plant configuration. These design choices include the design algorithms used to limit the size of the design space, as was discussed in paragraph 2.1.

To do so paragraph 5.1 will explain the general method used to decide upon a design choice and give a global overview of the complete design process of a power plant configuration.

Following this overview the Power Management Strategy (PMS) is described in paragraph 5.2. Then the design of the shaft configuration is described in paragraph 5.3. This is followed by the design of the propulsive power generation system(s), which is described in paragraph 5.4. The design of the electrical systems is then presented in paragraph 5.5 and a summary of the different fuel properties is presented in paragraph 5.6. Finally the method used to determine the emissions and the design methodology developed for the exhaust gas treatment systems are presented in paragraph 5.7.

5.1. System Design Selection and overall Design Process

In this paragraph the general method used to select the best possible system design is presented. Followed by a global overview of the complete design (and simulation) process.

5.1.1. Design Selection

There are several cases in the design process where an optimal design has to be selected from a set of possible design solutions. The selected design should be the best possible trade-off between the client's preferences. The method used for this selection is the same for every algorithm and is presented in this paragraph in a generalized form.

The start of each intermediate design algorithm is the creation of a set of feasible designs. For each of these designs an estimate of the performance and system dimensions is made.

Based on these estimates the designs are then assigned a score for each of the four characteristics. This score follows the logic that the lower the value of that characteristic, the higher the score. The maximum score is equal to the total number of design solutions and decreases with increments of 1.

The total rating ('R') of a design can be determined using equation (5.1), in which 'WF_N' represents the weight factor associated with characteristic 'N', these are the multi criteria weight factors determined in paragraph 4.3. The parameter 'S_N' indicates the score for characteristic 'N'.

$$R_{Design} = \sum WF_N * S_N \quad (5.1)$$

The algorithms then selects the design which has the highest rating, which is expected to be the best tradeoff between the client's preferences.

5.1.2. Overall Design Process

A global process flow diagram of the tool has been presented in paragraph 1.3 and this paragraph will present a more detailed overview of the design and simulation processes. This will be presented by discussing the general flow through the process and by presenting a single power plant configuration for which the entire design process is executed, this example is included in Appendix C.

This case includes (and/or repeats) some design algorithms that are discussed further along this chapter. The presented case can therefore best be used as a guide to better understand where the different design algorithms are located in the complete process.

The first step in the design process is the design and simulation of the different main propulsive engines and power take in engines. The performance simulation results in a fuel consumption, emissions and an additional electrical power demand (due to the exhaust gas treatment systems and/or PMSM). These additional power demands are added to the electrical power demands defined by the operational profile. This total electrical power demand is then used in the next step in the design process; the design of the electricity generation system.

The first step in the design process of the electrical systems is the division of the electrical power demand between the batteries and the generation system. This is done according to the power management strategy, which will be discussed in paragraph 5.2.

The power required from the electricity generation system is then used to design the engine driven generators, the PEM fuel cells or a combination of these two. The performance of the generation system is then simulated as well.

The final step in the power plant configuration design process is the design and application of the exhaust gas treatment systems.

After this stage the performance data (emissions and fuel consumption) is combined with the data obtained from the different design processes to form the input for the final multi criteria analysis.

The multi criteria analysis then ranks the different results, using the same methodology described earlier, and combines their rankings using the client preferences, which results in a single total score for each power plant configuration. The concept with the highest total score is then selected as the optimal concept.

5.2. Power Management Strategy

An important design choice, which is not left to an algorithm, is the Power Management Strategy (PMS). This strategy is not implemented into its own algorithm, but is implicitly present in other algorithms used throughout the design process. Therefore it is necessary to define the PMS before the intermediate design algorithms are discussed.

The main philosophy behind the power management strategy is that the consumption of fossil fuel is to be minimized. This is done because fossil fuels are both finite and a significant factor in the emission of greenhouse gases. Which means that minimizing their consumption is beneficial for the environment and also aids in creating a more 'future proof' ship design, even for owners that do not care about fuel consumption.

The following sub-paragraphs will describe the PMS for both the propulsive- and the electrical power supply systems (the latter of which can consist of storage and/or generation systems).

5.2.1. Propulsive power Generation Systems

For the propulsive power generation system (PGS) there are two main decisions that have to be made based on the power management strategy. The first decision is the division of the power demand over the main propulsive engine (MPE) and the power take in (PTI), and how to determine which systems delivers the required power at a certain moment in time.

The second decision is the number of engines which are operational at a given point in time, and how the load is divided over the running engines.

Load sharing between the propulsive engines

For this research a PTI systems functions as a booster of the delivered power provided by the MPE. To achieve this functionality the MPE is designed as such that it can deliver the second highest power demand. The power take in system will then be dimensioned so that it can deliver a power equal to the difference between the highest- and second highest power demand. This means that the highest power demand can only be met by both PGS systems together. The division of propulsive power is described using the Power Division Ratio (PDR) (see also paragraph 2.2.3 and equation (5.2)).

$$PDR_{shaft} = \frac{P_{MPE}}{P_{shaft}} = 1 - \frac{P_{PTI}}{P_{shaft}} \quad (5.2)$$

The PDR is not only used during to define the power required from each of the propulsive power generation systems, but also to divide the power demand over the two propulsion generation systems. To minimize the consumption of fuel, the engine loading has to be as close to the maximum continuous rating (MCR) as possible [8]. To achieve this, the loading of each PGS also has to be maximized as well.

During the design of the PGS an engine margin will be included and in addition to this engine margin, an operational margin of 10 % is also applied. This margin ensures that a PGS (when applied in practice) has some excess power available to cope with dynamically changing loads. To incorporate this operational margin a PGS is deemed capable of delivering power when the ratio $P_D(t)/P_N$ is smaller than or equal to 0.9. These design choices can be combined into a power management strategy. Which is presented in the form of a flow chart and presented in by Figure 11.

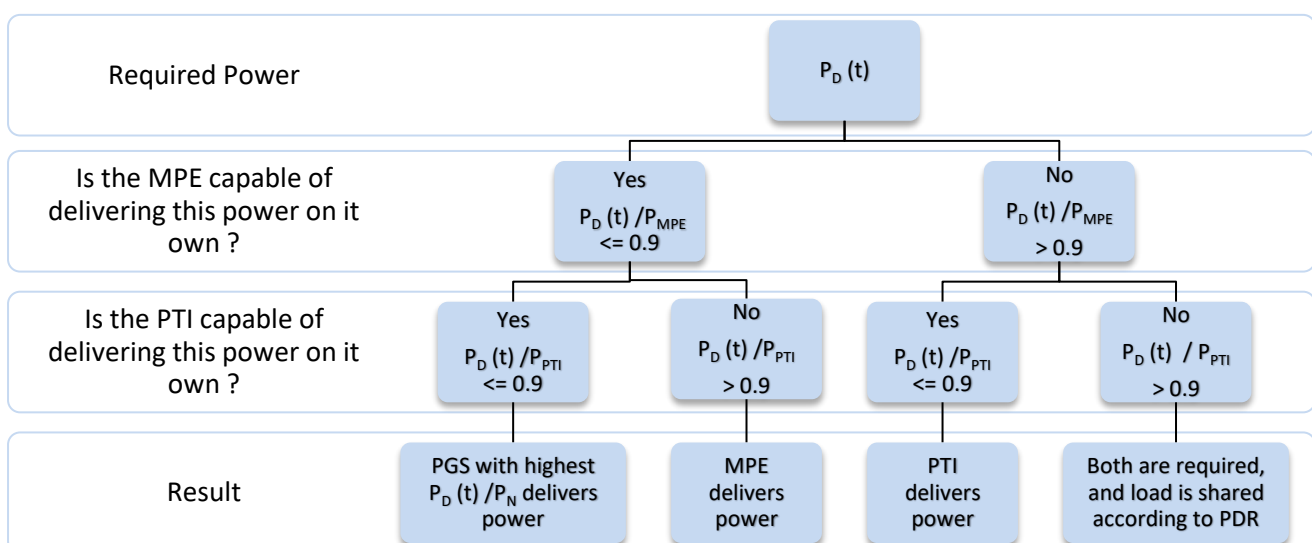


Figure 11: Propulsive power Generation Management flowchart

Engine Management

As stated in the previous paragraph, the load of each individual engine has to be maximized. This can be done by using the minimum amount of engines necessary to deliver the demanded power.

The demanded power is then evenly divided over the number of engines that are required to operate. This should result in the lowest possible specific fuel consumption, due to the non-linearity between the engine loading and the specific fuel consumption [35].

This strategy is once again shown as a flowchart, presented by Figure 12, which shows the PMS as it would be applied to a PGS containing three engines, as an example. Any other number of engines is also possible, but this example clearly illustrates the effect of PMS. For the electrical machines this strategy is not really applicable since a single engine is installed at all times (as discussed in paragraph 2.3).

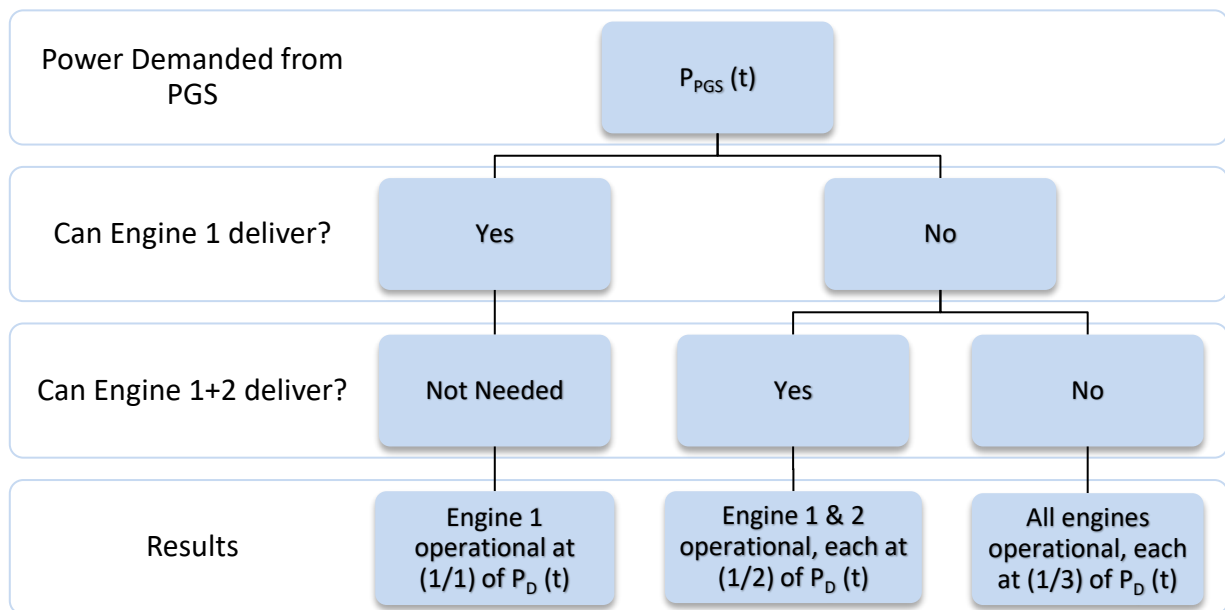


Figure 12: Engine Management flowchart (example for a PGS containing 3 engines)

5.2.2. Electrical Energy Supply

The supply of electric power can be done using three different systems, as summarized below.

- Only a generation systems delivers electric power
- Only a storage system delivers electric power
- A combination of both storage and generation systems to deliver the required electric power

For a storage system a very broad PMS is sufficient, since the demand of electrical power simply has to be met at all times.

However, the generation systems do require an additional PMS. For engine driven generators this strategy follows the same logic as applied to the PGS engines.

As such the minimal amount of generation systems required to meet the electric power demand are operational at any given time. And the power demand is again evenly distributed over the gensets. The flowchart for this part of the PMS is identical to the one defined for the engines and is therefore not repeated.

However, for fuel cell based generation systems this strategy is different, because the efficiency of fuel cells improves at part load conditions [4]. Although, fuel cells do not use fossil fuels it is beneficial to keep fuel consumption to a minimum. This can be achieved by maximizing the amount of fuel cells operational, therefore the demanded electrical power will always be shared over all installed fuel cells.

There is however also the possibility that both a fuel cell and an engine driven generation system are installed together. This combination of generation systems comes with two additional design choices made by the PMS. The first choice is the fraction of power each system delivers (this is defined as the Degree of Hydrogenization or 'DoH'). This design choice is not specified by the PMS, and instead a dedicated design algorithm will determine its value.

The second choice is the method used to determine which generation systems is delivering power at a given moment in time.

The developed power management strategy once again aims at the minimization of the consumption amount of (fossil) fuels. Which can be done by using the fuel cell whenever it can meet the power demand. Should the power demand exceed that of the fuel cell than the engine driven generator will deliver, without the fuel cell, so that the engine loading is maximized, once again improving the efficiency of the driving engine.

For cases where neither of the two systems can meet the power demand on their own, both systems will be operational. In those cases the generator set will be loaded until its MCR, so that once again the SFC of the genset is minimized and the fuel cell will deliver the remainder of the power, this also capitalizes on the fact that fuel cells have an increased efficiency in part load conditions. This strategy is also presented as a decision tree in Figure 13.

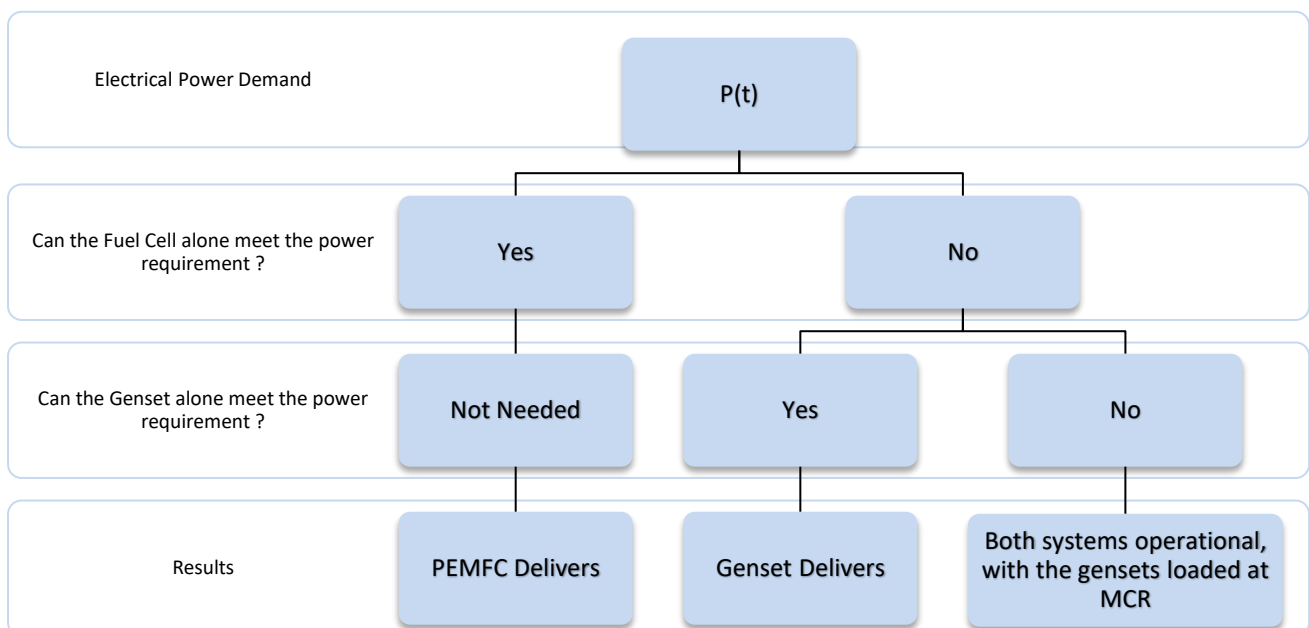


Figure 13: PMS of Hybrid Generation Systems

The final design choice concerning the management of the electrical power is the division of the electrical power demand between the storage and generation systems.

As discussed in paragraph 2.2.6, storage systems are used as an emission reduction measure. Such a reduction is always beneficial, but increasingly so near coastal regions, which are often busy places in terms of both ship traffic and number of people working and/or living in these areas. Therefore the energy storage system will be used to deliver the required electrical power during the operational stages at which the vessel is near a coastal region, so that the generation systems can be offline (and thus not consume fuel or produce exhaust gas).

However, as no geographical data is included in the operational profile it is not possible to indicate when a vessel is near a coastal region. This can be examined by examining the three operational profiles presented in chapter 4. From these profiles it can be observed that the propulsive power is lowest in coastal areas.

Therefore the energy storage systems will be used to deliver all required electrical power in the operational stages at which the propulsive power demand is minimal.

5.3. Shaft Configuration Gearbox Design

The shaft configuration gearbox divides the propulsive power demand between the two propulsive power generation systems. The required power is shared through a gearbox at the cost of a loss in transmitted power, which can be accounted for using equation (5.3) [8, p. 64]. This equation results in the total shaft power that has to be delivered to the shaft configuration gearbox. This shaft power is then shared between the two propulsive power generation systems, according to the PMS, which has been discussed in the previous paragraph.

$$P_{shaft} = \frac{P_D}{\eta_{shaft}} \quad (5.3)$$

The main unknown in equation (5.3) is the shaft efficiency, which is assumed to be 0.99 [%] [8] for concepts with a single propulsive power generation system, since the shaft configuration gearbox is non-existent, and therefore only shaft bearing losses have to be accounted for.

For the concepts which include a Power Take In, a more complex twin-input / single output (TISO) gearbox is required, these are relatively complex gearboxes, with relatively large power losses, with a value between 3 and 5 [%] of the power delivered to it [8, p. 167].

The efficiency obtained from the source does however include a reduction gearbox (which has between 1 and 2 [%] power loss, according to the same source), therefore a loss factor of 3 [%] is assumed for the shaft configuration gearbox.

The dimensions of this gearbox are determined using (a slightly adapted version of) the dimension prediction algorithm developed by Stapersma & de Vos [36], which is included in appendix D.

5.4. Propulsive power Generation System Design

This paragraph presents the algorithms used to design the different components found in the propulsive power generation systems. These components are shown in Figure 14, which shows the propulsive engines, the combinatory and reduction gearbox and the shaft configuration gearbox. The figure also shows the system boundaries of a propulsive power generation system.

During the design of a propulsive power generation system two components have to be designed. These are the driving engines together with the combinatory gearbox and the reduction gearbox. The design of both of these components is discussed in the following sub-paragraphs. This is done by first discussing the engine design procedure. Which is then used to design the reduction gearbox and with that the complete PGS.

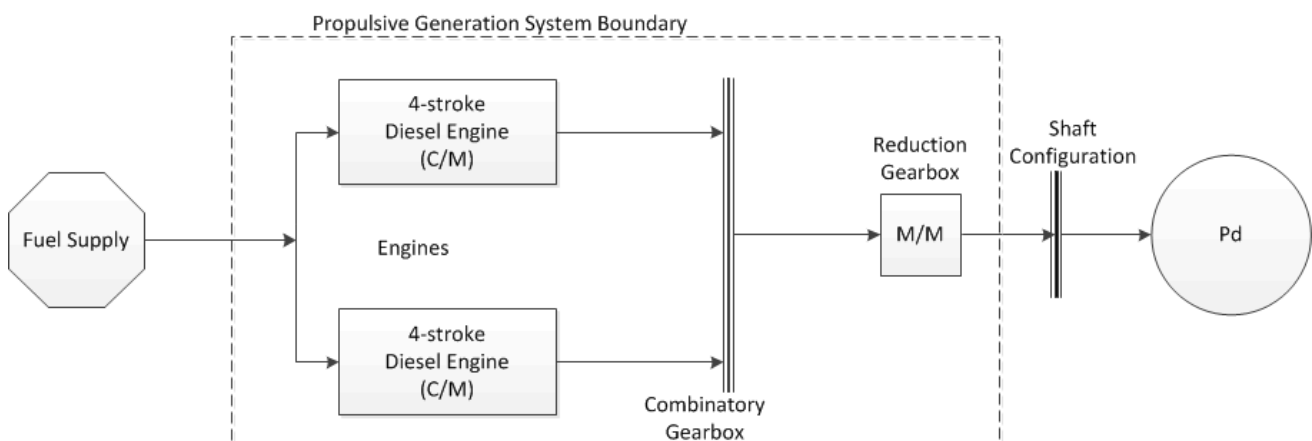


Figure 14: Components Propulsive power Generation System

5.4.1. Engine Design

In this paragraph the design processes developed for different engines inside a propulsive power generation system are discussed. Two main types of propulsive engines can be recognized; electrical machines and internal combustion engines (ICE). Both these systems require a different design approach and are discussed separately.

Electric Machines

For the propulsive power generation systems designed with electric motors a dedicated design algorithm is not required. Mainly because the total dimensions of two electric motors which both deliver half of the required power are identical in to those of a single electric motor which delivers all the required power. Additionally the (nominal) efficiency of these machines is not dependent on size.

For the determination of the dimensions of the electric machines the methodology presented by Stapersma & de Vos [36] is used. This method has already been implemented in an algorithm by Rietveld [3] and has been adjusted for the use on Permanent Magnet Synchronous Machines (PMSM) by ten Hacken [4]. This algorithm will not be discussed any further, and interested readers are referred to these reports instead.

A reference nominal efficiency for the PMSM is assumed to be 95%, based on the efficiency curve presented by ten Hacken [4].

Internal Combustion Engines

The installation of a single engine is not always possible for internal combustions engines. Therefore a dedicated algorithm is required to design the engines inside a propulsive power generation system. The entire design process is illustrated in Figure 15, which is located on the following page and the remainder of this paragraph discusses the developed method.

The engine design algorithm creates an engine design by first selecting a number cylinders per engine from a range of commonly found values. The algorithm then designs a concept PGS using engines with the selected number of cylinders. The detailed design process is presented in appendix E, in combination with all technological parameters required for this design process. The (optional) combinatory gearbox is discussed in appendix D (together with other gearbox designs).

This design process is repeated for every number of cylinders per engine included in the range.

The result of the design algorithm is an estimated fuel consumption, a total system mass and volume for each of the different engine designs.

From this set of concept PGS designs the optimal number of cylinders per engine is then selected using the method presented in paragraph 5.1.1.

During this selection process designs which have more than 4 separate engines are given such a ranking that these will only be selected if there is no other option available, since options with more than 4 engines are not used in practice.

During the execution of this algorithm the fuel type, engine speed and engine type are not varied and therefore the emissions are only related to efficiency of the engine(s). Therefore the fuel consumption is used to determine the ranking in terms of emissions as well.

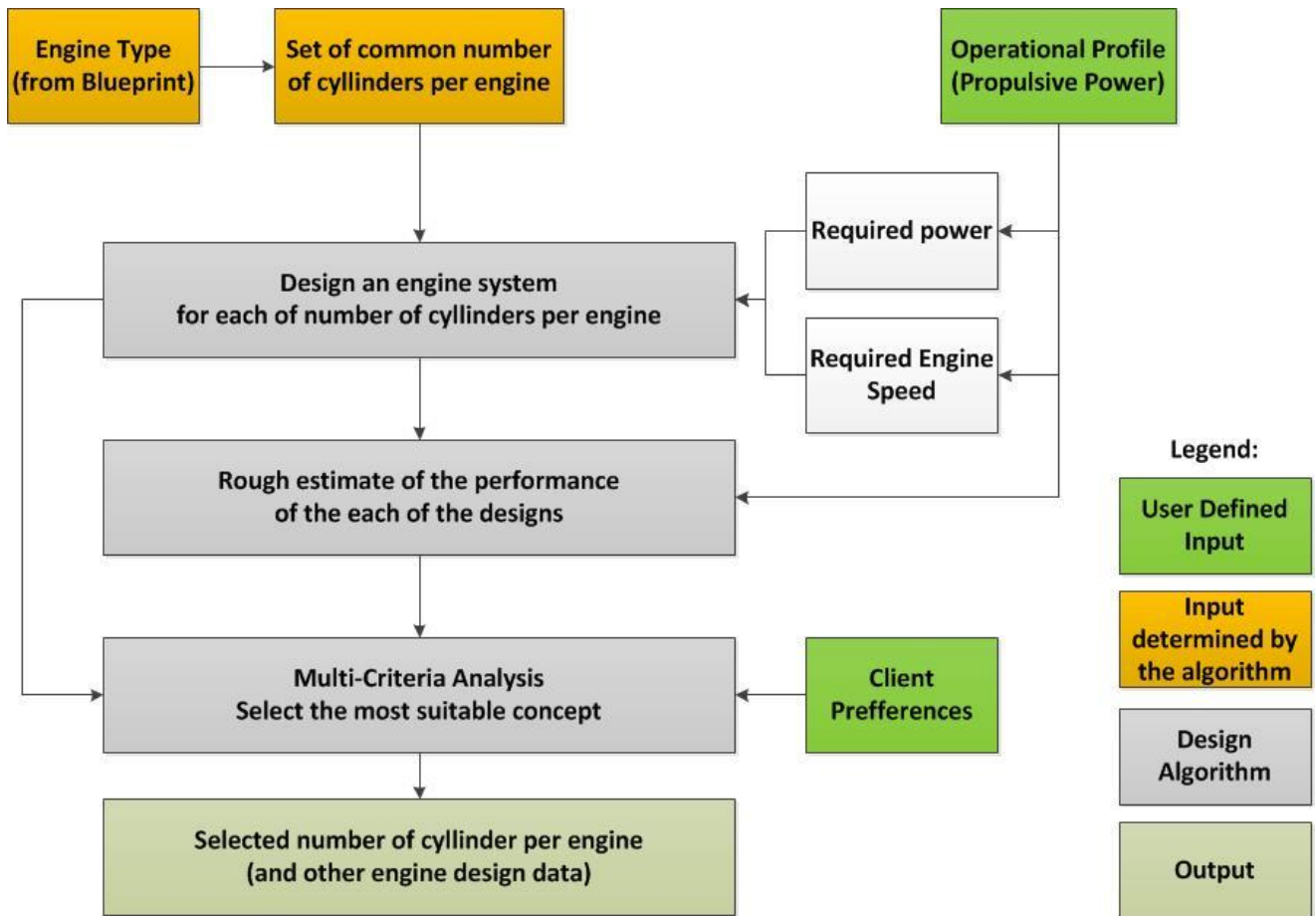


Figure 15: Process Flow Diagram Engine Design

Verification

Because the final dataset will be quite large, it is difficult to check whether the individual results are accurate enough. Therefore the untested design methodologies will each have to be verified individually.

The engine design is such an untested method, and therefore the working principles will have to be verified.

This verification is done by applying the developed algorithm to a case study and then comparing the generated results to reference engines found in different databases ([37], [38], [39], [40])

For the verification of the engine design algorithm a PGS is designed using 2-stroke engines which directly drive the propeller shaft, other input parameters are obtained from the cargo vessel case (presented in chapter 4), and these result in the design requirements presented in Table 9.

Table 9: Design requirements Case study Engine Design

Parameter	Value	Unit
Total Required Power	11.919	[kW]
Engine Speed	130	[RPM]
Preferences	[10 0 5 7]	[-]

The results of the design process are presented by Figure 16, Figure 17 and Figure 18 and the numerical results are presented in Table 10. In which the selected concept is made bold, while in the figures the intersection of the two lines mark the selected design.

Comparing the results to the engine databases mentioned earlier show that similar engines can be found in reference data and that the order of magnitude of the results is correct. As such the results of this algorithm are deemed accurate enough.

Table 10: Numerical Results of the MPE design for the example case

Number of Cylinders	Number of Engines	Average Fuel Cons.	Total Volume	Total Mass
[-]	[-]	[Ton/hour]	[m ³]	[Tonnes]
4	2	1.19	398.2	469.8
5	2	1.19	497.7	587.3
6	1	1.16	298.6	352.4
8	1	1.19	398.2	469.8
10	1	1.26	497.7	587.3
12	1	1.32	597.2	704.7
14	1	1.37	696.8	822.2

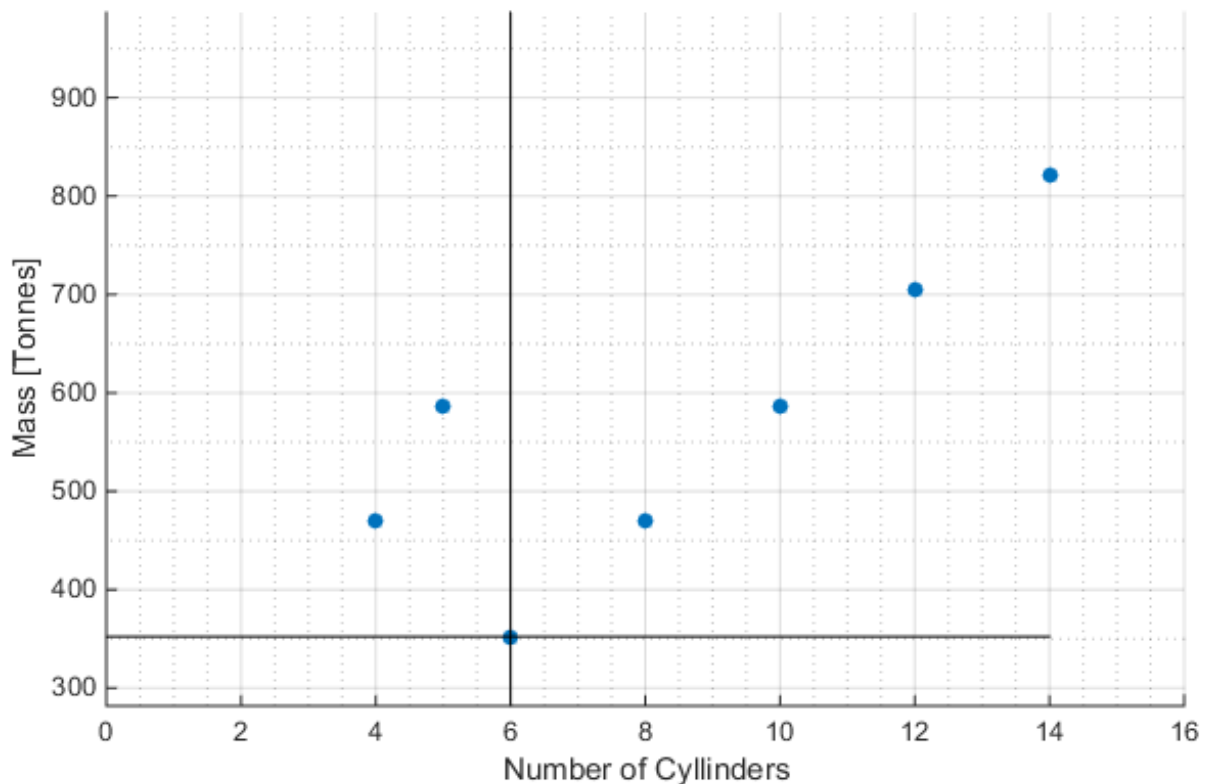


Figure 16: Total System mass per possible engine design

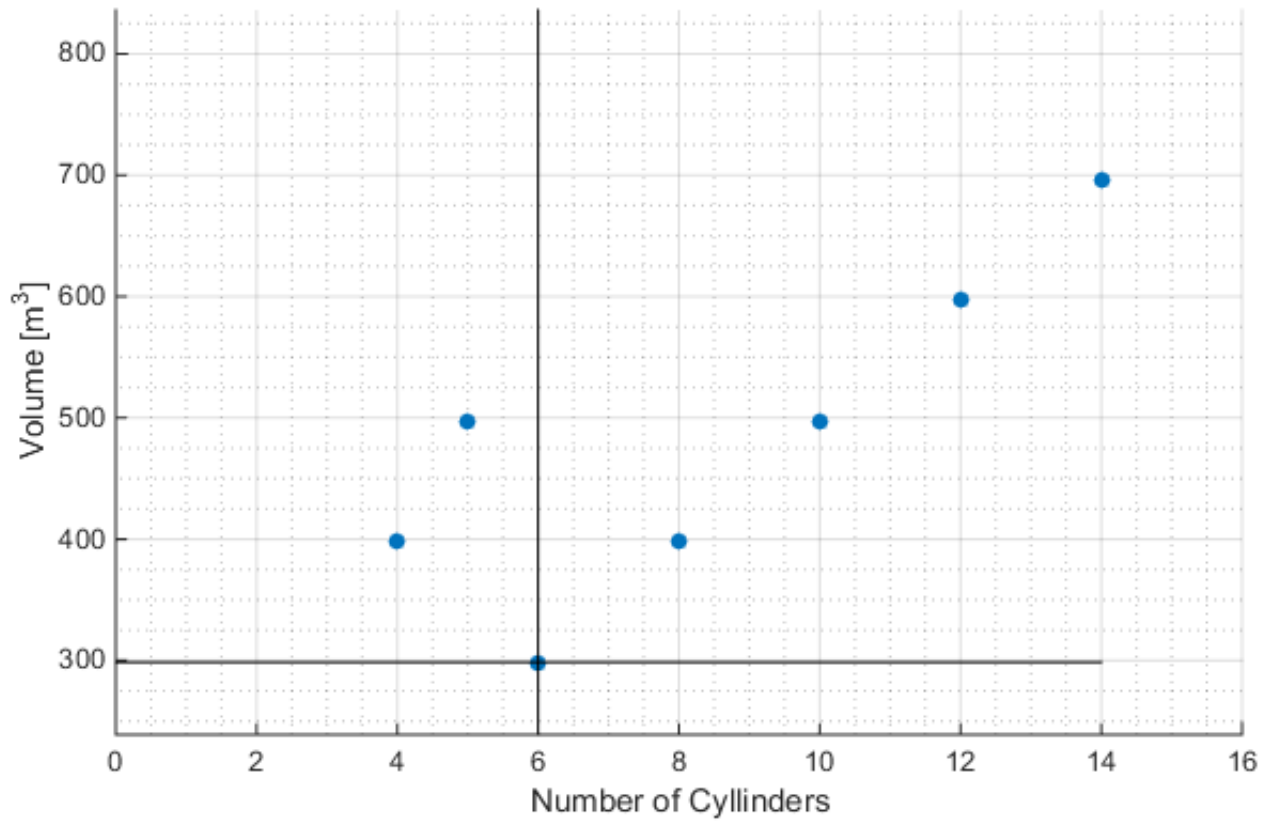


Figure 17: Total System Volume per possible engine design

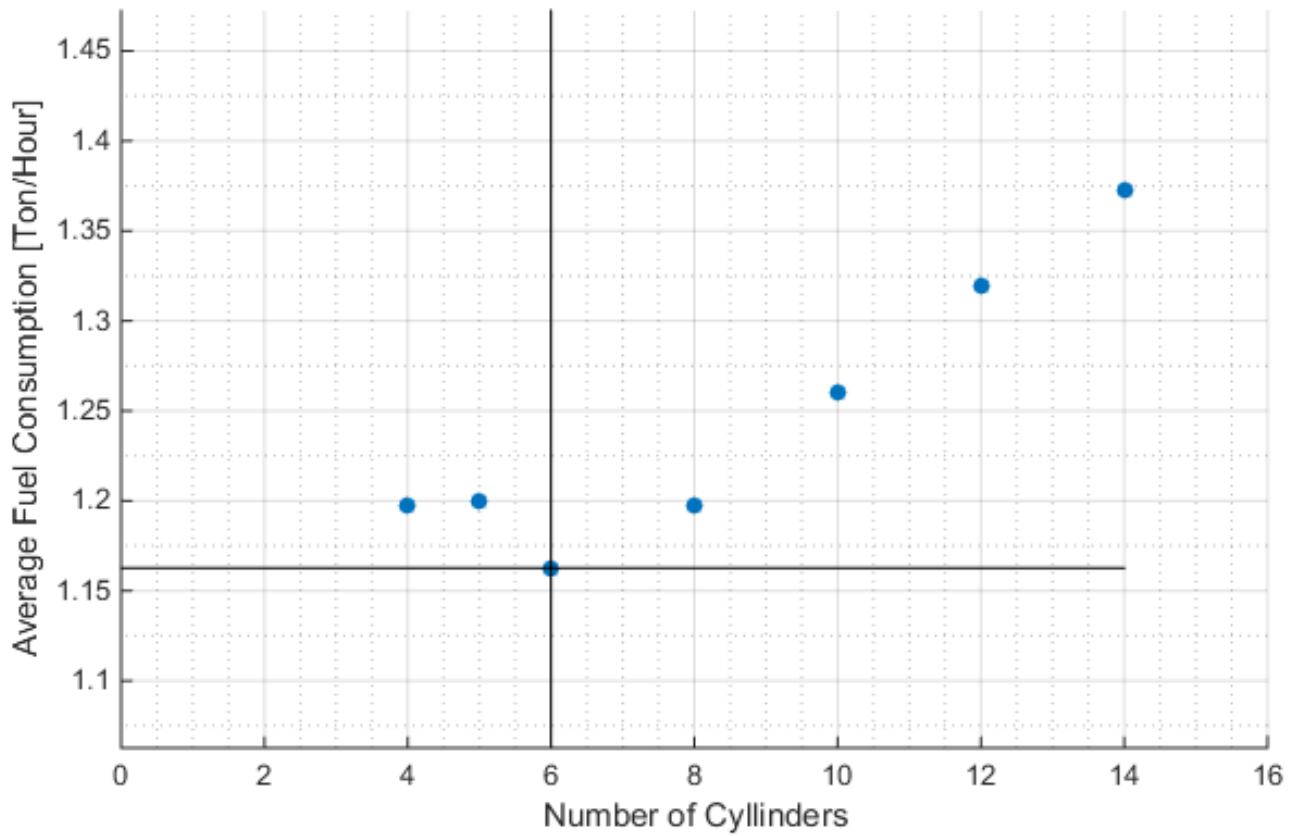


Figure 18: Average Fuel Consumption per possible engine design

5.4.2. Propulsive power Generation Systems Design

The other component inside a PGS that has to be designed is the reduction gearbox. The algorithm to determine the dimensions and performance of these gearboxes, given a required reduction ratio, is discussed in appendix D.

The gearbox design algorithm can then be combined with the engine design algorithm to form the PGS design algorithm, a schematic representation of which is presented by Figure 19 and the remainder of this paragraph discusses the algorithm in more detail.

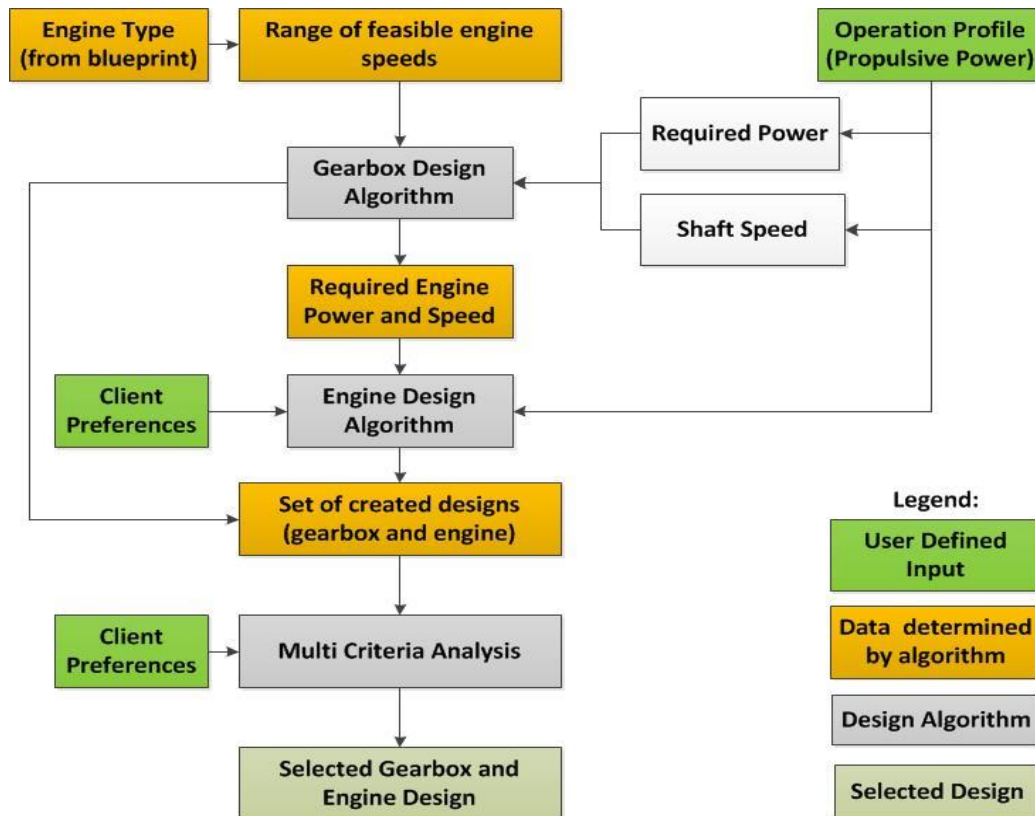


Figure 19: Process Flow Diagram, Propulsive power Generation System Design

The first step in the design algorithm is the determination of the range of allowable engine speeds. This range is engine type dependent and obtained from the databases presented by Stapersma [37] and verified/updated using the data provided by Rolls-Royce [38], MAN [39] and Wärtsilä [40].

The determined engine speed ranges are presented in Table 11. It is also possible for a concept to be created without a reduction gearbox (direct drive) in those cases this range is non-existent and the only allowable RPM is that of the propeller shaft.

For the permanent Magnet Synchronous Machine (PMSM) the range not based on a dataset because these machines can be constructed for almost any rotational speed. However, very high or low speed engines are somewhat unconventional (and therefore likely to be expensive). Instead the extreme limits of the combustion engines are used as range for the PMSM.

Table 11: Engine speed Ranges per engine type

Engine Type	Lower Limit	Upper Limit	Unit
2-stroke Diesel	60	250	[RPM]
4-stroke Diesel	400	2000	[RPM]
4-stroke Dual Fuel	400	1200	[RPM]
PMSM	60	2000	[RPM]

The PGS design algorithm selects an engine speed and designs a gearbox so that difference between the selected engine speed and the required shaft speed is bridged.

The results of the gearbox design are the dimensions and efficiency of reduction gearbox. With the efficiency of this gearbox known, the required power can be adjusted to determine the requirements for the engine. This adjustment includes an engine margin (EM), as seen in in equation (5.4).

This margin is applied to ensure that the engines do not run on their maximum possible load, which reduces the wear of the engine and improves the efficiency of the engine. [8, p. 417].

$$P_{required} = \frac{P_D}{\eta_{gearbox}} * (1 + EM) \quad (5.4)$$

A conventional value for the engine margin is 15% of the required engine power [8, p. 417]. However because the possibility exists that multiple engines are connected using a combinatory gearbox this margin is increased with another 3%, to account for the possible losses of such a gearbox, resulting in a total engine margin of 18%. Although the possibility still exists that only one engine is installed this engine will therefore have a slightly larger engine margin. However, an engine margin of 18% is not unheard of [8, p. 417] and this is therefore accepted.

This method of accounting for the possible losses of the combinatory gearbox is not ideal, but is the only practical way of doing so. Since the number of engines, which is a parameters of the engine design, is largely dependent on the required power, which is then again dependent on the efficiency of the combinatory gearbox, of which the application is determined by the number of engines and so on.

After the engine margin is applied, the required engine design algorithm (as discussed in 5.4.1) is executed, using the selected engine speed and the required total engine power. Then the results of the engine design process are saved, together with the results from the gearbox design.

The PGS design algorithm then selects a new engine speed, and the process repeats until the entire range of engine speeds has been processed. The results for each engine speed are then once again supplied to an intermediate MCA to determine the engine speed which is optimal, given the clients' preferences.

For the verification of the PGS design algorithm the cargo vessel case is again used. For this verification the algorithm is tasked with designing 4-stroke diesel engine, with a reduction gearbox. This case study has the design requirements summarized in Table 12.

Table 12: Design Requirements Case Study Gearbox Design

Parameter	Value	Unit
Total Required Power Gearbox	11.919	[kW]
Shaft Speed	130	[RPM]
Engine Speed Range	400 – 2000	[RPM]
Preferences	[10 0 5 7]	[-]

The results generated by the PGS design algorithm are presented by Figure 20, Figure 21 and Figure 22. The intersection of the black lines once again marks the selected design.

The algorithm selects a design which has the smallest spatial requirements, while assuring the highest possible efficiency. This is expectable, given the high weight factor assigned to fuel consumption (or efficiency). Lower total mass/volume solutions are present, however these have an efficiency which is lower than the selected concept.

The results of the algorithm seem to behave somewhat erratic, which is caused by the engine design algorithm selecting another engine design concept and the fact that the algorithms for the engine and the gearbox design both contain step functions.

The results seem of a correct order of magnitude, given gearbox and engine databases. Additionally the fact that the engines reduces in size when the reduction ratio (and therefore the engine speed) increases is recognizable.

While for the gearbox the opposite is true; the higher the engine speed (and reduction ratio) the larger the gearbox becomes. Which also is reasonable, since a larger reduction ratio, requires a larger gearwheel.

It is also clear that an increase in engine speed reduces both the gearbox efficiency and the engine efficiency. Although the gearbox efficiency is shown as separate data, its effects are visible in the difference between engine and total efficiency.

A final, somewhat more fundament indication of the fact that the algorithm functions properly, is the fact that the gearbox ratio has a slight discrete behavior (the step size between data points is not equal, while the engine speed range has a fixed step size), which is expectable since the number of teeth on both gearwheels has to be integer.

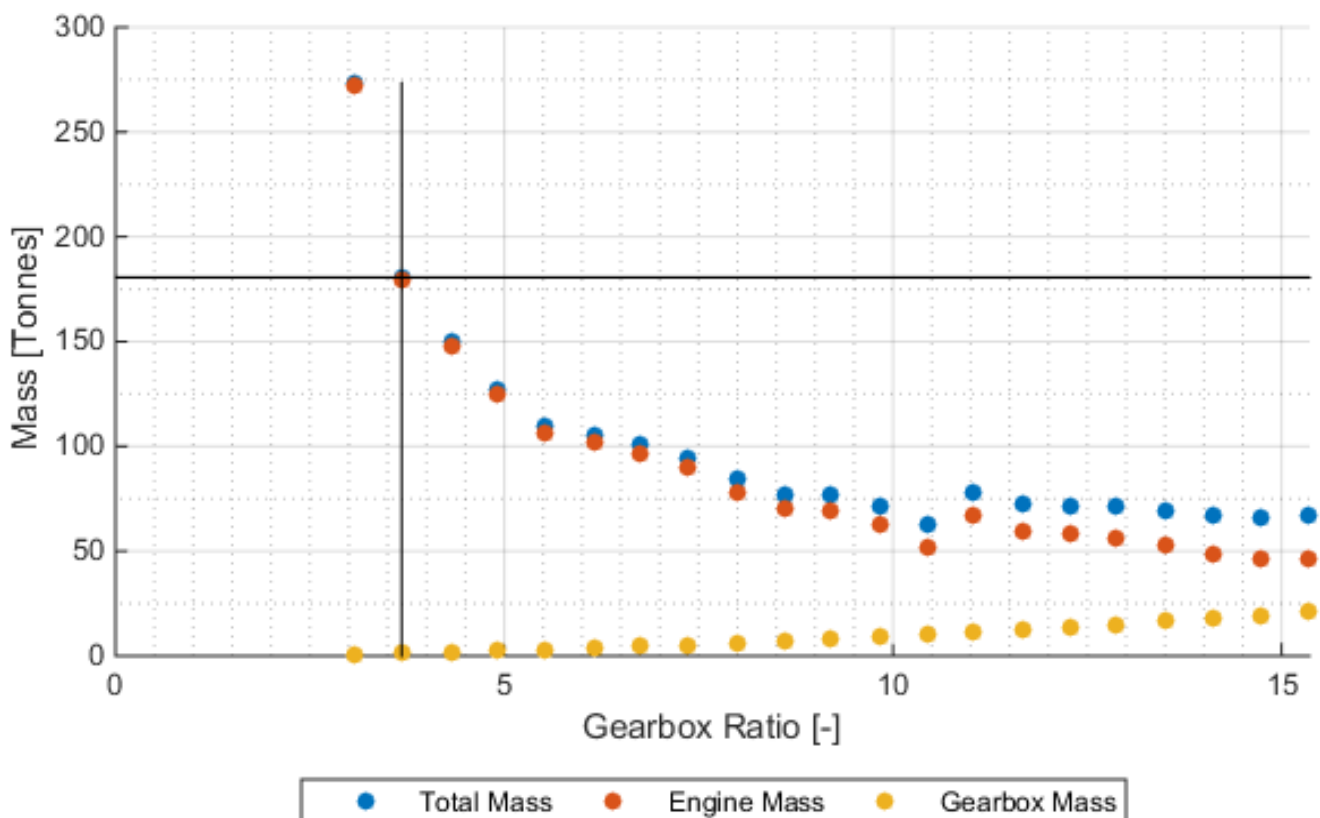


Figure 20: Engine, Gearbox and Total Mass versus Gearbox Ratio

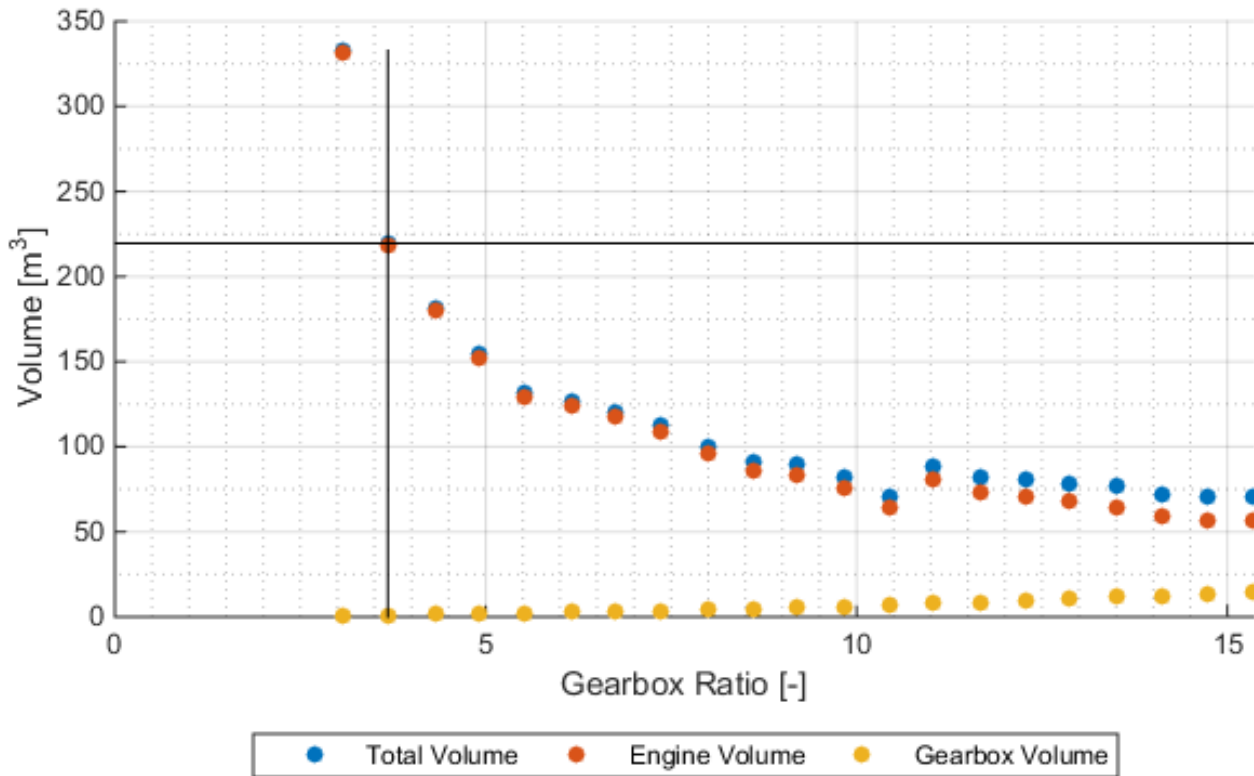


Figure 21: Engine, Gearbox and Total Volume versus Gearbox Ratio

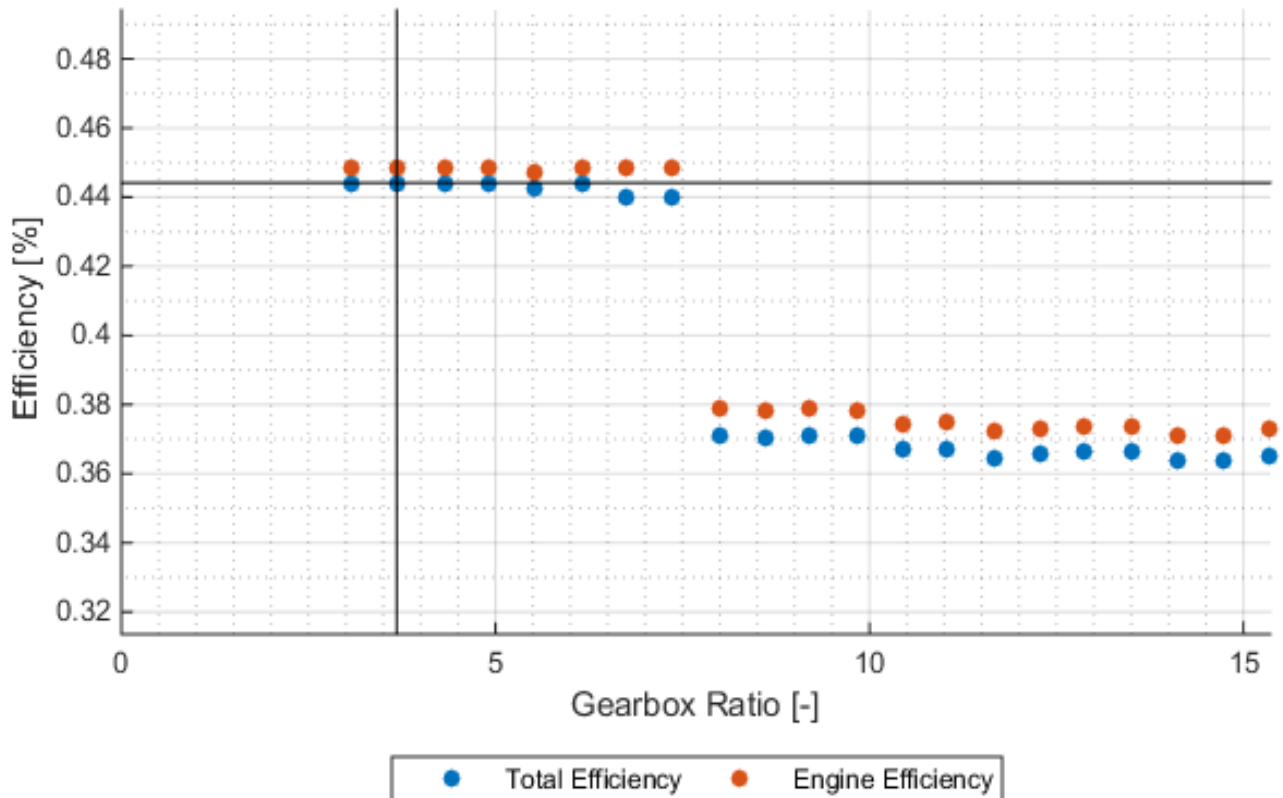


Figure 22: Engine and Total efficiency versus Gearbox Ratio

5.5. Electrical Energy Storage and Generation Systems Design

Another important set of systems found in a shipborne power plant are the systems which supply electrical power. The required systems that have to be designed are the electrical grid itself and the systems which provide electrical power to that grid and these are all discussed separately.

5.5.1. Electrical Grid

The electrical grid is an alternating current (AC) electrical grid (as discussed in paragraph 2.3.3), the voltage of which was left undetermined. This voltage is required before the electrical supply systems can be designed. To properly design the electrical grid it is first divided into two parts; the main grid to which the suppliers of electrical power are connected and the supply grids, which connect the consumers of electrical power to the aforementioned main grid. The created division is presented in the EFD found in Figure 23.

The voltage of the different supply grids can be 0, 230, 440, 690, 3300, 6600 or 11000 Volt, which are the most conventional voltages found on board of ships [41]. The voltages of these grids are determined first.

The exhaust gas treatment are assumed to be fed from a 690 [V] grid at all times ([12] & [42]). The other systems which consume electrical power will not have a predetermined supply voltage, instead the supply voltage is related to the power transferred by each supply grid.

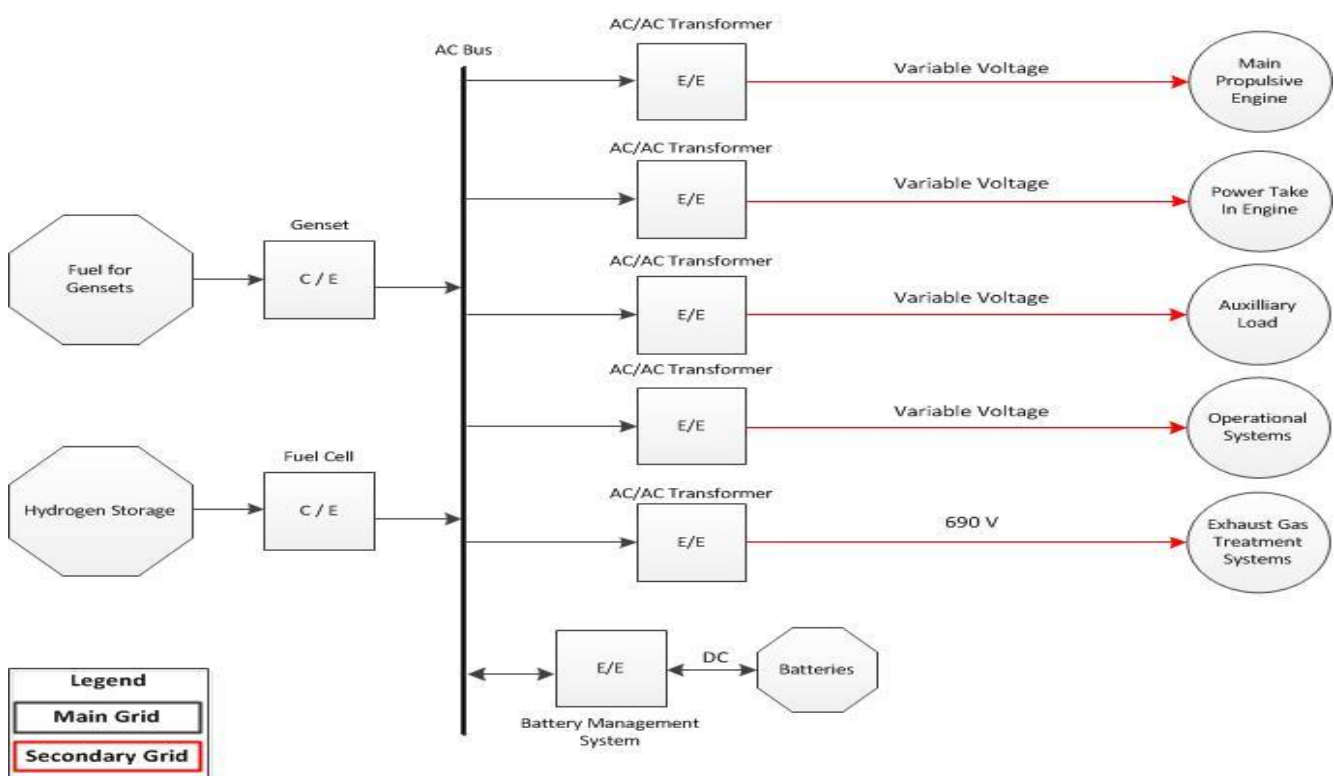


Figure 23: Detailed Energy Flow Diagram of the Electrical Grid

To determine the supply grid voltages, a step function based on the maximum electrical power is used. This step function is defined as shown by Table 13 and is derived using maximum continuous current limits, obtained from a circuit breaker manufacturer [43].

The data from this manufacturer is divided into two groups; low voltage (< 1 [kV]) and high voltages (> 1 [kV]), and based on this division there are two different maximum continuous currents.

For low voltage circuit breakers the maximum continuous current is 2000 [A] and for the high voltage circuit breakers this is 3000 [A] [43].

The limits presented by Table 13 can also be found in Figure 24, which shows the grid voltage and current as function of electrical power. In this same figure the aforementioned current limits are also plotted.

Using these limits, the voltages of the different supply grids can be determined, leaving only the main grid voltage as an unknown.

Table 13: Supply Grid Voltage as function of electrical power

Maximum Electrical Power [MW]	Supply grid voltage [Volt]
0	0
0.46	230
0.88	440
1.38	690
9.90	3300
19.80	6600
> 19.80	11000

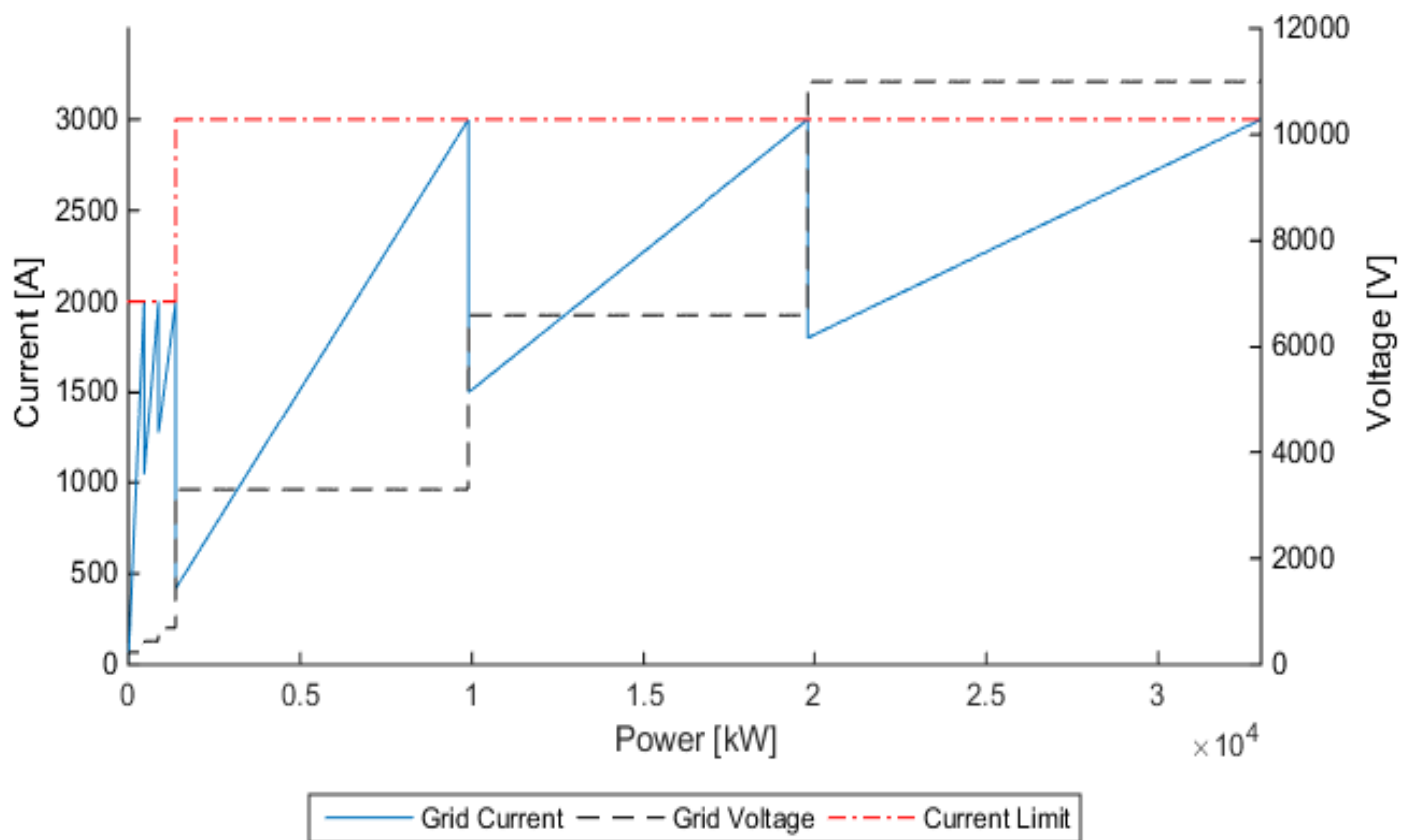


Figure 24: Grid Voltage, Current and Current Limits as function of the electrical Power

The main grid voltage is selected to be either 230, 440, 690, 3300, 6600 or 11000 [V] and where the main grid voltage is not equal to the supply grid voltage a transformer is installed. All possible transformers can be seen in the EFD presented by Figure 23, it is however likely that a power plant configuration will include less.

This research will not design the transformers separately, instead a standardized mass, volume and efficiency is assumed, which will be applied for every case where a transformer is required. A standard transformer is estimated to have a volume of 4 [m³] and a mass of 4 tonnes [44] and a constant efficiency of 98 [%] [8].

The voltage of the main grid is selected, from the aforementioned range of voltages, so that the mass/volume of the transformers is minimal or so that the power losses due to the transformers are minimized. Which criterion is used to select the grid voltage depends on the client preferences; should the client favor low spatial requirements, than the total size of the transformers is minimized. If he/she favors efficiency then the voltage is selected so that the losses due to the transformers are minimal.

The entire design process of the electrical grid is also schematically shown in Figure 25. With the determination of the electrical grids completed it is now possible to design the different electrical power suppliers.

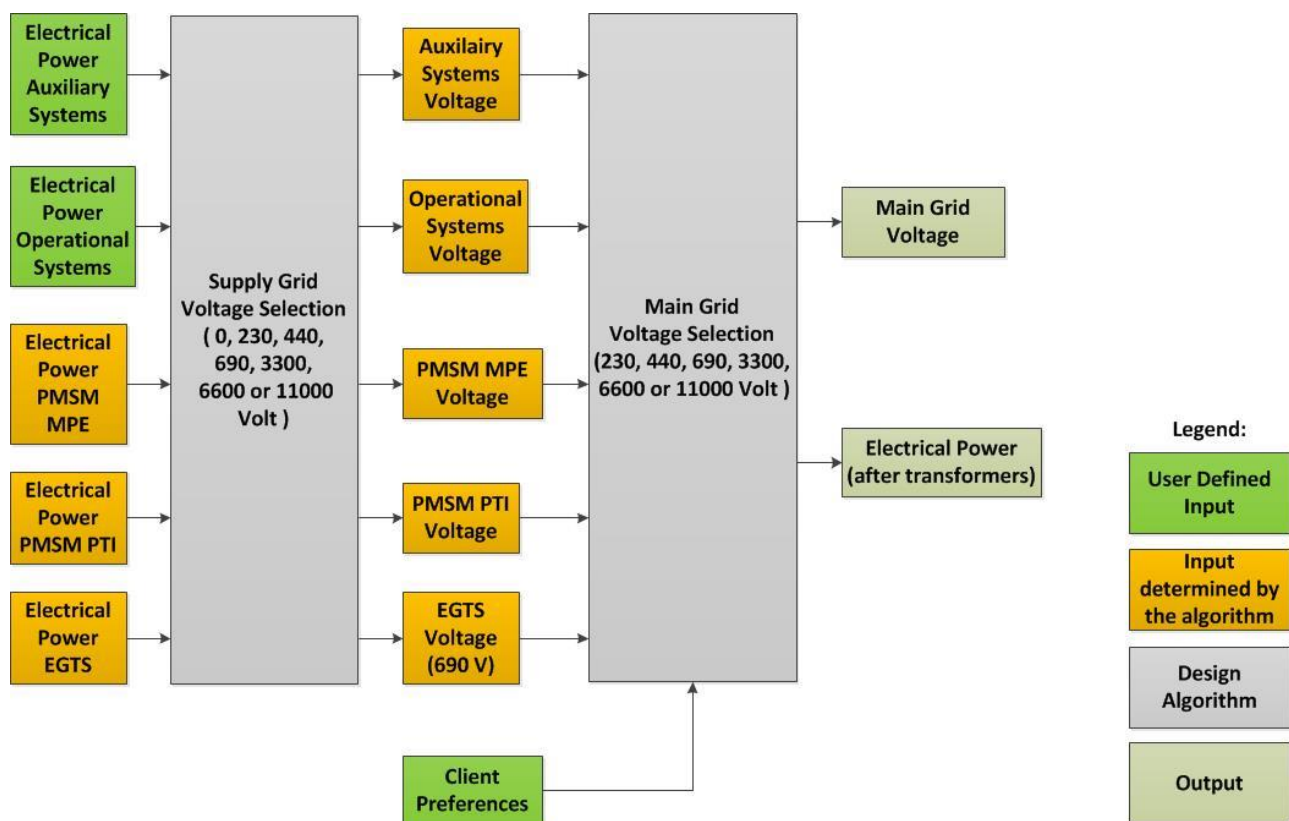


Figure 25: Process Flow Diagram, Electrical Grid Design

5.5.2. Energy Storage Design

As discussed in chapter 2 this research included batteries for the storage of electrical energy. An electrical power storage system based on batteries has the global configuration as shown by Figure 26, which shows the battery management system and the considered configuration of the batteries.

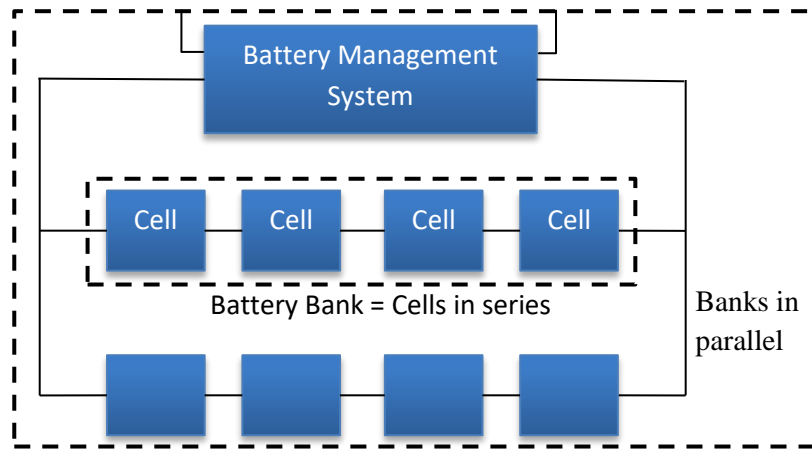


Figure 26: Battery Based EES Lay-Out

From Figure 26 it can be derived that the mass and volume of the batteries are related to the amount of cells in series and the amount of battery banks in parallel and the mass/volume of each individual cell. The mass and volume of the complete ESS can then be determined using equation (5.5).

$$\begin{aligned} M_{EES} &= \#_{banks} * (\#_{cells} * M_{cell}) + M_{BMS} \\ V_{EES} &= \#_{banks} * (\#_{cells} * V_{cell}) + V_{BMS} \end{aligned} \quad (5.5)$$

Battery Management System Dimensions

The Battery Management System is considered to consist of an inverter and a rectifier. The inverter is used in case the batteries supply power, while the rectifier is used when the batteries are being charged.

It is assumed that both the inverter and the rectifier are identical in terms efficiency (which is assumed to be 99% [4]) and their dimensions.

This means that the mass and volume of the BMS is exactly two times the mass (and volume) of the required inverter alone.

The mass and volume of the inverter are all scaled using the power that passes through the inverter. A set of inverters developed by ABB [45] is used as reference.

Based on these reference inverters several relationships for the estimation of the principal dimensions can be established. These relationships are shown by Figure 27 and Figure 28, located on the next page.

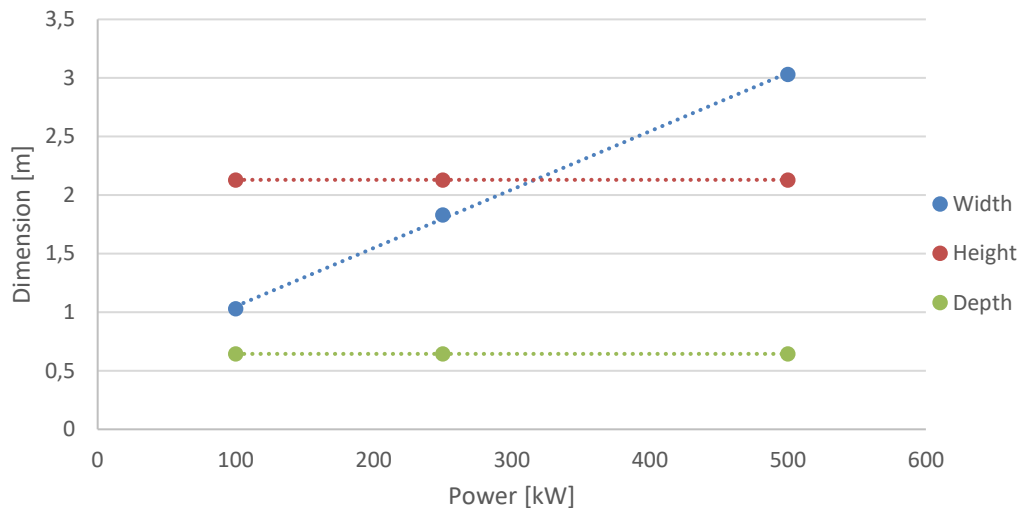


Figure 27: Main dimensions of an inverter as function of power

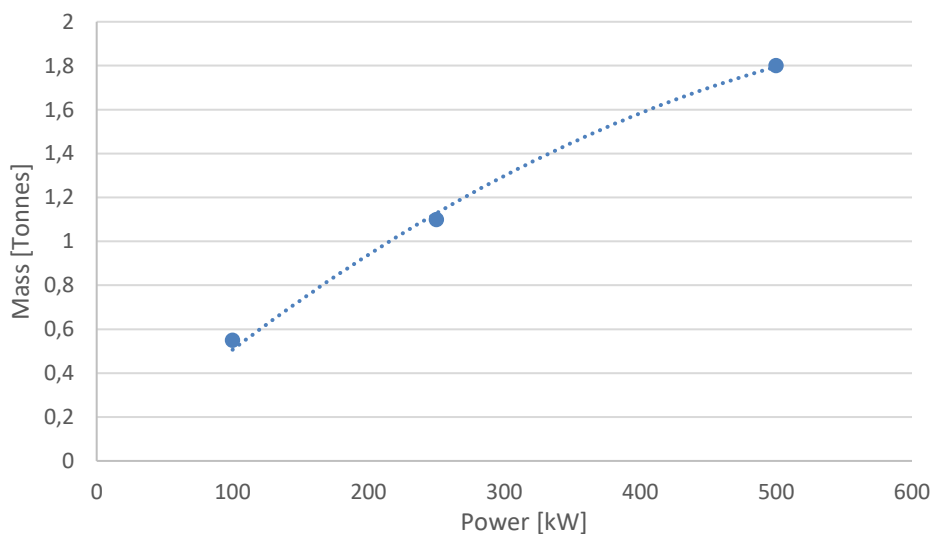


Figure 28: Inverter mass as function of inverter power

Battery Design

As stated earlier in this paragraph, the main variables which determine the dimensions of the batteries are amount of cells in series, the amount of battery banks in parallel and the mass/volume of an individual cell.

Because the batteries are connected to the electrical grid, the voltage of the EES has to be similar to that of the electrical grid. Which means that the number of cells in series can be determined as soon as the voltage of a single cell is known.

The voltage of single cell is a dependent on the state of discharge (SoD) and the discharge current of the battery [46]. Because losing power at a given time is not an option for a ship owner, the batteries will be designed for a worst case scenario. This is defined as a highly discharged battery required to deliver the maximum electrical power demand found during the operation of those batteries.

Based on the modeled discharge behavior of the battery [46] (see also Appendix F) it is assumed that batteries are not to be discharged beyond a SoD of 80%, since a very steep voltage drop occurs after this point. Therefore this SoD is assumed to represent a highly discharged battery.

Figure 29 and Figure 30 show the voltages at 80% SoD, as function of the discharge current for both battery types. The discharge current is limited to 6000 [A] for lead-acid batteries and 400 [A] for li-ion batteries [3].

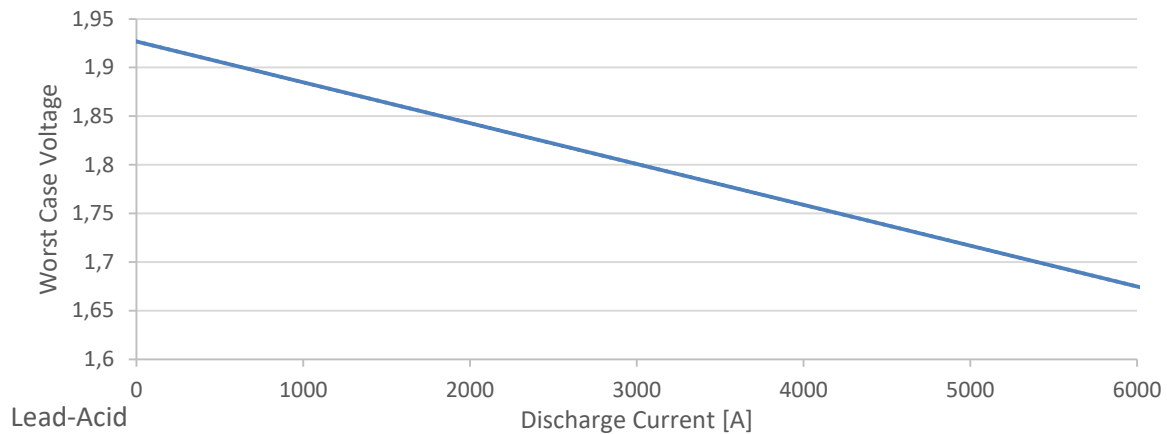


Figure 29: Lead-Acid Batteries, Cell voltage as function of discharge current

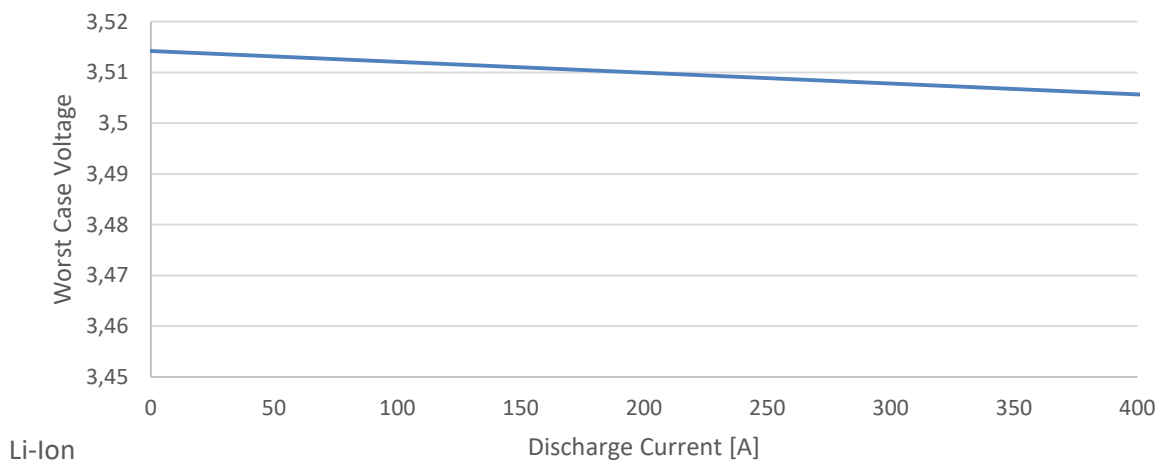


Figure 30: Li-Ion Batteries, Cell voltage as function of discharge current

The required number of cells can then be determined using equation (5.6), the result of which has to be rounded up towards the nearest integer.

$$\#_{cells} = \frac{U_{grid}}{U_{cell}} \quad (5.6)$$

If the required number of cells and the discharge current limit cause the available power of a single battery bank to be lower than the required power then additional battery banks are installed in parallel until the power demand can be met. Once the power demand can be met the number of battery banks in parallel is known.

With the number of banks and the number of series known, the only unknown parameter required to determine before the dimension of the complete system (see equation (5.5)) are the dimensions of a single cell.

These dimensions are directly related to the capacity in ampere-hour [Ah] of that same cell, which can be determined using equation (5.7).

$$C_{cell} = C_{bank} = \frac{C_{required}}{\#_{banks}} \quad (5.7)$$

Which is dependent on the total required capacity of the batteries (in Ah) which can be determined using equation (5.8).

$$C_{required} = \frac{C_{required_kwh}}{U_{main_grid}} = \frac{\int P_{electrical_ESS_delivering} dt}{U_{main_grid}} \quad (5.8)$$

The mass and volume a single cell can then be determined using equation (5.9), which apart from the previously discussed parameters includes a correction factor. Which is there to include the battery conditioning monitoring systems that are required for Li-Ion batteries, the values for these factors are obtained from Rietveld [3] and summarized in Table 14.

$$M_{cell} = f_{mass} * \frac{C_{cell}}{SBC} \quad (5.9)$$

$$V_{cell} = f_{volume} * \frac{C_{cell} * \rho_{battery}}{SBC}$$

The Specific Battery Capacity (SBC) is however also a function of the discharge current, as expressed by equation (5.10) [3]. Which uses the characteristic discharge current (I_{char}) and the shape factor ' α '. Both these parameters are battery type dependent and have been obtained from Rietveld [3] and are summarized in Table 14.

$$SBC = SBC_{max} * (\alpha + \alpha * e^{-\frac{I_{dis}}{I_{char}}}) \quad (5.10)$$

Table 14: Battery parameters for the considered battery types [3]

	Lead-Acid	Lithium-Ion	Unit
Maximum Discharge Current	6000	400	[A]
Cell Density	2650	1981	[kg/m ³]
Maximum Specific Battery Capacity	28.6	51	[Ah/kg]
α	0.518	0.882	[-]
I_{char}	4.098	11.384	[A]
Volume Correction Factor	1	1.6	[-]
Mass Correction Factor	1	1.3	[-]

Other methods to design a battery based energy storage system exist, such as the optimization algorithm developed by Rietveld [3]. Who uses a time-based simulation to optimize the battery capacity. This method produces more accurate results, but does require a lot of time for even one design to be created, which renders this approach impractical for this research.

5.5.3. Electricity Generation System lay-out Design

Several systems to generate electrical power are considered during this research. These are Polymer Electrolyte Membrane Fuel Cells (PEMFC), a generator driven by either a diesel engine or a dual fuel engine and a combination of an engine driven generator (both types) and a PEMFC.

PEMFC based generation system design

The dimensions of a fuel cell based generation system are determined using the methodology presented by ten Hacken [4]. This algorithm was specifically developed for the use on board submarines and the methodology is therefore adjusted for the fact that this research considered surface vessels. This is done by adding the dimensions an inverter, which is required to obtain an AC voltage and a compressor which is needed to deliver air (which contains the required oxygen) to the PEMFC. The complete methodology used to determine the dimensions of a PEMFC system is included in appendix G.

The main variables in this methodology are the cell area of a single fuel cell and the nominal current density used to design the fuel cells. These two parameters are determined using intermediate design algorithms. This algorithm uses a range of feasible cell areas and current densities to design a series of fuel cell based generation systems, from which the optimal concept is selected, a process flow diagram of the design algorithm is found in Figure 31.

The cell area of a fuel cell is limited, due to the fact that the hydrogen still has to be dispersed over the entire cell area. Ten Hacken [4] presented 0.025 up to 0.12 [m²] as range of feasible cell areas and this range is also used for this research. The current density [A/m²] is varied between 0 and 16000, which are the feasible limits for PEMFC's [4].

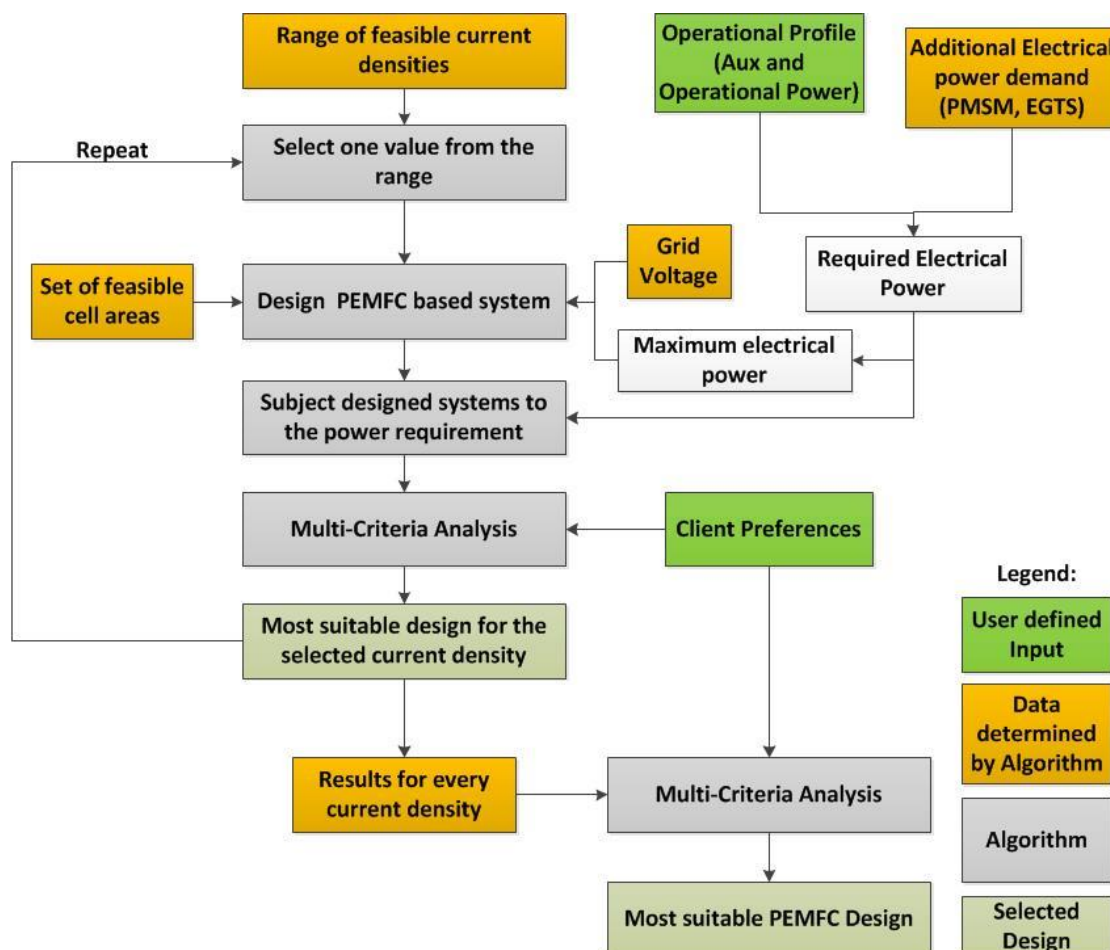


Figure 31: Process Flow Diagram of the PEMFC design Algorithm

Combustion Engine driven Generators

For the concepts which require an engine driven generator, the methodology presented by Rietveld [3] is used. This algorithm uses the dimension prediction method described by Stapersma & de Vos [36], in combination with the rescaling of a reference generator.

However, Rietveld used data of diesel generators which were specifically designed for submarine applications. Since this research does not consider submarines, it would be unfair to use the same values. Therefore the average cylinder values used by Rietveld are updated using genset data obtained from Wärtsilä [47]. Additionally, values for the design of dual fuel driven generation sets are added, these values are also obtained from Wärtsilä [47]. Both sets of design parameters are also verified using the engine databases mentioned in appendix E.

Table 15: Average Cylinder Data Generator driving Diesel Engines

	Diesel	Dual Fuel	Unit
i_{engine}	[4 6 8 12 16]	[6 8 10 12 14 16]	-
k	2	2	-
P_{me}	25	22	Bar
c_m	8.4	9.3	m/s
N_{engine}	900	1200	RPM
L_s/D_b	1.4	1.4	-
L_s	0.28	0.28	m
D_b	0.2	0.2	m

The developed algorithm first determines required mechanical power, using a reference efficiency of the generator. Using the design parameters an average power per cylinder is determined and using this average power the number of cylinders required to deliver the required mechanical power is calculated.

The algorithm then determines the number of engines needed to supply that minimum amount of cylinders. It does so by comparing the required number of cylinders to the most conventional engines used to drive generators.

For diesel engine driven generators these are 4, 6, 8, 12 and 16 cylinders [3] & [38], while for dual fuel driven generators 6, 8, 10, 12, 14 and 16 cylinders are more common [47].

For which it is assumed that the 4, 6 and 8 cylinder engines are line engines, and the 12 and 16 cylinder engines are V type engines, which is again based on the engine manufacturer data.

The manufacturer data is also used to estimate an average specific fuel consumption (SFC) is also estimated to be 197 [g/kWh], which is once again adjusted for the engine load using the method described by Jalkanen et al [35].

This process creates a set of different genset designs, which can all deliver the required electric power. These designs are then ranked according to the clients preferences and the one which best suits those preferences is selected.

The voltage delivered by a diesel generator is not important for its design since a voltage regulator is normally included in a genset (an example from Caterpillar can be found in their catalogue [48]). Therefore a transformer is not required. This means the total mass and volume can be determined using equation (5.11).

$$\begin{aligned}
 M_{\text{system}} &= M_{\text{genset}} * \#_{\text{gensets}} \\
 V_{\text{system}} &= V_{\text{genset}} * \#_{\text{gensets}}
 \end{aligned}
 \tag{5.11}$$

5.5.4. Hybrid Generation Systems

The last option for the supply of electricity generation is the application of both a fuel cell and an engine driven generator. These systems have one additional degree of freedom, which is the Degree of Hydrogenization (DoH), see also equation (5.12)). To determine the value for the DoH an additional algorithm is developed.

$$DoH_{hybrid} = \frac{P_{PEMFC}}{P_{max}} \quad (5.12)$$

The algorithm selects a DoH from a range of 10 to 90 % with increments of 20%. The required electrical power is divided over the fuel cells and the gensets based on the selected DoH and the PMS discussed in paragraph 5.2. The algorithms then calls the design algorithms for both generation systems and saves the results.

This process is executed for the entire range of DoH's and once all designs have been created another MCA to select the DoH which bests meets the specified preferences. In this comparison the fuel consumption is the summation of both the fuel required by the combustion engine and the hydrogen required by the system. This design process is also shown by Figure 32.

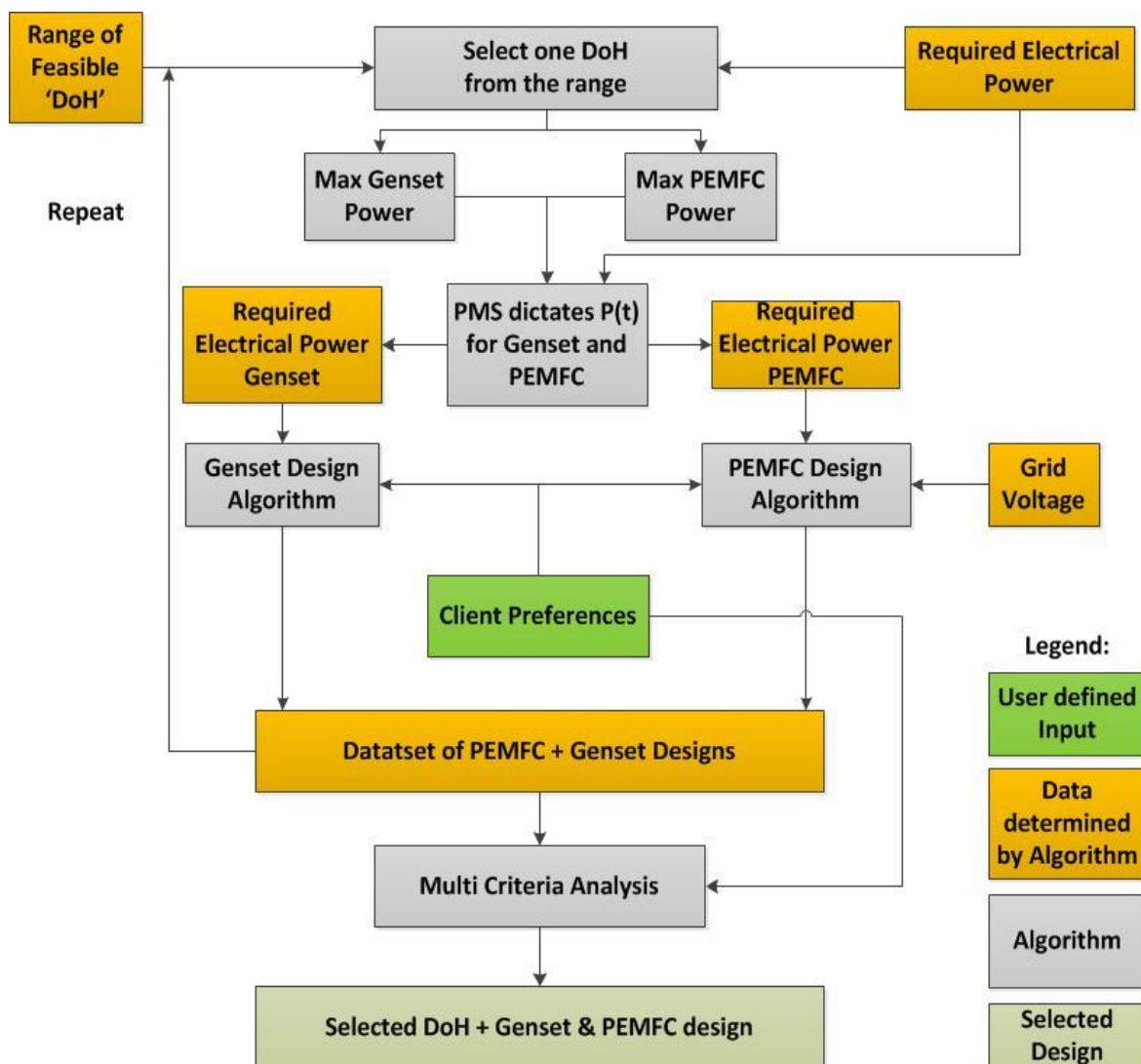


Figure 32: Hybrid Generation System Design Flow

5.6. Fuels: Chemical properties and Storage

In this paragraph the properties of the different fuels are presented. This paragraph also presents the method used to account for the application of dual fuel engines and the method used to account for the storage requirements.

5.6.1. Fuel characteristics

The most important characteristics for all included fuels are summarized in Table 16, which also includes the sources used to obtain the data.

Note that the mass percentages do not always add up to a 100%, this is caused by the fact that there are trace elements (nitrogen, oxygen, vanadium, and ash) present in the fuel and these are not included in this summary.

Table 16: Fuel Characteristics per fuel

	Lower Heating Value	Density	Carbon Content	Hydrogen Content	Sulphur Content	Specific Tank Mass	Sources
	[MJ/kg]	[kg/m ³]	[Mass %]	[Mass %]	[Mass %]	[Kg tank / kg fuel]	[-]
Marine Diesel Oil (MDO)	42	880	87	12	0.2	0 ²	[14, p. 705], [49, p. 558], [50], [51]
Heavy Fuel Oil (HFO)	40.5	1010	85	10	3.5	0 ²	[14, p. 705], [49, p. 558], [50], [51]
LNG (CH ₄)	48.6	470	75 ¹	25 ¹	0	0.48	[52] [53], [54]
CNG (CH ₄)	46.9	180	75 ¹	25 ¹	0	1.18	[55], [52], [56]
Hydrogen (H ₂)	120	42	0	100	0	17.5	[52], [57], [4]
Ammonia (NH ₄)	18.65	683	0	18 ¹	0	1.91	[58], [52], [59]

1. Calculated from the chemical composition of the gas, assuming a pure composition
2. MDO and HFO are stored in the double hull of a ship, therefore no additional tank mass is required.

5.6.2. Dual Fuel Application

For cases where different fuels are used (i.e. dual fuel engines) the properties of each fuel are combined in order to obtain a (fictional) fuel blend. In practice dual engines inject both fuels separately, however accurately modeling this is, due to the time constraints posed to this research, not possible.

The properties of the fuel blend can be determined using equation (5.13), in which 'X' presents the property being calculated and 'R_F' is the ratio total fuel to pilot fuel. These ratios are presented in Table 17, along with the sources used to obtain them.

Note that this approach cannot be used to determine the specific tank mass or the tank volume since both fuels are stored separately.

$$X_{blend} = X_{pilot_fuel} * R_F + X_{dual_fuel} * (1 - R_F) \quad (5.13)$$

Table 17: Dual Fuel blending Ratios for all considered dual fuel types

Duel Fuel Type	R _F [%]	Source
Liquefied Natural Gas	1	[60]
Compressed Natural Gas	1	[60]
Ammonia	40*	[61]

* A value of 5% is also mentioned by the same source, but it also indicates this was an idealistic case and a ratio of 40 [%] resulted in better combustion properties. Therefore this value is used.

5.6.3. Fuel Storage Requirements

The volume required for the storage of the different fuels has to be taken into account. Therefore the required tank volume and tank mass is added to the (invariable) system volume/mass. These are accounted for using the fuel density and the specific tank mass (m_{tank}) [kg tank/kg fuel], both of which are included in Table 16. The equations to determine the tank volume and tank mass are presented by equation (5.14).

$$V_{tank} = \frac{M_{fuel}}{\rho_{fuel}} \quad (5.14)$$

$$M_{tank} = M_{fuel} * m_{tank}$$

5.7. Engine Emissions & Exhaust Gas Treatment System Design

As discussed in chapter 3 a constraint was added, which allowed for the removal of the exhaust gas treatment systems from the concept definition. Instead the exhaust gas treatment systems would be installed when required by the emission regulations. Therefore the emissions and their regulatory limits are discussed in the first sub-paragraph. Then the design of the exhaust gas treatment systems is discussed in the second and third sub-paragraph.

5.7.1. Engine Emissions

In this paragraph the methods to estimate the different emissions are discussed. The first of which is the exhaust gas mass flow produced by all combustion engines together. Secondly the methods used to determine the emissions of CO₂, NO_x, and SO_x are discussed individually.

Exhaust gas Mass Flow

The total mass flow of the exhaust gas is the result of the summation of the exhaust gas produced by all internal combustion engines. The mass flow a single combustion engine can be determined by establishing a mass balance over a cylinder.

This mass balance states that the mass exiting the engine has to be equal to the amount of mass going into the engine. The latter of which consists of the mass of the fuel and air required for combustion, this is also shown by equation (5.15).

$$\dot{M}_{exhaust,n} = \dot{M}_{fuel,n} + \dot{M}_{air,n} \quad (5.15)$$

The mass flow of the fuel is determined during the performance simulations, so when a formulation can be established, the exhaust gas mass flow can also be determined during this same simulation. The mass flow of air can be determined using the air to fuel ratio (AFR) [8, p. 207]. This ratio consist of the stoichiometric ratio (σ) and the air excess ratio (λ), as shown by Equation (5.16).

$$\dot{M}_{air} = \dot{M}_{fuel} * AFR \quad (5.16)$$

$$AFR = \sigma * \lambda$$

These relationships can then be combined to determine the total mass of the exhaust gas, as shown by equation (5.17).

$$\dot{M}_{exhaust} = \sum_{n=1}^3 \dot{M}_{fuel,n} * (1 + AFR_n) = \sum_{n=1}^3 \dot{M}_{fuel,n} * (1 + \sigma_n * \lambda_n) \quad (5.17)$$

The air excess ratio accounts for the amount of air required for the scavenging process in the cylinder, and is only engine type dependent. The air excess ratio is assumed to be 2.8 for 2-stroke engines and 1.8 for 4-stroke engines [8, p. 207].

The stoichiometric ratio defines the exact amount of air required for the (complete) combustion of the fuel. This ratio is completely dependent on the chemical composition of the fuel, which has been presented in paragraph 5.6, and can be determined using equation (5.18) [8, p. 206].

$$\sigma_n = \frac{\%C * \frac{32}{12} + \%H * \frac{16}{2} * \%S * \frac{32}{32}}{0.23} \quad (5.18)$$

Carbon Dioxide Emissions

The amount of carbon dioxide (CO₂) emitted by the combustion engines can be related to the consumed fuel, using a pollutant emission ratio (per), which is expressed in grams per kilogram fuel.

The 'per' for CO₂ is completely dependent on the amount of carbon inside the fuel and can be determined using equation (5.19) [14, p. 704].

$$PER_{CO_2} = 3150 * \frac{\%C}{86} \quad (5.19)$$

Sulphur Oxide Emissions

The sulphur inside the fuel is converted to several different sulphur oxides by the combustion process. These different oxides are often summarized under the term SO_x. The amount of SO_x emitted (expressed as 'per') is only dependent on the sulphur content in the fuel and can be determined using equation (5.20) [8, p. 478].

$$PER_{SO_x} = 20 * \%S \quad (5.20)$$

The IMO also poses a limit to the amount of sulphur that is allowed to be emitted. This limit is defined as a maximum allowed sulphur content of the fuel. These limits and their resulting 'per' are summarized in Table 18 [11].

At the time of this research the sulphur cap outside of SECA's is 3.5 [%]. However, in the year in the year 2020 this cap will be reduced to 0.5 [%] [33]. This limit is implemented so that the selected power plant configurations are more future proof than they would be under the current sulphur limits.

Table 18: Sulphur Emission Limits per ECA

Emission Control Area	Sulphur Content Limit	Sulphur emission limit
	[%]	[gram / kg fuel]
Global	< 0.5	10
Sulphur Emission Control Area	< 0.1	2
NO _x Emission Control Area	< 0.5	10
Total Emission Control Area	< 0.1	2

Nitrogen Oxide Emissions

For conventional diesel engines the total NO_x emissions, again expressed as 'per', can be determined using Figure 33, which is obtained from Klein Woud & Stapersma [8]. Which curve is used depends on the engine designation, these indications have been included in Table 19 and are also presented by Klein Woud & Stapersma [8].

Table 19: Engine Designations based on engine speed [8]

Engine Indication	Engine Rated Speed [RPM]
Slow Speed	$N_{\text{engine}} < 130$
Medium Speed	$130 < N_{\text{engine}} < 1200$
High Speed	$N_{\text{engine}} > 1200$

Dual fuel engines have a NO_x emission, which is 80 % lower than diesel engines due to the decrease in combustion temperature [62]. This results in the NO_x emissions as shown Figure 34, in which the same engine designations are used.

This effect also exists for dual fuel engines running on ammonia, although not to the same extent. This is due to the fact that there is more fuel borne nitrogen, which results in high NO_x emissions at low engine loads. The behavior of the NO_x emissions for dual fuel engines running on ammonia is estimated using data obtained from the Iowa State University [63] and the results are presented in Figure 35, which again uses the same three engine designations

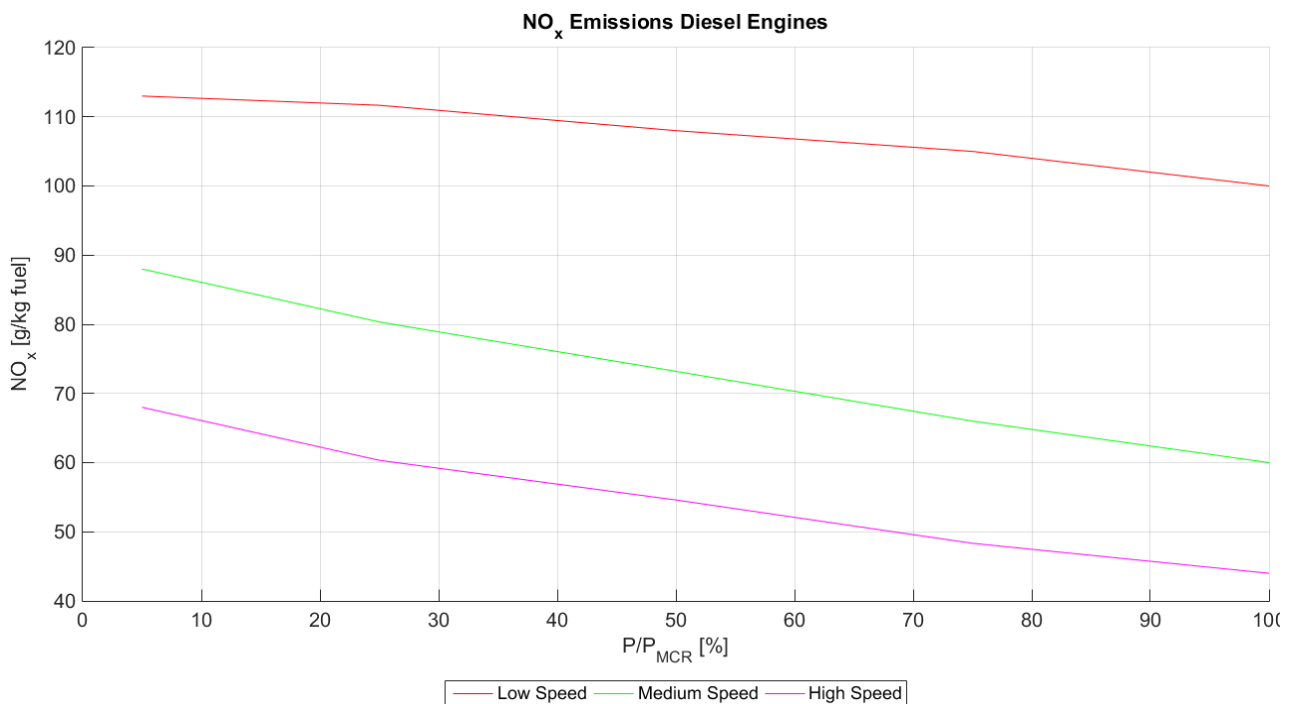


Figure 33: NO_x emissions as function of engine loading for Diesel Engines

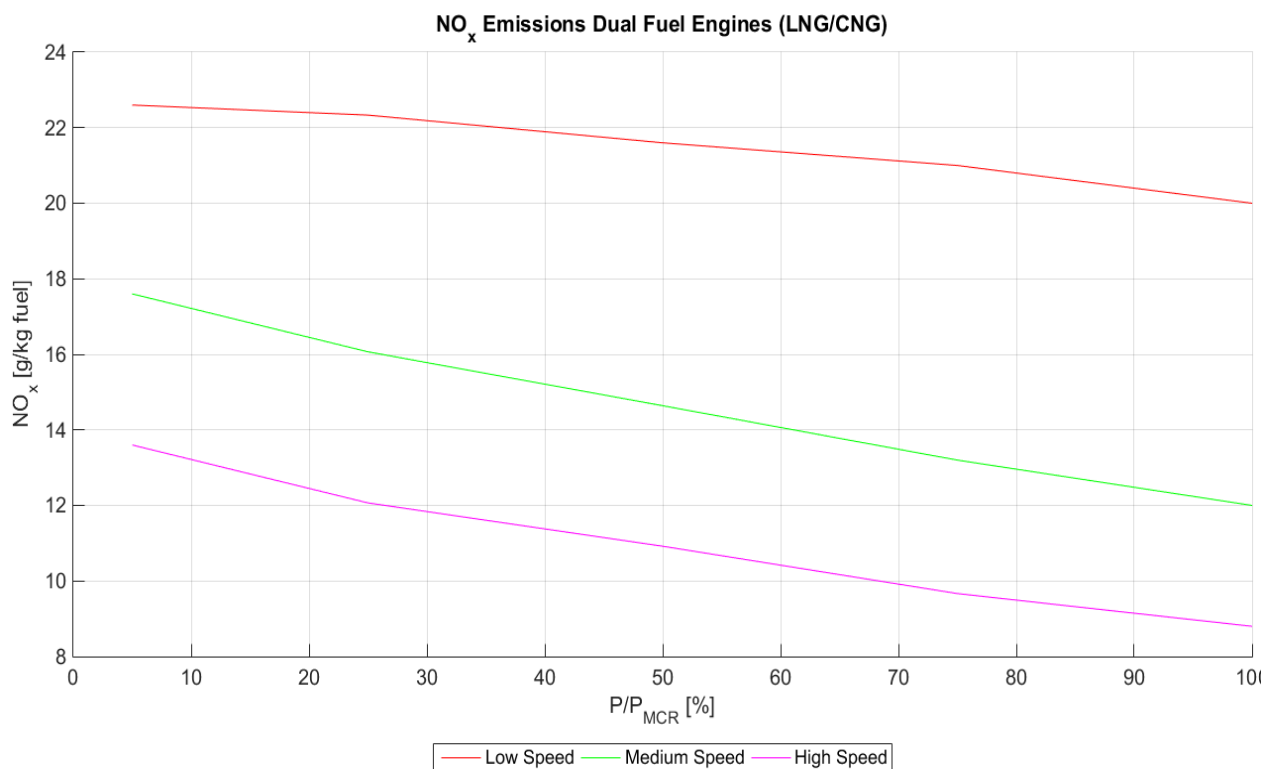


Figure 34: NO_x emissions as function of engine loading for Dual fuel Engines

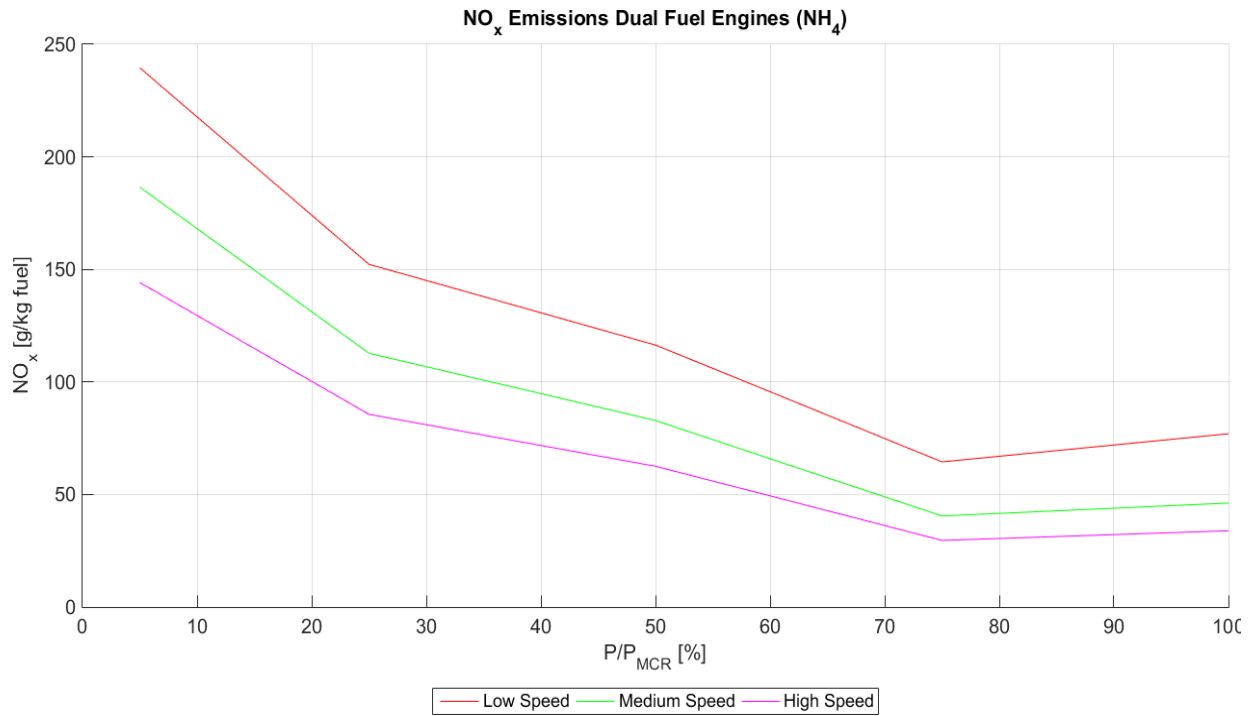


Figure 35: NO_x emissions as function of engine loading for DF engines supplied with ammonia

The emission of NO_x is limited by the IMO in 'MarPol Annex VI [11] and these limits are summarized in Table 20. These limitations were posed in 2005 and since then several adjustments have been made, which also have to be accounted for.

Table 20: IMO NO_x limits per engine designation [11]

Engine Indication	Engine Rated Speed [RPM]	NO _x limit [g/kwh]
Slow Speed	$N_{\text{engine}} < 130$	17.0
Medium Speed	$130 < N_{\text{engine}} < 2000$	$45 * (N/60)^{-0.2}$
High Speed	$N_{\text{engine}} > 2000$	9.8

The adjusted emission limits are determined using an adjustment factor, which is also prescribed by MarPol Annex IV, see also equation (5.21). The value for 'F' is dependent on the emission control area in which the vessel operates and a summary of these values is found in Table 21 [14, p. 759].

$$NO_{x-adjusted} = NO_{x-2005} * (1 - F) \quad (5.21)$$

Table 21: NO_x Limit Reduction factors for each ECA (valid from 2016 onwards)

Type of Emission Control Area	F
Global (No Emission Control Area)	0.2
Total Emission Control Area	0.8
NO _x Emission Control Area (NECA)	0.8
SO _x Emission Control Area (SECA)	0.2

Now that all engine emission, and their limits, can be determined, it is possible to determine whether a certain exhaust gas after-treatment system is required and to design that treatment system as such the emitted exhaust gas exactly complies with the appropriate regulations.

5.7.2. Scrubber System

This research only considers open loop scrubber systems (as discussed in paragraph 2.2). The components of such a scrubber are shown by Figure 36. Which is based on a schematics obtained from Wärtsilä [12] and information provided by the United States EPA [64]. The pumps necessary for the transportation of the scrubbing water are not included in this diagram and are not included in the dimension estimates. For each of the components shown the dimensions will be determined.

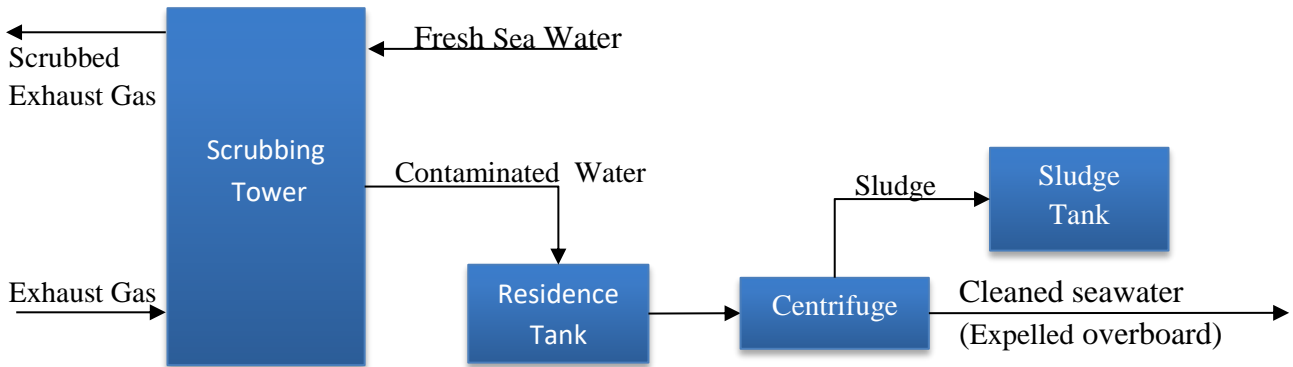


Figure 36: Scrubber System Components

Scrubbing Tower Dimensions

The first component for which the dimensions have to be determined is the scrubbing tower. The volume of this tower can be defined using equation (5.22).

$$Vol_{tower} = A_{tower} * H_{tower} \quad (5.22)$$

This equation requires an overall height and overall floor area of the scrubbing tower. The overall floor area is mainly determined by the circular area of the spray tower vessel, as shown by Figure 37 (based on [12]).

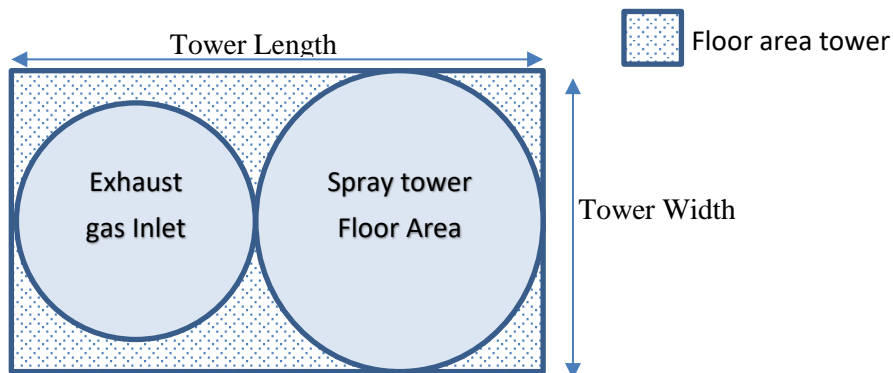


Figure 37: Scrubbing Tower floor area and principal dimensions

The circular area of the tower is not the only thing influencing the total floor area of the scrubbing tower. This floor area is also influenced by structural elements and the inlet of the exhaust gases.

To estimate the overall floor area of the scrubbing tower these influences have to be accounted for. This is done by defining the tower width and length as shown by Figure 37. The floor area of the scrubbing tower can then be determined using equation (5.23).

$$A_{tower} = W_{tower} * L_{tower} \quad (5.23)$$

The principal dimensions of the scrubbing tower can all be related to the diameter of the spray tower. The required relationships are obtained using a dataset provided by Wärtsilä [12] and these relationships are presented in Figure 38 and mathematically presented by equation (5.24).

$$\begin{aligned} L_{tower} &= 1.84 * D_{spray_tower} \\ W_{tower} &= 1.09 * D_{spray_tower} \\ H_{tower} &= 1.59 * D_{spray_tower} + 2.395 \end{aligned} \quad (5.24)$$

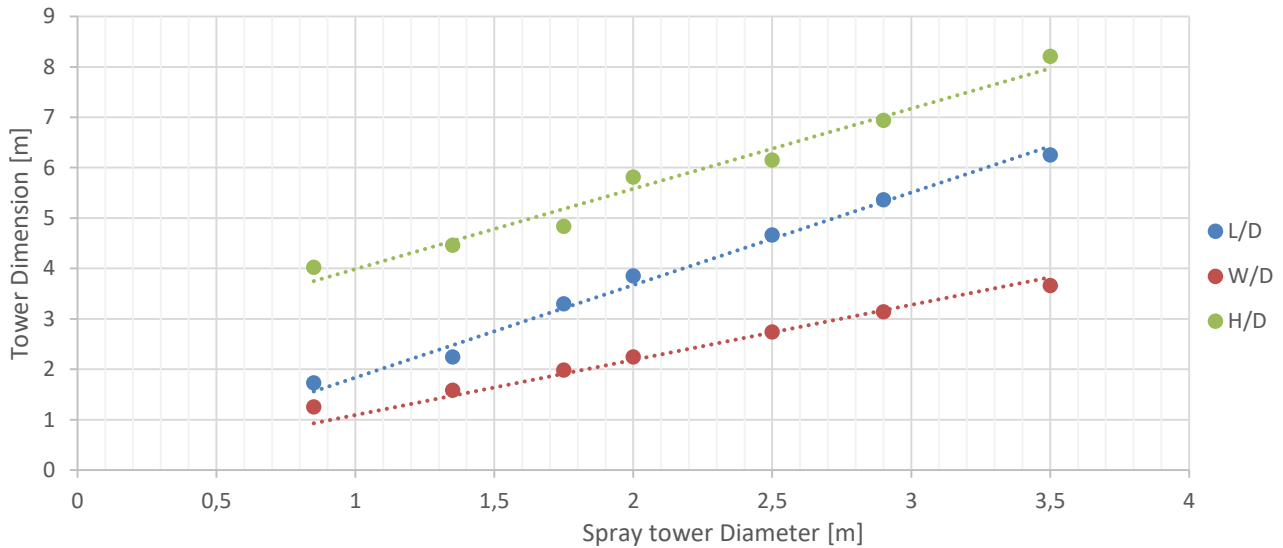


Figure 38: Regression of Spray Tower dimensions [12]

The diameter of the scrubbing tower is directly related its surface area, which can be determined using equation (5.25). This equation uses the fact that the exhaust gas has a maximum allowable velocity to ensure that the scrubbing water does not get carried upwards by the exhaust gas. This maximum allowable velocity is assumed to be 3 [m/s] [12].

$$A_{spray_tower} = \frac{\dot{Q}_{exhaust}}{v_{gas_max}} \quad (5.25)$$

Because the mass flow of the exhaust gas has been determined earlier in this paragraph it is possible to determine the circular floor area of the spray tower using equation (5.26). For this equation the exhaust gas density is assumed to be 1.2 [kg/m³], which is the density of (ambient) air. This value is used because the exhaust gas is scrubbed (and cooled in the process) using ambient temperature seawater.

$$A_{spray_tower} = \frac{1}{v_{gas_max}} * \frac{\dot{M}_{exhaust}}{3600 * \rho_{exhaust}} \quad (5.26)$$

Therefore all principal dimensions of the scrubbing tower can be determined. However, the regression analysis executed to obtain the numerical values presented in equation (5.24) was done using scrubbing systems designed so the scrubber could cope with a sulphur content (of the combusted fuel) of 3.5 %.

Therefore a scrubbing system designed for a system running on a fuel with a lower sulphur content will be oversized, since the minimum cleaning efficiency is lower. To compensate for this phenomenon an adjustment factor is introduced, related to the required cleaning efficiency.

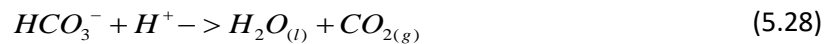
An important term in the determination of the removal efficiency is the residence time of the exhaust gas inside the spray tower [65]. The residence time of the exhaust gas is directly related to the height of the spray tower. Therefore the height of the spray tower is adjusted for cases where a lower removal efficiency is required, this is done using equation (5.27).

$$H_{corrected} = H_{overall} * f_{eta} = H_{overall} * \frac{\%S_{fuel_actual}}{\%S_{fuel_maximum}} = H_{overall} * \frac{\%S_{fuel_actual}}{3.5} \quad (5.27)$$

Now that the overall volume of the scrubbing tower is known it is possible to determine its weight. The data obtained from Wärtsilä [12] is used once again in order to determine this density. Which is found to be 0.15 [ton/m³].

Residence Tank Dimensions

Because the pH value of the expelled water is limited to a value of 5.5 [64], the wash water cannot be expelled to sea directly. However, seawater is a natural alkaline, which causes the scrubbing water to undergo the reaction shown in equation (5.28). To allow time for this reaction and the separation of the gas and the liquid which are the product of this reaction, a residence tank is included in the scrubbing system.



The dimensions of the residence tank are directly related to the wash water flow through the scrubber. The water has to reside in the residence tank for approximately 2 minutes [12, p. 59] to allow the pH balancing reaction to take place. This leads to the residence tank volume being defined as shown by equation (5.29).

$$Vol_{tank} = 120 * Q_{washwater} \quad (5.29)$$

The wash water flow is related to the total exhaust gas production using the Liquid/Gas ratio (R), which is assumed to be 0.006 [-] using the data provided by Wärtsilä [12, p. 59] and this value is verified using a range of commonly found values (0-1*10⁻³) [66]. The volume of the residence tank can then be determined using equation (5.30).

$$Vol_{tank} = 120 * \dot{Q}_{exhaust} * R_{L/G} \quad (5.30)$$

Centrifuge Dimensions

The next components for which the dimensions have to be determined is the centrifuge. Which removes the contaminants from the scrubbing water before it is expelled overboard.

The dimensions of the centrifuge are dependent on the amount of water that has to be processed. This processing capacity [m³/s] has to be equal to the flow towards the residence tank, since the residence tank is not allowed to overflow or become drained.

The dataset from Wärtsilä for the “Hydrocyclone” system [12, p. 28] shows that there indeed is a strong relationship between the volume of the centrifuge and the processing capacity. This can also be seen in Figure 39, and equation (5.31) presents the algebraic relationship.

$$Vol_{centrifuge} = 11.17 * \dot{Q}_{exhaust} * R_{L/G} \quad (5.31)$$

For the determination of the mass of the system an average system density based on the “Hydrocyclone” series is used. This average systems density is assumed to be 0.85 [ton/m³]. Which includes the water inside the centrifuge.

$$M_{centrifuge} = Vol_{centrifuge} * \rho_{system} \quad (5.32)$$

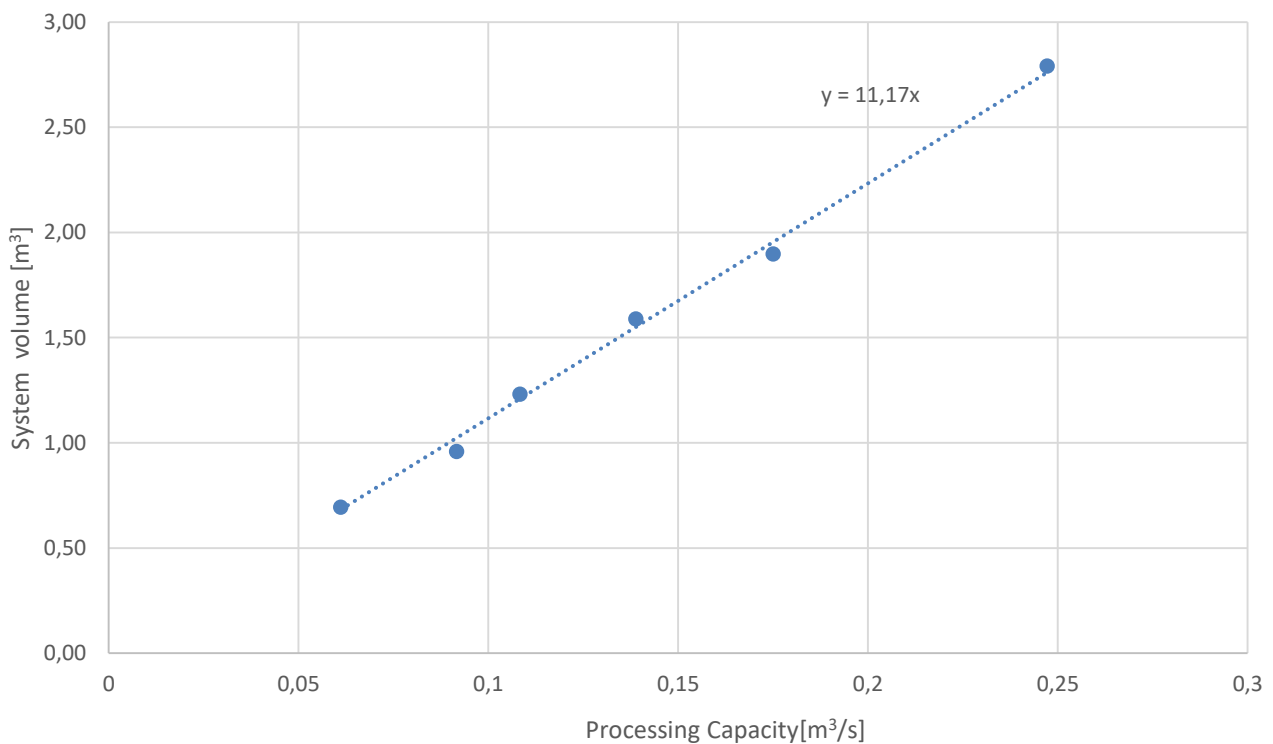


Figure 39: Regression of the ‘Hydrocyclone’ Dataset [12]

Sludge Storage Tank Dimensions

The last component of the scrubber system is the sludge storage tank, which will be designed using the results of the simulation. The minimum required volume of the sludge storage tank can be found using time integration of the sludge volume flux. This flux can be determined using equation (5.33).

$$Q_{sludge}(t) = \frac{SPF}{\rho_{sludge}} * P_b(t) \quad (5.33)$$

The density of the sludge assumed to be 970 [kg/m³] [67]. Which only leaves the Sludge Production Factor to be determined. The amount of sludge produced is dependent on the composition of the scrubbing water (silt/sand content, calcium content, and more), which can vary greatly depending on the area of operation, of which no data is included in this research.

Instead an estimate provided by Wärtsilä is used [12, p. 60], this estimate is 3.5-5 [kg/MWh]. The upper limit of this range is assumed so that a conservative estimate of the required tank volume is made.

The tanks used for sludge are standardized containers of 0.69 [m³]. [12, p. 61] These tanks are used because they can easily be exchanged for empty ones when the vessel is in port. Each of these tanks has an empty weight of 60 [kg] [12, p. 61].

The number of required tanks can be determined using equation, the result of which has to be rounded up towards the nearest integer.

$$\#_{sludge_tanks} = \frac{\int Q_{sludge}(t)dt}{V_{tank}} = \frac{\int Q_{sludge}(t)dt}{0.69} \quad (5.34)$$

The volume and mass of the sludge storage can then be determined using equation (5.35).

$$\begin{aligned} M_{storage} &= M_{tank} * \#_{tanks} \\ V_{storage} &= V_{tank} * \#_{tanks} \end{aligned} \quad (5.35)$$

Verifying the developed dimension prediction model is omitted since the developed dimension prediction method is relies heavily reference scrubbing systems,. Therefore it is only expectable that the tool can estimate these reference vessels.

Power Consumption

Lastly a nominal power requirement of the total system also has to be determined. This power requirement is indicated by Wärtsilä to be approximately 2% of the nominal engine power being scrubbed [12, p. 78].

5.7.3. Selective Catalytic Reduction System

An SCR system is assumed to consist of two components; the SCR reactor and the reagent storage tank and both will have to be dimensioned.

The dimensions of the reactor have to be as such that the system can deal with the highest possible engine load. The dimensions of the reagent storage tank can only be determined after a time based simulation and this will therefore be discussed in chapter 6.

SCR Reactor

The dimensions of the reactor vessel can be determined using equation (5.36). This equation uses the cross sectional area and height of the reactor. The square area of the reactor consists of a (metal) shell and the catalyst (also shown in Figure 40).

$$V_{reactor} = A_{reactor} * H_{reactor} \quad (5.36)$$

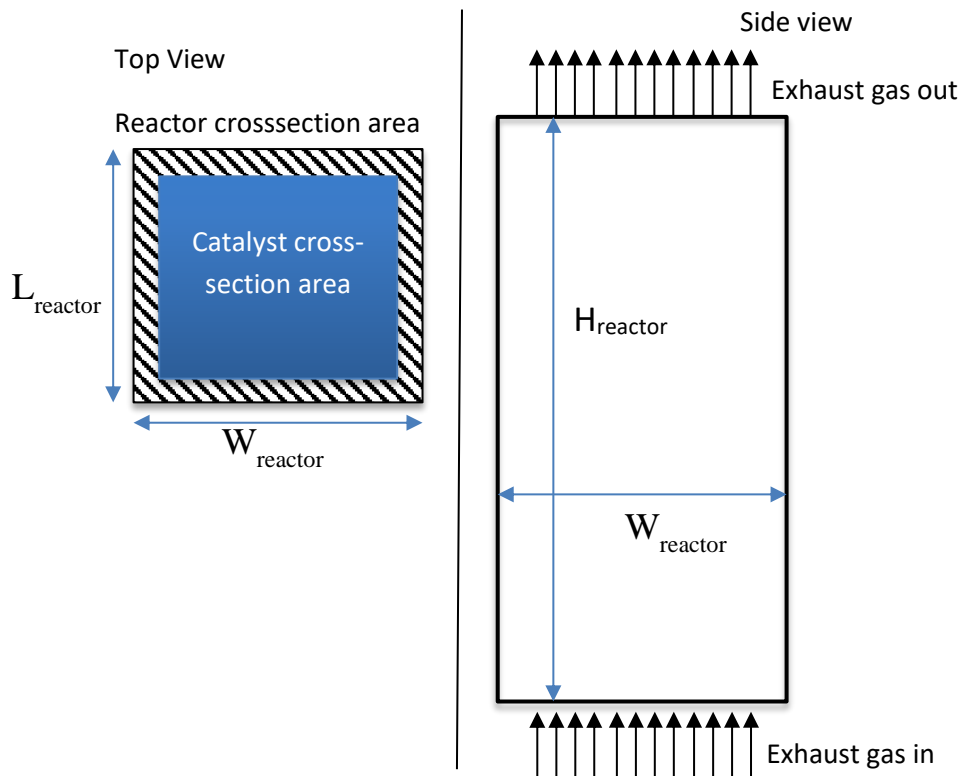


Figure 40: Schematic representation of SCR dimensions

The first step in determining the dimensions of the SCR reactor is the determination of the floor area of the reactor, which can be determined as shown by equation (5.37).

$$A_{reactor} = W_{reactor} * L_{reactor} \quad (5.37)$$

The reactor width and length are defined as shown by equation (5.38), which contain a core dimension (width or length) and a correction factor to account for the auxiliary systems (e.g. the sooth blowing system) and structural elements.

$$\begin{aligned} W_{reactor} &= W_{catalyst} * f_{width} \\ L_{reactor} &= L_{catalyst} * f_{length} \end{aligned} \quad (5.38)$$

By fitting the core dimensions to the smallest SCR system included in a dataset provided by Caterpillar [42] a value of 1.1 is found for both correction factors.

This effectively results in an increase of the square area of 21 %, which is slightly larger, but in the same order of magnitude as a correction factor suggested by the US EPA [68]. However, the correction factor defined by the US EPA is specifically determined for stationary SCR applications. These SCR require less structural rigidity since they encounter far lower (if any at all) loads caused by accelerations. Therefore the increase in correction factor is deemed acceptable.

The two principle dimensions of the catalyst can be determined using equation (5.39). In which the wall thickness (τ_{wall}) of the catalyst is found. This thickness is assumed to be 0.7 [mm] [69].

$$\begin{aligned} L_{catalyst} &= W_{catalyst} = \#_{channels_side} * (D_{channel} + \tau_{wall}) + \tau_{wall} \\ A_{catalys} &= L_{catalyst} * W_{catalyst} \end{aligned} \quad (5.39)$$

The diameter of each channel can be determined using the Reynolds number, which is defined as presented by equation (5.40). A maximum value of 1000 is assumed for the Reynolds number, because SCR's have to operate in the laminar flow regime. [70]

Apart from this Reynolds number, the exhaust gas has a maximum allowable velocity. However, different sources present large variations (0.7 up to 5 [m/s]) in this maximum velocity ([66], [68], [70]). An average value of 2.5 [m/s] is assumed, which should be sufficiently high to prevent excessive sedimentation of particulates and not too high to cause corrosion ([68] & [56]).

$$D_{channel} = \frac{Re_{max} * v_{gas}}{V_{gas_max}} \quad (5.40)$$

This leaves the number of channels per side to be determined. To do so equation (5.41) has to be used to determine the minimum flow area necessary to ensure that the maximum allowable velocity is not exceeded.

$$A_{flow} = \frac{Q_{exhaust}}{V_{gas_max}} = \frac{M_{exhaust}}{\rho_{exhaust} * V_{gas_max}} \quad (5.41)$$

The exhaust gas mass flow was determined previously and the exhaust gas density is assumed to be 1.96 [kg/m³], which is the density of air subjected to exhaust gas conditions caused by an engine running at its nominal rating, these conditions are a temperature of approximately 350 °Celsius and a pressure of 3.5 [Bar] [71].

Assuming the SCR catalyst is square shaped and constructed with square channels [56] results in the minimum amount of channels in a single direction to be determined using equation (5.42).

$$\#_{channels_required} = \sqrt{\frac{A_{flow}}{D_{channel}^2}} \quad (5.42)$$

However, each catalyst layer is also divided into square blocks with a cross section of 150x150 [mm] [70]. This means the number of channels per block is also limited. The number of channels per block can be determined using equation (5.43). The result of this equation has to be rounded down towards the nearest integer, since only whole channels can fit inside the block.

$$\#_{channels_blockside} = \frac{W_{block}}{D_{channel} + \tau_{wall}} = \frac{0.15}{D_{channel} + \tau_{wall}} \quad (5.43)$$

The amount of blocks per side, can be determined using equation (5.44), the result of which has to be rounded up towards the nearest integer, since partial blocks or not possible.

$$\#_{blocks_required} = \frac{\#_{channels_required}}{\#_{channels_blockside}} \quad (5.44)$$

With the number of blocks known, it is now possible to determine the actually installed amount of channels, as shown by equation (5.45).

$$\#_{channels_actual} = \#_{blocks_required} * \#_{channels_blockside} \quad (5.45)$$

This number of channels can now be used to determine the actual catalyst width and length using equation (5.39). Which then results in the surface area of the catalyst and the reactor.

Because the surface area of the catalyst and the reactor have now been determined, the only unknown dimension of the reactor is the height of the reactor.

The height of the reactor is mainly dependent on the height of the catalyst and is expressed as shown by equation (5.46). This equation includes a correction factor (f_{height}), to account for structural elements, a flow straightener and other empty spaces required [42]. Based on schematics obtained from Caterpillar [42] a value of 1.9 is assumed for F_{height} .

$$H_{\text{reactor}} = f_{\text{height}} * H_{\text{catalyst}} \quad (5.46)$$

However, the height of catalyst still has to be determined. To do so a schematic construction of an SCR reactor shown by Figure 41 (based on [42]) is used.

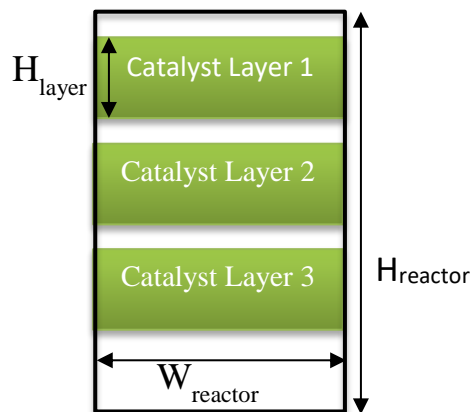


Figure 41: Reactor Construction (derived from [20] & [42])

From the presented figure an expression for the height of the catalyst is derived, which depends on the height of a single layer (assuming that all layers are equal in height) and the number of layers. Each layer comes with a small margin to include the air ducts required for sooth blowing, which is required to prevent excessive buildup of particulates [72]. This margin is assumed to be 30 [cm] per layer (and is obtained by scaling data presented by the US EPA [68]). The height of the catalyst can now be determined using equation (5.47).

$$H_{\text{catalyst}} = \#_{\text{catalyst_layers}} * (0.3 + H_{\text{layer}}) \quad (5.47)$$

Both parameters found in equation (5.47) still have to be determined. This can be done once the total reactive height (indicated by the green areas in Figure 41) is known.

The total reactive height of the catalyst can be determined using equation (5.48). Which requires four new parameters. Which are; the mass flow inside a single channel, a required NO_x removal efficiency, the perimeter of each channel and the overall mass transport coefficient.

The overall mass transport coefficient is assumed to be 0.0140 [$\text{kg}/\text{m}^2\text{s}$] [69], which is the appropriate value for the exhaust gas conditions mentioned earlier in this paragraph.

$$H_{\text{reactive}} = \frac{\dot{M}_{\text{gas_channel}} * \ln(1 - \eta_{\text{no}_x})}{-per_{\text{channel}} * K_{\text{overall}}} \quad (5.48)$$

To determine the perimeter of a single channel and the mass flow of exhaust gas per channel it is first required to determine the hydraulic diameter of each channel, and the total mass of exhaust gas, both of which are shown by equation (5.49).

$$\dot{M}_{gas_channel} = \frac{\dot{M}_{exhaust}}{\#_{channels_actual}^2} \quad (5.49)$$

$$per_{channel} = 4 * D_{channel}$$

So the only unknown variable that still has to be determined in order to design the SCR system is the required NO_x removal efficiency. This efficiency is defined as shown by equation (5.50), in which the 'NO_{x,in}' is the amount of NO_x produced by the engines. The value of 'NO_{x,out}' is assumed to be the maximum allowable emission of NO_x. Both the emission of NO_x and the regulatory limits related to NO_x emissions have been discussed in paragraph 5.7.1.

The required removal efficiency has to be determined for each of the exhaust gas producing machines and the SCR unit will then be designed to meet the highest (required) efficiency.

$$\eta_{no_x} = \frac{NO_{x-in} - NO_{x-out}}{NO_{x-in}} \quad (5.50)$$

Now that all unknown parameters have been determined, it is possible to estimate the reactive height of the catalyst. However, as was already visible in the schematic overview of the catalyst construction (Figure 41), the catalyst is not just one large block of catalyst material. It is instead divided into layers for ease of both transportation and maintenance. Each layer has a standardized height of 60 [cm] (excluding the empty space mentioned earlier) [69] & [70].

The number of layers can then be determined using equation (5.51). The result of which has to be rounded up towards the nearest integer.

$$\#_{layers} = \frac{H_{active}}{H_{layer}} \quad (5.51)$$

The mass of the SCR system consists of the mass of the flow straightener, which is estimated to be 400 [kg] (based on reference SCR data [42]) and an average system density, which includes the catalyst, the structural elements but also the empty spaces. An average system density of 0.25 [ton/m³] is found, again based on reference SCR data [42]. Both terms are shown by equation (5.52).

$$M_{SCR} = M_{static} + \rho_{system} * Vol_{reactor} \quad (5.52)$$

Power Requirement

The nominal power requirement of the SCR system is estimated to be 0.5 % of the power of the engines which deliver exhaust gas to the SCR is connected [68].

Verification

The only thing left to do, during the development of this algorithm, is determining whether this design algorithm correctly estimates the dimensions of the SCR reactor.

For the purpose of validation the algorithm is tested. This is done using the data provided by Caterpillar [42], which consists of both engine and SCR dimensions for several cases. The algorithm is provided with the engine data and the target efficiency of 90 %, which is an often claimed maximum efficiency for SCR systems ([68] & [69]). The predicted dimensions are then compared to those presented by the data obtained from Caterpillar [42].

The results of this comparison are shown in Figure 42 and Figure 43. The designs are decent matches for the presented main dimensions. Although the total spatial requirements do show some large deviations of approximately 30 %. These are mainly significant at low engine powers and some improvement is necessary here.

However, finding additional data to improve the design algorithm has proven difficult. Because the algorithm does correctly predicts when to add a block of channels. And because the algorithm predicts the other principle dimensions with a decent accuracy, the large deviations (which are mainly present in the system mass) are accepted. Though an effort should be made by future research to improve the weight estimate, especially in the low engine power range.

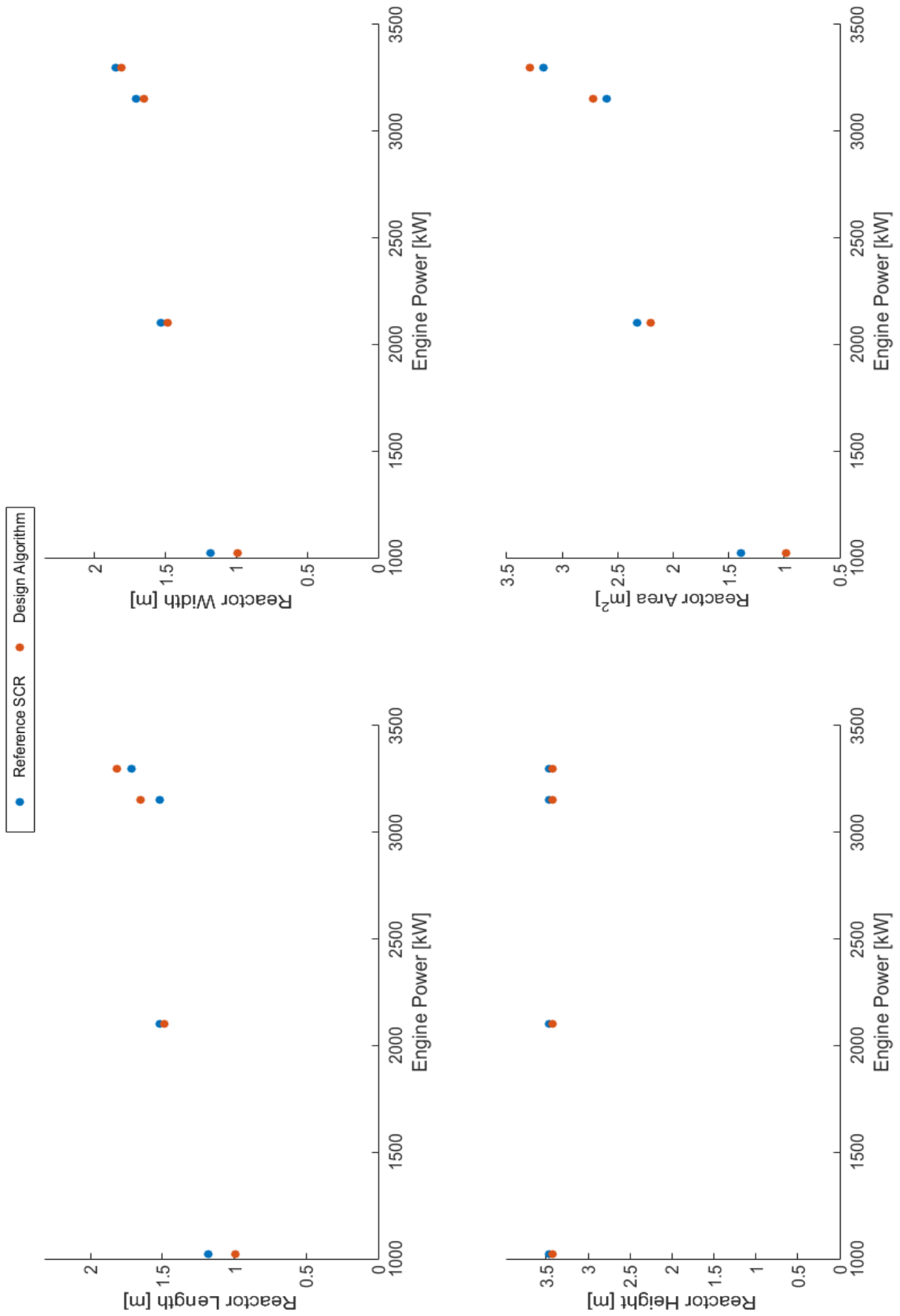


Figure 42: SCR dimension Prediction results - Main dimensions

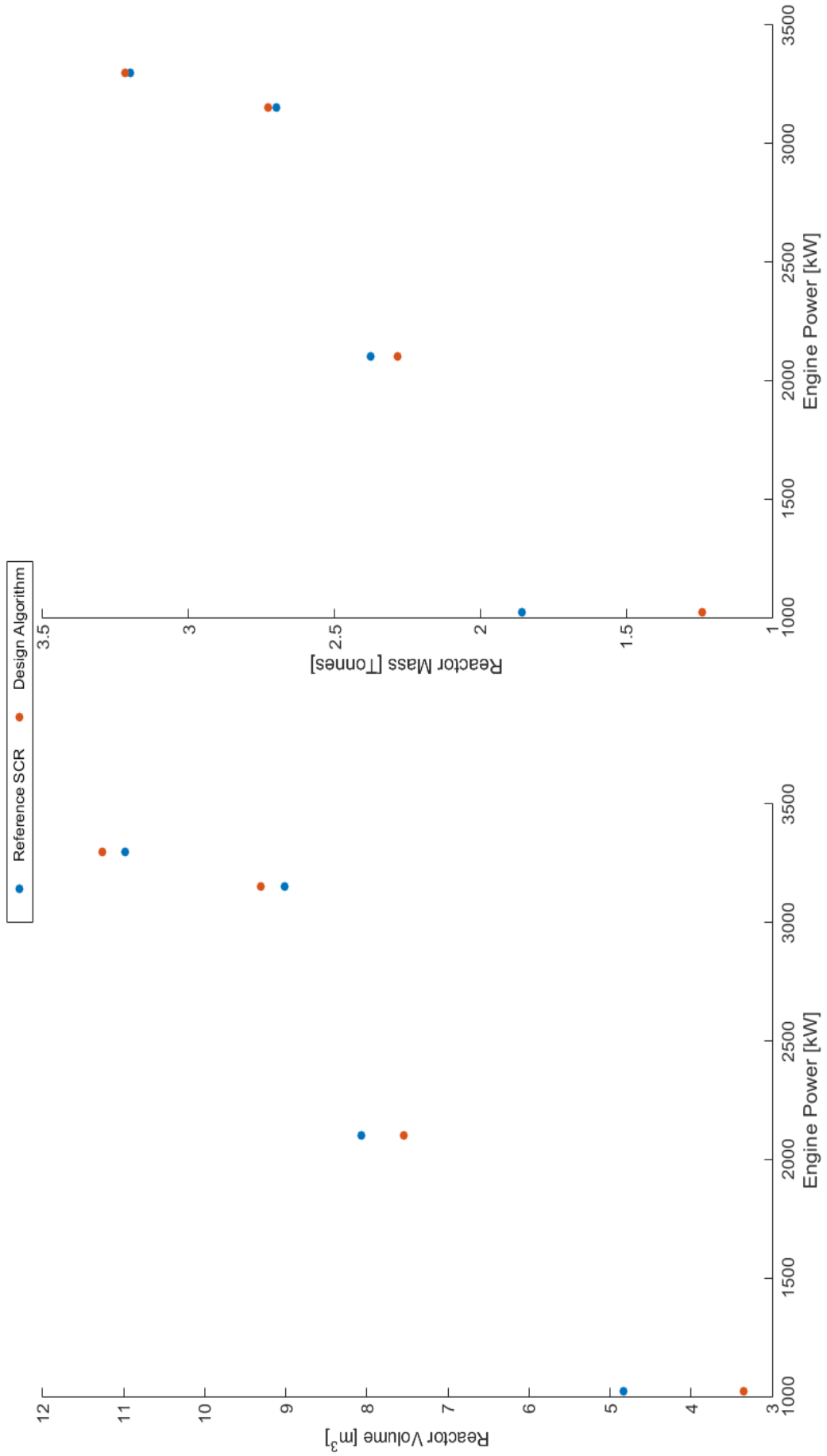


Figure 43: SCR dimension Prediction results - Spatial Requirements.

6. Performance Models

In this chapter the used performance models are discussed. A summary of the available and un-available models is given in paragraph 6.1. Following this summary each of the available models is shortly discussed. The working principles behind the available models are not discussed in depth and interested readers are instead referred to their developers instead. For the system for which a performance model is not available, a simplistic performance estimation is established.

6.1. Existing models

An overview of the required performance models is presented in Table 22. In this table the models which are available to this research have been marked. For the other components, the exhaust gas treatment systems, there is no model available to this research and a performance estimation will be established.

For dual fuel engines no models exist, however these engines are based on similar combustion principles as conventional diesel engines. Therefore it is decided to mark the model as existing and use the model developed for the diesel engines instead. The dual fuel nature of these engines is accounted for in the fuel properties, as discussed in paragraph 5.6.

Gearboxes (both reduction and the shaft configuration gearbox) are not listed here and these are assumed to be constant efficiency 'machines'. The same is applicable for the fuel types, which do not have a variable performance.

Table 22: Availability of performance models for the considered systems

Propulsive Engines	Electric Energy Storage	Electric Power Generation (EPG) System	EGTS 1	EGTS 2
Diesel engines (2- stroke)	Li-Ion Batteries	Fuel Cells (PEMFC)	Selective Catalytic Reduction (SCR)	Scrubbers (Open Loop)
Diesel engines (4- stroke)	Lead-Acid Batteries	Engine driven Generators		
Dual fuel engines (4-stroke)				
Electric motor (PMSM)				

6.1.1. Propulsive Engines

Internal Combustion Engines

For the simulation of the diesel and dual fuel engines the so called ‘Mossel’ model [73] is used. This model uses a set of performance curves to approximate the behavior of an engine.

Originally this model included a method to estimate engine emissions. However, these methods were algebraic functions, fitted to real engine data. Although this approach is accurate enough, it did not allow for a simulation of different engine types. Therefore the methodologies discussed in paragraph 5.7 are used as emission estimate instead.

The performance curves implemented result in a produced torque and engine speed as function of the fuel injection. This injection is then controlled through a PI controller so that the engine model reaches the delivered power required. This then results in a fuel consumption and emissions. The transient behavior of the load and engine are accounted for using equation (6.1).

$$\dot{\omega} = \frac{M_{engine} - M_{load}}{I_{total}} \quad (6.1)$$

In which the load torque is the torque demand from that engine by the propeller. I_{total} represents the total moment of inertia of both the load, the engine and the reduction gearbox combined. The ‘Mossel model’ also includes an estimation of both the engine and gearbox moment of inertia which is dependent on the size and type of those systems. For the moment of inertia of the load (the propeller) a constant value was assumed. As stated earlier, this engine model is also used for simulation of dual fuel engines. However, the fuel dependent parameters are now those of the fuel blend (as discussed in paragraph 5.6).

More complex engine model is also available. This model actually uses the (ideal) combustion processes that occur inside the cylinder and thus finds its foundations in the basic principles of thermodynamics. These models are arguably more accurate than the ‘Mossel model’. However, this model requires a lot more computational power, which is likely to decrease the speed of the entire simulation.

This, combined with the fact that the thermodynamic model requires more parameters, which at this point are not known and thus introduce a lot more uncertainty, make this research use a simplified model.

Permanent Magnet Synchronous Motor

For the simulation of the performance of the PMSM the model developed by ten Hacken [4] is used to determine a normalized engine speed/efficiency and speed/torque curves. Both of which are also presented by ten Hacken [4]. These curves are then used to determine the available engine torque and required electrical power. This simplification is made because the developed first principle model is rather sensitive to the parameters contained within the model and these parameters cannot be accurately determined at this design stage.

The fit model does include some transient behavior, which is modeled using the same principle as discussed for the combustion engines. However, for PMSM no estimation of the moment of inertia was available. The moment of inertia is estimated using the estimated using equation (6.2), in which the density of steel is assumed to be 7860 [kg/m³].

$$I_{engine} = \frac{1}{2} * m_{rotor} * R_{rotor}^2 \quad (6.2)$$

$$m_{rotor} = (\pi * R_{rotor}^2 * L_{rotor}) * \rho_{steel}$$

6.1.2. Electrical Systems

Proton Exchange Membrane Fuel Cell

For the performance estimation of the PEM fuel cell a model has been developed the EFIN project [74]. This model is used for this research as well. With the only alteration that is implemented, is the possibility install multiple fuel cells in parallel.

The used model is based on the polarization curve (see also Appendix G) and already includes the air compressor required for the necessary air supply.

Engine Driven Generators

An engine driven generation system (or genset) consists of two separate systems, the generator and the driving engine. The generator itself is assumed to be a constant efficiency machine, with an efficiency of 95% [3], which is not entirely accurate, however the change in efficiency at part load conditions of the generator are negligible when compared to the change in efficiency of the driving engine.

The driving engine is modeled using the 'Mosel model' discussed earlier. Although the moment inertia of the load is of course different from that of the propulsive power generation engines. An approximation of this is also included in the 'Mosel model' and this approximation is used.

Batteries

For the performance models of the batteries the models developed by Stapersma [46] is used. This model has already been verified and validated by Rietveld [3]. The parameters used for the simulation of both li-ion and lead-acid batteries are all obtained from Rietveld [3].

The simulation of these systems does not have a very large influence on the performance of the other systems, due to the used design methodologies. This influence is reduced further due to the fact that batteries do not consume fuel or emit any of the considered exhaust gases. Although they do influence the NO_x emissions (which are expressed in gram/kwh), since they do deliver power (or kWh).

6.2. Exhaust Gas Treatment Systems

For the exhaust gas treatment systems no suitable models were available for this research. The nominal power consumption of these was previously determined for the maximum load.

This power demand is variable, since the system will not be loaded at the nominal conditions at all times. The assumption is made that there is a direct correlation between the required power of the treatment systems and the loading of the engines of which the exhaust gas is treated. This relationship is also shown by equation (6.3).

$$P(t) = \frac{P_{engine}(t)}{P_{engine_nom}} * P_{egts_nom} \quad (6.3)$$

6.2.1. Scrubbing Systems

The initial assumptions made during the design of the scrubbing system were made in order to guarantee a SO_x removal efficiency of 98%. However, the dimensions were also adjusted for to account for a lower allowable efficiency. This correction is also accounted for during the simulation. Equation (6.4) shows the method used to calculate the emitted SO_x after the scrubber.

$$SO_{x_out}(t) = SO_{x_in}(t) * (1 - \eta_{removal_SOx}) \quad (6.4)$$

The scrubbing efficiency is mainly dependent on the Liquid/Gas ratio and other design parameters. These are assumed to be constant and therefore the scrubbing efficiency is assumed to be constant. Keeping the liquid to gas ratio constant does mean that less scrubbing liquid is required at lower loads. This is translated to the changing power requirements mentioned in the first section of this paragraph.

The production of scrubbing sludge, and the dimension related to the storage of this sludge has been related to the total engine power (in kWh) being scrubbed (see also paragraph 5.7.2). Therefore this sludge production is not included in the performance simulation of the scrubbing system itself and not repeated here.

6.2.2. Selective Catalytic Reduction System

The equation used for the determination of the height of the SCR system can simply be rewritten to express the efficiency as function of the exhaust gas mass flow (as shown by equation (6.5), which in practice is variable over time.

$$\eta_{removal} = 1 - e^{-\frac{k_{mass} * per_{ch} * H_{active}}{M_{exhaust}}} \quad (6.5)$$

However, in practice the mass transfer coefficient is (highly) dependent on the operating temperature [68] & [69], this effect was omitted in the design process by designing the SCR system with a fixed value for the mass transfer coefficient (k_{mass}). However, the exhaust gas temperature can change dramatically during off design conditions as demonstrated by Skogtjärn [71]. Therefore the temperature dependence of the efficiency can no longer be omitted during the performance simulation of the SCR systems. The change in efficiency due to the operating temperature is accounted for using a correction factor (F_{eta}), as shown by equation (6.6).

$$\eta_{removal,corrected} = (1 - F_{eta}) * \eta_{removal} \quad (6.6)$$

The correction factor is determined using reference SCR data [68] & [75], which is presented by Figure 44. During the simulation linear interpolation will be used to determine values which do not coincide with the available data.

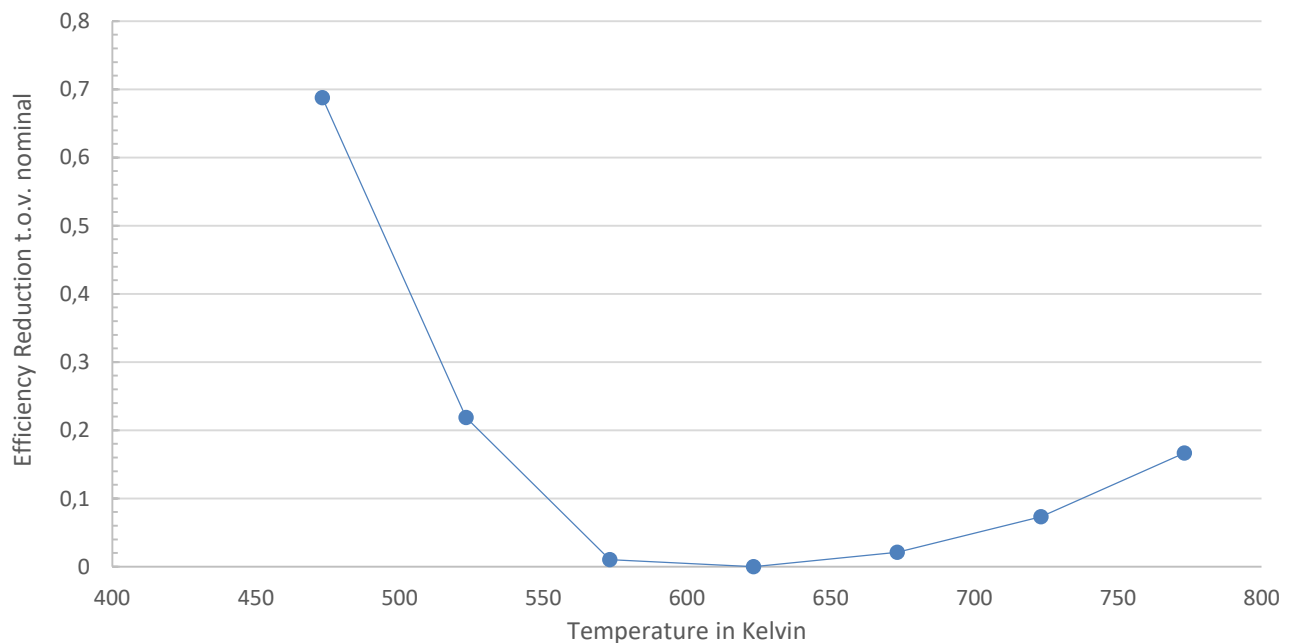


Figure 44: SCR Efficiency Correction factor as function of Temperature

The operating temperature of the SCR is equal the temperature of the exhaust gas, which can be estimated using equation (6.7) [71]. The exhaust gas mass flow has been determined earlier and the specific heat at constant pressure of the exhaust gas is 813 [J/kgK]. The inlet temperature of air is assumed to be 328 [K], which is the minimum air inlet temperature for normal engine operation according to MAN Diesel [76].

$$T_{exhaust} = T_{inlet} [K] + \frac{\sum_{n=1}^3 Q_{5-1_n}}{\sum_{n=1}^3 \dot{M}_{exhaust_n} * c_{p,exhaust}} \quad (6.7)$$

With Q_{5-1} being the total heat added to the exhaust gas, by the combustion engine. However, this a value for this added heat is not determined by the used engine models and an approximation is required.

The total heat transferred to the exhaust gas can be estimated using the overall engine efficiency, which is known, since all exhaust gas producing machinery has been designed prior to this design step, and the part-load efficiencies are determined by the performance models.

It is assumed that approximately 75% (F_{split}) of the provided heat ends up in the exhaust gas, this ratio is higher than is normally the case (where approximately 50% of the heat losses are found in the exhaust gas.) However, to account for both the heat losses and the fact that the engine outlet temperature is higher than the inlet temperature the value for F_{split} is assumed higher. The heat provided to the exhaust gas can then be determined using equation (6.8).

$$Q_{51_estimate} = P_{break}(t) * (1 - \eta_{engine}(t)) * F_{split} \quad (6.8)$$

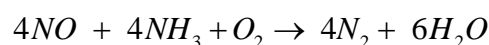
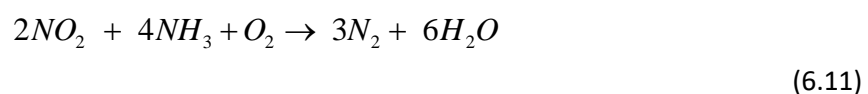
The total NO_x emissions can now be determined by a time integration of the emitted NO_x , which is determined using equation (6.9).

$$NO_{x_out}(t) = NO_{x_in}(t) * (1 - \eta_{removal,corrected}) \quad (6.9)$$

Reagent Consumption

And lastly an estimate of the required reagent storage capacity has to be made. This capacity can be determined by integrating the usage rate of the reagent over time. This usage rate can be determined using equation (6.10). This equation is related to the chemical reaction(s) taking place in the SCR system, which are shown by equation (6.11).

$$m_{ammonia}(t) = \frac{NO_{x_in}(t) * \eta_{removal,corrected}}{MW_{NO_x}} * SR * MW_{reagent} \quad (6.10)$$



In equation (6.10) three previously unmentioned parameters are found. The first of these is the Stoichiometric Ratio (SR). This ratio prescribes the number of moles of (pure) ammonia that is required for the removal of 1 mole of NO_x. Based on the chemical reactions presented by equation (6.11), this ratio is determined to be '2'. Which is the ratio required for the removal of NO₂, and this is the highest stoichiometric requirement and thus ensures enough ammonia will be present for the SCR to operate.

The Molecular Weight (MW) of both the NO_x and the reagent are also required, the MW of NO₂ is 46.01 [g/mole]. This value is used since NO₂ is largest fraction of the emitted NO_x.

The MW of the reagent is equal to the molar weight of ammonia, which is 17.03 [g/mole]. Thus the usage rate of pure ammonia in [g/s] is now known.

This can then be used to determine the total amount of ammonia that has to be stored and from that the spatial requirements caused the storage of ammonia.

Once determined, the volume and mass of the reagent storage are added to the system- mass and volume of the SCR system. The reagent consumption is added to the fuel consumption, since the SCR reagent is also a consumable (and possibly a fuel).

7. Results

In this chapter the results of the concept exploration process are presented for each of the three cases defined in chapter 4. To do so, the first paragraph will summarize the method used for the final multi criteria analysis. Following the final MCA, the results for each of the three ship types are presented in the second, third and fourth paragraph respectively. Each of these paragraphs consists of two sub-paragraphs. The first of which presents the power plant configurations that are selected based on each of the characteristics individually (i.e. before the final MCA). The second sub-paragraph presents the optimal power plant configuration concept selected by the final MCA. The final paragraph of this chapter presents the sensitivity analysis and its results.

The presented results will not include the detailed design data determined by the intermediate algorithms. Because the tool is developed to be a concept exploration tool. To ensure the results of this tool do not create (subconscious) constraints for future designs phases, the selected power plant configuration is described using the definitions found in chapter 2 and 3.

7.1. Final Multi Criteria Analysis

The first step in the multi criteria analysis is the verification whether a designed and simulated configurations meets the emission limits (as they are discussed in paragraph 5.7.1). Doing so seems redundant since the installation of exhaust gas treatment systems and/or primary emission reduction methods should guarantee that this happens. However, due to part-load conditions the performance of the EGTS designs could be reduced causing the emissions to exceed the regulatory limits.

Therefore this constraint remains important in order to guarantee the regulatory compliance of the created power plant designs.

The final multi criteria analysis is executed after the configurations which do not meet the emission limits have been removed. This analysis follows the same procedure as discussed in paragraph 5.1. However, there are three types of emissions (NO_x , SO_x and CO_2) on which a concept can be judged and only one MCA weight factor related to emissions. Using the specified weight factor for each emission would cause the importance of the weight factor to become too large. To prevent this from happening, the weight factor is evenly divided over the three emissions. This leads to the client preference being defined as shown by equation (7.1) for the final MCA. The remainder of the MCA then follows the same logic as the intermediate design choices, which has been discussed in paragraph 5.1.

$$\begin{aligned}
 WF_{fuel} &= WF_{fuel} \\
 WF_{NOX} &= \frac{1}{3} * WF_{emissions} \\
 WF_{SOX} &= \frac{1}{3} * WF_{emissions} \\
 WF_{CO2} &= \frac{1}{3} * WF_{emissions} \\
 WF_{mass} &= WF_{mass} \\
 WF_{volume} &= WF_{volume}
 \end{aligned} \tag{7.1}$$

7.2. General Cargo Vessels

This paragraph presents the results for the general cargo vessel case, for which the input values were defined in chapter 4. The first sub-paragraph will present the configurations, which are optimal for each of the separate characteristics. The second sub-paragraph will then present the selected power plant configuration.

7.2.1. Optimal Configuration per characteristic

The power plant configurations, which are selected when a selection is made based on a single characteristic, are presented in Table 23, which also includes the numerical results for each of those configurations.

When examining these results, and the ones found for other ship types, it is important to be aware of the fact that there are concepts which have identical numerical results for one characteristic. The tool still selects a specific concept from those concepts with identical results. An example of this phenomenon is seen for the configurations selected for fuel consumption and emissions as shown by Table 23. Both concepts have identical results for the emissions (a value of zero), yet a different power plant concept is selected for both. This is caused by the fact that the algorithm ranks concepts with equal results according to the order they are found in the library of feasible concepts. This means that the first concept with zero emissions encountered in the library is assigned the highest rank, with following concepts (with zero emissions) receiving a (slightly) lower ranking for emissions.

This effect is also expectable for the other ship types, since the numerical results for emissions and fuel consumption are not dependent on the user defined input, due to the systems in these configurations.

Table 23: Optimal Concepts, per characteristic, Cargo Vessel

		Optimal Concept per Characteristic			
		Fuel Cons.	Emissions	Mass	Volume
Component	Shaft Configuration	Single Shaft	Single Shaft	PTI	Single Shaft
	MPE - Engine Type	PMSM, Direct	PMSM, Direct	4-stroke DE, Geared	2-stroke, Geared
	MPE - Main Tank	-	-	MDO	MDO
	MPE - Sec. Tank	-	-	-	-
	PTI- Engine Type	-	-	4-stroke DE, Geared	-
	PTI - Main Tank	-	-	MDO	-
	PTI - Sec. Tank	-	-	-	-
	Generation System	-	PEM Fuel Cell	Diesel Genset	Diesel Genset
	Genset – Main Tank	-	-	MDO	MDO
	Genset – Sec. Tank	-	-	-	-
	Hydrogen Storage	-	Pressurized Hydrogen	-	-
	Electrical Energy Storage	Li-Ion Batteries	Li-Ion Batteries	-	-
	NOX Reduction	-	-	SCR	SCR
	SOX Reduction	-	-	Open Loop, Scrubber	Open Loop, Scrubber
Numerical Results	Fuel Cons. [Tonnes]	0	205.4	520	484
	Emissions : NO _x /SO _x /CO ₂ [g/kwh]/[g/kg fuel]/[tonnes]	0/0/0	0/0/0	11.3/2/1656	4.4/2/1503
	System Mass [tonnes]	238277	4474	159	258
	System Volume [m ³]	14926	5530	800	785

For the cases where a concept would be selected purely on fuel consumption or emissions then a power plant with electric propulsion, without engine driven generation is selected. This is unexpected, since an optimization towards these characteristics, implies that the highest possible efficiency is preferred. Which is exactly where electric propulsion loses to ICE based propulsion, due to additional conversion losses [8]. However, once the other systems in the configuration are examined, the reason for electric propulsion can be found. The selected power plant configurations capitalize on the fact that electricity can be generated (or stored) without emissions (or fuel consumption). Given the spatial requirements of these configurations (which were included in Table 23) it is not likely that these configurations will be selected as optimal power plant configuration, even though fuel consumption is rated to be very important.

The optimal concepts for volume or mass alone are both pure diesel engine driven concepts, equipped with both exhaust gas treatment systems. The inclusion of a PTI system is remarkable for a cargo vessel, since its operational profile is not really suited for one. [8]

The selection of diesel engine driven concepts is expectable, since diesel fuels have the highest energy density [MJ/m³] of all considered fuels, although the disregard of HFO as fuel is unexpected, especially for a concept which is selected based on volume alone. This could be due to the fact that MDO requires a smaller scrubber (as discussed in paragraph 5.7) and thus become more interesting.

Another remarkability is the application of both treatment systems. This is theoretically possible, but not seen in practice (yet) due to the large initial investments. It is however not unthinkable that this combination of treatment systems becomes a feasible (retrofit) option for ship owners once the implemented emission regulations come into force.

7.2.2. Optimal Configuration

The selected, optimal, configuration contains the components listed in Table 24. In this table the installed power of the different systems is also included. To enable a relationship between the components and the operational profile to be established. The numerical results for the different characteristics are shown in Table 25. These numerical results are mainly interesting for validation purposes, and should not be used as design requirements, since the accuracy of the results has not been validated.

Table 24: Components, optimal Configuration, Cargo Vessel

	Node Name	System
Component	Shaft Configuration	Single Shaft
	MPE - Engine Type	2- stroke DE, Direct (11.9 MW)
	MPE - Main Tank	MDO
	MPE - Sec. Tank	-
	PTI- Engine Type	-
	PTI - Main Tank	-
	PTI - Sec. Tank	-
	Generation System	PEMFC (618 kW)
	Genset – Main Tank	-
	Genset – Sec. Tank	-
	Hydrogen Storage	Pressurized Hydrogen
	Electrical Energy Storage	-
	NOX Reduction	SCR
	SOX Reduction	Scrubber

Table 25: Numerical Results Selected Configuration, Cargo Vessel

Characteristic	Value	Unit
Fuel Consumption	447	[ton]
NO _x emissions	7.24	[gram/kWh]
SO _x emissions	2	[gram/kg fuel]
CO ₂ emissions	1370	[ton]
System Mass	614	[ton]
System Volume	1153	[m ³]

The selection of a single shaft configuration driven by an internal combustion engine is expectable. Since this type of propulsion chain is the most common one found in cargo vessels, since these are highly fuel efficient [8, p. 106]. The fact that the concept exploration tool selects this type of propulsion chain (given the specified operational profile and characteristics) gives some initial confidence in the working principles of developed tool.

What is unexpected is the fact that a 2-stroke diesel engine combined with both exhaust gas treatment systems is favored over the application of a dual fuel engine. A likely explanation for this the fact that the storage requirements of the gaseous fuel (which is required for dual fuel engines) are more severe than the spatial requirements of both exhaust gas treatment systems.

Another explanation could be the fact that the large costs necessary to install both exhaust gas treatment systems are not included as a tradeoff.

Although, the inclusion of costs could also increases the likelihood of HFO being selected as fuel (since HFO is a relatively cheap fuel [8]), which in turn would require a scrubber. Because of the tradeoff between fuel price and system costs (such as the one mentioned earlier), it is especially interesting to keep both investments (purchase) separate from operational costs.

The application of a fuel cell as generation system is not expected since these are not yet found in practice. Instead it was expected that a diesel driven genset would be installed, since these gensets are by far the most commonly applied method to supply electric power [8, p. 115]. However, the fact that a fuel cell was not expected, because in practice other generation systems are used, is somewhat skewed. Since fuel cells are not as mature as other generation systems and have therefore less time to be included in ship design.

The favoring of a fuel cell over an engine driven genset is likely due to the fact that fuel consumption is measured in tonnes. Which is where hydrogen beats all the other fuels, since it is (by itself) very light (see also paragraph 5.6) and the high preference towards fuel consumption causes the tool to minimize the fuel mass.

In general the selected power plant configuration matches the expectations. And possible unexpected results can be explained. Both these considerations grant some initial confidence in the working principles of the newly developed concept exploration tool. Although other ship types will have to be investigated as well before a final verdict on the working principles of the tool can be given.

Additionally the numerical values seem to be of the right order of magnitude for an initial estimate. As can be seen from the fact that according to the operational profile a total of 2.548.086 [kWh] of power is required, which can be delivered with 447 tonnes of fuel.

This translates to an average fuel consumption of 175 [gram/kWh], which is a decent value for a completely engine driven systems [8, p. 136].

In this case averaging the fuel consumption and comparing that average to another reference, is a slightly skewed comparison, since a fuel cell is not engine driven and hydrogen is a lot lighter than the consumed diesel fuel. However, given the large difference between the propulsive power (11 MW) and the electric power (618 kW) (see also Table 24) the error made by averaging the results of the considered configuration, to an existing engine based one is relatively small.

The emissions of NO_x are low, when compared to commonly found values, which are between 6 and 22 [g/kWh] [8, p. 212] (and the NO_x emissions of 2-stroke diesel engines normally in the upper regions of this range). These low emissions are however expectable since the power plant configurations are force to comply with the most stringent emission regulations, such as the Tier III NO_x emissions (see also paragraph 5.7).

7.3. Harbor Tug

This paragraph presents the results for the harbor tug case, for which the input values were defined in chapter 4. The first sub-paragraph will present the configurations, which are optimal for each of the separate characteristics. The second sub-paragraph will then present the selected power plant configuration.

7.3.1. Optimal Configuration per characteristic

The power plant configurations, which are selected when a selection is made on one characteristic alone, are presented in Table 26. The numerical results are harder to verify for these vessels, since numerical values from reference vessels is very scarce. This verification is complicated further by the fact that there is more variation in both the operational profile and the applied power plant configurations. Therefore it is likely that the results cannot be verified using reference power plant configurations alone. Therefore more fundamental (marine engineering based) knowledge is likely necessary to verify whether these results are indeed feasible.

Table 26: Optimal Concepts, per characteristic, Harbor Tug

		Optimal Concept per Characteristic			
		Fuel cons.	Emissions	Mass	Volume
Component	Shaft Configuration	Single Shaft	Single Shaft	Single Shaft	Single Shaft
	MPE - Engine Type	PMSM, Direct	PMSM, Direct	4-stroke DE, Geared	4-stroke DE, Geared
	MPE - Main Tank	-	-	MDO	MDO
	MPE - Sec. Tank	-	-	-	-
	PTI- Engine Type	-	-	-	-
	PTI - Main Tank	-	-	-	-
	PTI - Sec. Tank	-	-	-	-
	Generation System	-	PEM Fuel Cell	PEM Fuel Cell	PEM Fuel Cell
	Genset – Main Tank	-	-	-	-
	Genset – Sec. Tank	-	-	-	-
	Hydrogen Storage	-	Pressurized Hydrogen	Pressurized Hydrogen	Pressurized Hydrogen
	Electrical Energy Storage	Li-Ion Batteries	Li-Ion Batteries	-	-
	NOX Reduction	-	-	SCR	SCR
	SOX Reduction	-	-	Open Loop, Scrubber	Open Loop, Scrubber
Numerical Results	Fuel Cons. [Tonnes]	0	0.5	1.2	1.2
	Emissions : NO _x /SO _x /CO ₂ [gr/kwh]/[g/kg fuel]/[tonnes]	0/0/0	0/0/0	4.6/2/3.4	4.6/2/3.4
	System Mass [tonnes]	110	55	33	33
	System Volume [m ³]	92	60	43	43

The first interesting results observable in Table 26 are the selected configurations when judging on either emissions or fuel consumption alone. These are the same as the configurations selected for the cargo vessel case. This is expectable, since their selection is caused by the ranking methodology as discussed in paragraph 7.2.1. Although relatively high, the spatial requirements are more feasible than those of the cargo carrier case. This is an indication that for vessels with a short mission (or low power requirements) battery powered configurations might be interesting alternatives, which has also been suggested by the ITF [1].

For a selection based on mass or volume alone the concepts which are selected are identical to each other, and different from those selected for the cargo vessel. The fact that both are identical is somewhat unexpected, since this was not the case for the cargo vessel. Again HFO is not selected as fuel type, which could be due to the same reasons as discussed for the cargo carrier, but, given the preferences of this case, also due to the fact that HFO is more polluting than other fuels.

7.3.2. Optimal Configuration

The selected, optimal concept, contains the components listed in Table 27, which also presents the installed power of the different systems, so that a relationship between the components and the operational profile can be established. The numerical results for the different characteristics are shown in Table 28.

Table 27: Components, optimal Configuration, Harbor Tug

	Node Name	System
Component	Shaft Configuration	PTI
	MPE - Engine Type	PMSM, Direct (1.2 MW)
	MPE - Main Tank	-
	MPE - Sec. Tank	-
	PTI- Engine Type	Dual Fuel Engine, Geared (1.2 MW)
	PTI - Main Tank	MDO
	PTI - Sec. Tank	LNG
	Generation System	PEM Fuel Cell (1.2 MW)
	Genset – Main Tank	-
	Genset – Sec. Tank	-
	Hydrogen Storage	Pressurized Hydrogen
	Electrical Energy Storage	-
	NOX Reduction	-
	SOX Reduction	-

Table 28: Numerical Results Selected Configuration, Harbor Tug

Characteristic	Value	Unit
Fuel Consumption	0.55	[ton]
NO _x emissions	0.35	[gram/kwH]
SO _x emissions	0.02	[gram/kg fuel]
CO ₂ emissions	0.68	[ton]
System Mass	48	[ton]
System Volume	56	[m ³]

Given the defined operational profile it is expectable that a PTI is selected [8, p. 111]. The installation of an electrical MPE and a dual fuel engine PTI (instead of the other way around is given the high preference towards emissions also expectable, because the running (and thus emitting) hours of the combustion engine are minimized.

The fact that a 4-stroke engine is selected for the power-take in is also expectable, given the higher power density of these engines [8] (but also (implicitly) seen in Appendix E) and the weight factors related to the spatial requirements.

The selection of a fuel cell based generation system is somewhat expectable since both emissions and fuel consumption were assigned relatively high weight factors and both of which are important pros of fuel cells. Because very little reference data is available the numerical results are not very useable. Although A comparison between the smallest configuration (the one selected for mass/volume alone) to the selected configuration shows that a low emission tug can be designed without severe increases in dimensions.

7.4. Trailing Suction Hopper Dredgers

This paragraph presents the results for the trailing suction hopper dredger case, for which the input values were defined in chapter 4. The first sub-paragraph will present the configurations, which are optimal for each of the separate characteristics. The second sub-paragraph will then present the selected power plant configuration.

7.4.1. Optimal Configuration per characteristic

Again the concepts for both fuel consumption and emissions are identical to those selected for other cases. Which is still expectable, since these configurations will always have zero emissions / zero fuel consumption, due to the components in those systems.

Comparing the configuration that is selected for mass and volume to those selected for the other ship types show that again different configurations are selected. Especially interesting is the switch from fuel cell to engine driven genset, when a comparison is made with the results of the harbor tug case.

Apparently fuel cells are more interesting for lower power demands, while for higher powers gensets become more interesting. This is reasonable, since for higher powers the fuel tank mass becomes the dominant part of the system mass (which is in favor of diesel fuels), while for lower powers this is the generation system mass (which favors the lighter fuel cell). This is another indication of the influence of the operational profile.

The fact that the exhaust gas treatment systems are not installed in these concepts expectable since the most lenient emission regulations are applied to this this case.

Table 29: Optimal Concepts, per characteristic, TSHD

		Optimal Concept per Characteristic			
		Fuel cons.	Emissions	Mass	Volume
Component	Shaft Configuration	Single Shaft	Single Shaft	Single Shaft	Single Shaft
	MPE - Engine Type	PMSM, Direct	PMSM, Direct	4-stroke DE, geared	4-stroke DE, geared
	MPE - Main Tank	-	-	MDO	MDO
	MPE - Sec. Tank	-	-	-	-
	PTI - Engine Type	-	-	-	-
	PTI - Main Tank	-	-	-	-
	PTI - Sec. Tank	-	-	-	-
	Generation System	-	PEM Fuel Cell	DE Genset	DE Genset
	Genset – Main Tank	-	-	MDO	MDO
	Genset – Sec. Tank	-	-	-	-
	Hydrogen Storage	-	Pressurized Hydrogen	-	-
	Electrical Energy Storage	Li-Ion Batteries	Li-Ion Batteries	-	-
	NOX Reduction	-	-	-	-
	SOX Reduction	-	-	-	-
Numerical Results	Fuel Cons. [Tonnes]	0	46	127	127
	Emissions : NO _x /SO _x /CO ₂ [gr/kwh]/[g/kg fuel]/[tonnes]	0/0/0	0/0/0	11.7/4 /403	11.7/4 /403
	System Mass [tonnes]	6202	1854	221	221
	System Volume [m ³]	4051	1981	407	407

7.4.2. Optimal Configuration

The selected, optimal configuration, contains the components listed in Table 30, which also presents the installed power of the different systems, so that a relationship between the components and the operational profile can be established. The numerical results for the different characteristics can be found in Table 31.

Table 30: Components, optimal Configuration, TSHD

	Node Name	System
Component	Shaft Configuration	PTI
	MPE - Engine Type	PMSM, Direct (8.8 MW)
	MPE - Main Tank	-
	MPE - Sec. Tank	-
	PTI- Engine Type	Dual fuel, Geared (2.2 MW)
	PTI - Main Tank	MDO
	PTI - Sec. Tank	LNG
	Generation System	PEM Fuel Cell (23 MW)
	Genset – Main Tank	-
	Genset – Sec. Tank	-
	Hydrogen Storage	Pressurized Hydrogen
	Electrical Energy Storage	-
	NOX Reduction	-
	SOX Reduction	-

Table 31: Numerical Results Selected Configuration, TSHD

Characteristic	Value	Unit
Fuel Consumption	59	[ton]
NO _x emissions	0.17	[gram/kwH]
SO _x emissions	0.01	[gram/kg fuel]
CO ₂ emissions	44	[ton]
System Mass	1053	[ton]
System Volume	1380	[m ³]

The selection of a power take in based propulsion system is somewhat unexpected, since the overall efficiency of PTI based configurations is lower than the efficiency of a single shaft configuration and a relatively high weight factor was assigned to fuel consumption (and therefore implicitly to efficiency).

Although unexpected, the selection of a PTI is not unreasonable, since a single shaft configuration would cause either a large propulsion generation system in combination with a large electricity generation system (since both power demands are quite high) or an even larger electricity generation system than is required for the selected configuration.

The selected PTI configuration (a PMSM as main propulsive engine and a dual fuel engine as PTI, as seen in Table 30) combines the application of electric propulsion, while still keeping the electricity generation systems from becoming excessively large in terms of installed power.

Additionally, the most load variations are present for the PMSM, which suffers less from part load conditions than the dual fuel engine. Which could be an important reason for the selection of a PMSM as Main engine, and a combustion engine as power take in, instead of the other way around.

The application of a dual fuel engine (instead of any other engine type) as power take in engine is expectable, given the relatively high weight factor for emissions.

The selected generation system (a PEM fuel cell) is, given the relatively high preferences towards fuel consumption and emissions, also expectable, since hydrogen is a light fuel and fuel cells do not emit any of the considered exhaust gasses, resulting in a zero emission electricity generation system. Although it should be noted that the application of fuel cells (especially of this size) is not (yet) seen in practice [77].

Instead the most commonly applied generation system on board these vessels are still the (diesel) engine driven gensets. However, the increase in environmental awareness (as discussed in chapter 1) do make a shift towards fuel cells likely.

Interesting to note, is that the emission regulations applied to case are the most lenient of all cases, and the tool still selected a power plant configuration, which also has the potential to meet more stringent demands without any retrofitting.

As a final note to the selected configuration is that it is certainly not the only option for dredgers. The selection of this configuration is strongly related to the assumption that the dredging pumps are driven using electric motors. Which increases the electrical power demand quite dramatically, which in turn creates a stronger tradeoff between propulsion and electrical power demand.

In practice electrically driven pumps can be found, but a PTO + CPP configuration or diesel engine driven pumps are far more common. Especially the PTO + CPP configuration is very common in industry. So common in fact that a designer will have to make a very strong case before a dredging company will turn away from CPP based configurations [29].

The fact that the selected configuration is not likely to be accepted for a TSHD [29] is an indicator of the fact that it should be beneficial for the tool to be expanded, so that a CPP and/or PTO system is considered as well.

7.5. Remarks

From the obtained results, a tendency towards the application of fuel cells can be recognized, since all configurations selected after the final MCA contain one. This is likely due to the excellence in term of fuel consumption (when measured in tonnes, as it is during this research) and emissions.

Another cause could be the fact that an important downside of a PEMFC (the storage requirements of pure hydrogen) is never assigned a weight factor that is higher than others.

This tendency towards fuel cells also gives rise to some initial (preliminary) recommendations, which are presented below.

The first and foremost recommendation is to replace, or supplement, the indication of fuel consumption with a dimensionless parameter, such as an overall system efficiency. This would reduce the impact of the fact that hydrogen is a very light fuel. Therefore changing the indication of fuel consumption would level the playing field for other generation systems and allow for a fairer tradeoff in the PEMFC/ genset electricity generation system.

Another remark is that the tool not been constrained in terms of state of the art limits. An example of which is the fact that the largest (immobile) PEMFC based power plant ever created is approximately 2 [MW] [77]. This limit has not been implemented, since there is no fundamental reason as to why this limit could not be extended. However, extending this limit is likely going to be a very costly process and it is not unthinkable that a ship owner might not want to be the (first) one to invest in such a process.

Another preliminary recommendation that could level the playing field for other (non-fuel cell based) generation systems is the fact that fuel cells are not as mature as other technology and as such the costs of designing and installing them could be rather high. This major downside of fuel cells is not accounted for during the design and selection process since costs (both purchase and operational costs (or CAPEX and OPEX) are not included as a criterion.

Including these terms as characteristics allows for more tradeoffs to be considered, and should therefore result in more reliable results.

An added benefit of the inclusion of costs, is that it allows for a better tradeoff between the different fuel types, such as MDO, which more expensive but cleaner and HFO which is cheap and 'dirty'. [8]

7.6. Sensitivity Analysis

The sensitivity analysis focusses on the influence of the client's preferences and not on the influence of the operational profile. Therefore the analysis can be done for one ship type, by executing the concept exploration methodology, while keeping all input values, except the client preferences constant.

For this analysis the cargo carrier case is used, the input parameters of which were determined in chapter 4. The MCA weight factor for each characteristics is varied between 1 and 10 with increments of 3 and preferences close to their original values are omitted. This leads to three additional variations per characteristic. This creates four different datasets, each of contains three different variation to the original benchmark case. The client preferences for the newly created cases are presented in Table 32, along with the original case.

Table 32: Used Cases for the Sensitivity Analysis

Case:	Weight Fuel Consumption	Weight Emissions	Weight Mass	Weight Volume
Original:	10	0	5	7
A.	1	0	5	7
B.	4	0	5	7
C.	7	0	5	7
D.	10	4	5	7
E.	10	7	5	7
F.	10	10	5	7
G.	10	0	1	7
H.	10	0	7	7
I.	10	0	10	7
J.	10	0	5	1
K.	10	0	5	4
L.	10	0	5	10

For each of the defined variations, the numerical results will be compared to the original case. This is done for each characteristic individually and these comparisons are presented in the form of a scatter diagram.

This results in a total of 6 scatter diagrams per varied weight factor and a total of 24 scatter diagrams. An example of such a scatter diagram is presented in Figure 45 and discussed in the remainder of this paragraph. After the discussion of the example results, all cases are discussed. The corresponding scatter diagrams are however not presented in the main body of this report and interested readers are referred to Appendix H instead. The general lay-out of the scatter plots is presented using the example results found in Figure 45.

The x-axis of each scatter diagram represents the concept number, which is a reference to the concept library. This number alone gives very little information about the power plant configuration, making a somewhat obsolete parameter to plot against. However, it does enable a (graphical) comparison of each individual concept under the influence of the changing client preferences.

The y-axis of the scatter diagrams shows the change (delta) in the considered characteristic, expressed as a percentage with respect to the original benchmark case. The value of which can be determined using equation (7.2), in which 'X' is the characteristic under consideration.

$$\delta_{X,case} = \frac{X_{case} - X_{original}}{X_{original}} * 100 \quad (7.2)$$

The example presented in Figure 45 shows a magnified version of the scatter diagram found in appendix H. Figure 45 shows the change in fuel consumption, under the influence of a changing weight factor for fuel consumption (Case A, B and C in Table 32). In the title of each figure it is mentioned which weight factor is changed, and which characteristic is shown.

The presented magnification does show some interesting patterns, but does omit some extreme spikes. However, because this figure is mainly included to present the way the created diagrams can be read this is not a problem. Instead the omitted spikes and the patterns which are shown, are discussed in the sub-paragraph dedicated to a changing MCA weight factor for fuel consumption.

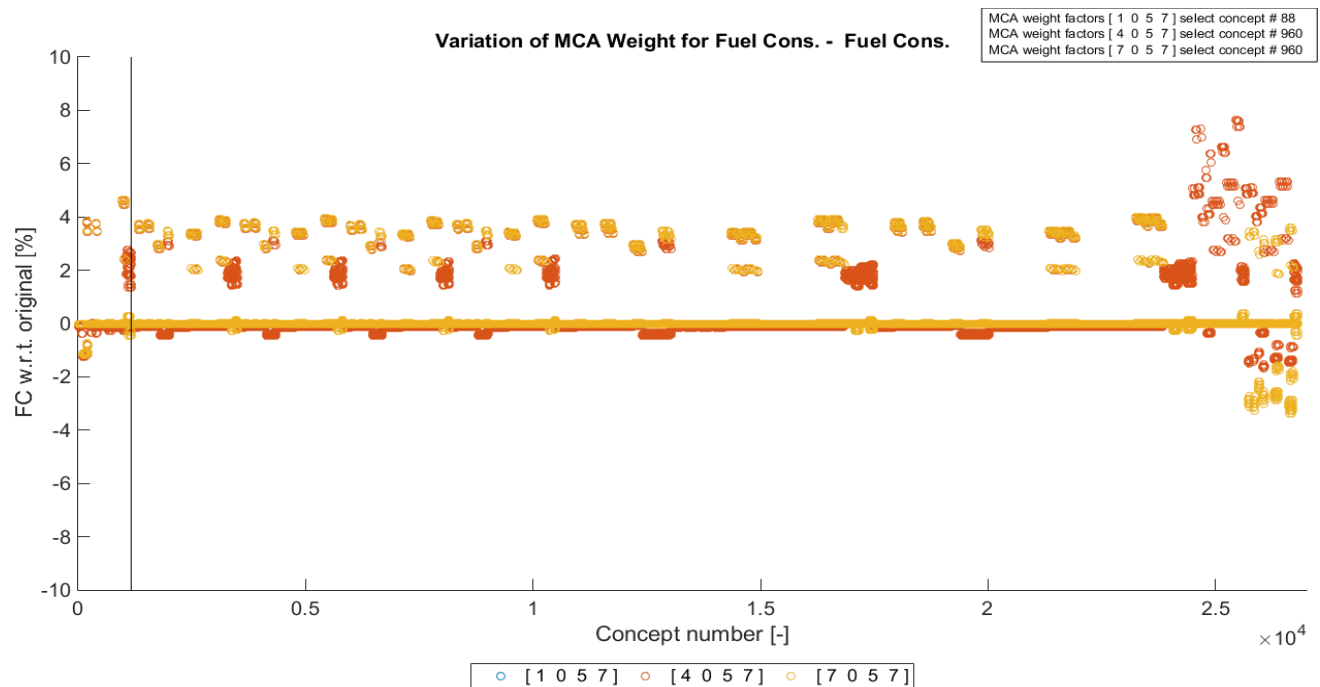


Figure 45: Example of Sensitivity Analysis Results

The legend presents the client preferences (or MCA weight factors) used during the creation of each dataset. As can be seen (from the legend) in Figure 45, each figure contains three different datasets, each with their own color. Every dataset contains every power plant configuration found in the design space, for the given set of MCA weight factors.

To each figure an annotation is added, which presents the selected power plant configuration for each set of client preferences, once again using the concept number.

In the example shown in Figure 45 a black line (at # 1166) marks the split between single shaft and power take in power plant configurations. This line is not seen in the appendices and its location does not change depending on the preferences, but it remains useful to (at least) be aware of its location.

The most remarkable phenomenon seen in Figure 45 are the intermitted (orange) clusters. These are caused by the fact that electrical propulsion engines are found here. These machines cause an increase in the electrical power demand and therefore magnify the effect of the design choices related to the electricity generation systems, which in turn causes an increase in sensitivity to the weight factors.

Interestingly the reoccurring pattern seen in these spikes changes around # 10000. The main reason for the change in pattern is the fact that here the dual fuel engine based propulsion systems are found.

There are more feasible dual fuel concepts, since there is more variation in the fuel type that can be applied. Which in turn causes an increase in the period of the reoccurring pattern discussed earlier.

The largest deviation from the aforementioned pattern is found around # 24000 which is where full electric, PTI configurations can be found. Here the design choices concerning the electricity generation systems become (even more) dominant. This can be seen from the fact that the change in fuel consumption for these cases has more deviations and the observed deviations are relatively high.

The fact that these orange spikes exist indicates that the more design choices that are stacked on top of each other, the more sensitive the results become to those choices. This is expectable, since more choices means an increase in influence and thus an increase in sensitivity as well. From this reasoning it is expectable that the electricity generation systems, and their design choices, have a larger influence on the results than the propulsive power generation systems. Since these systems are more likely to stack onto each other (given the developed algorithms discussed in paragraph 5.5).

However, the previously discussed patterns were all explained by the propulsion engines changing. Which is contradicting the expected sensitivity of the generation systems.

That all the observed deviation can be explained with changes in the propulsive engines, is explainable by considering the case used during the analysis. This was the cargo carrier, which has a propulsive power demand, which is higher than the electrical power demand (± 10 MW vs ± 600 kW as seen in chapter 4). It is only expectable that a design choice influencing a machine of several megawatts will have a greater influence on the total results than the design choice which influences a system of only a couple hundred kilowatts.

This dependency shows that not only does the operational profile influence the design of the power plant configuration itself, it also changes the sensitivity of the tool. Since the operation profile can cause a specific set of design choices to become more or less dominant over other design choices.

7.6.1. Varying the preference for Fuel consumption - Numerical data

The cases A,B and C (as defined in Table 32) are used to investigate the influence of the MCA weight factor for fuel consumption. The created scatter diagrams shows that, as expected, increasing the importance of a low fuel consumption, reduces the amount of consumed fuel. Which can be seen from the fact that the majority of the numerical data has a positive deviation (and thus consumes more fuel) from the benchmark case (which had the highest weight factor).

There are some extreme spikes, which were excluded from the magnified example case, they are however visible in appendix H. These spikes have two causes, which are closely related to each other. To better illustrate both causes the detailed design data of a single configuration, which has such an extreme spike has been included in Table 33.

The first cause of the observed spike is a change in degree of hydrogenation ('DoH', see paragraph 5.5.4 for its definition). This change in DoH has a quite significant impact on the results, because a large electrical machine (11 MW, as seen in Table 33) is present. This causes the change in DoH to significantly reduce the amount of hydrogen consumed, while at the same time increasing the amount of consumed diesel. Since diesel is heavier than hydrogen it causes an increase in (consumed) fuel mass.

The other cause for the increases in fuel consumption is found, when the results for the NO_x emissions are examined as well.

At exactly the same locations as the spikes in fuel consumption the NO_x emissions increase quite dramatically, again due to the changing DoH, which increases the size of the genset (which emits NO_x) while the delivered power (kWh) remains approximately the same (since the operational profile does not change).

The change in NO_x is significant enough for an SCR system to be required, while it was not required for the original case (as can be seen in Table 33). This again further increases the mass of the consumed fuel (since the SCR reagent is also added to the consumed fuel mass, as discussed in paragraph 6.2.2).

Table 33: Design Data for a single configuration located at an extreme spikes in fuel consumption

System	Original Case	Case B
<i>Shaft Configuration</i>	Power Take In	Power Take In
<i>MPE - Engine Type</i>	Dual Fuel Engine (844 kW)	Dual Fuel Engine (844 kW)
<i>MPE - Main Tank</i>	MDO	MDO
<i>MPE - Sec. Tank</i>	LNG	LNG
<i>PTI- Engine Type</i>	PMSM, Geared (11.4 MW)	PMSM, Geared (11.4 MW)
<i>PTI - Main Tank</i>	-	-
<i>PTI - Sec. Tank</i>	-	-
<i>Generation System</i>	PEMFC & DE Genset (9795 kW & 1347 kW)	PEMFC & DE Genset (1108 kW & 12354 kW)
<i>Genset – Main Tank</i>	HFO	HFO
<i>Genset – Sec. Tank</i>	-	-
<i>Hydrogen Storage</i>	Pressurized Hydrogen	Pressurized Hydrogen
<i>Electrical Energy Storage</i>	Li-Ion Batteries	Li-Ion Batteries
<i>NOX Reduction</i>	N/A	SCR
<i>SOX Reduction</i>	Wet Scrubber	Wet Scrubber

The emissions of CO₂ show only small deviations, with the only significant changes found at the same locations as aforementioned changes in DoH. This is expectable, since the only way to alter CO₂ emissions is to alter the amount of carbon containing fuel that is consumed or to change the amount carbon in that fuel. The latter of which happens when the DoH is changed.

The other patterns seen for this emission follow behavior of the fuel consumption which is expectable since it for those concepts the only influence on the CO₂ emissions comes from the amount of consumed fuel.

The emissions of SO_x show both a rather large deviations and a large spread in the value of those deviations. This is interesting, since the only way to alter the emission of SO_x (determined in gram SO_x per kg fuel) is to alter the fuel composition. The only design choice which could vary the 'average' SO_x per kg fuel is the DoH, since for other concepts the average fuel composition does not change.

The highest spikes are, as expected, once again found at the locations where electric machines are applied as propulsive engines.

The behavior of the deviations found for the mass and volume are very similar. The majority of the results show limited deviation w.r.t. to the original configuration. However, there are large spikes in both the mass and volume of the complete system. These spikes coincide with the locations where the fuel consumption showed the largest deviations.

Here the increase in system mass is likely caused by the installation of an SCR as discussed previously. While, the decreases in mass are likely caused by the decrease in DoH, which increases the amount of diesel fuel required. Which in turn reduces tank mass (as discussed in paragraph 5.6).

7.6.2. Varying the preference for Emissions - Numerical data

The cases D,E and F (found in Table 32) demonstrate the effect of a changing weight factor related to the emissions. The change in weight factor has a limited influence on the results. This can be seen from the fact that it is rather difficult to separate the three different cases. Which implies, that although there are some significant deviations, they are not (or hardly) influenced by the change in weight factor.

This is likely caused by the fact that the weight factor related to emissions is dominated by the high weight factor for fuel consumption. These two weight factors are closely related to each other, because emissions were expressed as Pollutant Emission Ratios ('PER'), which have the unit of gram 'emission' per kilogram fuel and the influence of the client preferences on the 'PER' is very limited (instead it is mainly dependent on the type of system present inside a concept).

The other cause for the observed insensitivity is the fact that emissions are also under the influence of the (objective) IMO regulations, which were assumed to be non-negotiable design criteria. These design criteria can only be influenced by the choice of emission control area, which has not been varied during this sensitivity analysis.

7.6.3. Varying the preference for Mass - Numerical data

The cases G,H and I, found in Table 32 demonstrate the influence of a changing value for the weight factor related to mass. Interestingly the fuel consumption shows the same behavior for a change in weight factor for mass as it did for a changing weight factor for fuel consumption.

This is somewhat remarkable, since in general the more efficient (slow running) 2 stroke engines, are significantly larger (and thus heavier). This makes it unexpected that the tool still finds solutions which have lower fuel consumption than the benchmark. The most likely explanation for the seen reduction is the fact that the weight factor for fuel consumption is still very high.

For cases, where the weight factor for mass is the lowest (the blue scatter), reductions in the NO_x emissions are seen. This is somewhat expectable, since a smaller engine (for the same power requirements) can be achieved by using engines with a higher nominal engine speed (as show by Figure 20, found in paragraph 5.4.2). The selection of a higher engine speed has additional benefit of emitting less NO_x (as discussed in paragraph 5.7.1).

However, when the weight factor for mass is increased further this effect is lost, and even results in an increase in the emissions of NO_x, with some extreme spikes appearing as well. The largest spikes are again found at electrical propulsion systems, which as discussed for Figure 45 remains somewhat expectable.

Other, less extreme, but still significant increases NO_x emissions, are likely due to the relatively high weight for fuel consumption, which might result in the selection of a larger, slow speed engine.

The emissions of SO_x do not show a clear pattern and for each variation of the weight factor both large positive and large negative deviations can be seen. This is likely due to the fact that the emission of SO_x are only affected by fuel composition, something which is only influenced by the application of combined electricity generation systems.

This suspicion is confirmed by the fact that the most extreme deviations are again found at the electric propulsive engines, which as stated several times before, magnify the impact of the design choices involved with the electricity generation system.

The emissions of CO₂ show very little deviations, with the exception of the spikes found at the electric propulsion systems, which were encountered numerous times before.

The numerical results for mass show that, as expected, the system mass decreases w.r.t. the benchmark case when a higher weight factor is assigned. The opposite, an increase in system mass for a decrease in weight factor is also seen.

There are some deviations from the expected behavior, which could be caused by the DoH of the combined generation system changing. These changes are likely caused by the high weight factor for fuel consumption, which causes an increase in hydrogen consumption w.r.t. to diesel fuel (and thus a decrease in total consumed fuel mass). This increase in hydrogen consumption comes at the price of an increase in (fuel) tank mass and volume.

The volume shows roughly the same behavior as was discussed for the mass, and is therefore not discussed in greater detail.

7.6.4. Varying the preference for Volume - Numerical data

The same trends as described for the variation of mass can be seen, when altering the preference for volume (case J,K and L), which is expectable, since these are strongly correlated.

What is interesting is that again combined electricity generation systems have the largest variation in their numerical values.

Once again affirming that the ratio between spatial requirements and fuel consumptions has a large impact on the numerical results of the tool.

These (and the previous) variations also demonstrate that especially mass and/or volume criticality are dominant terms in the design of a power plant configuration.

7.6.5. Changes in Optimal Concepts under varying preferences

For this part of the sensitivity analysis the optimal power plant configuration is selected for every case. The selected concepts numbers are summarized in Table 34. These numbers remain rather vague, since they are only a references to the library of feasible concepts. It is used nonetheless, since it does show whether the selected power plant configuration has changed.

Table 34: Selected optimal concepts per sensitivity analysis case

Case Name	Changed Preference	Numerical Change	Concept Number
Original	-	-	89
A	Fuel Cons.	10 -> 1	88
B	Fuel Cons.	10 -> 4	960
C	Fuel Cons.	10 -> 7	960
D	Emissions	0 -> 4	975
E	Emissions	0 -> 7	975
F	Emissions	0 -> 10	975
G	Mass	5 -> 1	1026
H	Mass	5 -> 7	960
I	Mass	5 -> 10	960
J	Volume	7 -> 1	975
K	Volume	7 -> 4	975
L	Volume	7 -> 10	960

Because the selected concept numbers presented in Table 34 give very little information about the actual power plant configuration, the systems present in those power plant configurations are presented in Table 35. In this table only concept number 960 and 975 are presented, since these are selected by the final multi criteria analysis quite dominantly.

Table 35: System types present in the most dominantly selected concepts

		Concept Number (Nnumber of occurrences)	
		960 (5)	975 (5)
Component	Shaft Configuration	Single Shaft	Single Shaft
	MPE - Engine Type	Dual Fuel Engine, Geared	Dual Fuel Engine, Geared
	MPE - Main Tank	MDO	MDO
	MPE - Sec. Tank	LNG	LNG
	PTI- Engine Type	-	-
	PTI - Main Tank	-	-
	PTI - Sec. Tank	-	-
	Generation System	Dual Fuel Genset	PEM Fuel Cell
	Genset – Main Tank	MDO	-
	Genset – Sec. Tank	LNG	-
	Hydrogen Storage	-	Pressurized Hydrogen
	Electrical Energy Storage	-	-
	NOX Reduction	-	-
	SOX Reduction	-	-

The configurations presented in Table 35 show a number of trends in the design of the cargo carrier vessel. Among these trends are some indicators for possible improves to the tool and therefore also some preliminary recommendations are discussed alongside these trends.

The first trend is that, for the considered case, the tool favors single shaft configurations. This behavior is expectable (as discussed in paragraph 7.2) and gives some confidence in the validity of the tool.

A very interesting trend is the selection of dual fuel engines as the propulsive engines. These engines are quite dominantly selected, as can be seen from the fact that a configuration which contain one is selected (at least) 10 out of 13 times. Given the increased emission regulations this is expectable, since their application eliminates the need for exhaust gas treatment systems.

Another trend that can be seen is also related to the application of dual fuel engines. These engines are always supplied with LNG (as seen in Table 35 and the selected power plant configurations presented for the different ship types). Ammonia and CNG apparently never result in a power plant configuration which is more favorable. This is somewhat expectable, given the properties presented in paragraph 5.6. This could however change if fuel treatment systems are accounted for as well. Doing so adds an incentive towards the minimization of the amount of different fuels used. This might make ammonia more interesting as fuel, since (for this research) SCR systems require ammonia as well.

Another remarkability is found, when considering the selected fuel types. There seems to be a complete disregard for HFO as fuel. This is unexpected, since HFO has the highest energy density and is currently the most commonly used fuel in the maritime sector [8]. Although the latter could very well change, given the upcoming sulphur cap.

The disregard of HFO is likely caused by the fact that MDO and HFO do not differ very much in terms of chemical properties and of these two MDO simply requires a smaller scrubber and/or less compensation from other fuels to comply with the implemented sulphur emission limits.

Additionally, the biggest downside of MDO when comparing it to HFO is the higher price, which is not accounted for. Therefore it is again (it was already done in paragraph 7.5 as possible solution to another remarkability) recommended to add both Capex and Opex to the tool as design criteria.

Another trend that can be recognized is the fact that the selection algorithm favors the application of primary emission reduction measures, instead of secondary ones. This tendency makes it interesting to investigate the influence of the fuel properties on the configurations.

Especially investigating a case where the sulphur content of MDO is reduced below 0.1 [%] is interesting, because this would cause MDO to meet the emission regulations (in any emission control area) without EGTS.

The weight factor relating to emissions has little influence on the selection of another configuration. This can be deduced from the fact that changing the weight factor from 0 to any other value, causes another configuration to be selected, but further increasing the weight factor does not cause a change in configuration. This again indicates that the tool is somewhat insensitive to the weight factor relating to emissions. This is somewhat expectable. Mainly because the influence of emissions on the design is more objective in nature than characteristics, due to the emission regulations.

The exact influence of these regulations on the design could be investigated in the future, by varying the emission control area while keeping all other input parameters constant.

Another remarkability is that fact that the selected configurations either includes a fuel cell or an engine driven genset, but never a combination of these two, while these two systems together should have promising features [18].

A first suggestion to improve the attractiveness of these combined systems was mentioned in paragraph 7.5 (in another context). In that paragraph the suggestion was made to include state of the art feasibility limits. Such a limit could, for higher power demands, cause standalone fuel cells to become infeasible and a combination of fuel cells with an engine driven generation system to become more interesting.

Another possible cause for this disregard of combined generation systems could be the fact that gensets and fuel cells are very different systems and that their interaction with each other is not modeled correctly due to the relatively simplistic performance models. This could also be due to the power management strategy, which might not suited for these combined generation systems.

And finally, the combination of difficult to store hydrogen and easy to store diesel could also be an unintended cause for the disregard of combined generation systems. This issue could be resolved by included other methods to supply PEMFC with hydrogen (such as fuel reformers). Since this would then greatly reduce the storage requirements posed by the hydrogen, which is the largest downside of the PEMFC that is encountered by the tool.

[This page has intentionally been left blank]

8. Conclusions and Discussion

In this chapter the conclusions of this research are presented and discussed. The first paragraph presents the conclusions of this research. The second paragraph then discusses the limitation of this research and their influence on the presented conclusions.

8.1. Conclusions

To select an optimal power plant configurations as function of the operation profile and the preferences of a client, a design space exploration tool has been developed. This tool allows for a comparison of numerous power plant configurations. Such a large scale comparison is necessary because the number of possible fuel types, generation systems and exhaust gas treatment systems has increased rapidly in the last couple of years (and is still increasing). Which has made it difficult for any engineer to keep up with, and include, all these developments during the design and selection of a power plant configuration.

Each power plant configurations is compared to other ones, based on fuel consumption, emissions, mass and volume. An indication of the mass and volume of the system is obtained using first principle dimensioning approaches. The fuel consumption and emissions are estimated using a performance simulation of the entire mission of the vessel. This approach is used so that the performance of the power plant can be estimated for the different conditions the power plant ‘encounters’ during the mission of the vessel.

To develop the design exploration tool, with the aforementioned functionalities, several sub-questions had to be answered. The answer to these sub-questions will presented before the main research question.

The first step in the creation of any automatic concept exploration tool is the definition of which concepts have to be considered and how those concepts can be created and/or specified. This lead to the first sub-question;

- What is the most suitable method to create the configuration concept library ?

The most suitable method to create the required concept library (for this research) is to vary the systems present in each configuration, while keeping the connections between these systems fixed. This method was made even more suitable for this research, by only specifying the type of systems. The tool then utilizes several functions to determine the parameters required for a (decently accurate) performance simulation. An in depth discussion of this method, and possible alternatives, can be found in chapter 2.

Using the selected method, the configuration concept library is populated, which is discussed in chapter 3. The population process consist of a complete enumeration of all possible combinations and the application of a series of technological and regulatory constraints. These constraints ensure that the considered configurations are able to provide both propulsive and electrical power without excess systems and they also ensure that emission limits posed by the IMO are not exceeded.

For the purpose of developing and testing the concept exploration tool, three example cases (a general cargo carrier, a harbor tug, and a trailing hopper suction dredger) were used. These cases had to be defined, which led to the following sub-questions:

- For each of the three case studies considered by this research:

What is the operational profile ?

What are possible client preferences ?

The operational profile for each of the three considered cases have been determined using reference vessels to specify several stages in the mission of these vessel. For each of these stages a duration and a power requirement for the propulsive, auxiliary and operational systems has been determined.

The client preferences where determined by considering the preferences a possible owner of each ship type might have. This did introduce a large degree of subjectivity, since the selected values reflect the author's opinion on the operations of these vessels. In practice these preferences could be determined using a (to be developed) questionnaire or by discussing them with a client. Both the determined operational profiles and client preferences are presented in detail in chapter 4.

Because of the subjective nature of the client preferences the tool has been subjected to a sensitivity analysis, the results of which are discussed in paragraph 7.6 and the most important conclusions of this analysis will be presented after the remaining research questions have been answered.

Not every design choice involved in the design of a power plant configuration is dependent on the preferences of a client. Therefore it is necessary to discern which design choices are, and which are not related to the preferences of a client. This leads to the definition of the third sub-question of this research;

- Which design choices are influenced by the preferences of a client ?

The design choices that, according to this research, are influenced by the preferences of a client are the following:

- The number of propulsive engines present (and with that, the installed power per engine)
- The size of the reduction gearbox (and related to that again the dimensions of the engines (in combination with the previous design choice)
- The voltage of the electrical grid, and with that the location of the electrical transformers.
- The size and number of engine driven gensets (similar to the propulsive engines).
- The size and design point of the installed fuel cells.
- The division of power between fuel cell based and engine driven generation systems

For each of these design choices a dedicated function has been developed, and these are all discussed in greater detail in chapter 5.

To investigate the influence of the final selection procedure, the results of the design process have to be examined prior to the final selection as well. This gave rise the last sub-question of this research;

- For each of the three case studies considered by this research:
For each of the different characteristics considered, which configuration would be the ideal choice ?

For both fuel consumption and emissions the same power plant is selected for each of the three cases. This was found to be caused by the selection process.

For mass and volume different concepts are selected per case study. It was also observed that a concept which is optimal for mass is also often optimal for volume. Which is not unexpected, since a smaller system is often lighter as well. All selected power plant configurations and the systems within those configurations, are presented in chapter 7.

Now that every sub-question has been answered (either here or elsewhere in this report), the main research question (repeated below) can also be answered.

“What is the optimal power plant configuration of a surface vessel given its operational profile and the preferences of its owner, when a comparison is made based on the fuel consumption, emissions and spatial requirements?”

The optimal power plant configuration has been determined for each of the three considered ship types and each of these can reasonably be agreed with, although there are some unexpected results. The actually selected power plant configurations, and their components are presented in chapter 7 and not repeated here.

In addition to the selected power plant configurations, the numerical results for each of the considered characteristics were also presented. These results are interesting for the verification of the newly developed concept exploration tool.

Especially the results of the general cargo carrier were found to be interesting, since both the input and the (expected) output are known with a high level of accuracy. Additionally, it is possible to explain, with some basic marine engineering knowledge, why a certain configuration had been selected.

That this is possible is especially valuable for cases where the results could not be easily compared to real designs, such as the harbor tug and trailing suction hopper dredger. These are harder to compare to real designs, since several different power plant configurations can be found for these vessels. The spread in applied power plant designs is caused by the operational profile of these vessels. For these vessels there is more variation in the operational profile, which has made it difficult for industry to pick ‘ideal’ configuration. The comparison with existing power plant configurations was complicated further by the fact not all components found in the power plants on board these vessels were included in this research. An example of such a component are controllable pitch propellers, which are commonly found on dredgers [29].

With the main research question answered for each of the three included cases. All that is left for this conclusion is the sensitivity analysis to which the tool has been submitted. This analysis focused only on the client preferences, since these are highly subjective and could therefore be a major point of discussion.

The sensitivity analysis shows that the majority of the configurations are influenced by the client preference, and these mostly show between 5 and 10 % change in their numerical results. Some extreme deviations were also observed. These extremes were caused by the application of electrical propulsion in combination with a change in the division of power between the engine driven genset and the fuel cell (which is described using a ratio; the ‘Degree of Hydrogenization’ or ‘DoH’). In those cases the electrical machine caused an increase in required electrical power, which in turn magnified the influence of a change in the degree of Hydrogenization DoH.

From this observed relationship it can be deduced that the sensitivity to the client preference is not only influenced by the value of the weight factor, but also by the operational profile.

The observed sensitivity is mainly present when the numerical results are compared and not as much as during the final concept selection.

This is caused by the fact that the numerical results are compared to each other, which causes the selection procedure to be less sensitive to a change in numerical results. This can also be seen from the fact that two different power plant configurations are dominantly selected, for varying preferences.

The creation of the concept library showed that even with the limited nodes and systems included in this research still a lot of possible configurations can be created (26.818 to be precise, as discussed in chapter 3). What makes this number remarkable is the fact that current marine engineering trends (partially) converge on the same results as the ones selected by the tool. This subtly implies that a marine engineer is already a very strong optimizer on his/her own. Since, even without considering every single one of the possibilities (which the tool does), current marine engineers have converged on the most ideal power plant configuration out of more than 26 thousand options !

8.2. Discussion

The most significant point of discussion of this research is that, even though a lot of design choices are left to the client's preferences, some had to be made beforehand so that the envisioned tool could be developed. Although it was attempted to keep these choices to a minimum, they could not be completely avoided. These choices do however influence the results of the developed tool, and disagreement with them could be an important reason to disregard the (suggested) optimal power plant configuration.

The most significant predetermined design choice is the power management strategy, which had to be determined before the tool could be developed. The influence of this strategy is quite significant, since this strategy is embedded in every single one of the developed design algorithms. During this research an attempt was made to keep the goal of this strategy as objective as possible, by considering trends observed in practice.

The design choices which were not predetermined during the development of the tool could also be argued with. Mainly because the considered preferences, and thus design choices, are limited. As a result systems which excel at the considered characteristics, while having their downsides in ones which are not, are often selected as strong concepts.

The selected preferences do however give a very graspable indication about the performance and dimensions of each configuration and they envelop some of the most important tradeoffs found during the design of a power plant. Nonetheless it remains possible, and necessary, to include more preferences, so that more tradeoffs can be considered.

Apart from the limitation of the number of preferences that can be specified, another simplification has been made. Which is the separation of the three power demands specified by the operational profile. In practice these three power demands are related to each other (and to the systems in a configuration) due to (for example) engine support and fuel treatment systems. These relationships are not accounted for and this could result in inconsistent power demands being defined by a user. Implementing these relationships would arguably result in better results, but likely cause a severe increase of the required computational time.

For the three considered cases it was attempted to avoid the possible inconsistency in the power demands by defining the different operation stages (as seen in chapter 4). These stages were then used to estimate the behavior of the different power demands. Additionally it was attempted the use several different sources to further reduce the risk of inconsistency.

Another point of interest concerning the design choices is the methodology used to determine the values for the different technological parameters. These values are determined using reference data obtained from the manufacturers of those systems.

This approach has been used, because it increased the likelihood that the selected power plant configuration is feasible in practice. Since the components used inside that configuration exist in practice.

The downside of this approach is that, because the design processes rely on reference data, the tool is limited in its ability to 'create' innovative system designs, since the tool cannot go beyond the implemented state of the art. This limitation was attempted to be reduced by using numerous different sources, so that at least the state of the art of each system is as up-to-date as possible.

Apart from the methods used to determine the detailed information, the level of detail itself should be reflected upon. The main issue one could have with the determined information is the fact that it is still superficial, and therefore does not allow for very accurate performance simulations. However, the used level of detail is sufficient for the used performance models, which are simplified 'curve-fit' models.

These models do not use fundamental principles (such as thermodynamics) to estimate system performance. Using these fundamental performance simulation could indeed results in more accurate results. However, such a simulation requires lot of (detailed) parameters, most of which are unknown at an early stage in the design of a power plant (which is where the developed concept exploration tool is expected to be most useful). Therefore the only way to obtain these parameters would be to estimate them. Doing so is possible, but would likely decrease the accuracy of the performance model to the point where the simplified curve fit models become more accurate.

Additionally, the numerical results of the different configurations are ranked and those ranks are used to determine which concept is optimal. This makes it less essential to have numerical results which are as accurate as possible. Instead this approach requires the accuracy of the results to be the same for every power plant configuration. This can be achieved by estimating the numerical values for each characteristic using the same method for each configuration, as has been done during this research.

However, there are two performance models, which could definitely be improved to increase the applicability of the concept exploration tool. These are the performance models of both exhaust gas treatment systems.

Nonetheless, the more complex performance models could be interesting during the following steps in the optimization of the selected power plant, since more and more detailed information becomes available during the following iterations in the design process.

Another important simplification is (again) found in the input required by the tool. These simplification should also be discussed, since they do influence the results of the tool. One of those simplification is the use of a single emission control area. In practice a ship will travel through several different emission control areas. Although it does have to be able to comply with the most stringent area it sails in, it is not unheard of control the power plant in such a way that it only complies with the emission regulations of the area it is currently in, for example by switching between fuels to limit the sulphur emissions.

In the previous paragraph it has been noted that the influence of the different design choices is not only dependent on the value of the different weight factors. Instead the operational profile also influenced which set of design choices (propulsive or electricity generation) had the largest influence. This seems expectable, since the largest influence on the design often comes from the most powerful system.

This sensitivity was not investigated further, due to time constraints posed to this research. Nonetheless it is important that this sensitivity is investigating so that the tool can be verified.

Additionally, the considered case used as benchmark for the sensitivity analysis had a high weight factor assigned to fuel consumption. This could have influenced the results, as was mentioned for the cases where the weight factor for emissions was varied (paragraph 7.6.2). Therefore it is useful to investigate the sensitivity to the client preferences further. Both by considering more combinations of client preferences and by varying the emission control area.

Another major point of discussion is the fact that certain, (conventional) systems, such as power take off systems, waste heat recovery and controllable pitch propellers were excluded in advance. As a consequence power plant configurations, which are feasible (and applied) in practice, were eliminated beforehand. This reduces the applicability of the developed tool, and therefore it is advisable to expand the considered components.

There is another issue with scope of this research, which was mentioned earlier in this discussion. This is the fact that fuel treatment systems were not included in this research. This negligence allows the tool to freely implement a lot of different fuel types inside a single power plant.

This is (theoretically) possible, but not seen in practice, since each fuel requires its own handling and treatment systems, which in turn increase spatial requirements. In reality the number of different fuels is often limited. Therefore it is likely that including fuel treatment systems in estimates could improve the results.

A final point of discussion related to this research would be the final remark found in the conclusions. From this remark one could argue that the developed tool is not very useful, since it only selects configurations which are expectable given some very fundamental marine engineering knowledge. It is however important to be aware of the fact that the used cases were selected, for exactly that reason. Since both input and output were known, with some certainty, it was possible to verify the working principles of the tool.

Additionally, the goal of the development of this tool has never been the replacement of the marine engineer. Instead the tool is meant to engage designers to consider systems or even entire power plant configurations, which they would not have considered otherwise.

Apart from promoting the consideration (and possible application) of less mature technologies, the tool could also serve as a jumpstart to a discussion. Since the developed tool allows a designer to ask a ship owner;

“Have you considered another power plant configuration, for example one with ... ?”

He/she could then support this question with some estimates on the performance and dimensions of the suggested power plant. Such a discussion becomes very interesting when conventionally applied systems become less interesting (or even infeasible) due to environmental considerations or regulatory pressure.

Additionally the tool is newly developed, and the research has been subjected to time constraints. It is not unthinkable (and highly recommended) that the tool is expanded in the future. Increasing the amount of systems and tradeoffs that are considered at a very early design stage could also result in less conventional power plant configurations being selected more often. Possibly resulting in new solutions to existing problems.

9. Recommendations

In this chapter the recommendations for future research are discussed. Some recommendations are derived from the results and the discussion of those results. Others are established based on the conclusions and the discussion of this research. The recommendations are separated into three paragraphs.

The first paragraph presents the recommendations concerning the 'library of feasible concepts'. The second paragraph then gives recommendations related to the user defined input. The third, and final paragraph then discusses the recommendations based on the results of the concept exploration process.

9.1. Recommendations concerning the Concept library

The most important recommendation concerning the concept library is somewhat of an open door; this is expansion of the list of components included in the tool. Some noteworthy components that could be included in the future are summarized below.

The first system that could be added is a Power Take Off (PTO) generation system, since PTO's are already an often implemented feature in combination with a CPP.

The addition of a CPP is also an interesting addition to the tool, given the fact that this type of propeller is often applied in (for example) dredgers [29]. This does come with some issues for the input (since the propeller law is no longer applicable in those cases), but these will be described in the following paragraph.

Given the fact that a combination of an engine driven gensets and a fuel cell is never selected as an optimal configuration by the tool it could be interesting to include other fuel cells and/ or other methods to supply the fuel cell with hydrogen, such a fuel reformers. These measures could allow for the applications of fuels which are less demanding in terms of storage requirements.

This would be increasingly beneficial when fuel handling/treatment systems are accounted for as well, which is another recommendation.

Doing so would cause configurations with several fuel types (and thus different treatment systems) to become less interesting than power plant configurations with a single (or only a few) fuel type(s).

The addition of more emission reduction systems, both primary (water injection, or exhaust gas recirculation [14, pp. 706-707]) or secondary (cleaning the exhaust gas) could also be interesting. Although the former likely required a more detailed performance model of the combustion engines.

A more detailed performance modelling of the exhaust gas treatment systems is another recommendation, since rather simplistic methods were used during this research. During this research several other researches have been completed, which developed performance models suitable for marine SCR systems. It should be investigated whether these models could be added to this tool, and if possible, do so.

Additionally, some ports (plan to) limit the (quality of) overboard discharge of scrubbing water beyond the IMO regulations. These limits reduce the feasibility of the open loop scrubber, but increase the feasibility of closed loop scrubbing systems. Implementing those discharge limits would require a more detailed set of constraints such as overboard discharge limits) related to the area the vessel has to operate in.

The final recommendation related to the scope of this research is the limited application of batteries. Since they were only used as an emission reduction measure. However, they could also be used for other applications, such as peak shaving/dip filling. Including other applications of storage systems could make batteries more useful and open the door for the application of other electricity storage systems, such as flywheels.

This would however require a more detailed (dynamic) description of the operational profile. Such a detailed operational profile would likely cause an increase in the required computational time. However, it is not known how much the computational time would increase. It is possible that this increase is not very severe and therefore acceptable, given the fact that a very feasible (and often seen) application of energy storage could then be incorporated. It should most definitely be investigated whether this such a more detailed description (and more dynamic simulation) is possible.

9.2. Recommendation concerning the Input

During this research the operational profile was defined as a delivered power, and as such eliminating the propeller and ship design from the tool. However, adding the possibility to include calculation prior to the delivered power, could enable the tool to be used even earlier in the design process. (Possibly even extending to a stage where a user only has to 'draw' an intended voyage ?)

Doing so would also enable for the list of considered propulsors to expand with Voith-Schneider- or a CP-propulsors for example. This would however force the propeller/RPM constant (C_4) to become variable over time as well (this is also necessary for the application of PTO/CP combinations).

Additionally the geographical data has been simplified to a single emission control area. It would however be interesting to use more detailed description, such a complete route or time based area definition. This could be especially interesting if fuel switching or deactivation of scrubbers/SCR systems when they are not needed is added to the simulation.

Additionally this geographical data could also be expanded to include, for example, overboard discharge limits, which is required when a more complex (closed loop) scrubbing system is included (as was recommended in the previous paragraph).

Additional design criteria should also be added, to allow the tradeoffs between the different designs to become more accurate. Important criteria that could be added are capex and opex, although care should be taken, since any owner will find costs (of any kind) very important.

On a different note, the electrical power demands were kept separate from each other. While in truth connections between these power demands exist, for example caused by fuel treatment system and engine support systems. These relationships have not been accounted for, since these systems were assumed to be part of the auxiliary, electrical, load.

Accounting for these effects would improve the results of the tool, at the cost of a (possibly severe) increase in computational time, however it should certainly be investigated whether a (simplified) relationship could be developed between the operational profile and the systems present in a configuration, since in practice these do exist.

9.3. Recommendations based on the Generated Results

The final set of recommendations is based on the results obtained from the sensitivity analysis and the three considered case studies. Several of these were already mentioned during the discussion of those results. Nonetheless they will be repeated in this paragraph.

The tool did not show a large sensitivity to a varying preference for emissions. This is likely due to the fact that the fuel consumption weight factor was quite high. Therefore it is recommend to investigate the sensitivity to the client preferences further.

Additionally the characteristic of fuel consumption should be changed to, or complemented with, total system efficiency, in order to prevent the fact that hydrogen is a light fuel becomes dominant in cases fuel consumption is assigned a high weight factor.

The influence of the operational profile, for a fixed set of preferences, has not been investigated, since the operational profile could be determined with more certainty than the client preferences. However, as discussed in paragraph 8.2, the operational profile influences the sensitivity of the tool, by making some design choices more significant than others.

Additionally, even without the design choices the operational profile influences the design of a power plant, as any marine engineer will confirm. Therefore it is recommend to investigate the sensitivity of the tool towards a changing operational profile, under constant client preferences as well.

Apart from the sensitivity to the input values a lot of parameters where introduced and their influence on the entire process should be investigated.

An example of such a set of parameters are the fuel properties. Which are interesting, since it is expectable, given the more severe sulphur cap, that the sulphur content of the diesel oil will be reduced. Especially a case where the sulphur content of MDO is lowered below 0.1% is interesting. Since this would cause diesel engines to instantly comply with the new sulphur cap, even in SECA's without after-treatment systems.

Bibliography

- [1] International Transport Forum , "Decarbonizing Maritime Transport - Pathway to zero-carbon shipping by 2035," International Transport Forum , Paris, 2018.
- [2] International Maritime Organisation , "UN body adopts climate change strategy for shipping," International Maritime Organisation, 13 April 2018. [Online]. Available: <http://www.imo.org/en/MediaCentre/PressBriefings/Pages/06GHGinitialstrategy.aspx>. [Accessed 2018 May 09].
- [3] L. Rietveld, *Optimization of a propulsion plant for a submarine based on first principles.*, Delft, Zuid-Holland, 2017.
- [4] M. ten Hacken, "Optimization of a submarine propulsion system by implementing a PEM fuel cell and a PMSM in a first principle model," TU Delft - Nevesbu, Delft - Alblasserdam, 2017.
- [5] P. de Vos and D. Stapersma, "Automatic Topology Generation for early design of on-board energy Distribution Systems," Expected to be published in: Ocean Engineering, Delft, To be Published in 2018.
- [6] I. Georgescu, M. Godjevac and K. Visser, "A New Perspective on the Complexity of On-board Primary Power Systems," Journal unknown, research done at Delft Univeristy of Technology , Delft, To be Published.
- [7] E. Silvas, T. Hofman, A. Serebrenik and M. Steinbuch, "Functional and Cost-Based Automatic Generator for Hybrd Vehicles Topologies," IEEE, 2015.
- [8] H. Klein Woud and D. Stapersma, Design of Propulsion and Electric Power generation Systems, London: IMarEST, 2008.
- [9] I. Ohashi, "Yanmar Technical Review," 27 July 2015. [Online]. Available: https://www.yanmar.com/global/technology/technical_review/2015/0727_2.html.
- [10] ABB, "Motors and Generators for Marine Industry," ABB, 2011.
- [11] International Maritime Organization , "MARPOL Annex VI," International Maritime Organization, London, 2005.
- [12] Wärtisilä, "Wärtisilä Scrubber Product Guide," Wärtisilä MOSS AS., 2014.
- [13] K. Chopra, "10 Technologies/Methods for Controlling NOx & SOx Emissions from Ships," Marine Insight, 9 October 2017. [Online]. Available: <https://www.marineinsight.com/tech/10-technologiesmethods-for-controlling-nox-sox-emissions-from-ships/>. [Accessed 2 November 2017].
- [14] D. Stapersma, Diesel Engines Volume 4: Emissions and Heat Transfer, Delft: TU Delft, 2010.

- [15] ABB, "Energy Storage Systems," ABB, 9 August 2016. [Online]. Available: <http://new.abb.com/marine/systems-and-solutions/power-generation-and-distribution/energy-storage>. [Accessed 21 November 2017].
- [16] Y. Kheng Tan and S. Kumar Panda, "Review of Energy Harvesting Technologies for Sustainable Wireless Sensor Network," National University of Singapore, Singapore, 2010.
- [17] T. Tronstad, H. Høgmoen Åstrand, G. P. Haugom and L. Langfeldt, "Study on the use of fuel cells in shipping," European Maritime Safety Agency.
- [18] L. van Biert, M. Godjevac, K. Visser and P. Aravind, "A review of fuel cell systems for maritime applications," Elsevier B.V., 2016.
- [19] S. Hench, "Why are car manufacturers ignoring hydrogen Engines," Forbes.com, 27 June 2017. [Online]. Available: <https://www.forbes.com/sites/quora/2017/06/27/why-are-car-manufacturers-ignoring-hydrogen-engines/#278af6144027>. [Accessed 1 November 2017].
- [20] United States Environmental Protection Agency, "Air Pollution Control Technology Fact Sheet - SCR," US EPA, 2003.
- [21] Marine Traffic, "Marine Traffic - All Vessels," Marine Traffic, 4 October 2017. [Online]. Available: www.marinetraffic.com/en/ais/index/ships/all. [Accessed 4 October 2017].
- [22] Man Diesel & Turbo, "Propulsion Trends in Bulk Carriers," Man Diesel & Turbo, 2014.
- [23] Maritime Connector, "Bulk Carriers," November 2017. [Online]. Available: <http://maritime-connector.com/bulk-carrier/>.
- [24] Offshore Ship Designers, "Azistern 2460," [Online]. Available: <http://offshoreshipdesigners.com/tug-design/harbour-tugs/azistern-246/>.
- [25] D. A. Argyriadis, "Modern Tug Design with Particular Emphasis on Propeller Design, Maneuverability, and Endurance," The Society of Naval Architects And Marine Engineers, New York, 1957.
- [26] S. Memis, "A terminal Tug's Annual Duty Profile and Fuel Consumption on High and Medium Speed Engines," 10 October 2014. [Online]. Available: <https://www.linkedin.com/pulse/20141010084248-90166035-terminal-tug-s-annual-duty-profile-and-fuel-consumptions-on-high-and-medium-speed-engines>.
- [27] D. Cavalier and S. Caughlan, "Design of a Low Emissions Harbour Tug," ITS 2008, Singapore, 2008.
- [28] Boskalis, "Trailing Suction Hopper Dredgers," 2017. [Online]. Available: <https://boskalis.com/about-us/fleet-and-equipment/dredgers/trailing-suction-hopper-dredgers.html>.
- [29] K. van Dijk*, *Personal Communications with Klaas van Dijk, Engineer at 'van Oord Dredging and Marine Contractors BV'*, Rotterdam, 2017.
- [30] Boskalis, "Equipment Sheet - Gateway," Boskalis, Westminster, 2010.

- [31] D. Wangli, J. Braaksma, R. Babuska, J. Klaassens and C. de Keizer, "Evaluation of Dredging Performance in a Trailing Suction Hopper Dredger".
- [32] I. Sørfonn, 9 October 2007. [Online]. Available: dynamic-positioning.com/proceedings/dp2007/design_sorfonn.pdf.
- [33] DNV-GL, "Maritime Global Sulphur Cap 2020," Det Norske Veritas (DNV) en Germanischer Lloyd (GL), Hamburg (Germany), 2016.
- [34] World Maritime News, "IMO Designates North Sea, Baltic Sea as NECA," World Maritime News, 08 November 2016. [Online]. Available: <https://worldmaritimeweb.com/archives/205936/imo-designates-north-sea-baltic-sea-as-neca/>. [Accessed 01 February 2018].
- [35] J. Jalkanen, L. Johansson, J. Kukkonen, A. Brink, J. Kalli and T. Stipa, "Extension of an assessment model of ship traffic exhaust emissions for particulate matter and carbon monoxide," Copernicus Publications, Helsinki, 2012.
- [36] D. Stapersma and P. de Vos, "Dimension prediction models of ship system components based on first principles," International Marine Design Conference, Delft, 2015.
- [37] D. Stapersma, Diesel Engines Volume 1 Performance Analysis, Delft: TU Delft, 2010.
- [38] Rolls-Royce, "Diesel and Gas engines, generator sets and propulsion systems," Rolls-Royce, 2015.
- [39] MAN Diesel and Turbo, "Marine Engine IMO Tier II and Tier III Programme 2015," MAN Diesel and Turbo, 2015.
- [40] Wärtsilä, "Dual Fuel Engines," Wärtsilä, 2018. [Online]. Available: <https://www.wartsila.com/products/marine-oil-gas/engines-generating-sets/dual-fuel-engines>. [Accessed 16 January 2018].
- [41] H. Dewan, "Shipboard High Voltage Application and Safeties," Hanif Dewan's blog for maritime education and knowledge, 26 September 2014. [Online]. Available: <https://dewan31.wordpress.com/2014/09/26/shipboard-high-voltage-application-safeties/>. [Accessed 2 November 2017].
- [42] Caterpillar Marine, "CAT SCR Systems Product Dimensions and Benefits," Caterpillar Marine, 2015.
- [43] Eaton Corporation plc, "Volume 4 - Circuit Protection Tab 3; Power Breakers, Contactors and Fuses," Eaton Corporation plc, Dublin, 2017.
- [44] A. Kana and E. Rotteveel, "Design Data for Submarine Design (Assignment)," Delft University of Technology, Delft, 2017.
- [45] ABB, "ABB Solar Inverters Product Flyer," ABB, 2011.
- [46] D. Stapersma, "Theory and model for battery charging and discharging," Royal Netherlands Naval College, Den Helder, Delft, 1998.

- [47] Wärtsilä, "Wärtsilä Generating Sets," Wärtsilä, [Online]. Available: <https://www.wartsila.com/products/marine-oil-gas/engines-generating-sets/generating-sets/wartsilagen-set-20>. [Accessed 31 January 2018].
- [48] Caterpillar, "Electric Power Generation C175-16 (60Hz)," Caterpillar Inc., 2017. [Online]. Available: https://www.cat.com/en_GB/products/new/power-systems/electric-power-generation/diesel-generator-sets/1000028916.html. [Accessed 04 January 2018].
- [49] D. Stapersma, Diesel Engines Volume 3: Combustion, Delft: TU Delft, 2010.
- [50] I. Martinez, "Fuel Properties," 201.
- [51] American Petroleum Institute, "Heavy Fuel Oil Category," American Petroleum Institute, 2012.
- [52] Alternative Fuel Data Centre, "Alternative Fuel Data Centre - Fuel Properties Comparison," Alternative Fuel Data Centre, 2014.
- [53] The international Group of Liquefied Natural Gas Importers, "LNG Information Papier No. 1," GIIGNL, 2009 .
- [54] CHART Inc., "LNG Equipment Solutions," CHART Inc., 2015.
- [55] Unitrove, "Compressed Natural Gas," 18 October 2017. [Online]. Available: <http://www.unitrove.com/engineering/gas-technology/compressed-natural-gas>.
- [56] Quantum Fuel systems, "Q-Lite Advanced CNG Fuel Storage Tanks," Quantum Fuel systems, 2018. [Online]. Available: <http://www.qtw.com/product/q-lite-lightest-cng-tanks/>. [Accessed 30 March 2018].
- [57] Air Liquide, "Storing Hydrogen," Air Liquide, [Online]. Available: <https://energies.airliquide.com/resources-planet-hydrogen/how-hydrogen-stored>. [Accessed 16 January 2018].
- [58] D. Hofstrand, "Renewable Energy Newsletter - Ammonia as a Transportation Fuel," May 2009. [Online]. Available: <https://www.agmrc.org/renewable-energy/renewable-energy/ammonia-as-a-transportation-fuel/>.
- [59] Hydro Instruments, "Ammonia Handling Manual," Hydro Instruments, 2013.
- [60] MAN Diesel & Turbo, "Dual Fuel Upgrade," MAN Diesel & Turbo, 2013.
- [61] E. A. Brohi, "Ammonia as fuel for internal combustion Engines," Chalmers University of Technology, Gothenburg, Sweden, 2014.
- [62] H. Schlick, *Potential and challenges of gas and dual-fuel engines for marine application*, Busan: 5th CIMAC CASCADES, 2014.

- [63] A. Reiter and K. Song-Chargn, *Demonstrate Ammonia Combustion in Diesel Engines*, 4th annual conference on Ammonia, 2007.
- [64] United States Environmental Protection Agency, "Exhaust Gas Scrubber Washwater Effluent," US-EPA, Washington, DC, 2011.
- [65] A. Bandyopadhyay and M. N. Biswas, "Modeling of SO₂ scrubbing in spray towers," Elsevier, 2007.
- [66] G. Caiazzo, G. Langella, F. Miccio and F. Scale, "Seawater SO₂ scrubbing in a spray tower for marine application," Meeting XXXV of the Italian section of the Combustion Institute, Napoli, 2012.
- [67] United States Department of Transportation, "FGD Scrubber Material," 08 03 2016. [Online]. Available: <https://www.fhwa.dot.gov/publications/research/infrastructure/pavements/97148/025.cfm>.
- [68] United States Environmental Protection Agency, "Air Pollution Control Cost Estimation Spreadsheet for Selective Catalytic Reduction," US EPA, Washington, DC, 2016.
- [69] L. S. Chladova, "Evaluation of Selective Catalytic Reduction for Marine Two-Stroke Diesel Engines - Master Thesis," Aalborg University, 2010.
- [70] S. Bernardi, "SCR Reactor Design Criteria," 2014.
- [71] P. Skogtjörn, "Modelling of the Exhaust Gas Temperature for Diesel Engines," Linköpings universitet & Scania CV AB, 2002.
- [72] K. Wicker and J. Staudt, "SCR maintenance fundamentals," Andover Technology, 2004.
- [73] D. Stapersma, *Mossel driven testbed (Matlab & Simulink Model)*, Delft: TU Delft, 2014.
- [74] H. T. Grimmelijs and P. de Vos, "Towards environmental-friendly inland shipping propulsion systems for inland ships using different fuels and fuel cells," Delft University of Technology, Delft, 2011.
- [75] Johnson Matthey, "Global Emissions Management- Focus on Selective Catalytic Reduction (SRC) Technology," February 2012. [Online]. Available: <http://www.google.co.uk/url?sa=t&rct=j&q=&esrc=s&source=web&cd=5&ved=0ahUKEwj-wOuZ-d7YAhVItRQKHV7AcUQFgg8MAQ&url=http%3A%2F%2Fect.jmcatalysts.com%2Fdocuments%2Ffocus-on-selective-catalytic-reduction-technology-scr&usg=AOvVaw1OcGIGhxVwcbD0S5UbrpX>. [Accessed 17 January 2018].
- [76] MAN Diesel & Turbo, "Influence of Ambient Temperature Conditions," MAN Diesel & Turbo, 2015.
- [77] FuelCellsWorks, "Nedstack sells world's largest PEM fuel cell power plant," 14 April 2016. [Online]. Available: <https://fuelcellsworks.com/news/nedstack-sells-worlds-largest-pem-fuel-cell-power-plant>. [Accessed 10 April 2018].
- [78] Den Herder Seaworks B.V., "Den Herder Seaworks - Our Fleet," Den Herder Seaworks, [Online]. Available: http://www.dhseaworks.com/english/our_fleet.php. [Accessed 20 February 2018].

- [79] SeaBoats - Marine Brokers, "5500 m3 Trailing Suction Hopper Dredger," SeaBoats Marine Brokers, [Online]. Available: <http://www.seaboats.net/5500m3-trailing-suction-hopper-dredger-xidp1265828.html>. [Accessed 20 February 2018].
- [80] Wärtsilä, "Wärtsilä Encyclopedia of Marine Technology : Dredging and Dredgers," Wärtsilä, [Online]. Available: <https://www.wartsila.com/encyclopedia/term/dredging-and-dredgers>. [Accessed 20 February 2018].
- [81] Rolls-Royce, "Reduction Gears," Rolls-Royce, 2017.
- [82] RENK aktiengesellschaft, "Single Marine Gear Units Type RSV/RSH," RENK aktiengesellschaft, Rodder Damm, 2014.
- [83] P. Odetola, P. Popoola, O. Popoola and D. Delport, "Electrode Position of Functional Coatings on Bipolar Plates for Fuel Cell Applications. A review," InTech, 2016.
- [84] Toyota, "Mirai Product Informatie," Toyota, 2016.
- [85] Elliott group, "Multi Stage Centrifugal Compressors," Elliott group, 2014.

*. No known familiar relationship with the author of this thesis. The fact that both share the same family name is purely coincidental

Automatic Selection of an Optimal Power Plant Configuration

Appendices

Author:

J.S. van Dijk

Email:

jittvandijk@gmail.com

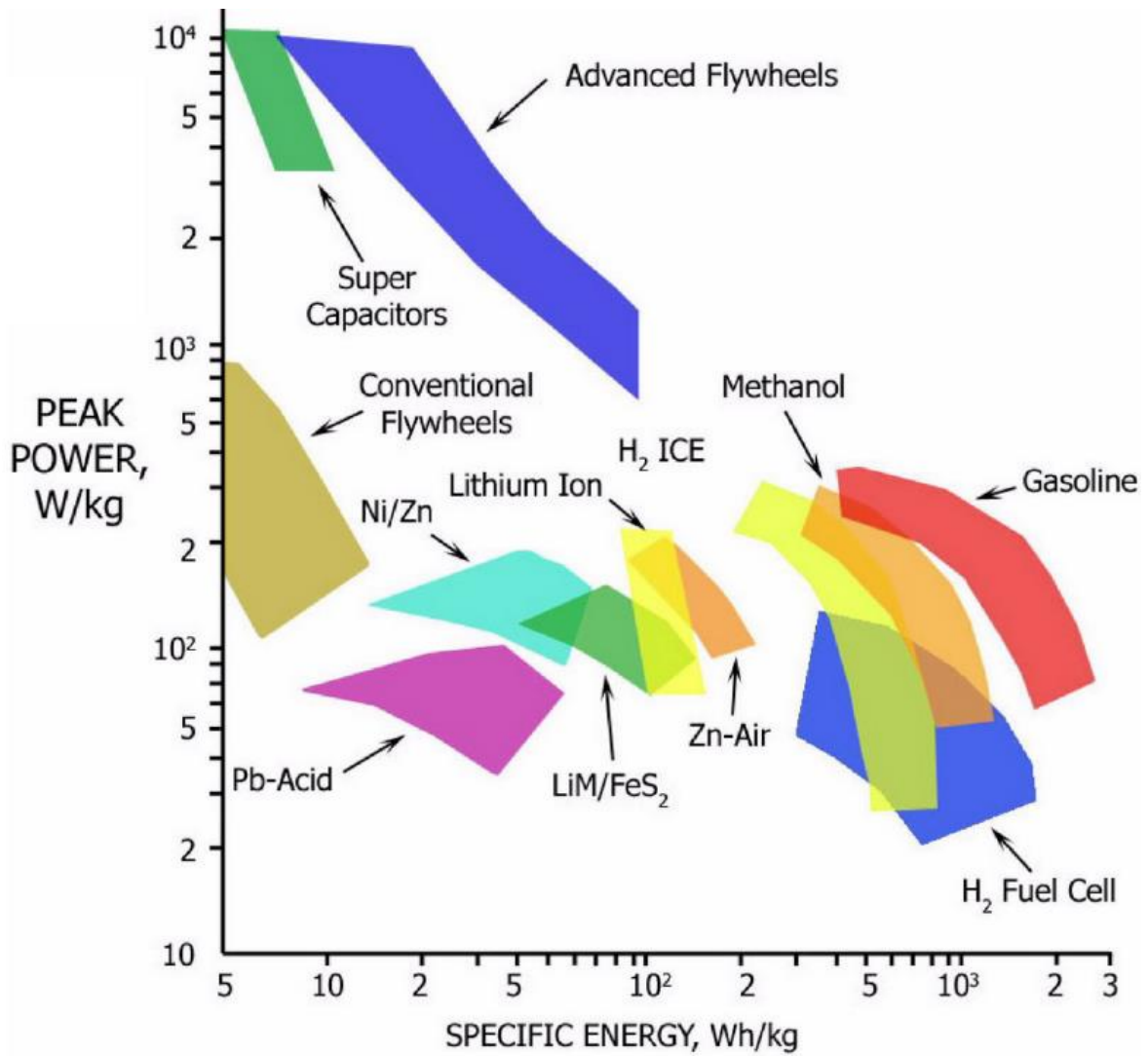
Student number:

4162056

Appendix :	Title :	Page :
A	Ragone Plot for the Comparison of Different Energy Storage Methods	1
B	Propeller Power/RPM curves and Reference Vessel Data	2
C	Overview of Design Processes	4
D	Combustion Engine Design Methodology	7
E	Gearbox Design Methodology	10
F	Battery Discharge Behavior	13
G	PEMFC Design Methodology	14
H	Sensitivity Analysis Results	19
J	Concept Paper	43

A. Ragone Plot for the Comparison of Different Energy Storage Methods

Source: Kheng Tan & Kumar Panda [16]



B. Propeller Power/RPM curves and Reference vessel Data

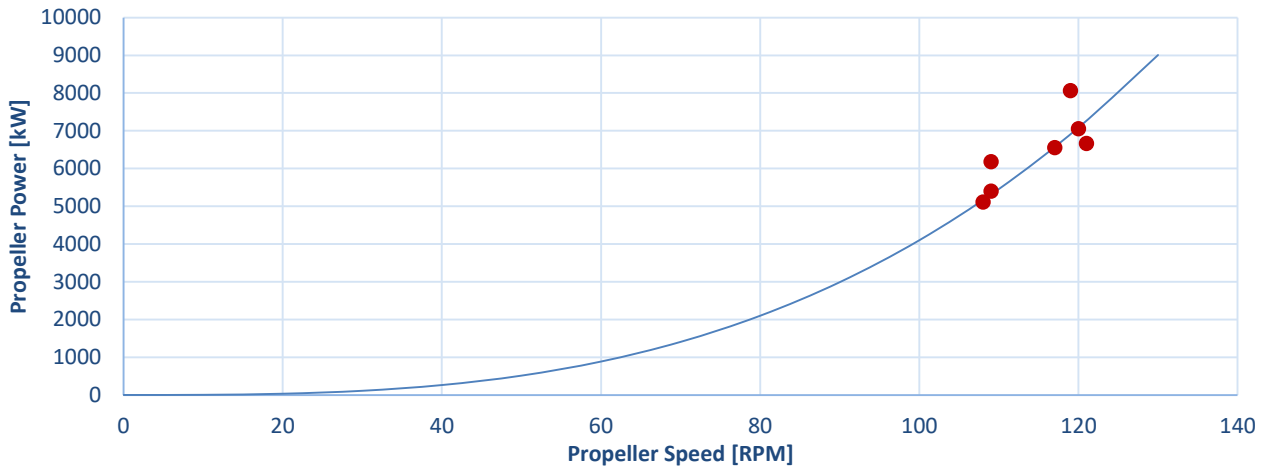


Figure 1: Propeller Power - RPM Curve of Cargo Vessels

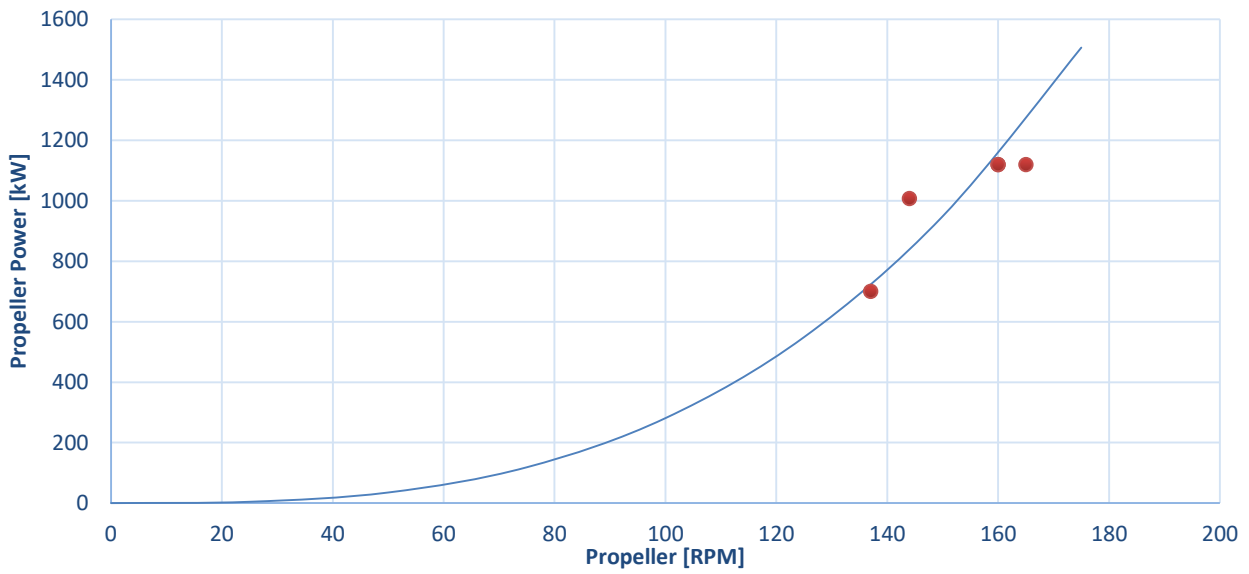


Figure 2: Propeller Power - RPM Curve of Harbor Tugs

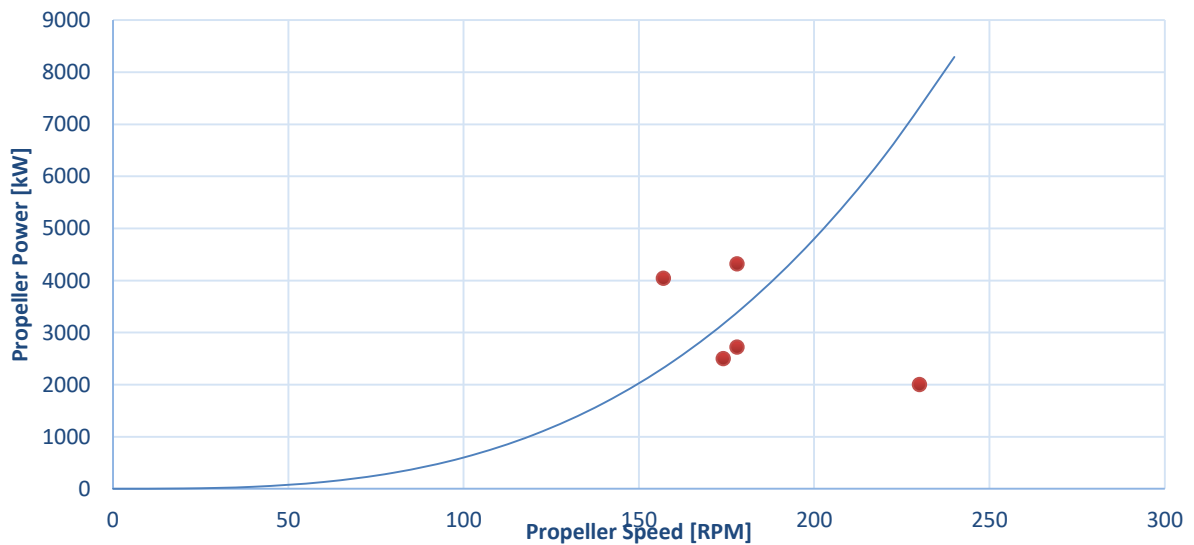


Figure 3: Propeller Power - RPM Curve of TSH Dredgers

n/a = Data not available

Table 1: Vessel Data Bulk Cargo Vessels (2 data points per vessel) [22]

Name/ Designation	V_{ship}	Size	Loa	B	T	D	P_{prop}	N_{prop}
[-]	[kts]	[dwt]	[m]	[m]	[m]	[m]	[kW]	[RPM]
1	14.5	n/a	200	23.7	10	11	6550	117
2	14.5	35000	178	28.0	9.5	10.5	7050	120
3	14.5	45000	185	30.4	10.3	11.6	8060	119
4	14.5	55000	190	32.26	11.2	12.7	8750	105
1	13.5	n/a	200	23.7	10	11	5110	108
2	13.5	35000	178	28.0	9.5	10.5	5400	109
3	13.5	45000	185	30.4	10.3	11.6	6180	109
4	13.5	55000	190	32.26	11.2	12.7	6720	95

Table 2: Vessel Data Harbor Tugs [25]

Name/ Designation	V_{ship}	Loa	B	T	D	P_{prop}	N_{prop}
[-]	[kts]	[m]	[m]	[m]	[m]	[kW]	[RPM]
YTB Design	12.75	32.9	8.5	3.5	4.7	700	137
143 ft Sea Rescue	14.3	43.6	10	4.3	5.2	1120	160
Ed. J. Moran	14	37	9	4	4.9	1120	165
Lack RR	13	32.1	7.9	3.4	4.4	1007	144
Grace Moran	13.5	32	7.9	3.5	4.5	1120	160

Table 3: Vessel Data TSH Dredgers [78], [79], [80]

Name/ Designation	V_{ship}	Loa	B	D	GT	P_{prop} Total	P_{prop}	N_{prop}
[-]	[kts]	[m]	[m]	[m]	[GT]	[kW]	[kW]	[RPM]
Scelveringhe (Den Herder)	n/a	116.8	18.6	6.4	5116	4320	4320	178
Swalinge (Den Herder)	n/a	82.2	14.6	6.3	2071	2720	2720	178
Spauwer (Den Herder)	n/a	142.8	21.6	8.5	9781	8076	4038	157
Wärtsilä Encyclopedia: Dredging	n/a	n/a	n/a	n/a	n/a	4000	2000	230
5500 TSHD (Ship Broker)	11.5	105	19	8	7260	5000	2500	174

C. Overview of the Design Processes

The design process is executed for a concept containing the components listed in Table 4. Which does not include the exhaust gas treatment systems, since these are only present when required to meet IMO emission regulations. The detailed design processes (grey in the diagrams), can be found in chapter 5 in the report. Parameters which are determined by the type of system, and thus specific for this case, are included between brackets “[..]”.

Table 4: Components Case Study

Node :	System Type :
Shaft Configuration	Single Shaft
Main Propulsive engine	2-stroke Diesel Engine + Gearbox
Power Take in	N/A
Electrical Energy Storage	Li-Ion Batteries
Main Fuel Main propulsive engine	Marine Diesel Oil (MDO)
Dual Fuel Main propulsive engine	N/A
Main Fuel PTI	N/A
Dual Fuel PTI	N/A
Generation System	Hybrid of Diesel Genset + PEMFC
Main Fuel Genset	Marine Diesel Oil (MDO)
Dual Fuel Genset	N/A
Hydrogen Storage	Pressurized Hydrogen

Propulsive power generation System Design [2-stroke, Diesel Engine on MDO + Gearbox]

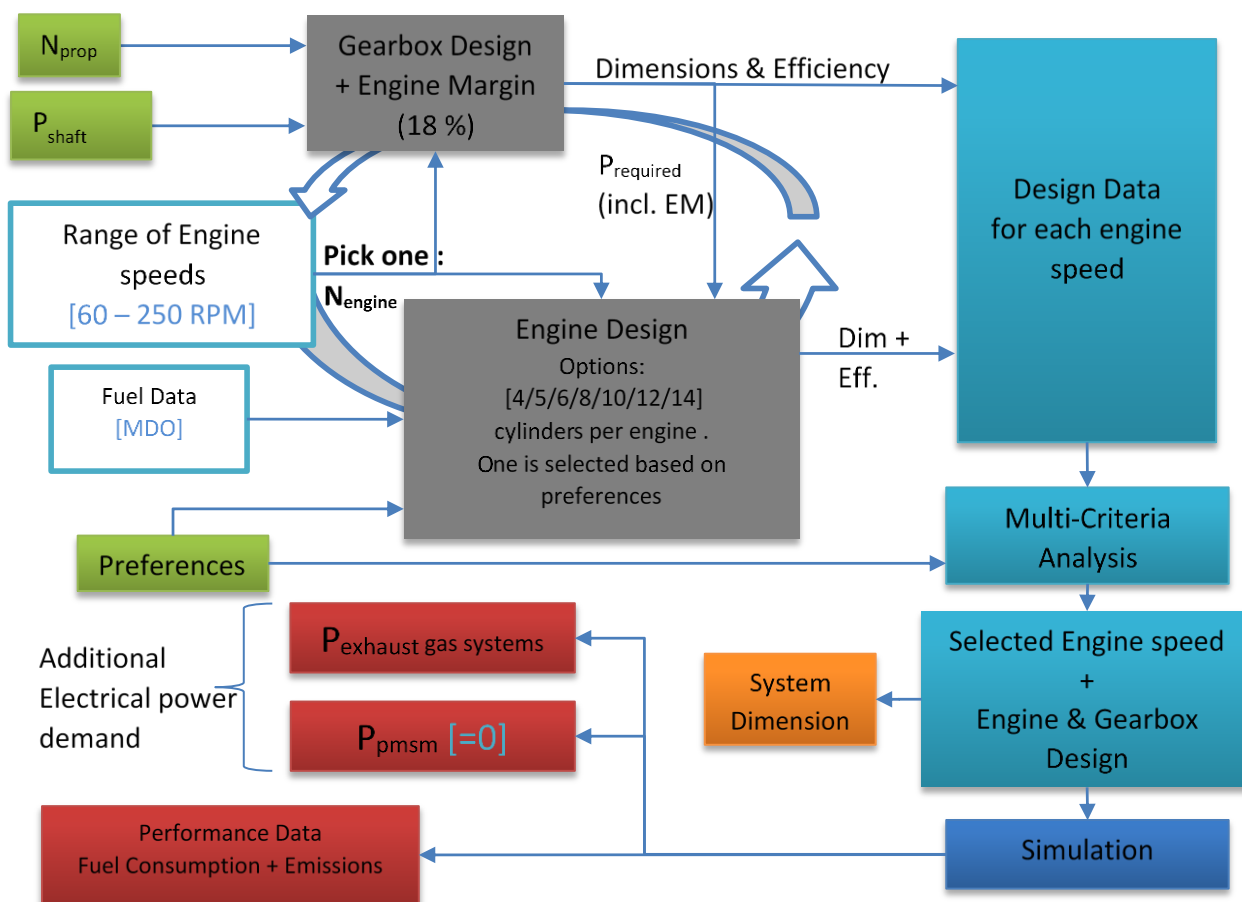


Figure 4: PGS Design, Green = User defined Input ; Blue = Algorithm ; Orange = Input obtain from other design algorithm / output towards other design algorithms. Red = Simulation results, output towards other designs & final MCA.

Electrical Grid Design (Power demands which are zero have been omitted from the figure)

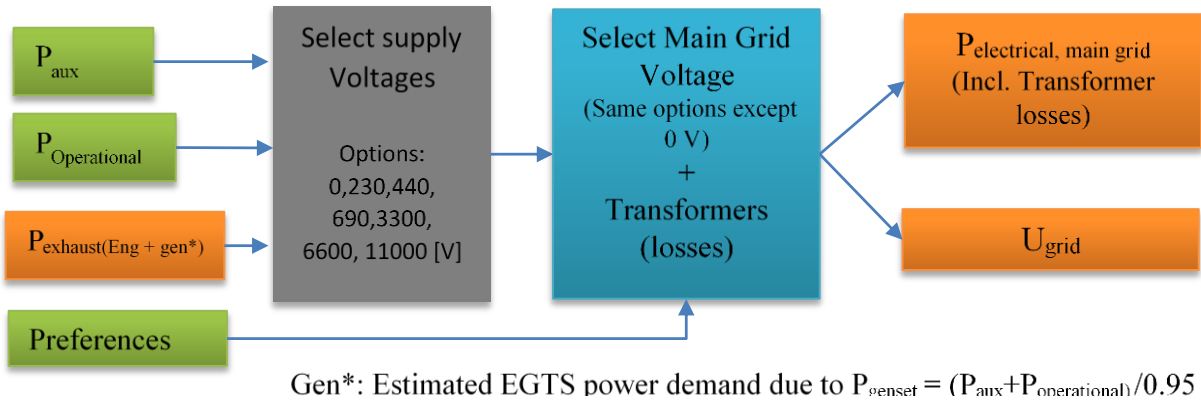


Figure 5: Grid Design, (legend same as previous figure)

Electricity Supply Design [Li-ion batteries + PEMFC + Diesel Genset running on MDO]

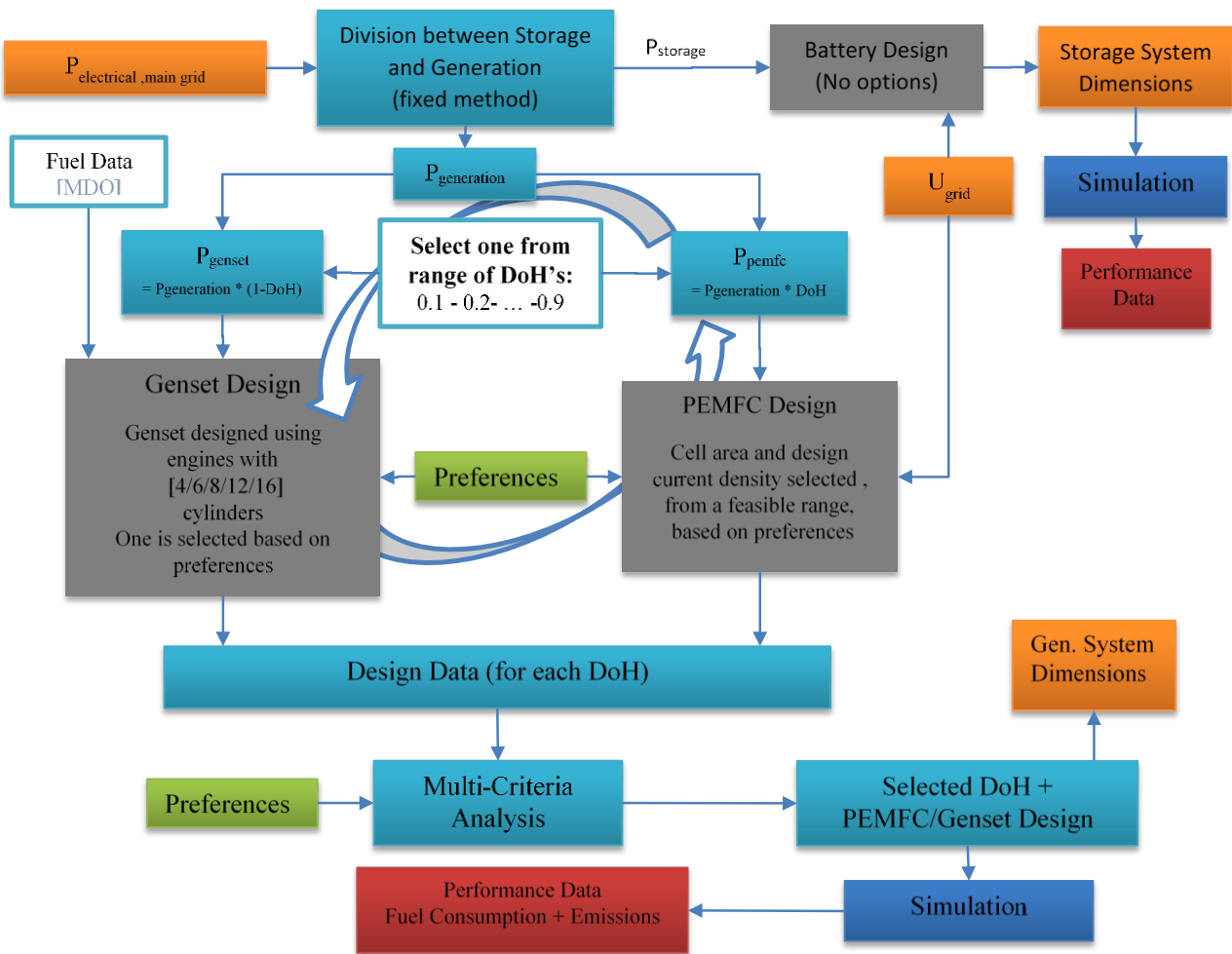


Figure 6: Generation System Design (legend same as other figures)

Exhaust Gas Treatment Systems Design & Application

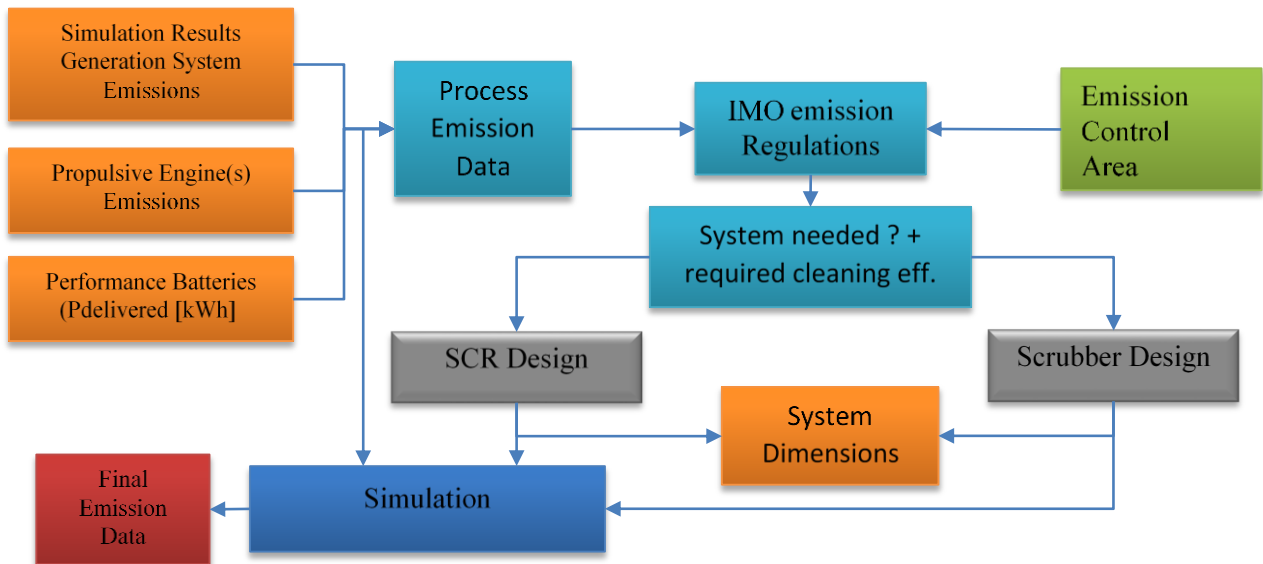


Figure 7: Exhaust Gas Treatment Design (legend same as other figures)

Final Multi Criteria Analysis

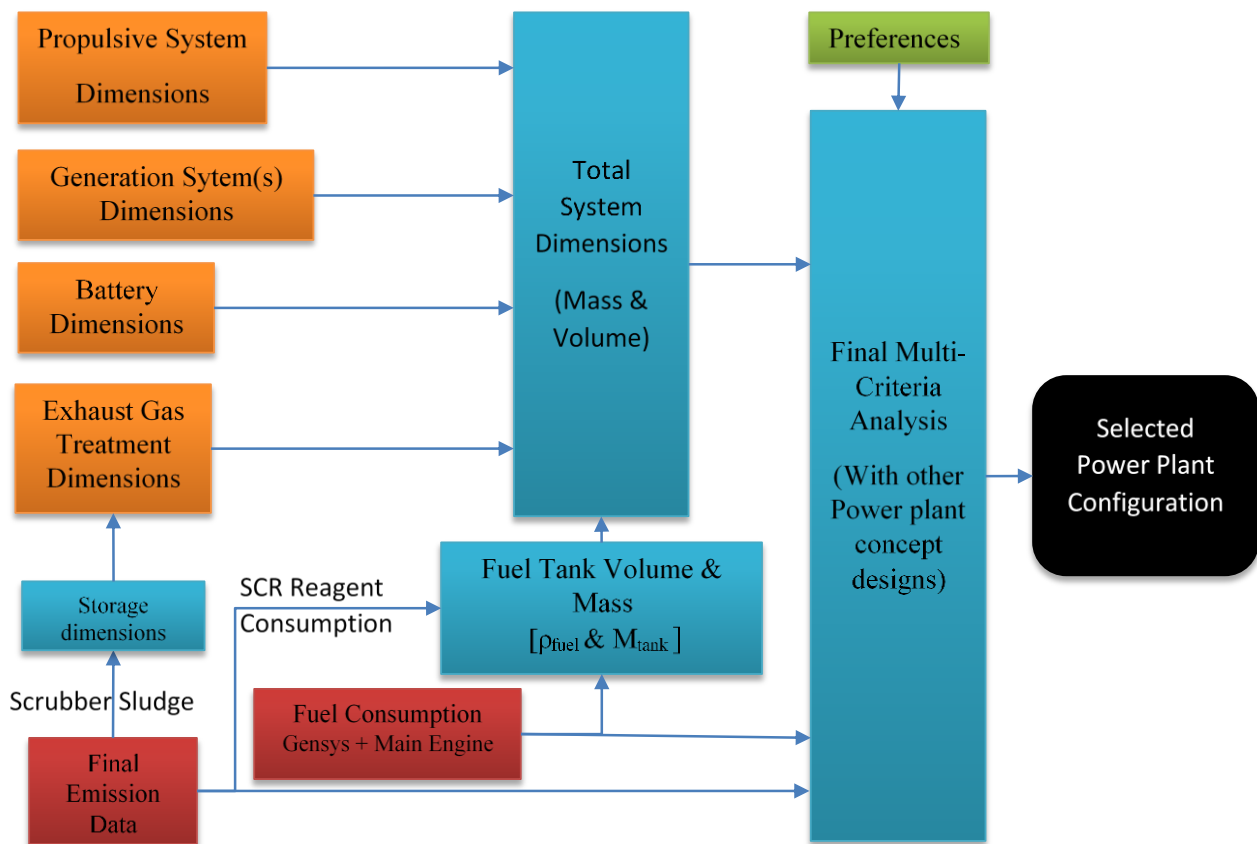


Figure 8: Final MCA; (legend same as other figures)

D. Gearbox Design Methodology

The gearbox dimensions are determined using the first principle methodology developed by Stapersma & de Vos [36]. This methodology requires several design parameters, which are obtained from the paper presenting the method and verified/updated using data from gearbox manufacturers such as Rolls-Royce [81] and RENK [82]. The selected values are summarized in Table 5.

For the special cases (the combinatory gearbox and the shaft combination gearbox) a separate dimension estimation methodology is developed, which will be discussed after the reduction gearboxes, nonetheless it is worth mentioning that the same design parameters are used by the ‘special’ gearboxes.

Table 5: Gearbox Design parameters and their values

	Symbol	Value	Unit
Tooth Shear Stress	τ_{tooth}	75	[GPa]
Maximum Tangential Speed	V_t	10	[m/s]
Lpinion/Dpinion	λ_{pinion}	0.9	[-]
Number of teeth	Z_p	25	[-]
Position pinion wheel t.o.v. main wheel	α	90	[degree]
A1/B1/C1	-	7/1.75/2	[-]

The principle dimensions of a gearbox are the dimensions of the pinion wheel and the main gear wheel, which can be determined using equation (10.1) [36].

$$D_{\text{pinion}} = \sqrt{\frac{2}{\pi} * \frac{z_p}{\tau_{ts} * v_t * \lambda_p} * P} \quad (10.1)$$

$$L_{\text{pinion}} = \lambda_{\text{pinion}} * D_{\text{pinion}}$$

$$D_{\text{wheel}} = D_{\text{pinion}} * i_{gb}$$

The only unknown parameter in the equations presented earlier is the gearbox ratio, which is defined as shown by equation (10.2).

$$i_{gb} = \frac{N_{\text{engine}}}{N_{\text{shaft}}} = \frac{z_{\text{wheel}}}{z_{\text{pinion}}}$$

or if $N_{\text{engine}} < N_{\text{shaft}}$ (10.2)

$$i_{gb} = \frac{N_{\text{shaft}}}{N_{\text{engine}}}$$

However, the number of teeth on the main wheel (z_{wheel}) has to be integer. This causes the gearbox ratio to not be completely free to select. To determine the gearbox ratio several steps are necessary.

The first step is the determination of the ‘requested’ gearbox ratio, which can be determined using the (selected) engine speed and the shaft speed.

This requested gearbox ratio is used to determine the required amount of teeth on the main gear wheel, which is then round up towards the nearest integer. This obtained, integer, number of teeth is then reverted back to an actually achievable gearbox ratio (and achieved engine speed), which is the ratio used during the design, this processes is also illustrated using equation (10.3).

$$i_{gb\text{-required}} = \frac{N_{engine\text{-required}}}{N_{shaft}}$$

$$z_{wheel} = z_{pinion} * i_{gb\text{-required}}; \text{ with } z_{wheel} = 1, 2, 3 \dots \text{inf}$$
(10.3)

$$i_{gb\text{-achieved}} = \frac{z_{wheel}}{z_{pinion}}$$

$$N_{engine\text{-achieved}} = N_{shaft} * i_{gb\text{-achieved}}$$

With the actual gearbox ratio known, the core dimensions of the gearbox can be determined, using equation (10.4) and these are also illustrated in Figure 9.

$$L_{core} = L_{pinion}$$

$$W_{core} = \max\left(\frac{D_{pinion} + D_{wheel}}{2} + \frac{D_{pinion} + D_{wheel}}{2} \cos(\alpha); D_{wheel}\right)$$

$$H_{core} = \max\left(\frac{D_{pinion} + D_{wheel}}{2} + \frac{D_{pinion} + D_{wheel}}{2} \sin(\alpha); D_{wheel}\right)$$
(10.4)

$$L_{gearbox} = A_1 * L_{core}$$

$$W_{gearbox} = B_1 * W_{core}$$

$$H_{gearbox} = C_1 * H_{core}$$

$$Vol_{gearbox} = L_{gearbox} * W_{gearbox} * H_{gearbox}$$

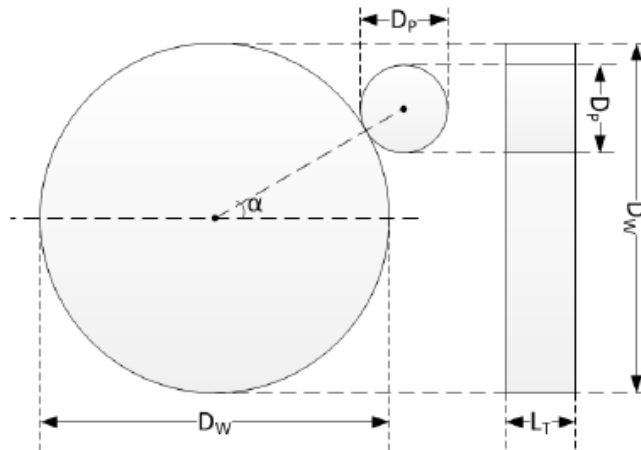


Figure 9: Reduction gearbox Dimensions [32]

The mass of a gearbox is assumed be directly proportional to its volume using an average system density. This density is determined using data obtained from RENK [82], and is found to be 1.5 [ton/m³].

$$Mass_{Gearbox} = Vol_{gearbox} * \rho_{gearbox} \quad (10.5)$$

The efficiency of the gearbox still has to be determined. This efficiency is assumed to be 99% [8, p. 167] for a single step reduction gearbox. However, a single step gearboxes has a maximum ratio of 6.25 [81] & [8, p. 156].

The losses inside a gearbox are mainly caused by friction losses caused by the bearings and suspensions needed for a shaft to be able to rotate. When a single step, and thus a single shaft, is no longer sufficient, an additional shaft is required. This adds another set of bearings and thus also introduces another 99% loss term. Therefore the efficiency of the gearbox is related to the number of reduction steps required to achieve the required gearbox ratio, as shown by equation (10.6).

$$\begin{aligned} \#_{steps} &= {}^{6.25} \log(i_{gb}), \text{ with } \#_{full_steps} = 0, 1, 2, \dots, n \\ \eta_{gb} &= 0.99^{1+\#_{full_steps}} \end{aligned} \quad (10.6)$$

Special Cases

However, there are cases where a gearbox is used in a different way. For this research these cases are the combinatory gearbox and the shaft configuration gearbox. Both of which do not change the rotational speed of the shafts (so the reduction ratio is equal to 1). However, their mass and volume still has to be determined. Since the gearbox has a reduction ratio of 1, the pinion wheel and main wheel have an equal diameter. However, the number of pinion wheels is variable. The influence of this variable number of gears can be seen in Figure 10.

Therefore the original dimensioning equations for gearboxes are adapted to suit these special cases. The equations which are changed are shown by equation (10.7) and equations or parameters which remain unchanged are not repeated.

$$\begin{aligned} D_{wheel} &= D_{pinion} \\ \alpha &= 0 \text{ degrees} \\ W_{core} &= \#_{gears} * D_{wheel} \end{aligned} \quad (10.7)$$

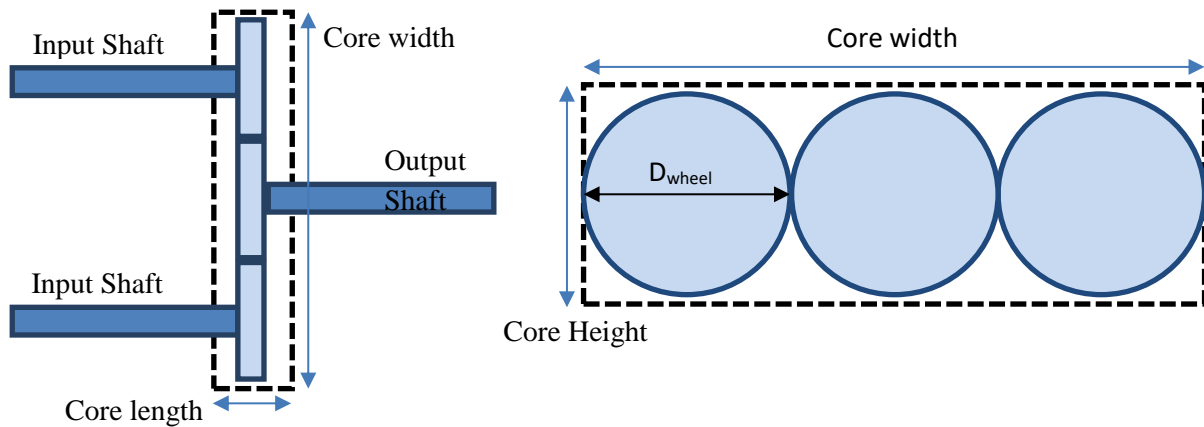


Figure 10: multiple-input, single output gearbox core dimensions

E. Combustion Engine Design Methodology

For the combustion engine design both the dimensions and the efficiency of the system have to be determined. The dimensions are estimated using the dimension prediction methodology developed for combustion engines presented by Stapersma & de Vos [36]. This methodology uses several, engine type dependent, design parameters. These parameters are estimated using engine databases presented by Stapersma [37, pp. 79-87], Rolls-Royce [38] and MAN [39] and Stapersma & de Vos [36]. All of the selected parameters are summarized in Table 6

One constant of importance in the determination of the dimensions of the engine is the cylinder configuration. For the (slow running) 2-stroke engines, this is a line build. However, the different sources show that 4-stroke engines are constructed in both line and V construction. It can be discerned from these same sources that until 10 cylinders these engines are in general constructed as line engines. For a higher number of cylinders this changes to a V construction. This same trend is implemented in the dimension prediction algorithm. Note that certain parameters such as the angle between the cylinders is also dependent on the construction type.

For dual fuel engines less extensive databases are available. Therefore the 4-stroke diesel engine parameters are used, and adapted where necessary. The main adaptations concern the mean effective pressure and the stroke to bore ratio. Which are different from those determined for the 4-stroke engines to prevent engine knocking [60].

Additionally the fit parameters are also different, since dual fuel engines have some additional auxiliary systems. The values for these fit parameters are determined using the data provided by Wärtsilä [40]. The selected parameters for dual fuel engines are also summarized in Table 6.

Table 6: Engine Design parameters and their values

	Symbol	2 – Stroke Engines	4 - Stroke Engines	Dual Fuel Engines (4-stroke)	Unit
Engine Type	K_{engine}	1	2	2	[-]
Conventional number of cylinders	i_{engine}	[4;5;6;8;10;12;14]	[6;8;9;12;16;18;20]	[6;8;9;12;16;18]	[-]
Mean Effective Pressure	p_{me}	21	25	22	[Bar]
Mean Piston Speed	C_m	9	11	11	[m/s]
Lstroke/Dbore	λ_{engine}	3.7	1.1	1.4	[-]
Reference Efficiency	η_{ref}	0.49	0.45(< 1000 RPM) 0.38(>1000 RPM)	0.45(< 1000 RPM) 0.38(>1000 RPM)	[-]
A1/B1/C1	-	Line : 2.1/2.2/1.5 V: n/a	Line: 2.5/4.2/5 V: 2.5/3/5	Line: 2.7/6/4.6 V: 3.5/3.5/4.6	[-]
Average Engine Density	ρ_{engine}	1.18	0.79	0.79	[Tonnes/m ³]
Construction Type	ct	Crosshead Piston $ct = 1$	Trunk Piston $ct = 0$	Trunk Piston $ct=0$	[-]
Cylinder Configuration	α	Line: $\alpha=0$ V: n/a	Line : ($\alpha=0$) ($i_{engine}<10$) V: ($\alpha=60$) ($i_{engine}>10$)	Line : ($\alpha=0$) ($i_{engine}<10$) V: ($\alpha=60$) ($i_{engine}>10$)	[degree]

With all design parameters known, the dimension and performance estimation can be discussed. The first step in the determination of the dimension of the engines is the estimation of the fundamental dimensions. Which for internal combustion engines are the dimensions of a cylinder, described as a stroke length and bore diameter. These dimensions are then used to determine an (inverse) power per cylinder ('C'), all of which are shown by equation (10.8) and (10.9) (with n_{nom} the engine speed in Hz). All these equations have been presented by Stapersma & de Vos [36].

$$L_{stroke} = 0.5 * \frac{C_m}{n_{nom}} \quad (10.8)$$

$$D_{bore} = \frac{L_{stroke}}{\lambda_{engine}}$$

$$C = \left(\frac{32}{\pi}\right) * \frac{\lambda_{engine}^2}{c_m^3} * n_{nom}^2 * \left(\frac{k}{P_{me}}\right) \quad (10.9)$$

Using the inverse power per cylinder, the minimum number of required number of cylinders necessary to meet the power demanded from the propulsive power generation system can be determined, as shown by equation (10.10), the result of this equation has to be rounded up towards the nearest integer, since a partial cylinder is not possible.

$$\#_{cylinders} = C * P_{PGS} \quad (10.10)$$

Then the number of engines required to meet the demanded amount of cylinders can be determined, since the number of cylinders per engine is predetermined by the algorithm. The number of engines can then be found using equation (10.11). The result of which has to be rounded up towards the nearest integer once again.

$$\#_{Engines} = \frac{\#_{Cylinders}}{i_{engine}} \quad (10.11)$$

Should this number of engines be larger than one, then the combinatory gearbox is required. The mass and volume of this gearbox is estimated using the methodology discussed in appendix D.

The volume of a single engine (and from that the mass) are determined using the methodology developed by Stapersma & de Vos [36], this method is also summarized, using the most important equations, on the following page. Note that the alfa used in these equations is the same alfa as mentioned by Table 6 but now in radians.

The engine mass and volume can then be combined with the installed number of engines to obtain the total mass and volume of the propulsive power Generation system.

$$L_{core} = i_{engine} * D_{bore} \text{ (for Line build engines)}$$

or

$$L_{core} = \frac{i_{engine}}{2} * D_{bore} \text{ (For V-build engines)}$$

$$W_{core} = 2 * \max\left(\left(\frac{L_{stroke}}{2} + (1 + ct) * L_{stroke}\right) * \sin(0.5 * \alpha) + \frac{D_{bore}}{2} \cos(0.5 * \alpha); \frac{L_{stroke}}{2}\right)$$

$$H_{core} = \frac{L_{stroke}}{2} + \max\left(\left(\frac{L_{stroke}}{2} + (1 + ct) * L_{stroke}\right) * \cos(0.5 * \alpha) + \frac{D_{bore}}{2} \sin(0.5 * \alpha); \frac{L_{stroke}}{2}\right)$$

$$L_{engine} = A_1 * L_{core}$$

$$W_{engine} = B_1 * W_{core}$$

$$H_{engine} = C_1 * H_{core}$$

$$Vol_{engine} = L_{engine} * W_{engine} * H_{engine}$$

$$Mass_{engine} = Vol_{engine} * \rho_{engine}$$

Now that all the dimensions of the engines have been determined, an indication of the performance of a given propulsion plant has to be estimated. This indication is determined based on a reference efficiency. Which is determined for an engine running at its Maximum Continuous Rating (MCR). The references values are included Table 6, for each engine type.

The given reference efficiency is first transformed to a reference Specific Fuel Consumption (SFC), which is defined in [gram fuel/kWh]. The conversion of efficiency to SFC is shown by equation (10.12) [37, p. 31]. The lower heating value is dependent on the fuel type and can be determined for each concept.

$$SFC_{ref} = \frac{3600000}{\eta_e * h^L} \quad (10.12)$$

However, this reference fuel consumption is that of an engine running at the MCR power that can be obtained from a certain cylinder geometry. Since it is possible for an engine to be designed for an MCR which is lower than this maximum, the nominal fuel consumption will also change. This change is accounted for using equation (10.13), which has been derived by Jalkanen et al [35] based on Wärtsilä data. The result of which is the SFC at the 'requested' MCR.

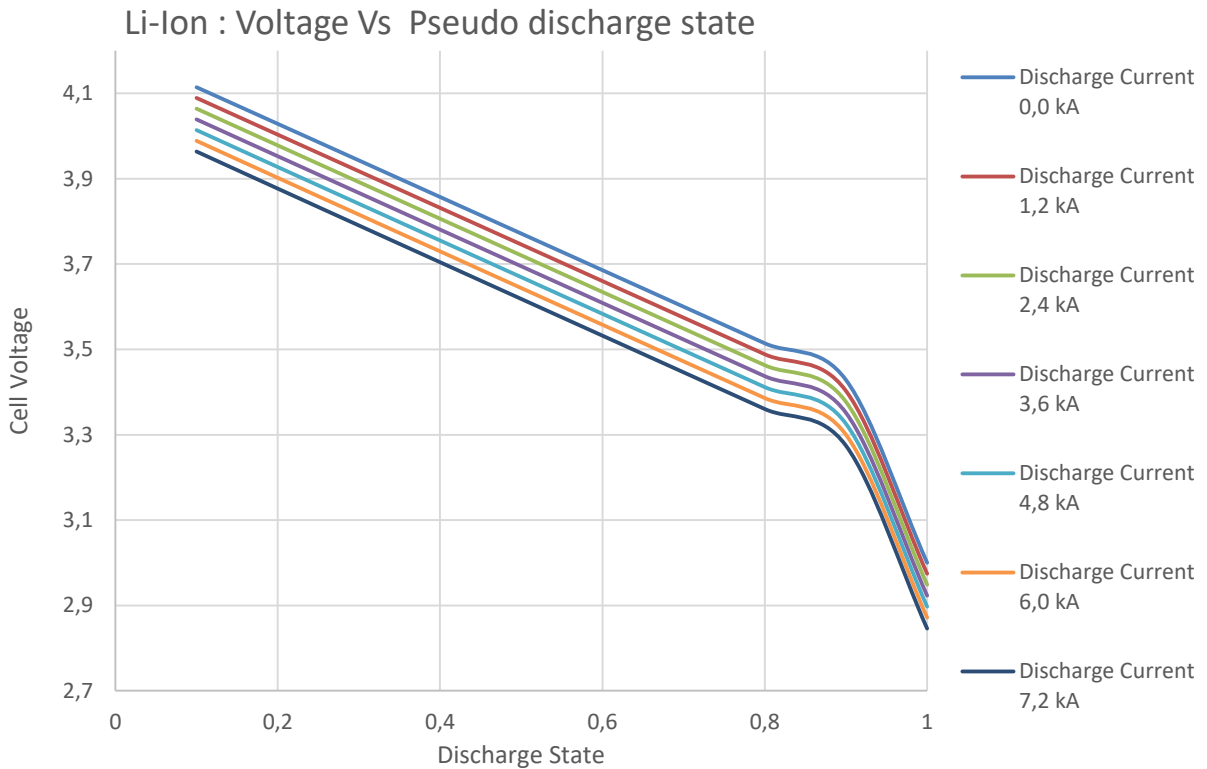
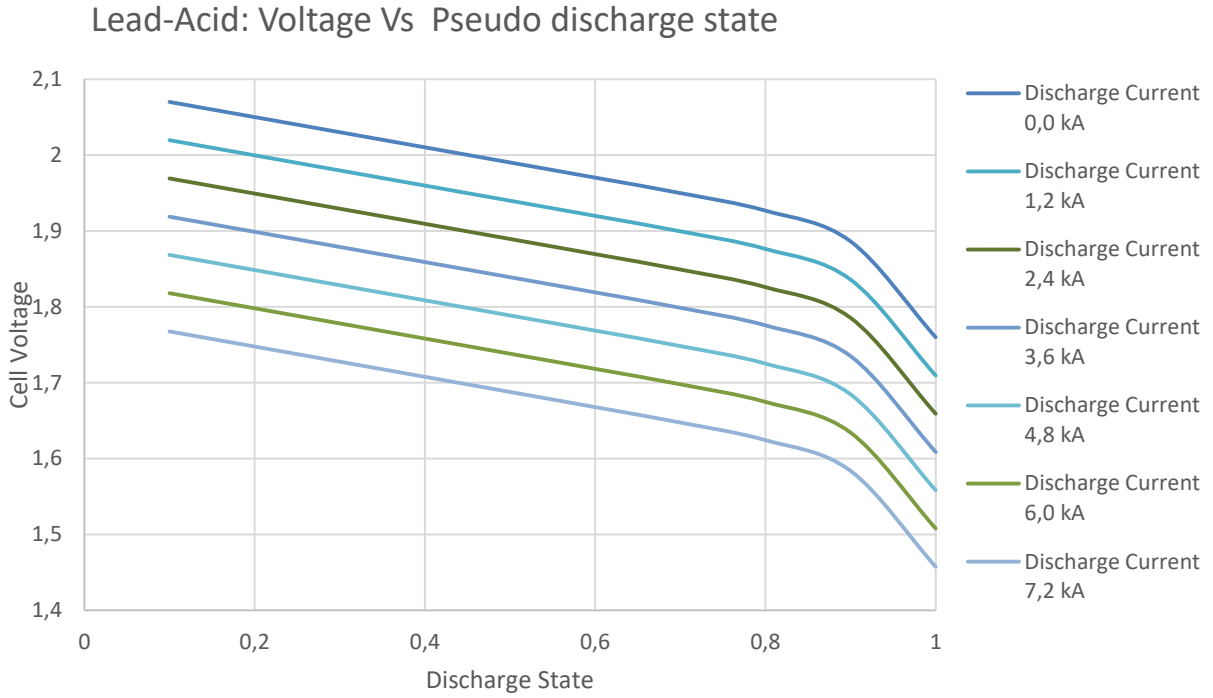
$$SFC_{MCR} = SFC_{ref} * \left(0.455 * \left(\frac{P_{load}}{P_{rated}}\right)^2 - 0.71 * \frac{P_{load}}{P_{rated}} + 1.28\right) \quad (10.13)$$

Equation (10.13) is also used to obtain a rough estimate of the fuel consumption at different parts of the operational profile. However, in those cases the reference sfc ("SFC_{ref}") is now the MCR fuel consumption. This results in a very broad estimate, and as such a performance estimate remains necessary to obtain more accurate estimates, after the selection of an engine design.

The emissions are mainly related to the fuel type and to the engine speed, which do not vary per engine design, and as such the fuel consumption can also be used as an indication for the emissions.

F. Battery Discharge Behavior

Voltage as a function of discharges state, for different discharge currents.



G. PEMFC Design Methodology

An electric energy generation system designed with fuels cells consists of an inverter, a number of fuel cell stacks in parallel and a compressor as shown by Figure 11 [74]. Each of the fuel cell stacks then consists of individual fuel cells connected in series as shown by Figure 12. The inverter is assumed to have a constant efficiency of 99% [45] and its dimension are estimated using the methodology presented for the energy storage system (paragraph 5.5.2 of the main report).

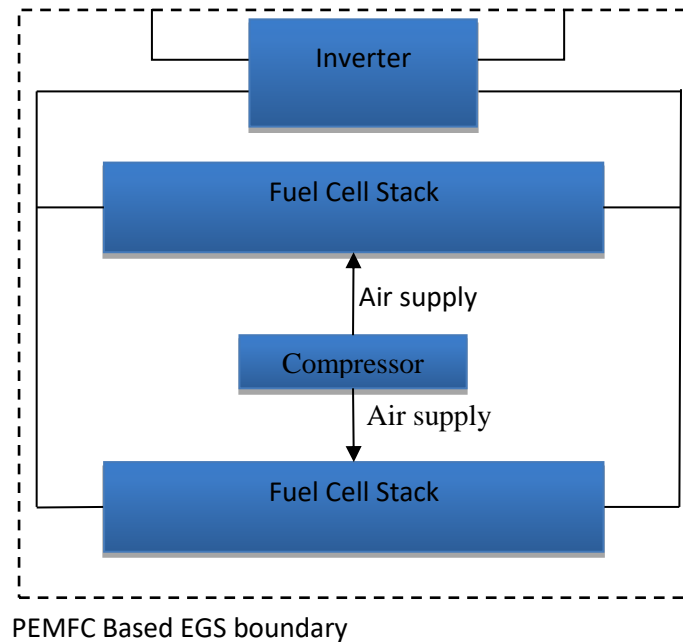


Figure 11: PEMFC based generation system lay-out

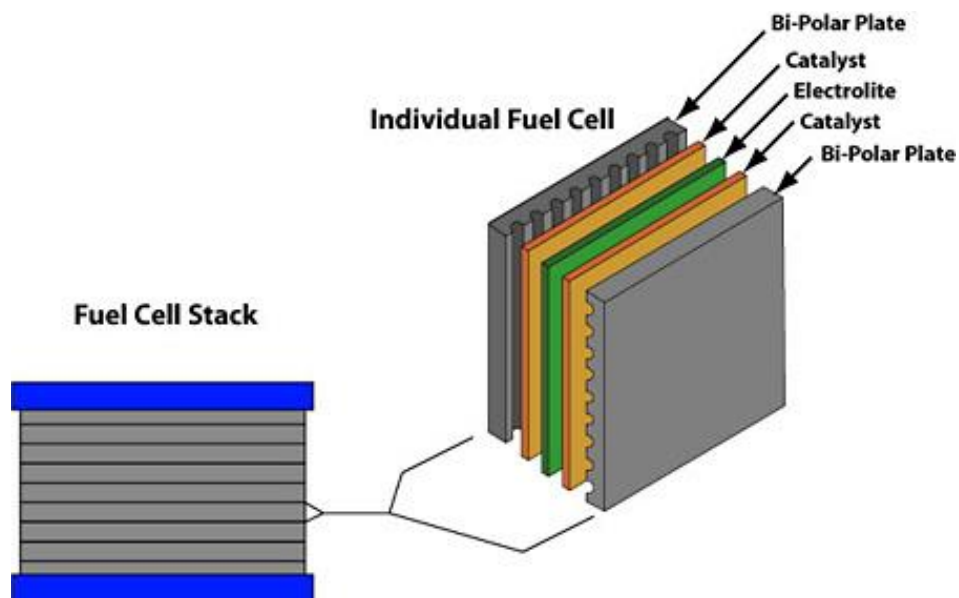


Figure 12: Fuel Cell Construction [83]

Therefore the main parameters in the construction of a fuel cell based system are the number of cells, the number of stacks and the size of a single cell. All these in some way related to the power required of the total system. These relationships will be discussed to obtain an indication of the system dimensions.

A fuel cell stack delivers a current which is equal to that of a single cell, which in turn is related to the surface cell area, as shown by equation (10.14) [4]. The cell area and nominal current density are varied by the design algorithm from a feasible range (see paragraph 5.5.3).

$$I_{stack} = I_{cell} = A_{cell} * i_{cell} \quad (10.14)$$

From the selected current density the voltage of a single cell can be determined using the 'polarization curve', which is represented by equation (10.15).

$$U_{cell} = E_o - (i + i_n) * r - A^{ln} * \ln\left(\frac{i + i_n}{i_o}\right) + B * \ln\left(\frac{i + i_n}{i_l}\right) \quad (10.15)$$

E_o = Open Cell Voltage

R = Gas Constant, $8.3145 \text{ [J} \cdot \text{mol}^{-1} \cdot \text{K}^{-1}]$

T = Temperature [K]

F = Faraday's Constant, $96485.3 \text{ [C} \cdot \text{mol}^{-1}]$

P_x = Partial Pressure of x [bar]

i = Actual Current Density $[\text{A} \cdot \text{m}^{-2}]$

i_o = Exchange Current Density $[\text{A} \cdot \text{m}^{-2}]$

i_n = Internal Equivalent Current Density $[\text{A} \cdot \text{m}^{-2}]$

i_l = Limiting Current Density $[\text{A} \cdot \text{m}^{-2}]$

r = Area Specific Resistance $[\Omega \cdot \text{m}^2]$

A^{ln} = Tafel Voltage loss coefficient on a ln base [V]

B^{ln} = Coefficient for mass transport voltage loss [V]

The polarization curve requires several technological parameters, for which numerous values can be found. Ten Hacken [4] presents values which are assumed to be the state of the art for these fuel cells, these values are used for this research as well, and summarized in Table 7.

The open cell voltage E_o is a function of the operating conditions of the fuel cell. These conditions obtained from ten Hacken [4] and the EFIN project [74]. However, ten Hacken adjusted for the application of pure oxygen, which is not the case for surface vessels. For surface vessels fuel cells are supplied with 'normal' air through a compressor. Some adjustment for the increased operating pressure as made by ten Hacken [4] can be maintained, since the compressor pressurizes the fuel cell. This leads to the operating conditions as summarized by Table 8.

Table 7: Technological Parameters PEMFC

Parameter	Value	Unit
i_n	100	$\text{A} \cdot \text{m}^{-2}$
$A^{ln}_{cathode}$	0.044	V
$i_{o-cathode}$	1.0	$\text{A} \cdot \text{m}^{-2}$
A^{ln}_{anode}	0.018	V
$i_{o-anode}$	1000	$\text{A} \cdot \text{m}^{-2}$
r	$1.0 \cdot 10^{-6}$	$\Omega \cdot \text{m}^2$
B	0.010	V
i_l	16000	$\text{A} \cdot \text{m}^{-2}$

Table 8: Operating Conditions PEMFC

Parameter	Value	Unit
Operating Temperature	80	$^{\circ}\text{C}$
Operating Pressure	5	bar
Open circuit voltage	1.1922	V
Fuel Utilization factor	1	-
Air Excess ratio (λ_{air})	2	-
Fuel cell current rate limit	0.08	$\text{A} \cdot \text{cm}^{-2} \cdot \text{s}^{-1}$

The presented design parameters and operating conditions result in the polarization curve as shown by Figure 13, which shows the influence of the different losses and the resulting polarization curve for a single fuel cell as function of the current density.

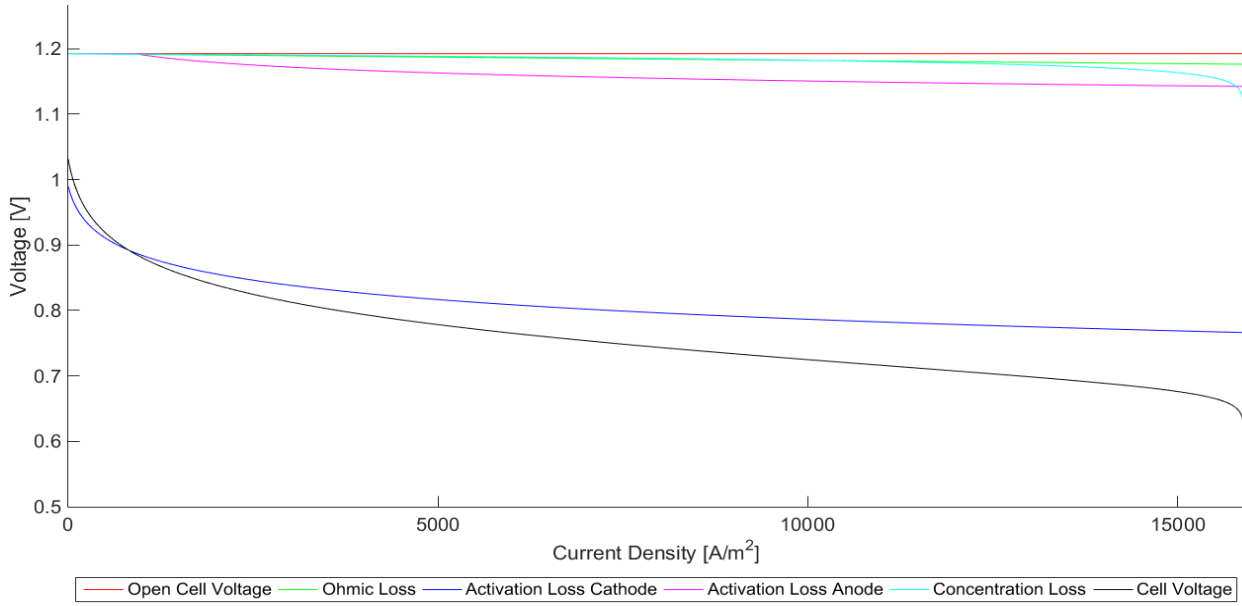


Figure 13: Polarization Curve of a PEM Single Fuel Cell

With the cell voltage and cell current known, the power of a single fuel cell can be determined, as shown by equation (10.16).

$$P_{cell} = U_{cell} * I_{cell} = U(i_{cell}) * (A_{cell} * i_{cell}) \quad (10.16)$$

The fuel cell system is assumed to be designed to deliver a voltage greater than or equal to the grid voltage, therefore the number of cells in series (inside a single stack) can then be determined using equation (10.17).

$$\#_{cells} = \frac{U_{grid}}{U_{cell}} \quad (10.17)$$

In practice the amount cells that can be placed in series in a stack is limited. However, it is possible to connect multiple stacks can be connected in series. Therefore this limit is not included. The power delivered by a single stack can be determined using equation (10.18).

$$P_{stack} = (\#_{cells} * U_{cell}) * I_{stack} \quad (10.18)$$

As mentioned earlier a compressor is required for the cooling of the fuel cells and the supply of oxygen to the fuel cell. Both the power demand and the dimensions of the compressor have to be included in the design as well. The power demand of a compressor, per fuel cell stack, can be approximated using the adiabatic compression power formula, also shown by equation (10.19)

$$P_{compressor} = Q_{air,stack} * \frac{\gamma * P_1}{\gamma - 1} * \left(\frac{P_2}{P_1}^{\frac{\gamma-1}{\gamma}} - 1 \right) \quad (10.19)$$

With P_1 the ambient pressure (1 [bar]), P_2 the required pressure (5 [Bar]) and the value of kappa is 1.4, which is the standard value for air.

The only unknown in this equation is the required air flow (Q), which has to be delivered to the fuel cells. The required airflow of a single stack can be determined using equation (10.20) [74]. With the stoichiometric ratio ‘v’ as 4, which is derived from the fact that one oxygen molecule delivers 4 electrons (derivable from the chemical reaction taking place inside a fuel cell, shown by for example [4]).

$$Q_{air,stack} = \lambda_{air} * \left(\frac{I_{stack} * \#_{cells}}{v * F} * \frac{1}{0.21} * \frac{M_{air}}{1000} \right) \quad (10.20)$$

The complete required power that has to be delivered by the fuel cell based system can then be defined as shown by equation (10.21)

$$P_{required} = (\#_{stacks} * P_{compressor}) + \frac{P_{electric}}{\eta_{inverter}} \quad (10.21)$$

The number of fuel cell stacks in parallel can now be determined using equation (10.22), the result of which has to be rounded up towards the nearest integer once again.

$$\#_{stacks} = \frac{P_{required}}{P_{stack}} \quad (10.22)$$

The two equations presented above can then be combined and rewritten to determine the required number of stacks in parallel, as shown by equation (10.23).

$$\#_{stacks} = \frac{P_{elec}}{\eta_{inverter}} * \frac{1}{P_{stack} - P_{compressor}} \quad (10.23)$$

The dimensions of a single fuel cell stack can then be determined using equation (10.24) [4]. Which included the surface area of a single fuel cell, the thickness of one fuel cell, which is assumed to be 1.34 [mm], which is the thickness of the fuel cells installed in the Toyota Mirai [84].

The volume factor ‘f’ is assumed to be 2.1 and the density of a single stack is 1.51 [kg/liter]. Both of which are state of the art values for fuel cell technology, based on the Toyota Mirai [84].

$$\begin{aligned} V_{core} &= A_{cell} * \tau_{cell} * N_{cell} \\ V_{stack} &= f_{volume} * V_{core} \\ M_{stack} &= V_{module} * \rho_{module} \end{aligned} \quad (10.24)$$

The dimensions of the total system can then be determined using equation (10.25). The inverter dimensions were discussed at the beginning of this paragraph. However, the compressor dimensions have been left underdetermined. These will be determined on the following page.

$$V_{system} = \#_{stacks} * V_{stack} + V_{compressor} + V_{inverter} \quad (10.25)$$

$$M_{system} = \#_{stacks} * M_{stack} + M_{compressor} + M_{inverter}$$

Compressor Dimensions

The dimensions of the compressor are estimated by scaling a reference air compressor. Because the airflow required by the fuel cells can quickly become quite large, while remaining at a relatively low pressure this reference compressor is selected to be an axial compressor with a maximum pressure rating of 7 bar [85] the values of which are summarized in Table 9.

Table 9: Reference Compressor Data [82]

Parameter	Value	Unit
Max. outlet Pressure	7	[Bar]
Q	535200	[m ³ /hour]
Length	8.255	[m]
Width	4.623	[m]
Height	4.630	[m]
Mass	122.47	[Tonnes]

The compression ratio of the selected reference compressor exceeds the required compression ratio. However, obtaining data for compressors which better match the requirements has not been possible. Therefore the selected reference compressor is first adjusted to better suit the requirements.

For an axial compressor the length is mainly a function of the number of steps required to obtain the required pressure difference. Therefore the length of the reference compressor is adjusted according to equation (10.26). Other reference values are kept the same.

$$L_{compressor_5bar} = L_{compressor_7bar} * \frac{5}{7} \quad (10.26)$$

The rescaling of the corrected compressor is done using the methodology presented by equation (10.27).

$$f = \frac{Q_{required}}{Q_{reference}}$$

$$L_{compressor} = L_{compressor_5bar} * f^{1/3}$$

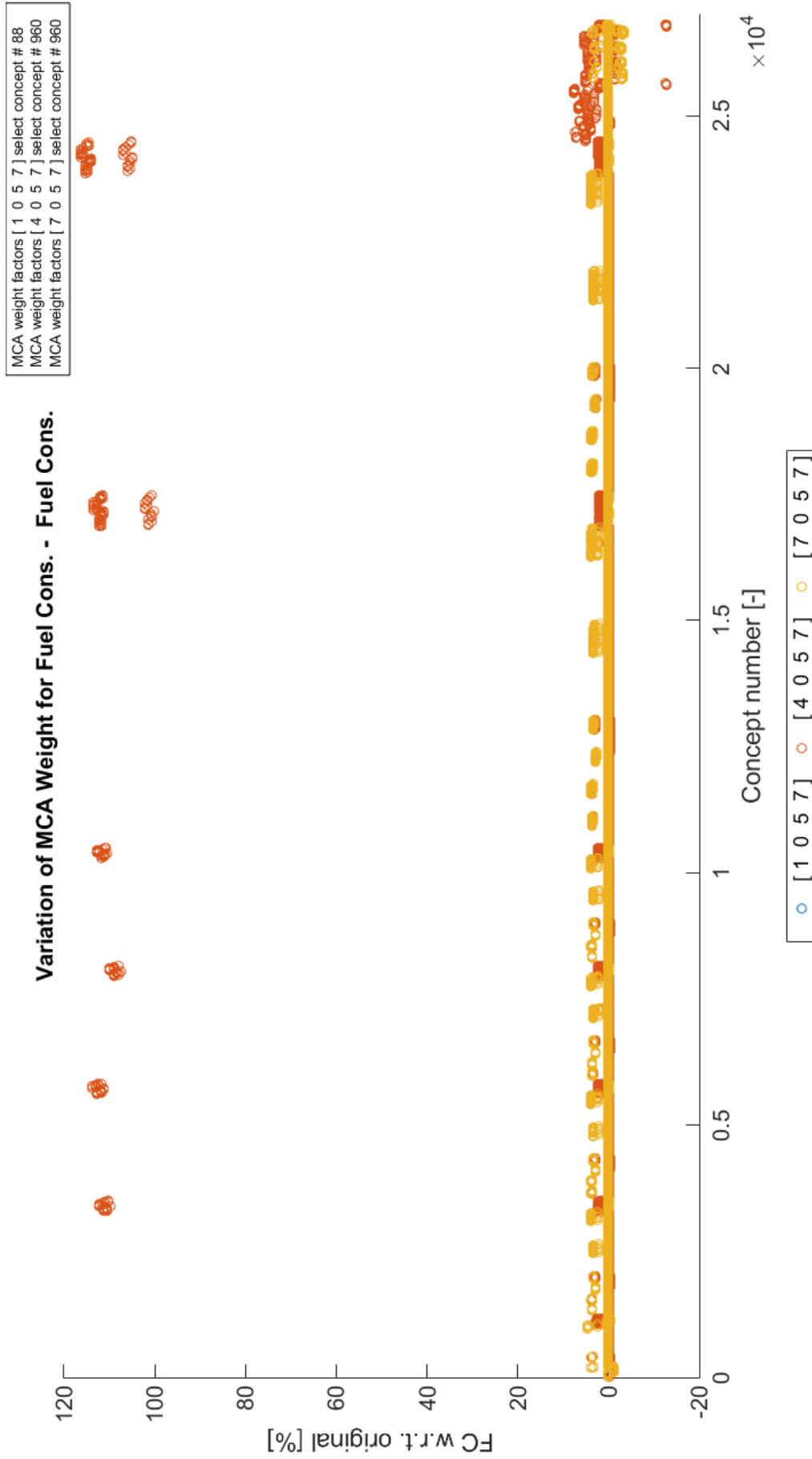
$$W_{compressor} = W_{reference} * f^{1/3} \quad (10.27)$$

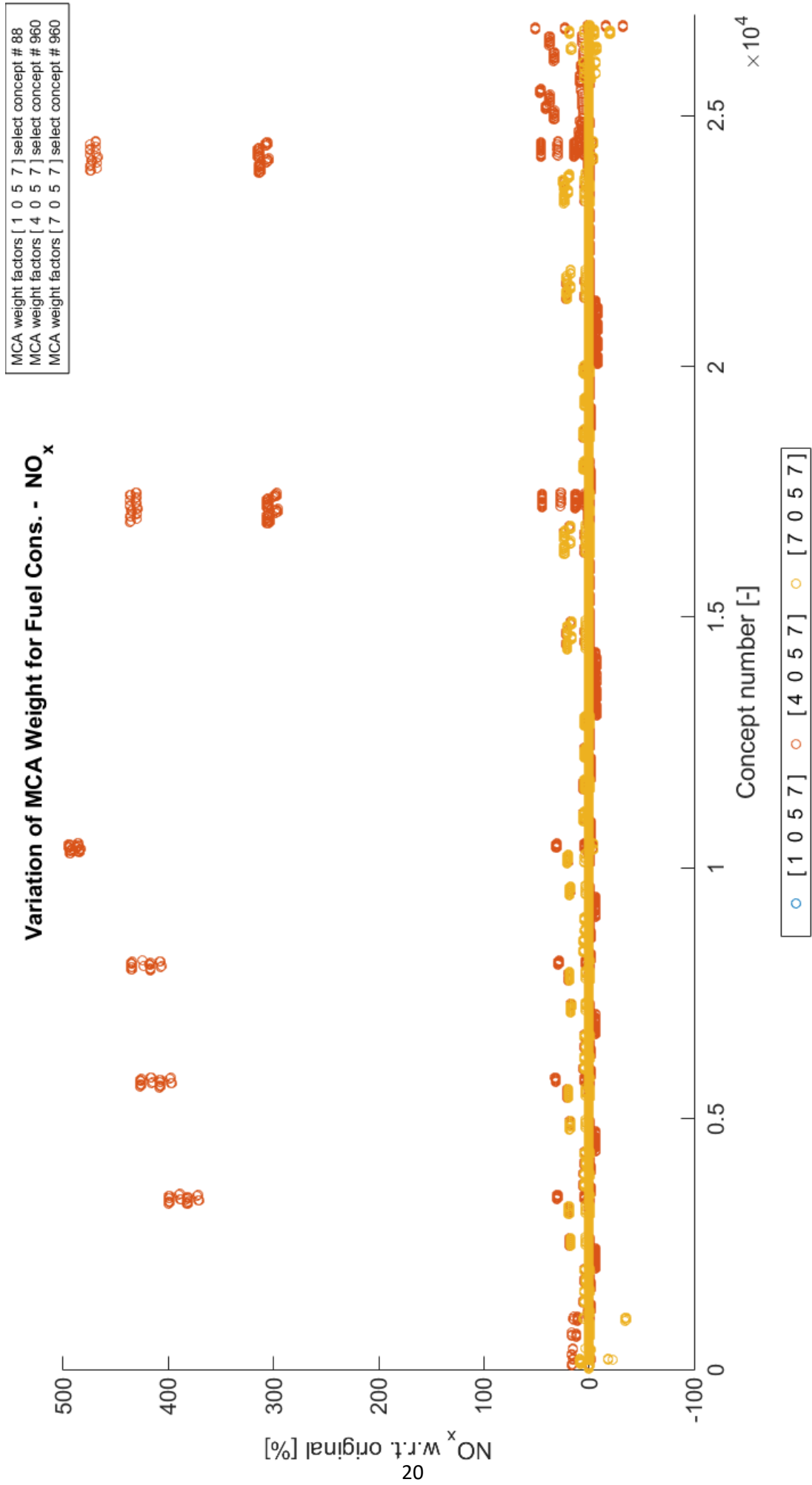
$$H_{compressor} = H_{reference} * f^{1/3}$$

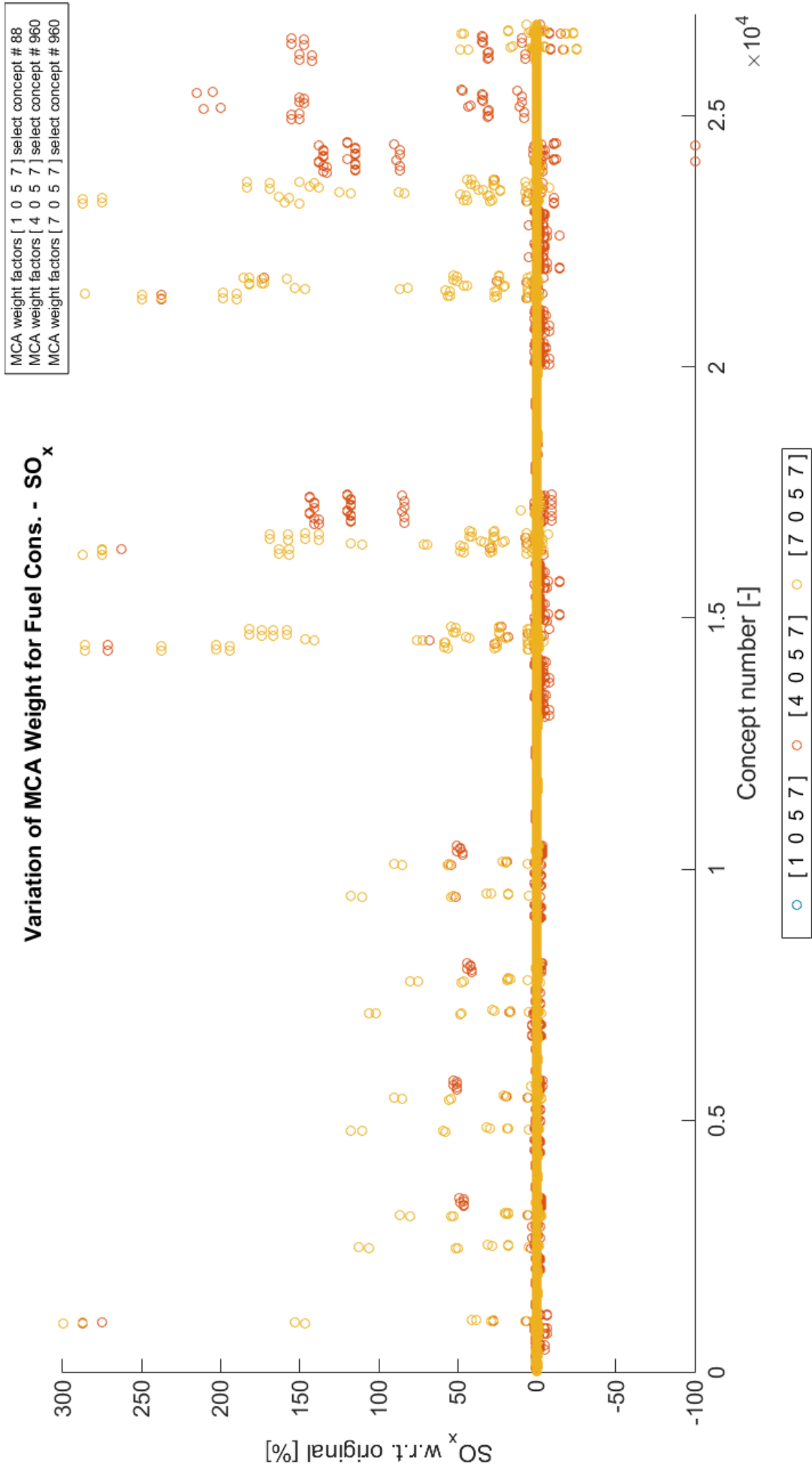
$$V_{compressor} = L_{compressor} * W_{compressor} * H_{compressor}$$

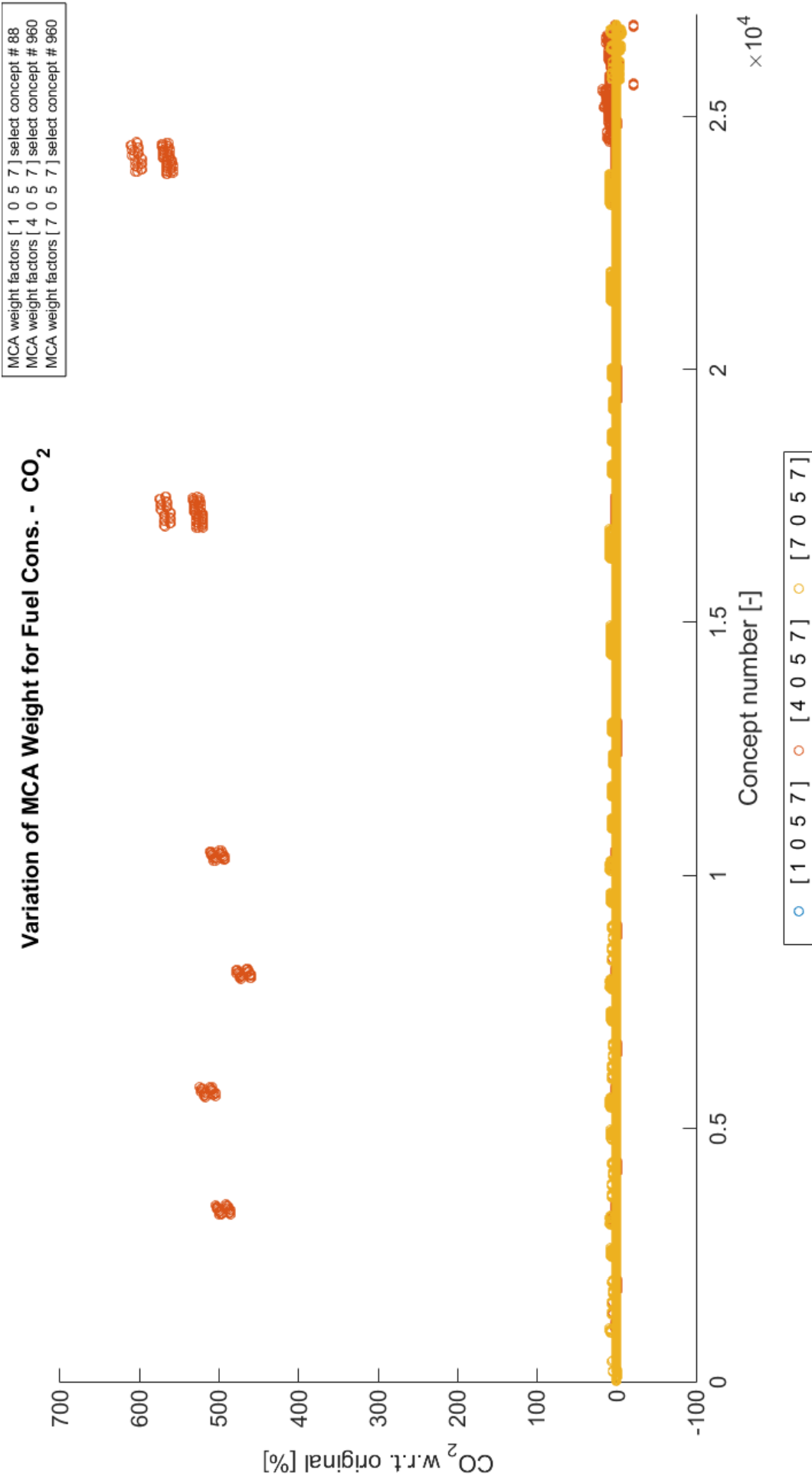
$$M_{compressor} = M_{reference} * f$$

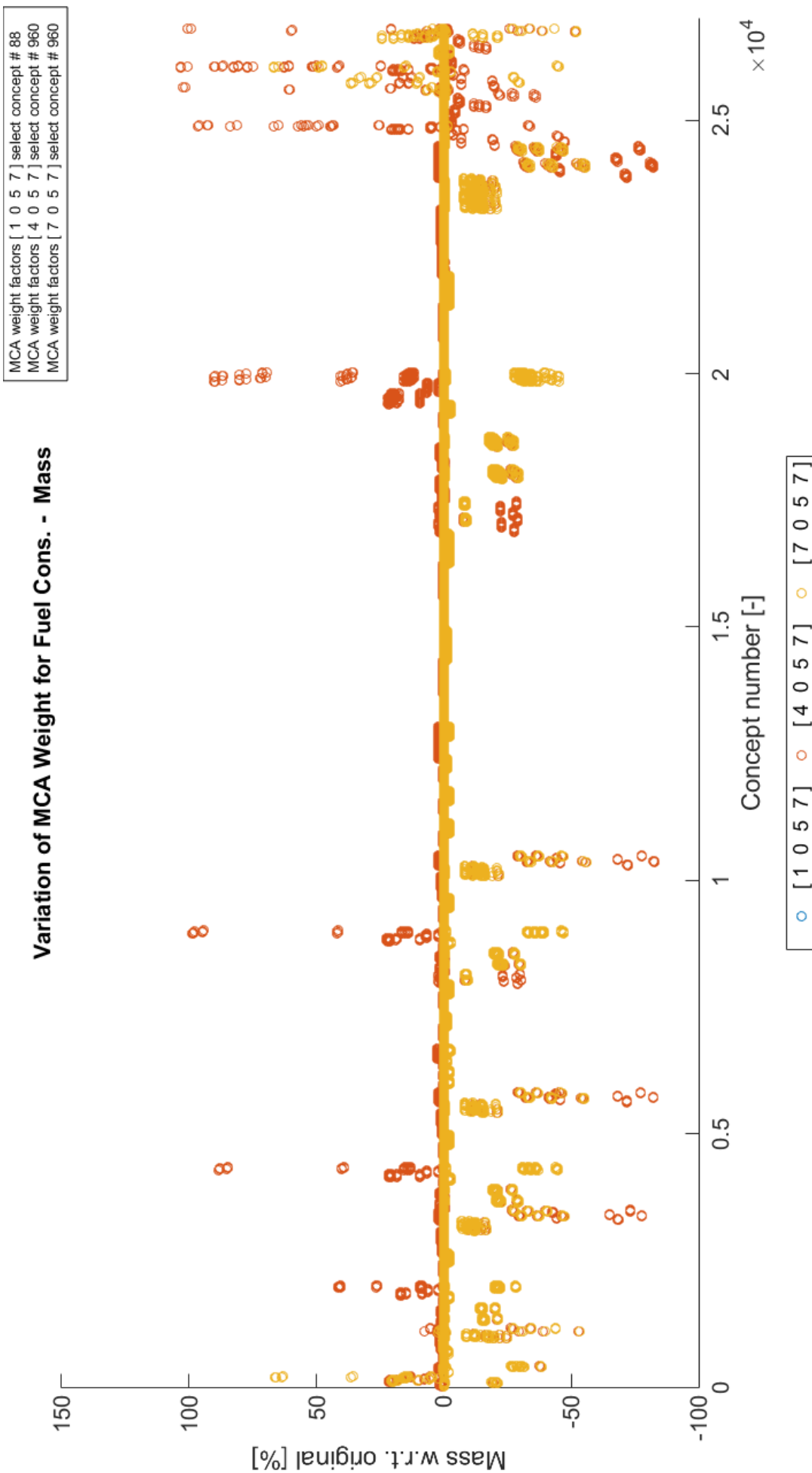
H. Sensitivity Analysis Results

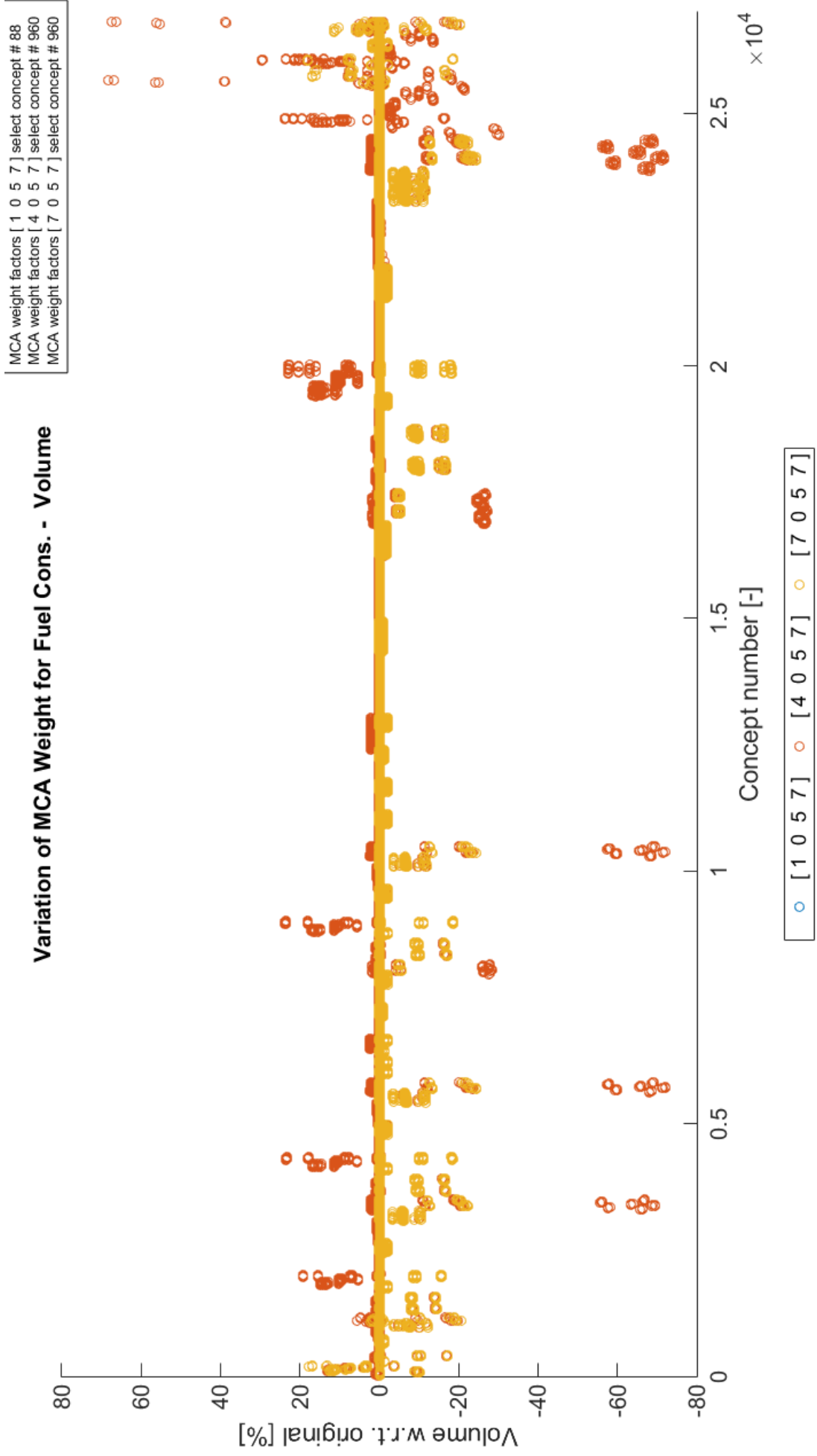


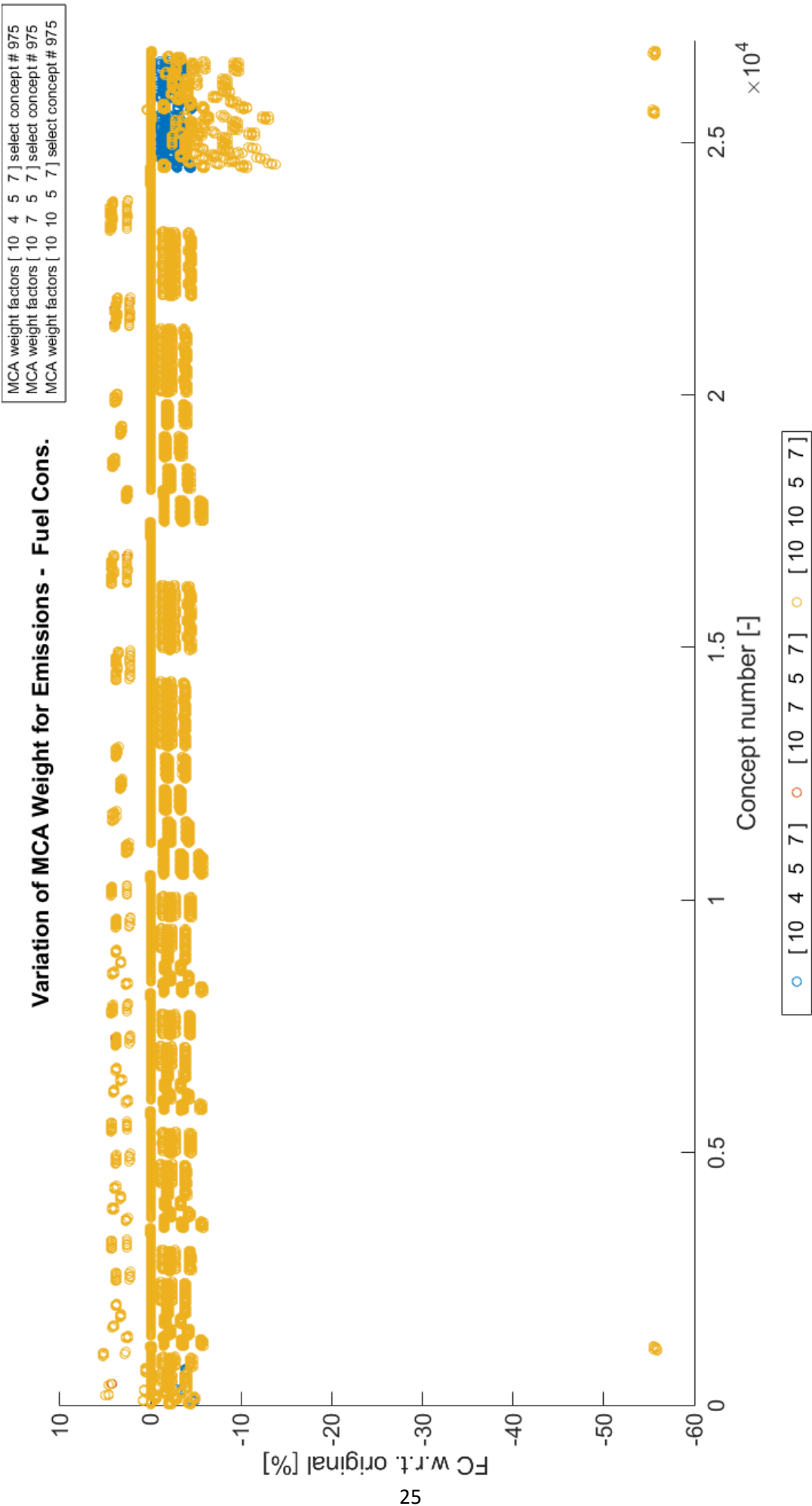


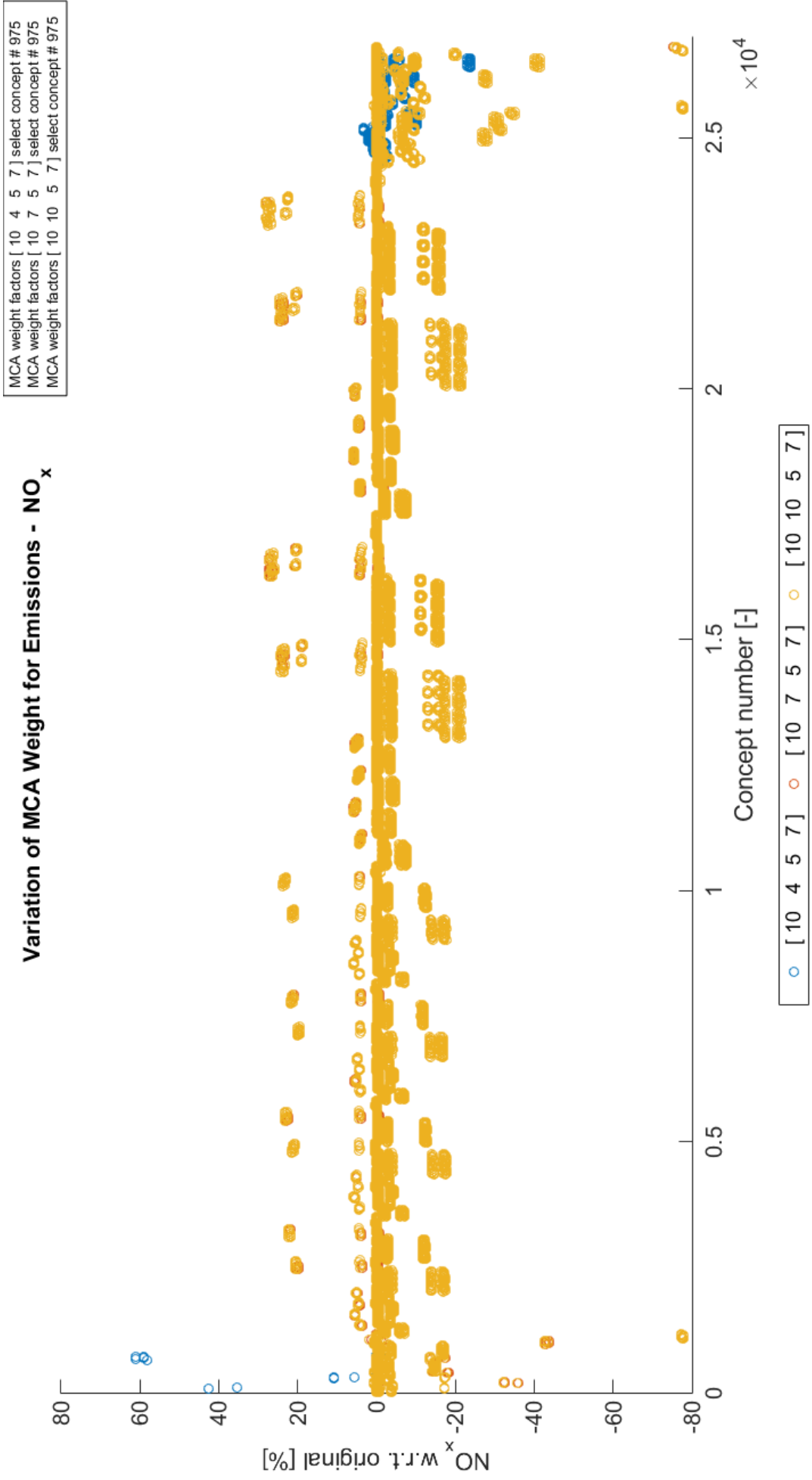


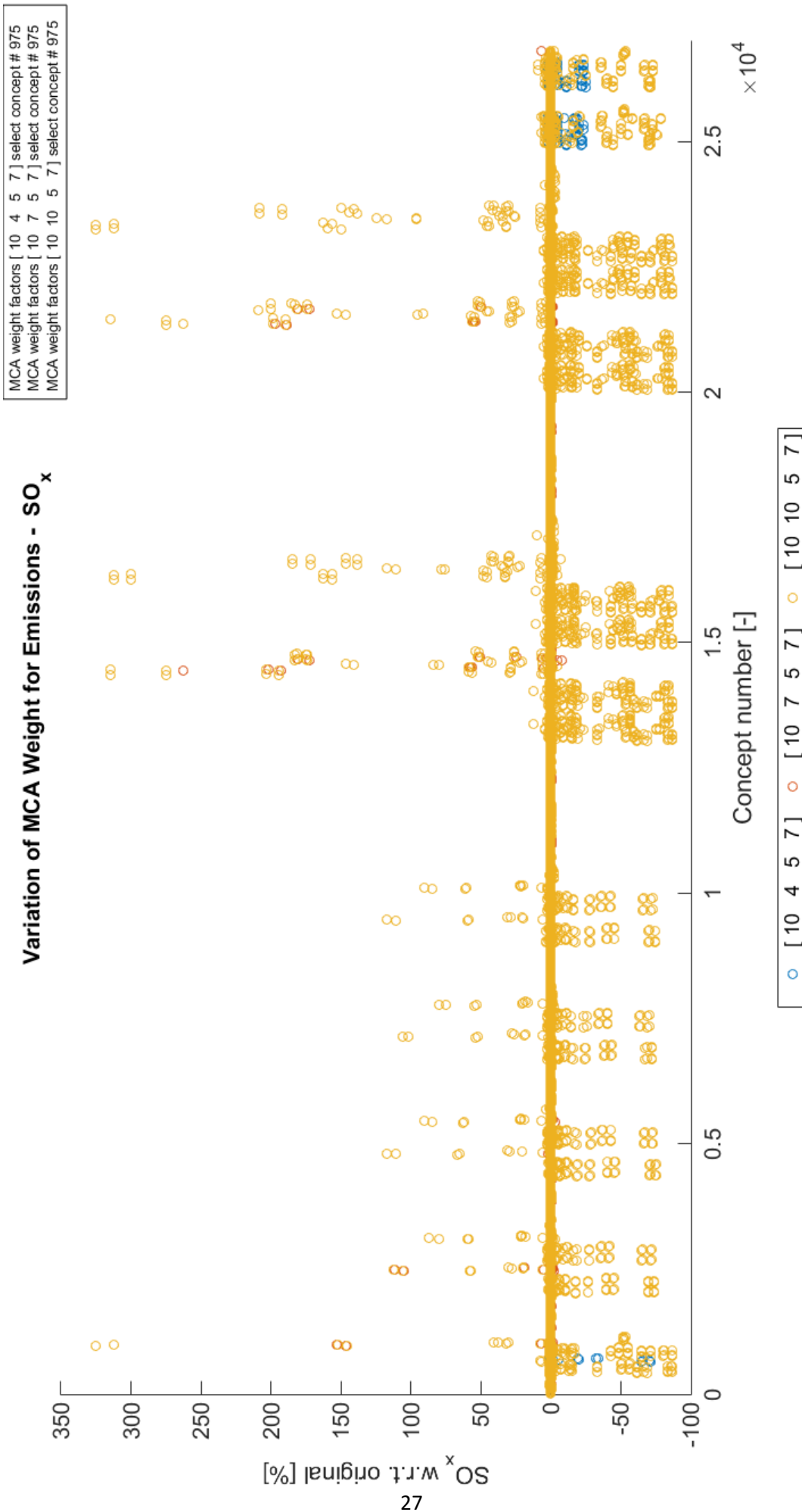


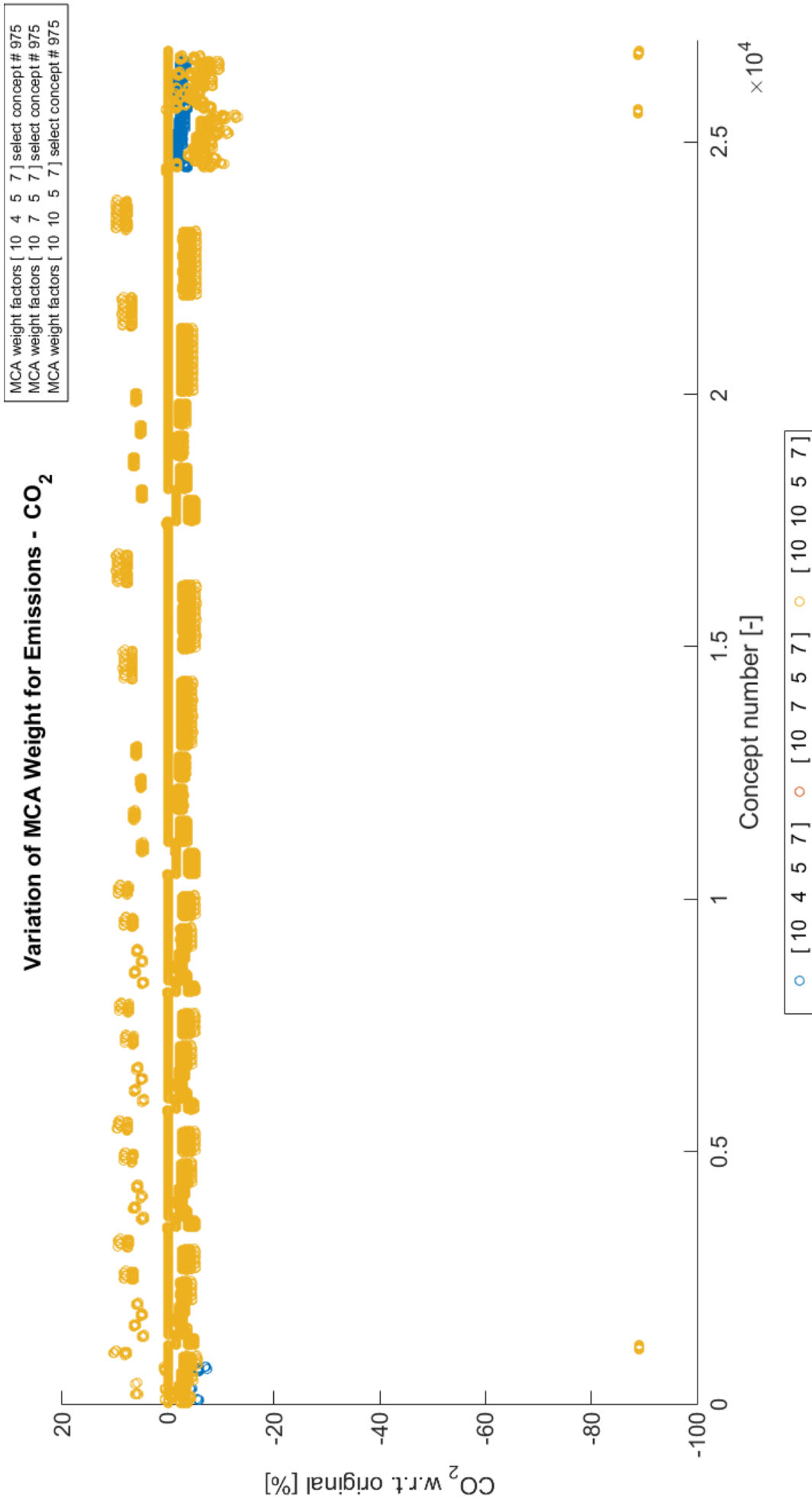


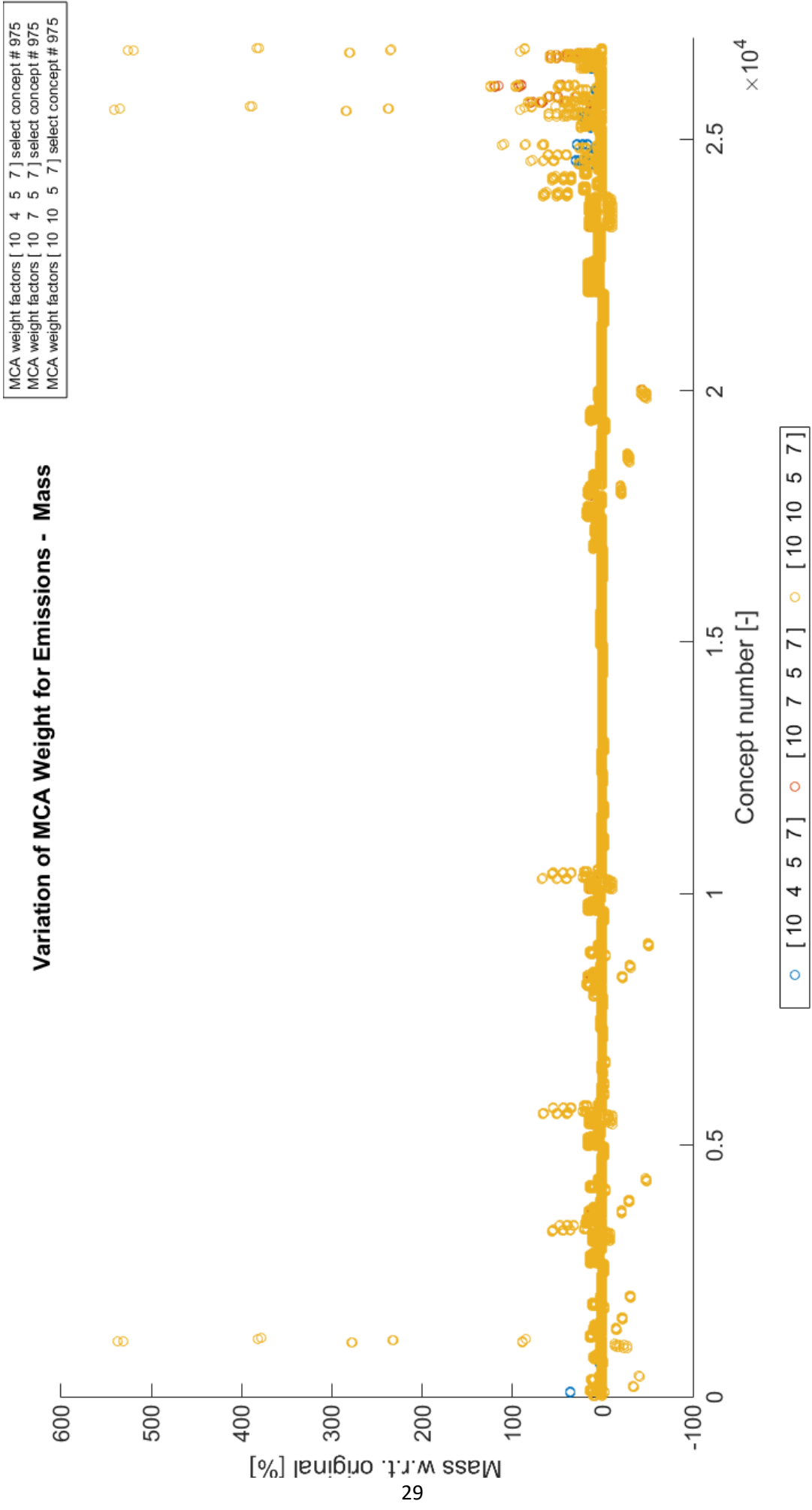


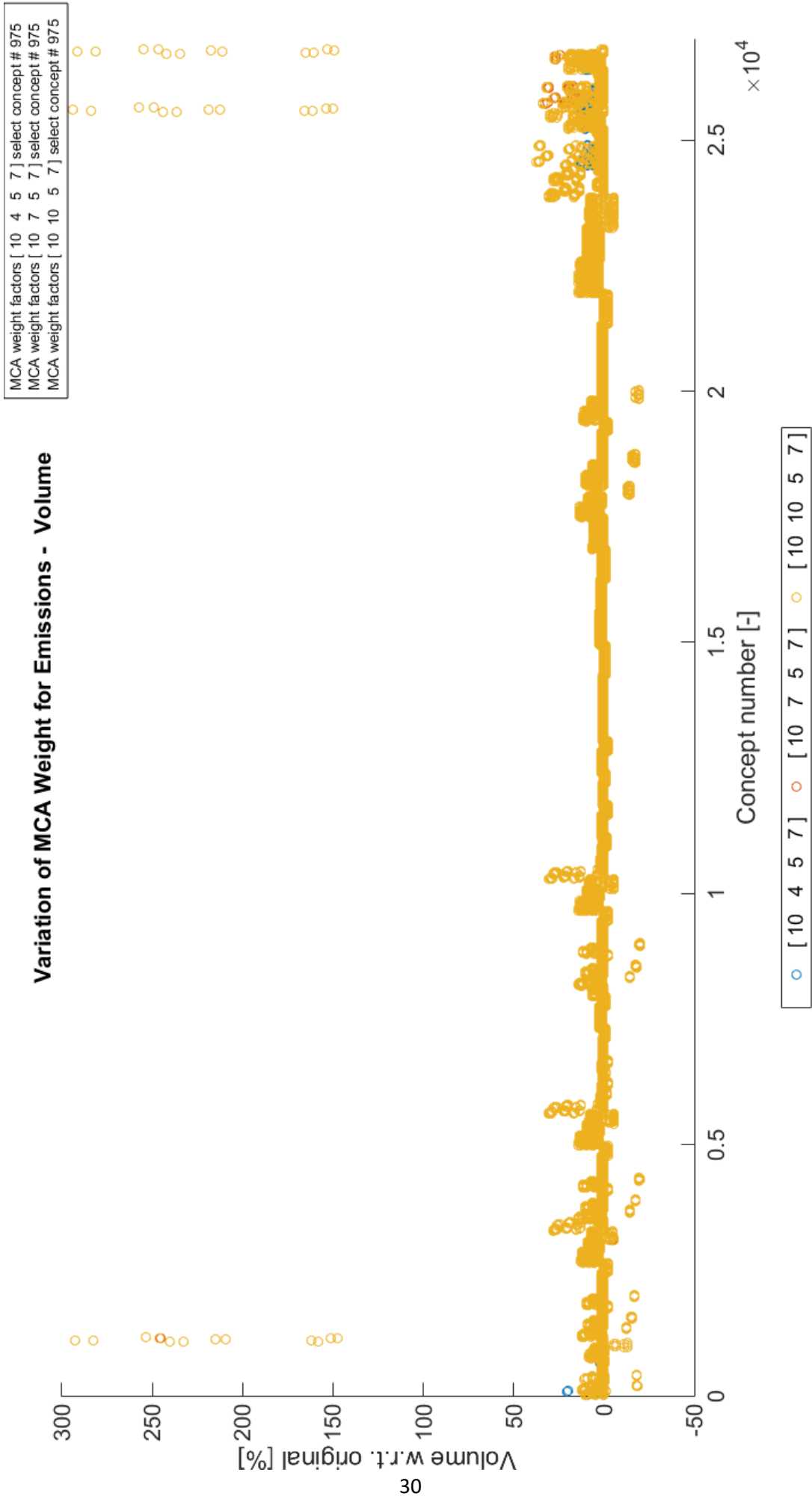


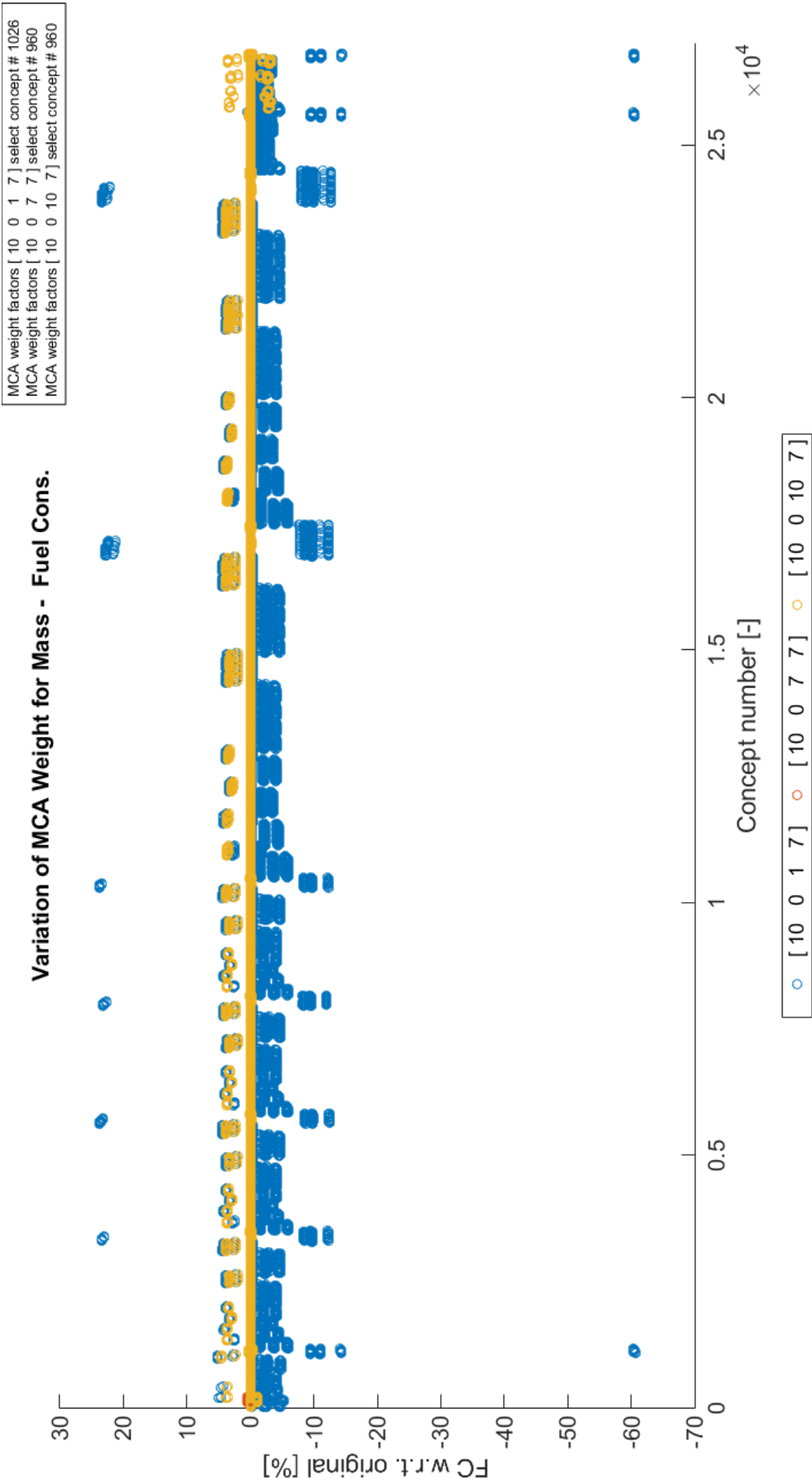


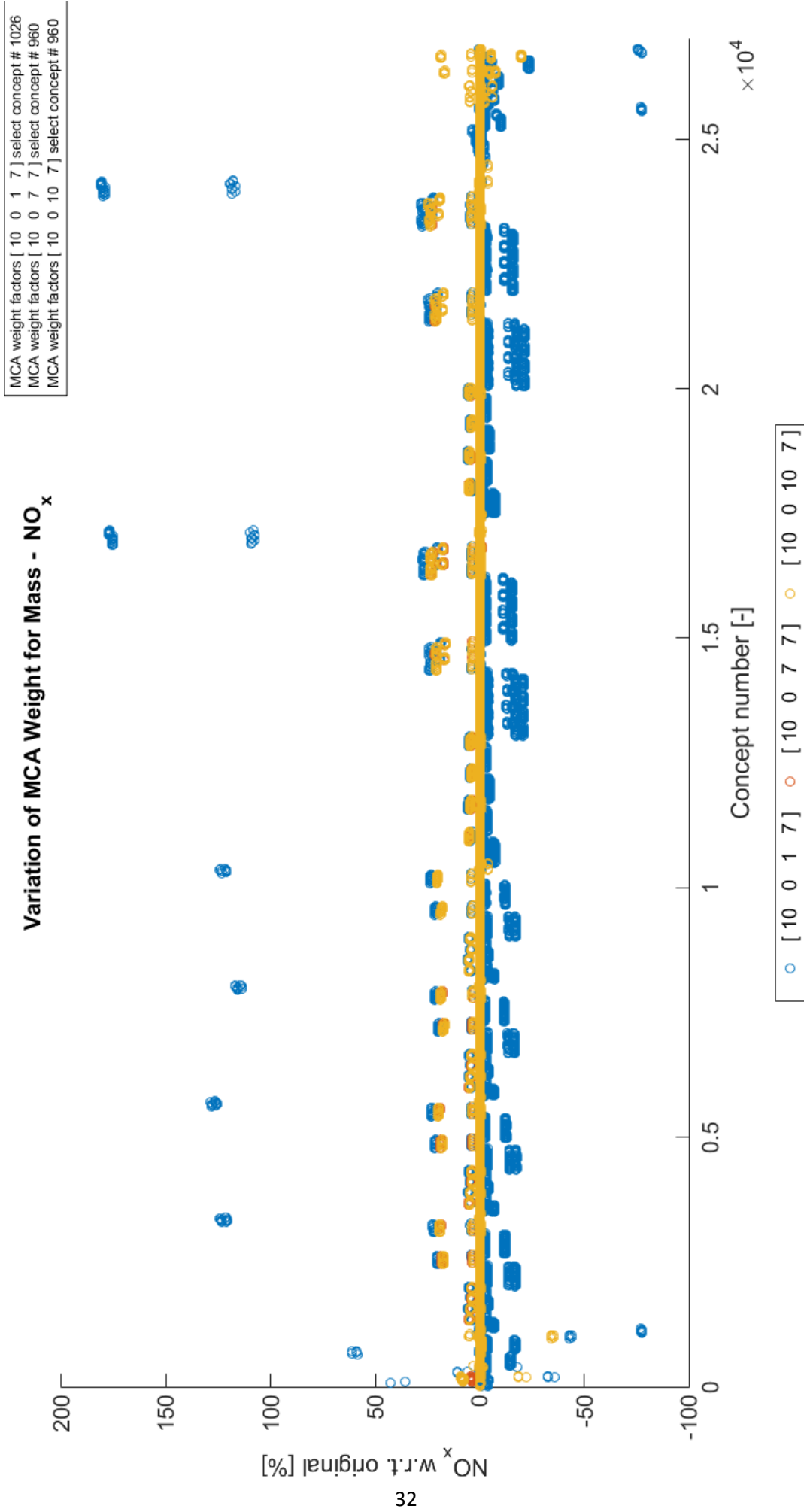


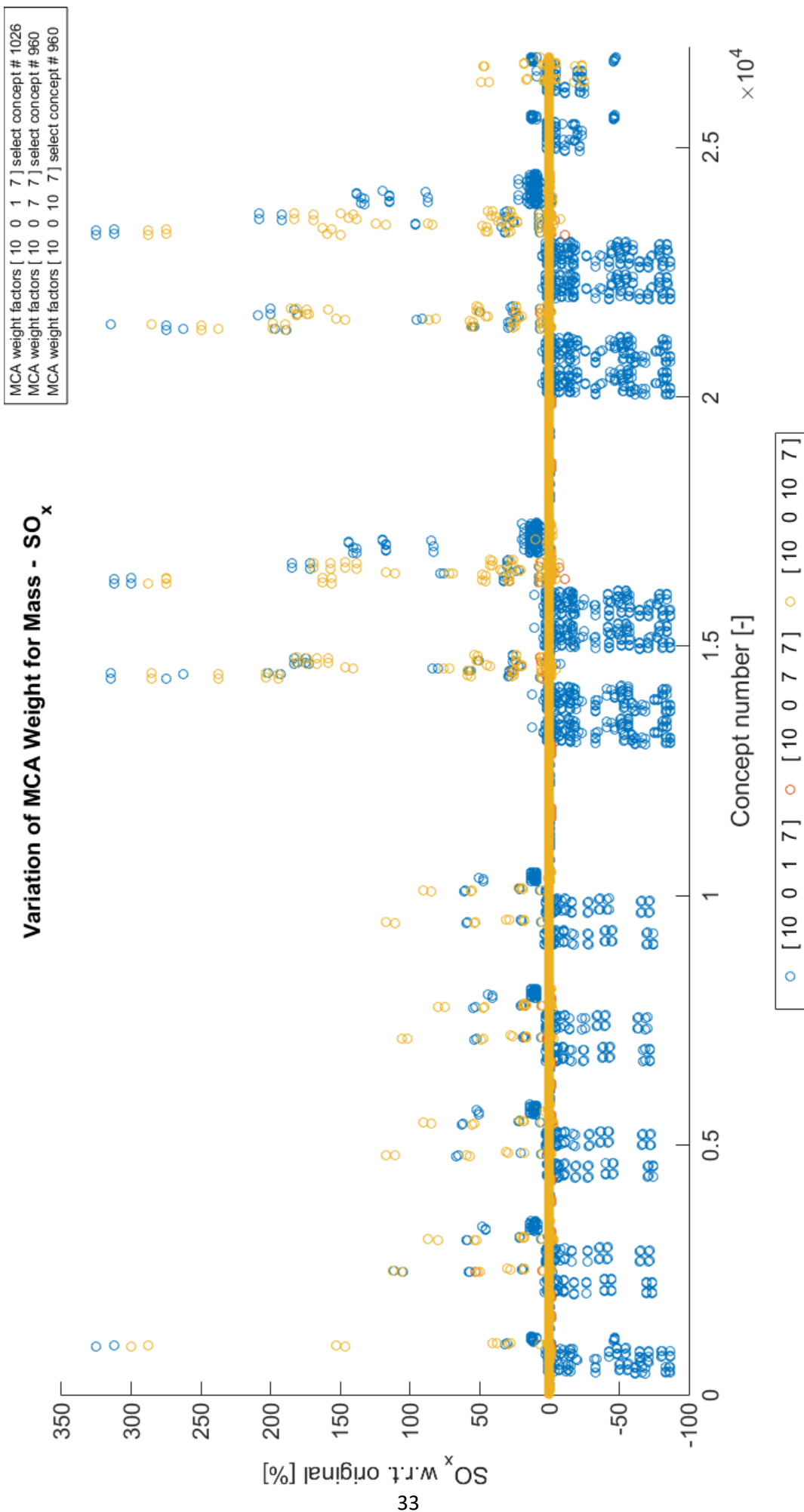


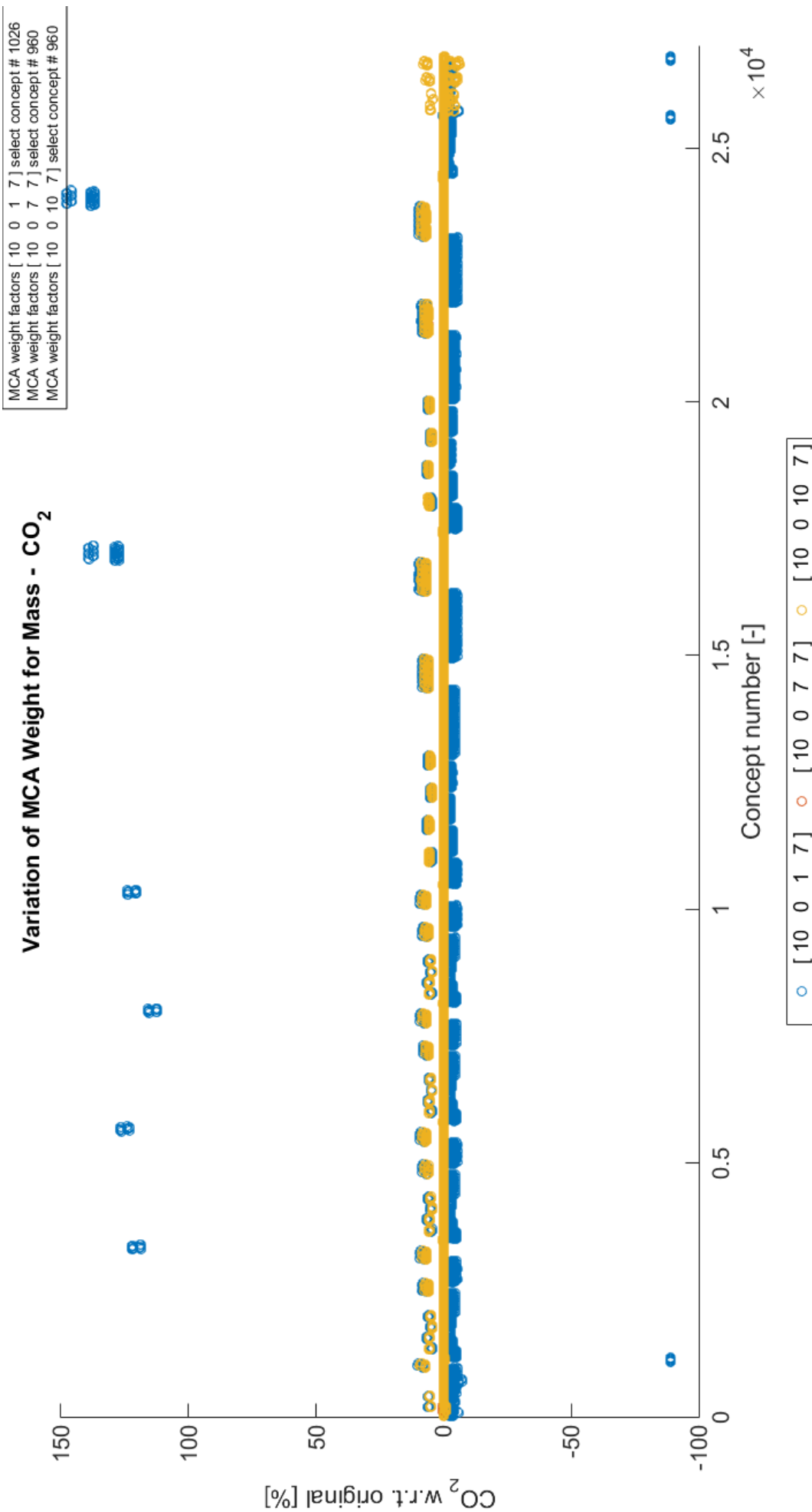






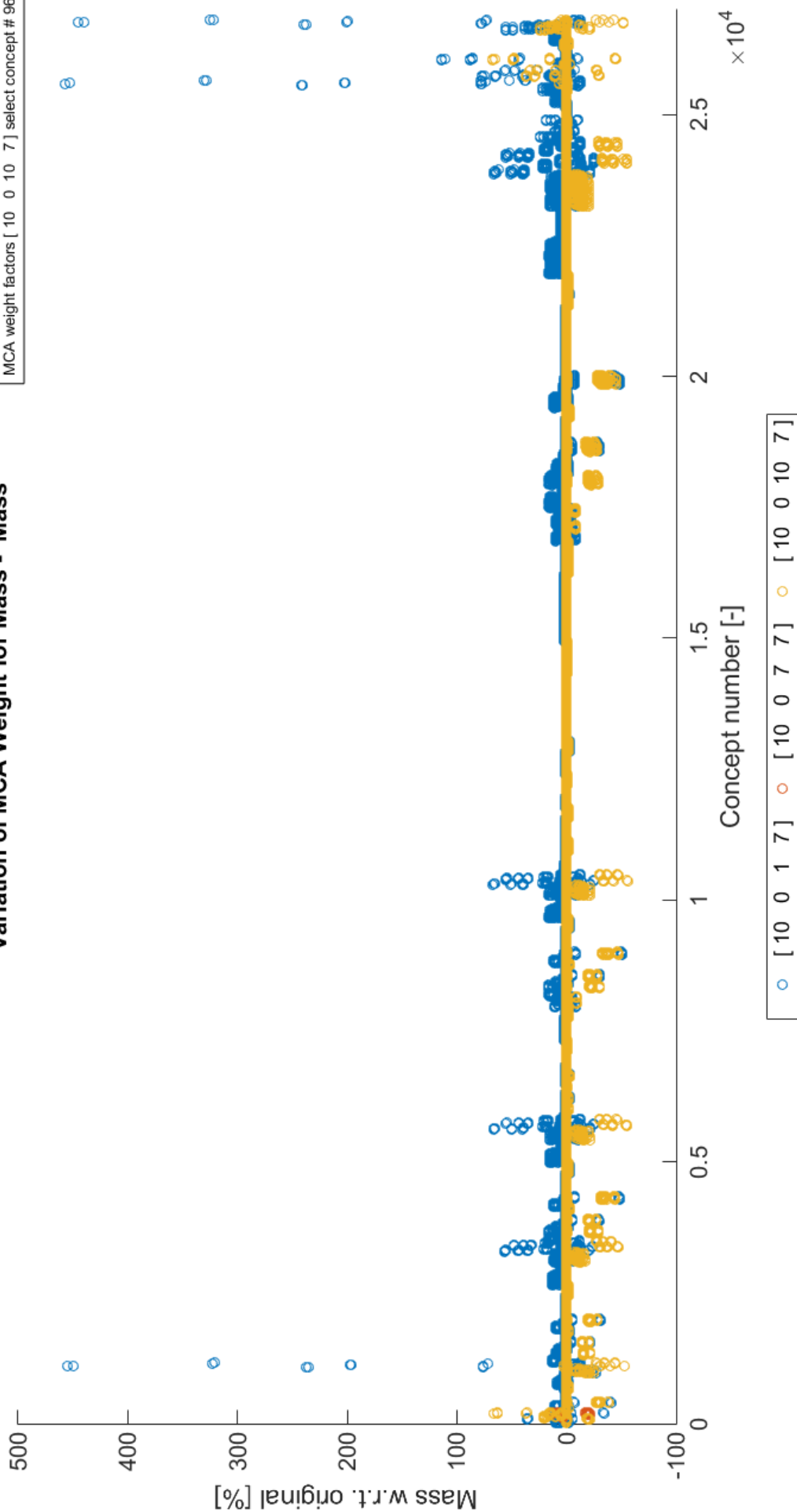


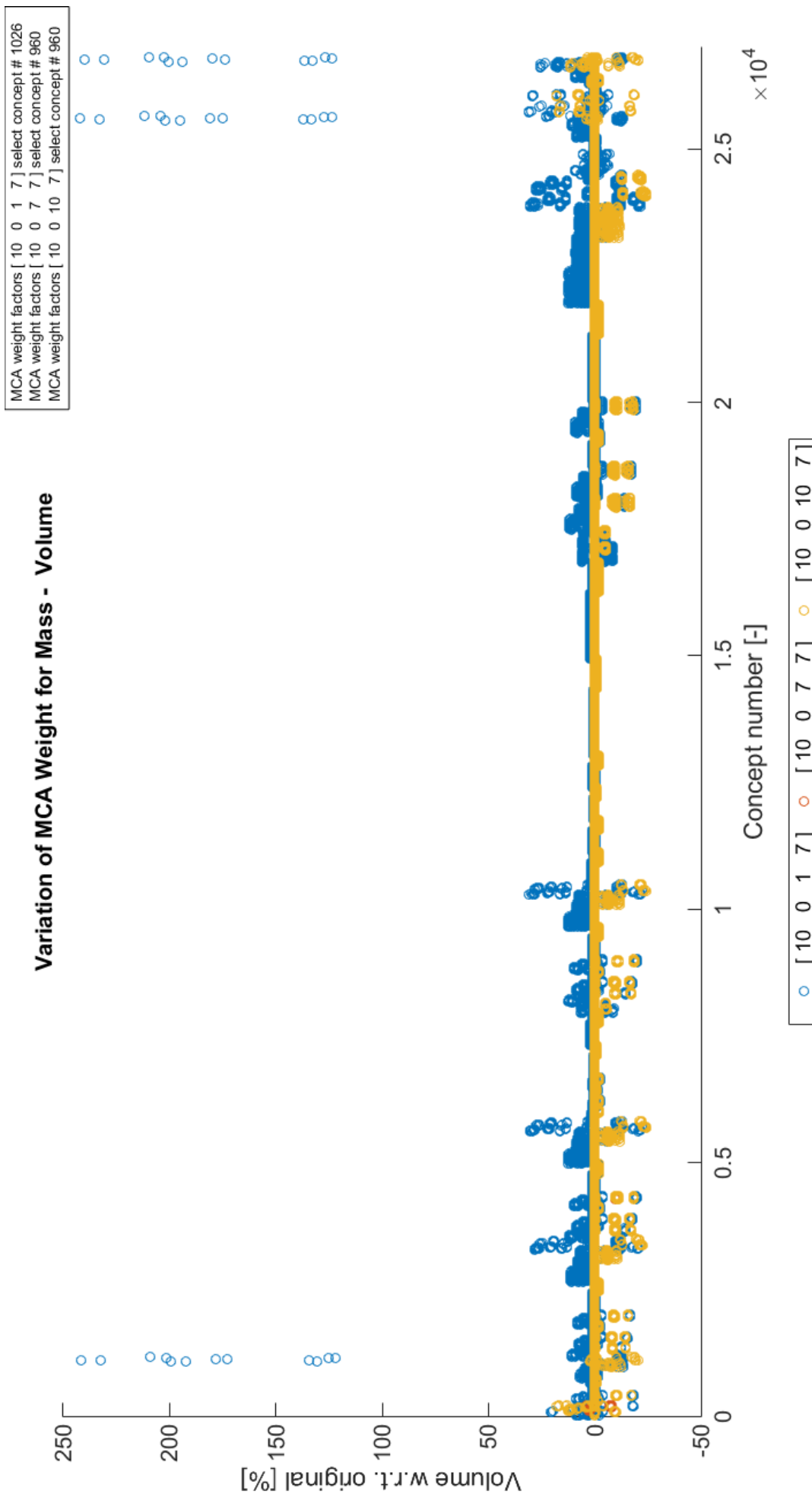


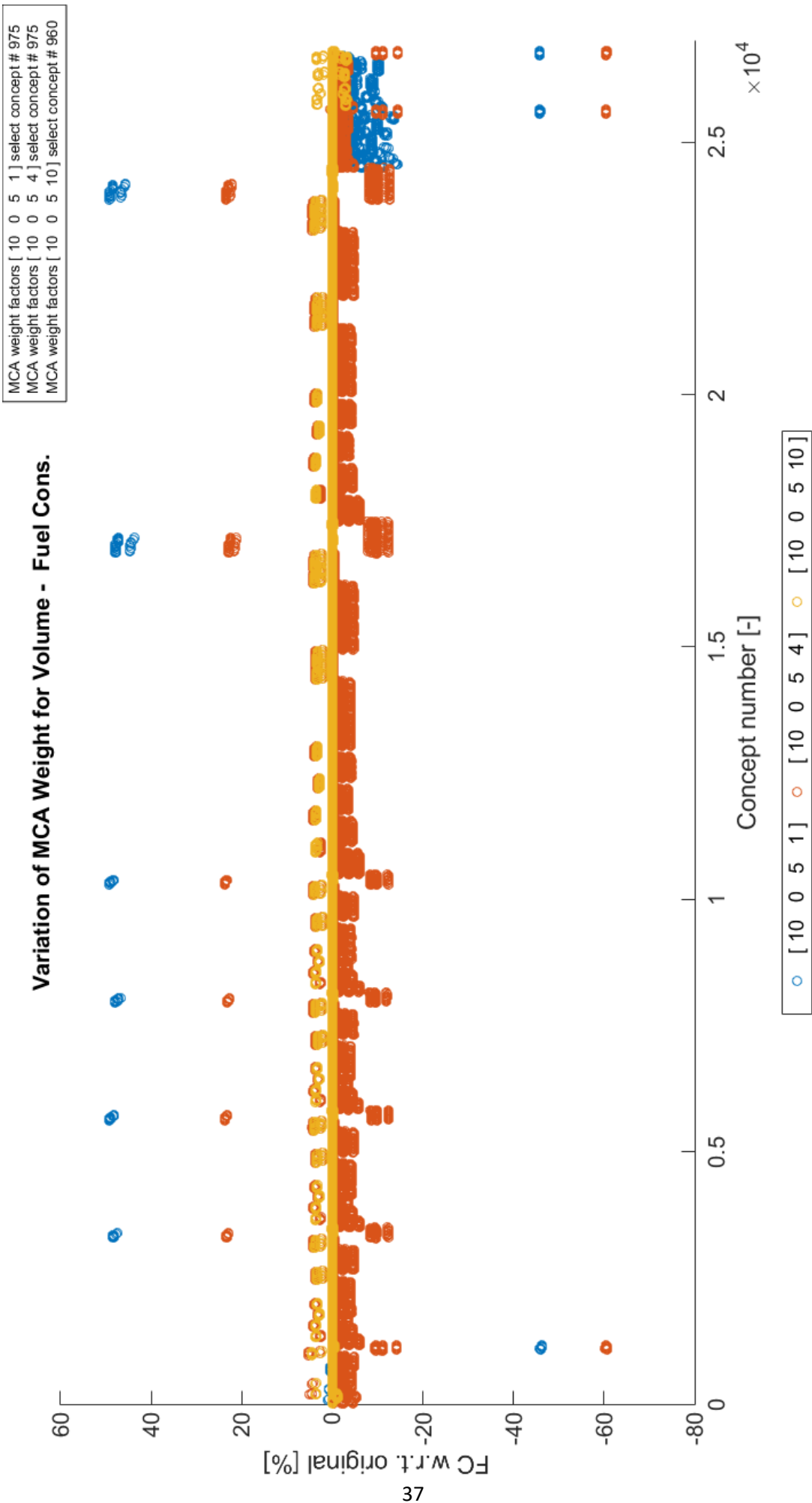


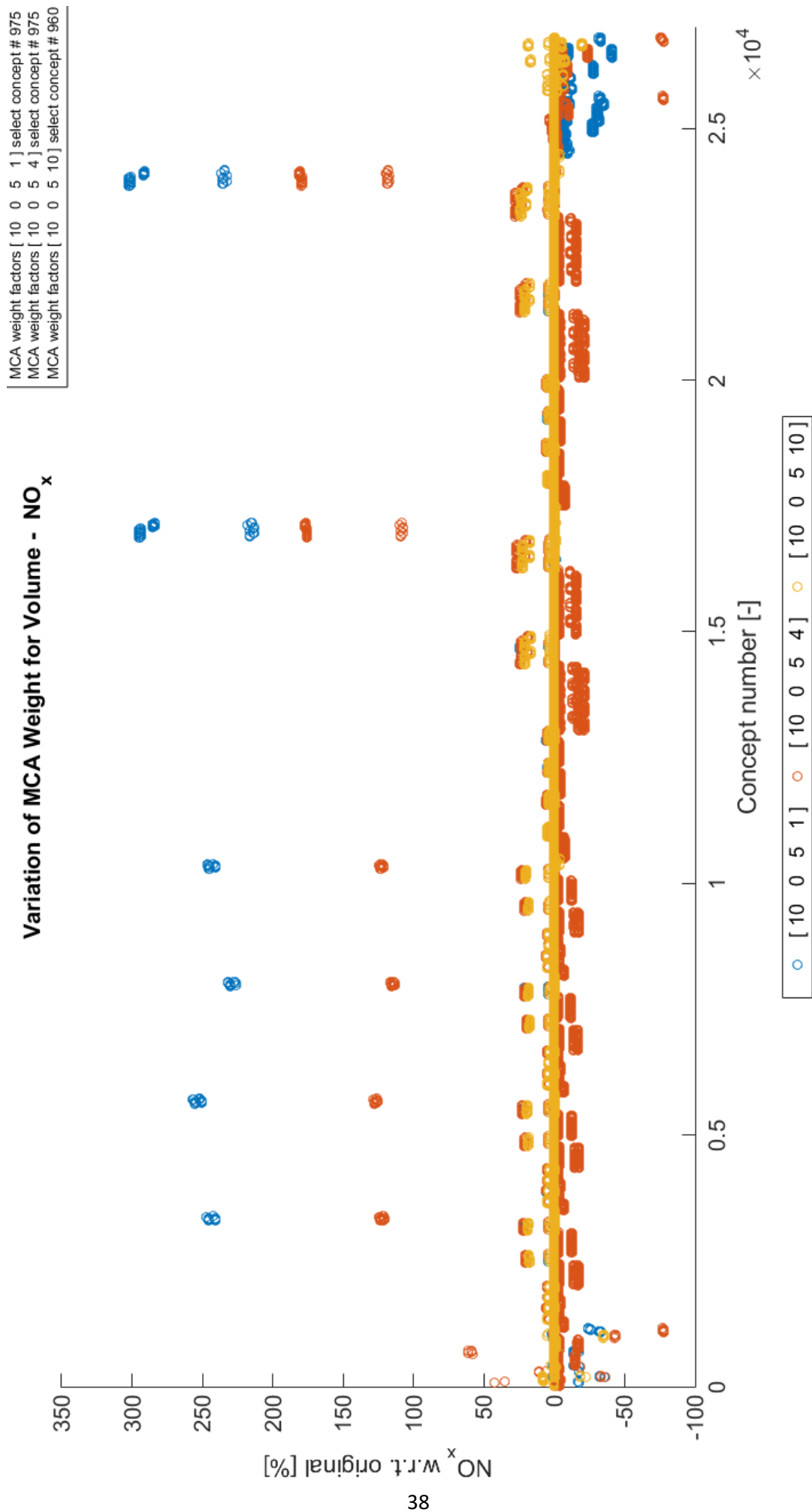
MCA weight factors [10 0 1 7] select concept # 1026
 MCA weight factors [10 0 7 7] select concept # 960
 MCA weight factors [10 0 10 7] select concept # 960

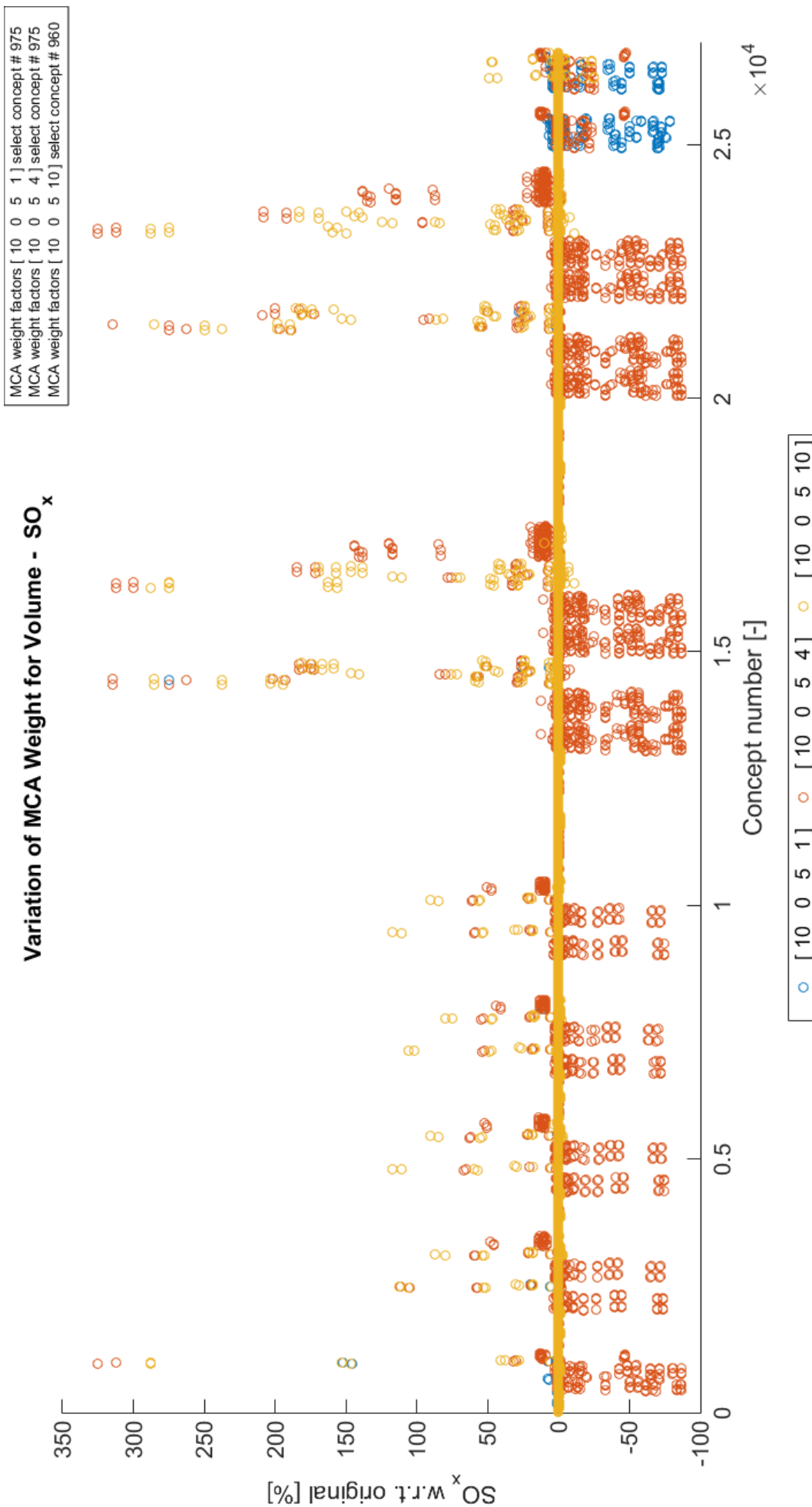
Variation of MCA Weight for Mass - Mass

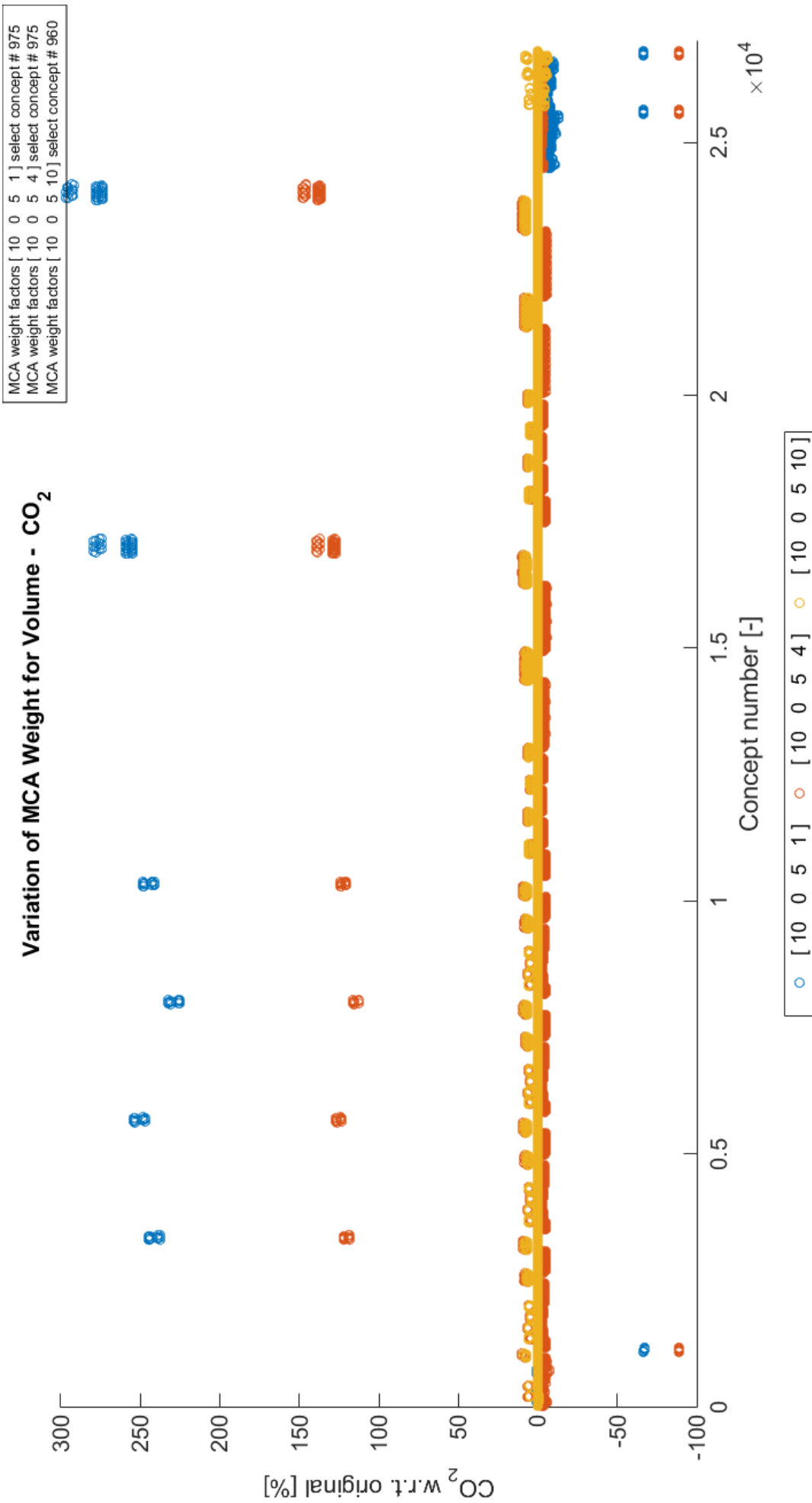






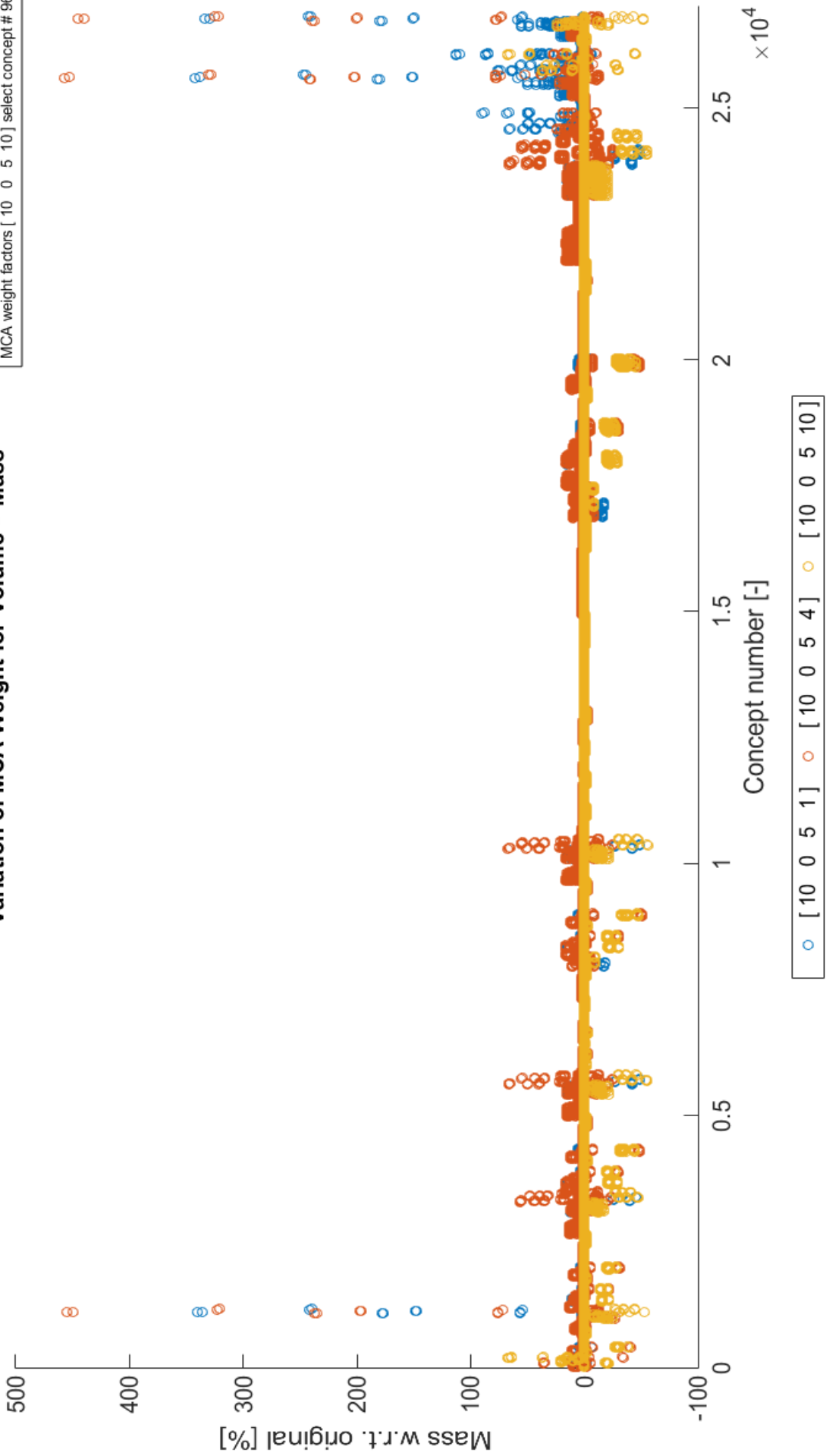


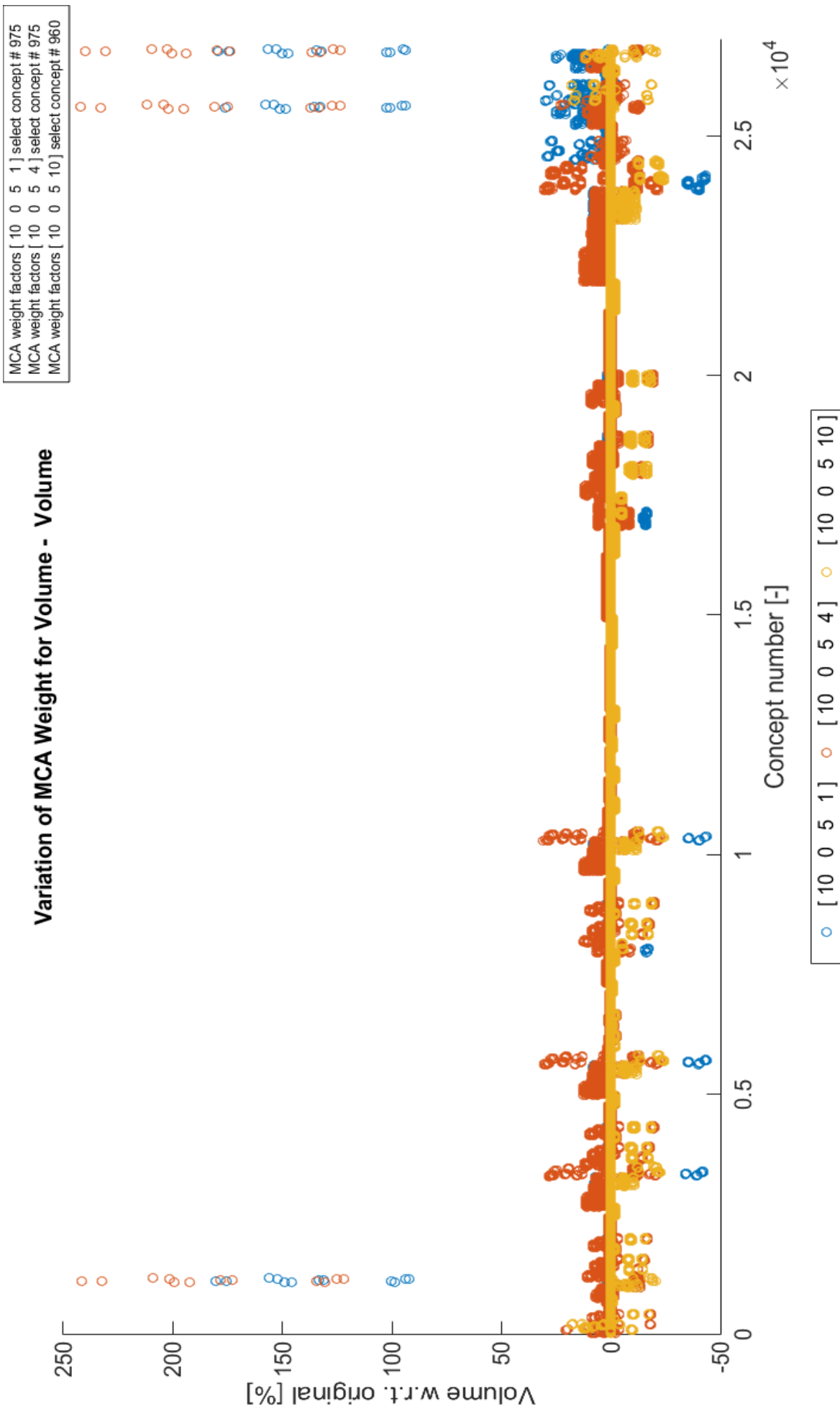




Variation of MCA Weight for Volume - Mass

MCA weight factors [10 0 5 1] select concept # 975
 MCA weight factors [10 0 5 4] select concept # 975
 MCA weight factors [10 0 5 10] select concept # 960





I. Concept Paper

In this appendix a concept paper is presented .

Automatic Selection of an Optimal Power Plant Configuration

Using Client Preferences and time based Operational Profiles

Jitte van Dijk

Delft University of Technology
Graduate Student at Nevesbu
Delft, The Netherlands

Not included for privacy purposes

Peter de Vos

Delft University of Technology
Marine Engineering Research Group
Delft, The Netherlands

Not included for privacy purposes

Rolf Boogaart

Nevesbu
Department of Marine Engineering
Alblasserdam, The Netherlands

Not included for privacy purposes

Abstract– Vessels are becoming more and more optimized towards their mission and an increasing amount of systems are considered during this optimization. Most of these considerations occur at an early design stage, where data is scarce and their impact is large.

This research aims to aid designers in considering this growing forest of possible system using concept exploration. During this exploration both the mission of the vessel and the wishes of the owner of said vessel (or client) are considered.

To do so a methodology is developed, which compares a large set of possible power plant configurations based on fuel consumption, emissions, system mass and volume. To obtain data for these four characteristics the design of each power plant is required. To obtain this the systems inside a power plant have to be designed individually. During the design of these systems several design choices are encountered.

These choices are solved using the preferences of the client, which are defined as multi criteria weight factors related to the aforementioned characteristics. And as such create individual systems and from that a power plant configuration, which is optimal according to the client. The entire selection process is demonstrated using three separate cases; a bulk cargo carrier, a harbor tug and a Trailing Hopper Suction Dredger.

Index Terms – optimization, concept exploration, design choices, Multi Criteria Analysis.

I. Introduction

Upcoming environmental awareness/regulations [1], [2] and the wish to maximize profits pressure ship owners to optimize their ships. This optimization mainly influences the power plant, since this is a large contributor to the operational costs of a ship and the biggest producer of emissions on board. During the design and optimization of these power plants a lot of possible components are considered, and the number of concepts is increasing rapidly.

The most commonly used approach to compare several plausible power plants is to create a set of preliminary designs, which are deemed promising in advance (based on the intended mission).

From this set of designs, one is selected, which best suits the owner. The selected design is then optimized further in the following design stages.

The wish exists to apply this method during the design of more commonly build vessels, without lengthening the design phase of these vessels. So that their design becomes less dependent on existing designs.

Therefore a concept exploration tool is developed. This tool ‘creates’ a set of pre-determined power plant configurations and estimates their performance over the entire mission of the vessel, using a performance simulation. Following these steps a configuration is selected, which according to the clients’ preferences is optimal.

This entire process is also shown by figure 1, which shows a process flow diagram of the developed tool.

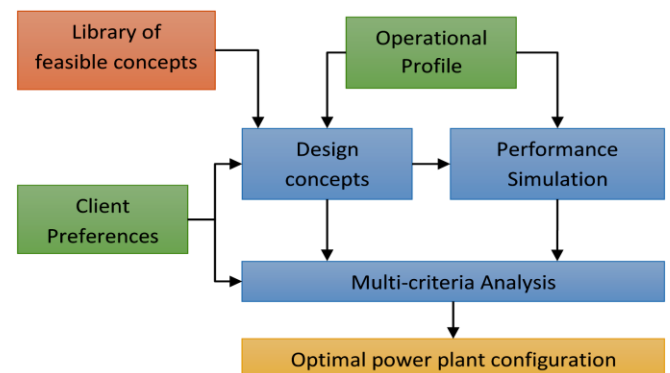


Fig 1. Schematic Process overview

In figure 1 a previously undiscussed component is shown; the ‘library of feasible concepts’. This specifies power plant configurations have to be designed and tested.

The creation of this library is discussed in chapter II. The third chapter then presents the required input (green in figure 1) for three considered cases. Chapter IV then discusses the design methodologies used to design the systems inside a power plant. Chapter V then presents the results for the three cases, and also discusses the sensitivity of the tool to the considered preferences. And finally chapter VI and VII present the conclusions and recommendations of the research.

II. The Library of Feasible Concepts

The library of concepts is created by defining a fixed topology, which is shown by figure 2, and by varying the type of system present in each node found in that topology. This definition of a power plant configuration is used, to limit the amount of considered concepts and to allow for a performance simulation to be possible.

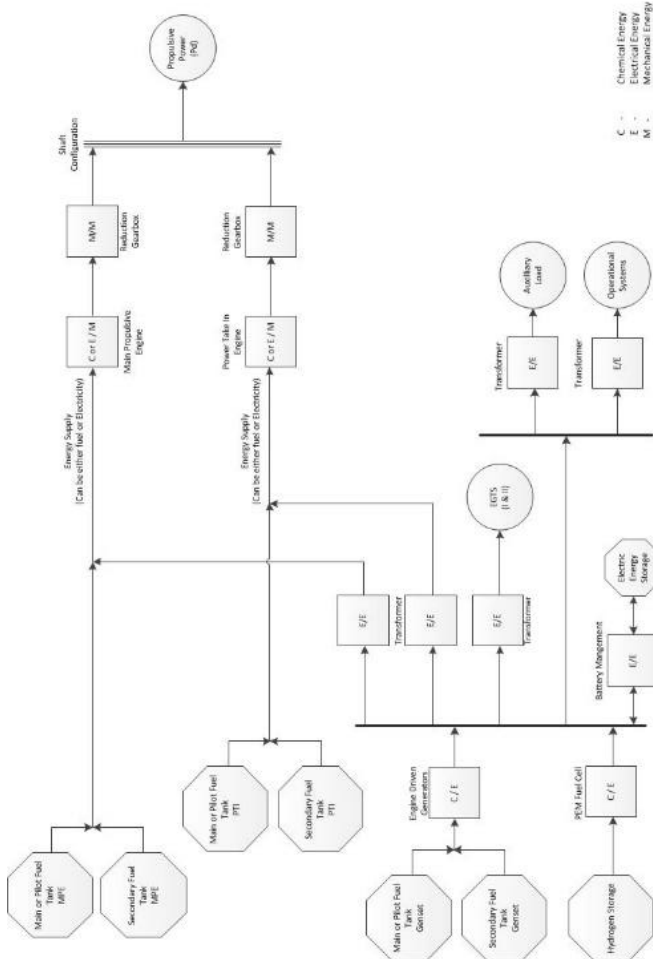


Fig 2: Considered (Overall) Power plant Configuration

For such a performance simulation to be possible a detailed description of the systems that are present is required. Using such a detailed description to define the different systems causes the amount of possible configurations to escalate. This is, due to the time constraints posed to this research and the wish to quickly generate results unwanted.

To circumvent such a large database and still obtain the level of detail required for the performance simulation, several objective functions are implemented. These functions will, given a rough description of a system (e.g. 2-stroke, diesel engine) create a set of feasible system designs and select one which according to the preferences of a client is optimal.

The discussed component definition and the presented topology are used to determine which systems are included during this research. A summary of the included systems presented in table 1. Note that on a single node a combination of two systems is not allowed.

Table 1. Considered nodes and systems

Node (Name) :	System / Type :
Shaft Configuration	Single Shaft Power Take In (PTI)
Propulsive Engine Types	2/4 stroke, Diesel Engines (DE), 4 stroke Dual Fuel engines (DF), Permanent Magnet Synchronous Machines (PMSM) (all with and without gearbox)
Fuel Type(s)	MDO / HFO / LNG / CNG / NH ₃ / Pressurized Hydrogen
Electricity Generation Systems	DE/DF Gensets / Proton Exchange Membrane Fuel Cell (PEMFC) Hybrid DE Genset + PEMFC Hybrid DF Genset + PEMFC
Electricity Storage	Li-Ion / Lead-Acid Batteries
Exhaust Gas Treatment Systems	Open Loop, Wet Scrubber. Selective Catalytic Reduction (SCR)

Given these boundaries, approximately $35.8 * 10^6$ possible power plant configurations can be created. Although the amount of concepts is already a lot less than other concept creation methods (for example the one developed by de Vos [3]), it is still too large to rapidly generate results.

This reduction is achieved by applying constraints to the power plant configurations. The first constrain is the requirement that exhaust gas treatment systems are only present when they are required to meet the IMO emissions regulations, which are summarized/presented in [4] & [5]. These regulations, some of which enter into force in 2020, are implemented to ensure the tool is 'future proof'.

More constraints are added to ensure the feasibility of the different power plant configurations.

For this research a secondary configuration is deemed infeasible when there are; fuel tanks or systems which are not needed, when the required fuel is not present, or when the concept design cannot perform the tasks required of a power plant (providing propulsive and electrical power).

These constraints remove a total of 99.93 [%] of the possible configurations, leaving a total of 26.818 configurations. These configurations are all deemed feasible and therefore included in the library of feasible concepts.

III. Considered Cases

The required input, apart from the operational profile and client preferences includes two additional parameters. The first of which is a relationship between the propulsive power and the propeller RPM, in accordance with the propeller law [5]. The second addition is an indication of the emission control area in which the vessel has to (be able to) operate, which is necessary for the constraint related to the exhaust gas treatment systems. All required input is determined for three cases; a bulk cargo carrier, a harbor tug and a Trailing Suction Hopper Dredger (TSHD). The required input parameters are determined using reference vessels and presented in figure 3,4 & 5 and Table 2.

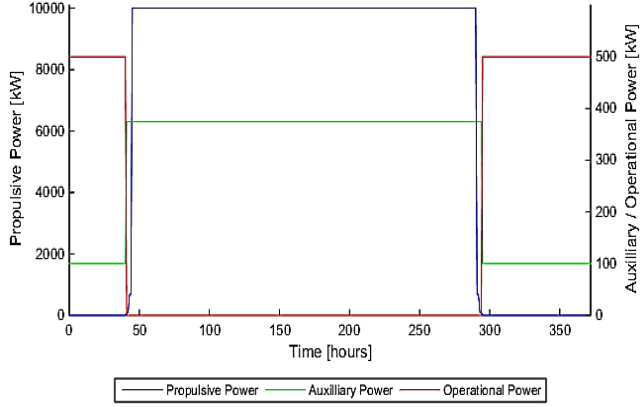


Fig 3: Operational Profile, Cargo Carrier

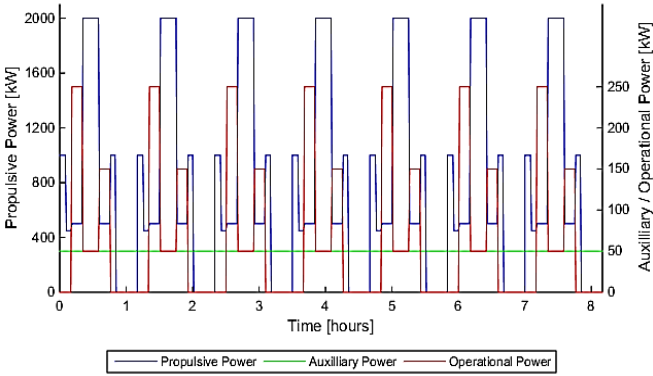


Fig 4: Operational Profile, Harbor Tug

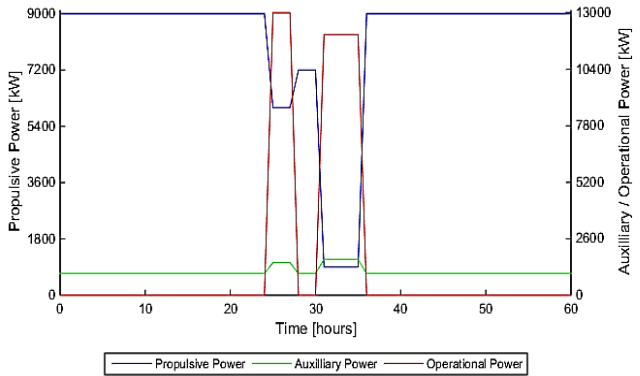


Fig 5: Operational Profile TSH Dredger

Table 2. Client Preferences, ECA's and C4's for all cases

		Cargo Carrier	Harbor Tug	TSHD
MCA Weight Factors	Fuel Cons.	10	6	8
	Emissions	0	8	6
	System Mass	5	3	5
	System Volume	7	5	5
	C4 [RPM/kW]	0.0041	2.81*10 ⁻⁴	0.0006
	Emission Control Area	SO _x + NO _x ECA	SO _x + NO _x ECA	Global limits

IV. Intermediate Design Algorithms

The first step in the design process, is the division of the propulsive power over the Main Propulsive Engine (MPE) and Power take In (PTI) (if both are present). This is done by designing the MPE so that it can deliver the second highest propulsive power demand, and the power take in delivers the different between the second highest and maximum power demand. The dimensions of the shaft configuration gearbox are estimated using a dimension estimation method [6], and the efficiency of this shaft configuration gearbox is assumed to be 99 [%] for single shaft configurations and 97 [%] for PTI configurations.

The division and efficiencies are also found in the equations below. These show the Power-Division Ratio (PDR), which defines the fraction of the total power, that is delivered by the MPE and it can have a value between 0 and 1. The value itself depends on the operational profile, but is not varied during the design process.

$$P_{MPE} = PDR * \frac{P_D}{\eta_{shaft}}$$

$$P_{PTI} = (1 - PDR) * \frac{P_D}{\eta_{shaft}}$$

With the division of power completed, the design of the engine based systems can be executed for both the main propulsive engine and the power take in engine. This process consists of the selection of the gearbox ratio and the number of cylinders per engine. Both of which are determined using design algorithms.

For the design of the PMSM an existing algorithm was used. [7] For the combustion engines a method is developed. This design process is presented in figure 6.

The dimensions of the engine(s) are determined using a dimension estimation method [6].

The nominal engine efficiency is estimated using reference engines and a relationship between the demanded power and the maximum possible engine power [8]. The latter of which is dependent on the cylinder geometry and the type of engine.

The same relationship is also used to obtain a very rough estimate of the part-load fuel consumption. So that a design choice can be made. The performance simulation itself uses a more accurate engine model so that a more accurate estimate can be obtained for the final comparison.

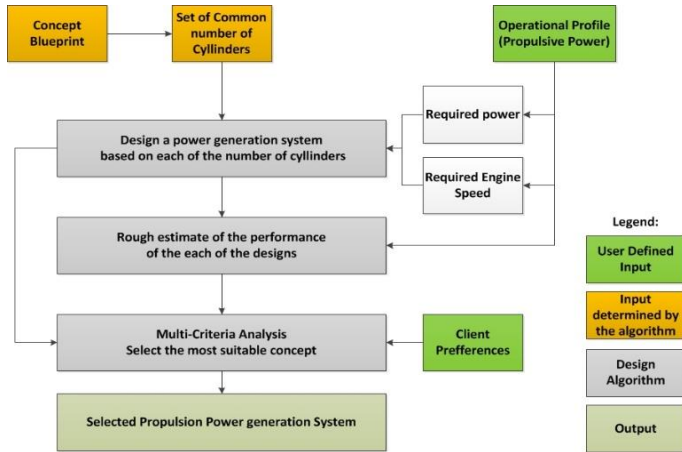


Fig 6: Engine Design Algorithm

The algorithm to determine the gearbox ratio, selects and engine speed from a feasible range. This range is determined using reference data and summarized in table 3.

Table 3: Engine speed ranges as function of engine type

Engine Type	Lower Limit [RPM]	Upper Limit [RPM]
2-stroke Diesel	60	250
4-stroke Diesel	400	2000
4-stroke Dual Fuel	400	1200
PMSM	60	2000

The algorithm then uses the previously discussed method to design the engines and another algorithm to determine the size and efficiency of the gearbox. These steps are then repeated for the entire range of engine speeds. From the set of designs created by this process one is then selected based on the client' preferences. The entire process is also seen in the diagram of this algorithm, which is shown in figure 7.

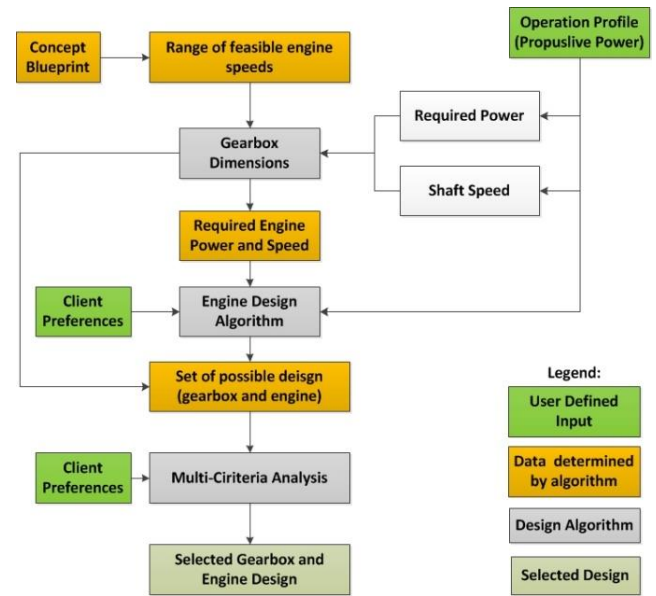


Fig 7: Gearbox Design Algorithm

After the completion of the design processes for both the MPE and the PTI, these systems are submitted to a performance simulation, which results in (among others) additional electrical power requirements, caused by the electrical power demand of the exhaust gas treatment systems and (if present) the PMSM.

These additional demands are accounted for during the design of the electrical -grid, -storage and -generation systems. The first step in the design of these systems is the determination of the electrical grid voltage.

This is done by first dividing the electrical grid in a main grid, to which the storage and generation system are connected, and a set of supply grids, which supply the different power consumers and obtain their power from the main grid.

The supply grid voltage is selected based on table 3, which includes the most common maritime voltages and is created using (circuit breaker) current limits.

Table 4. Supply grid voltage as function of power

Maximum Electrical Power [MW]	Supply grid voltage [V]
0.46	230
0.88	440
1.38	690
9.90	3300
19.80	6600
>19.80	11000

Based on the different supply grid voltages, the main grid voltage is then selected to either minimize the amount of transformers or to minimize the electrical power losses, due to those transformers, which are assumed to have an efficiency of 99 [%].

Which method is used depends on the client preferences.

For the design of engine driven gensets the design algorithm developed by an earlier research [9] is adjusted to include the fuel consumption, using the same methodology as discussed for the engine design.

The algorithms used to design a fuel cell determines the cell area of a single fuel cell and a nominal current density. It does so by creating a set of designs that fall within feasible ranges of these parameters. From these designs the one which best suits the client preferences is selected. The entire process is also shown by figure 8.

The dimensions and fuel consumption of each design are determined using previously developed methodologies [7] & [10].

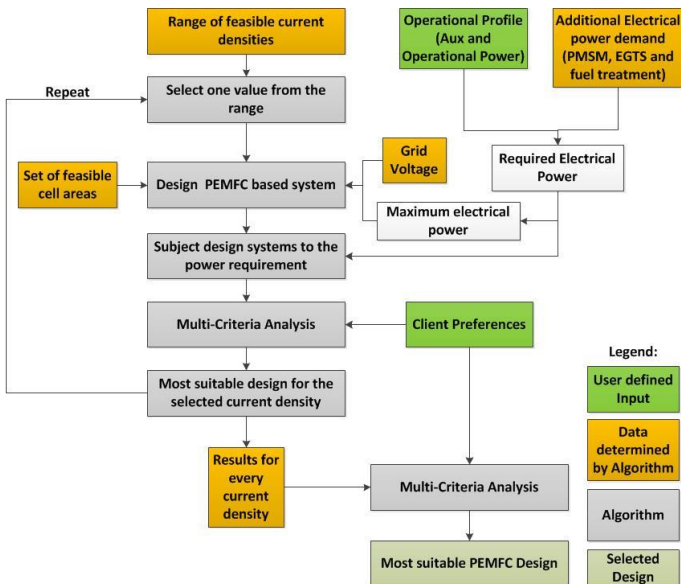


Fig 8: Fuel Cell Design Algorithm

As shown by table 1 the option for a hybrid generation system is also included. These systems have an additional design choice, which is the degree of Hydrogenization (DoH) (as shown below).

$$DoH = \frac{P_{PEMFC}}{P_{electrical}}$$

This is determined by designing a set of designs, for a value of DoH between 0.1 and 1 (with increments of 0.2) and designing an engine driven genset and a PEMFC using the previously discussed algorithms. Then the client's preferences are used to select the optimal DoH, an overview of this process is shown in figure 9.

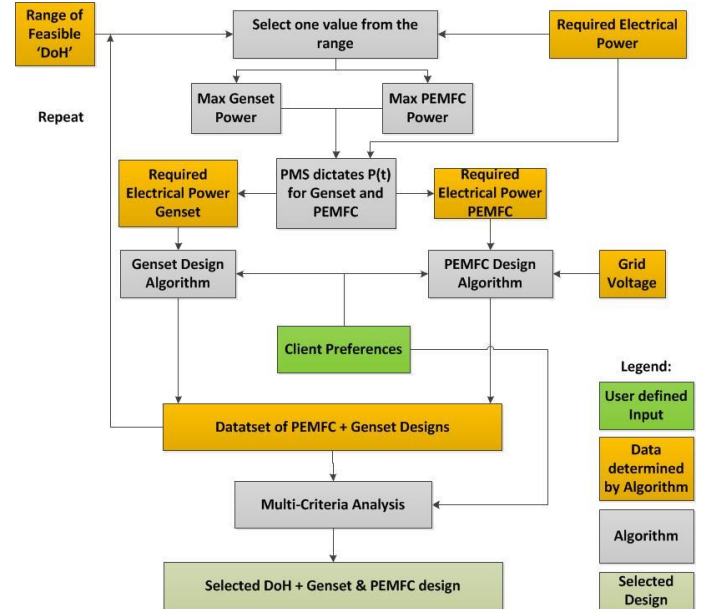


Fig 9: Hybrid Generation System Design

For case where both generation and storage of electrical power is present, the storage system is used as power supply during those stages in the operational profile, where the propulsive power is minimal (since this is often near shore) and thus reducing the engine emissions in those areas.

The batteries are then dimensioned using previously developed methodologies [9] and are designed to still meet the maximum power demand at 80% Depth of Discharge to assure that power demands can be met at all times.

After the design of the electrical generation and storage system(s) their performance is also simulated (using models developed by previous researches).

After which all engine emissions and fuel consumptions have been determined.

The engine emissions of the propulsive engines and the generation systems are then combined and compared to the IMO emission regulations, which depend on the selected emission control area.

If needed to meet the regulations exhaust gas treatment systems are installed and their dimensions are estimated. Their efficiency is then simulated, which results in a reagent consumption for the SCR system, a scrubbing sludge production and the post-treatment emissions.

All created designs and simulation results are then combined into a final multi criteria analysis in order to select the optimal power plant configuration.

V. Results

The results for each of the three cases (or ship types) are presented in table 4 and table 5. With table 4 presenting the numerical values for the different characteristics and table 5 presenting components of the selected power plant configurations, including an indication of the installed power.

Table 5. Numerical Results, All ship types

	Cargo Carrier	Harbor Tug	TSHD	Unit
Fuel Cons.	447	0.55	59	[Ton]
NO _x	7.24	0.35	0.17	[gram/kwH]
SO _x	2	0.02	0.01	Gram / kg Fuel
CO ₂	1370	0.68	44	Ton
Mass	614	48	1053	Ton
Volume	1153	56	1380	m ³

Table 6. Optimal power plant configuration per ship type

Cargo Carrier	Harbor Tug	TSHD
Single Shaft	PTI	PTI
2- stroke DE, Direct (11.9 MW)	PMSM, Direct (1.2 MW)	PMSM, Direct (8.8 MW)
MDO	-	-
-	-	-
-	Dual Fuel Engine, Geared (1.2 MW)	Dual fuel Engine, Geared (2.2 MW)
-	MDO	MDO
-	LNG	LNG
PEMFC (618 kW)	PEM Fuel Cell (1.2 MW)	PEM Fuel Cell (23 MW)
-	-	-
-	-	-
Pressurized Hydrogen	Pressurized Hydrogen	Pressurized Hydrogen
-	-	-
SCR	-	-
Scrubber	-	-

Most of the selected components can be explained given some basic marine engineering knowledge (most of which can be found works such as [5]) .

There are however, some unexpected components. For example the fact that HFO, which is a very conventional fuel, is not used as selected for any of the three cases. Instead MDO is always found in the selected concepts.

Another remarkable trend is the fact that fuel cells are selected in each of the three cases.

Because of the subjective nature of the client preference a sensitivity analysis is also executed. This is done by varying the client preferences for the cargo carrier case, while keeping all other input values the same.

The analysis is performed, by varying the preferences one at the time, with increments of 3, cases very similar to the original case, which is used as benchmark are omitted. Doing so creates a total of 12 additional, new, cases.

Both the final concept selection and the influence on the numerical results are investigated. With the influence in numerical results being expressed as a change w.r.t. to the benchmark case.

The complete set of numerical results are not included in this paper. Due to the large amount of data, however an example is included in figure 10 and figure 11. These figures show the same scatter diagram. But figure 11 shows a magnified version by omitting the largest spikes seen in figure 10.

The presented example shows the change in fuel consumption under influence of a changing weight factor related to duel consumption, for each individual power plant configuration.

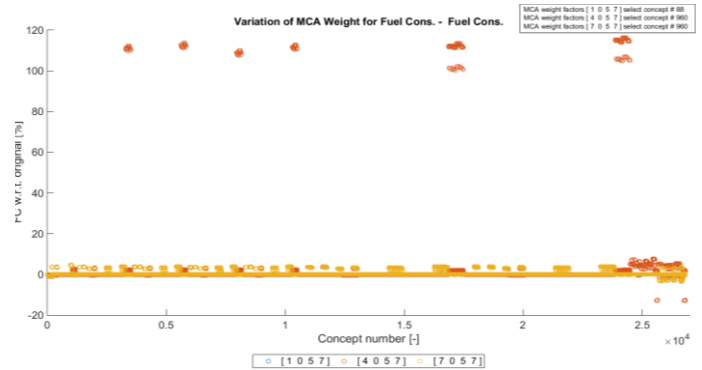


Fig 10: Example Results of the Sensitivity Analysis

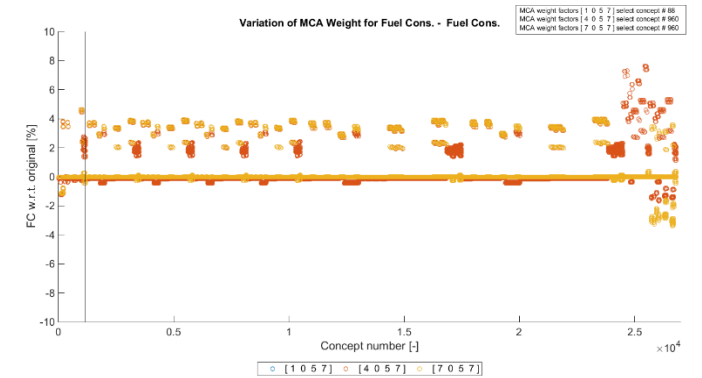


Fig 11: Magnified Example results

The numerical results presented in figure 11 show limited deviations, although there are some extreme deviations, as seen in figure 10. Both of these are discussed separately.

From the magnified changes in the numerical results (seen in figure 11) it can be seen that (as expected) the consumed fuel mass does indeed decrease when the weight factor is decreased.

The observed extreme deviations (visible in figure 10) are found in locations where electrical propulsion is applied in combination with a change in the DoH, this is also seen in the detailed design information of one such an extreme case, which is included in table 6.

In this table the large electric propulsive engine is found and the change in DoH can be observed from the fact that the power obtained from each generation system changes. From the detailed information two likely causes of the extreme increase in fuel consumption can be found.

The first is the fact that more diesel will be consumed, which is heavier than the hydrogen and thus the consumed fuel mass increases.

The other cause for the increase is the fact that because the DoH changed an SCR was required. The addition of an SCR increases the total system mass, but also requires reagent. This reagent is added to the consumed fuel, resulting in an enlarged increase in fuel consumption.

Table 7: Detailed design data, extreme deviation

	Original Case	Case B
Shaft Configuration	Power Take In	Power Take In
MPE - Engine Type	Dual Fuel Engine (844 kW)	Dual Fuel Engine (844 kW)
MPE - Main Tank	MDO	MDO
MPE - Sec. Tank	LNG	LNG
PTI- Engine Type	PMSM, Geared (11.4 MW)	PMSM, Geared (11.4 MW)
PTI - Main Tank	-	-
PTI - Sec. Tank	-	-
Generation System	PEMFC & DE Genset (9795 kW & 1347 kW)	PEMFC & DE Genset (1108 kW & 12354 kW)
Genset – Main Tank	HFO	HFO
Genset – Sec. Tank	-	-
Hydrogen Storage	Pressurized Hydrogen	Pressurized Hydrogen
Electrical Energy Storage	Li-Ion Batteries	Li-Ion Batteries
NOX Reduction	N/A	SCR
SOX Reduction	Wet Scrubber	Wet Scrubber

The fact that the propulsive engines have such a large influence on the entire design, is due to the fact that for this case, the power required from these systems is significantly higher than the electrical power demand.

Which implies that the influence of the weight factors is not only dependent on the value of those weight factors, but also on the operational profile.

In addition to the numerical results, the change in selected power plant configuration is also monitored. Two power plant configurations are selected multiple times, for different preferences, and these are presented in table, without the power indications.

Table 8. Most dominant concepts, sensitivity analysis

	Selected 5 times	Selected 5 times
Shaft Configuration	Single Shaft	Single Shaft
MPE - Engine Type	Dual Fuel Engine, Geared	Dual Fuel Engine, Geared
MPE - Main fuel tank	MDO	MDO
MPE - Secondary fuel tank	LNG	LNG
PTI - Engine Type	-	-
PTI - Main fuel tank	-	-
PTI - Secondary fuel tank	-	-
Electricity Generation System	Dual Fuel Genset	PEM Fuel Cell
Genset - Main fuel tank	MDO	-
Genset - Secondary fuel tank	LNG	-
Hydrogen Storage	-	Pressurized Hydrogen
Electrical Energy Storage	-	-
NO _x Reduction	-	-
SO _x Reduction	-	-

VI. Conclusions

The cargo carrier results, show that the developed tool selects an expectable power plant concept [5], given the more stringent emission regulations. This gives some confidence in the working principles behind the tool.

The other two cases also result in configurations which are explainable, given the operational profile and currently seen trends [5].

Although both the original cases and the sensitivity analysis show a high preference towards fuel cells and hydrogen storage. This is caused by the fact that fuel consumption was judged on a mass basis, which is hugely in favor of the application of hydrogen.

Additionally an important downsides of fuel cells, the fact that they are expensive, is not included in the tradeoff, since costs are not included as a criterion.

The sensitivity analysis showed that the tool is indeed sensitive to the preference. With average deviations of around 5 [%], although some extremes were observed as well. These extremes were caused by a combination of an electric propulsion system and a generation system which contains both a genset and a fuel cell.

From the combination of the different sensitivity analysis results and their causes it could also be deduced that the value of the weight factors is not the only thing which influences the sensitivity of the tool to those weights. Instead, the operational profile also has an influence on the sensitivity by influencing which set of design choices has a larger influence.

VII. Recommendations

The first recommendation of this research is the expansion of the list of considered components. Especially the inclusion of a power take off and other methods to store hydrogen (such as reformers or other fuel cell systems) should give some interesting results.

In addition to the list of components, the considered characteristics, and thus considered design choices, should also be expanded.

Especially the inclusion of life cycle costing could be interesting. Since this could change the tendency towards fuel cells. Additionally the inclusion of costs as a criterion could also reduce the application of MDO. Since MDO is a relatively expensive fuel (when compared to other conventional fuel types, such as HFO).

Another recommendation concerning the characteristics is to replace or complement the characteristic of fuel consumption with a total system efficiency. Doing so reduces the effect of the specific mass of a fuel. And could therefore also reduce the tendency towards fuel cells, and allow for a fairer comparison between the different systems.

The influence of the operational profile, should also be investigated, since it is expected that the operational profile greatly influences the results.

Another effect that should be included is the switching of fuels, during different stages found in the operational profile. This is often seen in practice, since this allows ships to operate for the lowest possible costs, while still complying with the regulatory limits posed to the area the vessel is in at that moment in time.

To do so, the emission control area would also have to become a time based preference as well.

And finally the influence of the defined technological parameters should be investigated, since these are likely to have an influence on the results.

An example of such a parameter, which is sure to be interesting to investigate, is the sulphur content of the applied fuels. Since, this parameter is expected to change in the near future, due to the upcoming sulphur cap [4].

VIII. References

- [1] International Transport Forum, "Decarbonizing Maritime Transport - Pathway to zero-carbon shipping by 2035," International Transport Forum, Paris, 2018.
- [2] International Maritime Organisation, "UN body adopts climate change strategy for shipping," International Maritime Organisation, 13 April 2018. [Online].
- [3] P. de Vos, D. Stapersma, "Automatic Topology Generation for early design of on-board energy distribution systems", expected to be published in 'Ocean Engineering', to be published in 2018
- [4] DNV-GL, "Maritime Global Sulphur Cap 2020," Det Norske Veritas (DNV) en Germanischer Lloyd (GL), Hamburg (Germany), 2016.
- [5] H. Klein Woud, D. Stapersma, "Design of Propulsion and Electric Power Generation Systems", IMarEST, London, 2008
- [6] P. d. Vos and D. Stapersma, "Dimension prediction models of ship system components based on first principles," International Marine Design Conference, 2015.
- [7] M. ten Hacken, "Optimization of a submarine propulsion system by implementing a PEM fuel cell and a PMSM in a first principle model," TU Delft - Nevesbu, Delft - Alblasterdam, 2017.
- [8] J. Jalkanen, L. Johansson, J. Kukkonen, A. Brink, J. Kalli and T. Stipa, "Extensions of an assessment model of ship traffic exhaust emissions for particulate matter and carbon monoxide", Copernicus Publications, Helsinki, 2012
- [9] L.P.W. Rietveld, "Optimization of a propulsion plant for a submarine, based on first principles", Master's thesis Delft University of Technology, 2017
- [10] H. T. Grimmelius and P. de Vos, "Towards environmental-friendly inland shipping propulsion systems for inland ships using different fuels and fuel cells," Delft University of Technology, Delft, 2011.